ESECMaSE

Enhanced **S**afety and **E**fficient **C**onstruction of **Ma**sonry **S**tructures in **E**urope

Project No. Coll – Ct - 2003 - 500291

ESECMaSE

Enhanced Safety and Efficient Construction of Masonry Structures in Europe

Horizontal Research Activities Involving SMEs

Collective Research

Work Package N°: 7

D 7.2b Test results on the earthquake resistance on improved masonry materials by pseudo dynamic tests

Prof. Dr.-Ing. habil. Dr.-Ing. E. h. K. Zilch, Dipl.-Ing. W. Finckh, Dipl.-Ing. S. Grabowski, Dr.-Ing. D. Schermer, Dipl.-Ing. W. Scheufler,

Due date of deliverable: 01.06.2008
Actual submission date:01.09.2008

Start date of project: 10.June 2004 Duration: 36 month

Draft N°: …1

Technical University of Munich
Department of civil engineering and geodesy
Chair of Structural Concrete
80290 Munich

Project co-funded by the European Commision within the Sixth Framework Programme (2002-2006)		
Dissemination Level		
PU	Public	X
PP	Restricted to other programme participants (including the Commission Services)	
RE	Restricted to a group specified by the consortium (including the Commission Services)	
CO	Confidential, only for members of the consortium (including the Commission Services)	

TECHNISCHE
UNIVERSITÄT
MÜNCHEN

Institut für Bau-stoffe und Kon-struktion

MPA BAU

Lehrstuhl für Massiv-bau
Univ.-Prof.
Dr.-Ing. K. Zilch

Arbeitsgruppe 4
Mauerwerk

ESECMASE

No. sw-2408202
Date....2008-08-21

Deliverable D7.2 b: **Test results on the earthquake resistance on improved masonry materials by pseudo dynamic tests**

Project: Enhanced Safety and Efficient Construction of Masonry Structures in Europe

Client: European Commission
RESEARCH DIRECTORATE-GENERAL

Person in charge: Dipl.-Ing. W. Scheufler

The investigation report includes: 16 Pages
104 Annex

MAILING ADDRESS:	D-80290 MUENCHEN	PHONE +49 / 89 / 289 - 23038/39	FAX +49 / 89 / 289 - 23046
ADDRESS:	BUILDING N6	THERESIENSTR. 90	D-80333 MUENCHEN
BANK DATA:	BAYER. LANDESBANK MUENCHEN	ACCOUNT NO: 24 866	BANK CODE: 700 500 00
CONTACT PERSON:	DIPL.-ING. W. SCHEUFLER	E-MAIL:esecmase@mb.bv.tum.de	PHONE +49 / 89 / 289-23025

Contents

1. Introduction

Deliverable 7.2 of ESECMaSe deals with the pseudo-dynamic tests on masonry walls. Since the pseudo dynamic wall tests of the ESECMaSe project were carried out at two different laboratories, the deliverable is divided into two parts:

⇒ D 7.2 a – University of Kassel (UNIK)
⇒ D 7.2 b – Technical University of Munich (TUM)

This report describes the pseudo dynamic wall tests with a test set-up developed in WP 6 on different kinds of masonry (clay, calcium silicate, lightweight aerated concrete) with different specimen dimensions, carried out at Technical University of Munich.

2. Material properties

2.1.1. Walls made of Clay units

Two wall specimens (Clay03 and Clay04) were built with vertically perforated clay bricks, type: Bellenberg HLZ – Plan – 12 – 0.9 9DF, optimized 2. The width of the brick was 175mm, the height 249mm and the length 363mm. The head joints were left unfilled according to the groove and tongue of the units. As mortar for the bed joints, a thin layer mortar type “Bellenberger Planziegel Dünnbettmörtel (DIBT Zul.-Nr. Z.17.1-261)” was used

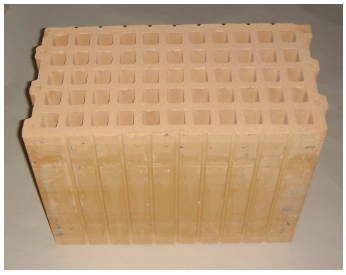

Figure 1: Clay units: Bellenberg HLZ – Plan – 12 – 0.9 9DF, optimized 2

2.1.2. Walls made of Calcium silicate units

Three different types of calcium silicate units were used. Specimen CS08 and CS09 were built with optimized calcium silicate bricks type KSP 20-1.8-6DF (248x175x248 mm) in combination with a thin layer mortar (class M10, according to DIN EN998-2) for the bed joints. The head joints were left unfilled because of the groove and tongue of the bricks.

Furthermore two walls (CS12 and CS13) were build with calcium silicate “Quadro E“ units. The units were square 498 x 498 mm with a thickness of 175 mm. The walls were confined with one Ø 16 mm reinforcing steel bar, at each end of the wall. The holes of the units in which the steel bars were placed, were completely grouted with mortar type “quick-mix AVG-

QM Ankermörtel". The mortar for the bed joints was a thin layer mortar class M10 according to DIN EN 998-2, the head joints were left unfilled because of the groove and tongue of the units.

For the other specimen CS014 and CS15, large-sized units, type KS XL-PE (width: 175mm, height: 623mm, length: 998 mm) with an internal reinforcement (three reinforcing bars, diameter 12 mm, per unit) in conjunction with the thin layer mortar type: "KS-Werkplanmörtel,", In the following referred to as "WEP", were used. The head joints of these Specimens were filled with the same mortar ("WEP").

Figure 2: KSP 20-1.8-6DF (175), optimized

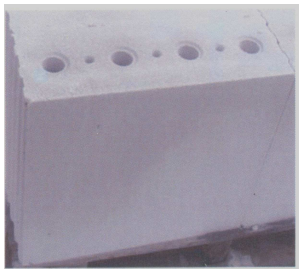

Figure 3: "Quadro-E" Unit, 498x175x498 mm

Figure 4: KS XL-P (175) with internal reinforcement

2.1.3. Walls made of Lightweight Aerated Concrete units

Four wall specimens (LAC01 – LAC04) were constructed of Lightweight Aerated Concrete units. The width of the brick was 175mm, the height 248mm and the length 247mm. The head joints were left unfilled according to the groove and tongue of the units. As mortar for the bed joints, a thin layer mortar type "Bisotherm heat-insulating", class M10 (according DIN EN 998-2) was used.

Figure 5: Lightweight Aerated Concrete units: Bisophon VBL- 12 - 2.0 6DF (175)

3. Pseudo dynamic tests

3.1. Test method

The PSD-test method with sub-structure-technique allows testing and simulating big structures under dynamic loadings, where just the relevant structural member is tested directly within the experiment. The rest of the structure during these tests is simulated just numerically as sub-structure. Therefore the loading of the specimen test can be driven quasi-static because the dynamic restoring forces are calculated exclusively numerically. The structural and dynamic properties (especially the stiffness parameters) of the sub-structure (e.g. the shear walls of the other storeys) are generally determined within preceding tests..
The equation of motion of the structure under the base acceleration is solved numerically in discrete time steps within the test procedure by the application of the implicit Newmark-algorithm. The interaction of applied target displacements and the measured restoring forces is covered during the calculation process.
For the following tests the complex structural system of the building was simplified to the basically load bearing structures. This reduced structure was numerically simulated using a finite-element model.

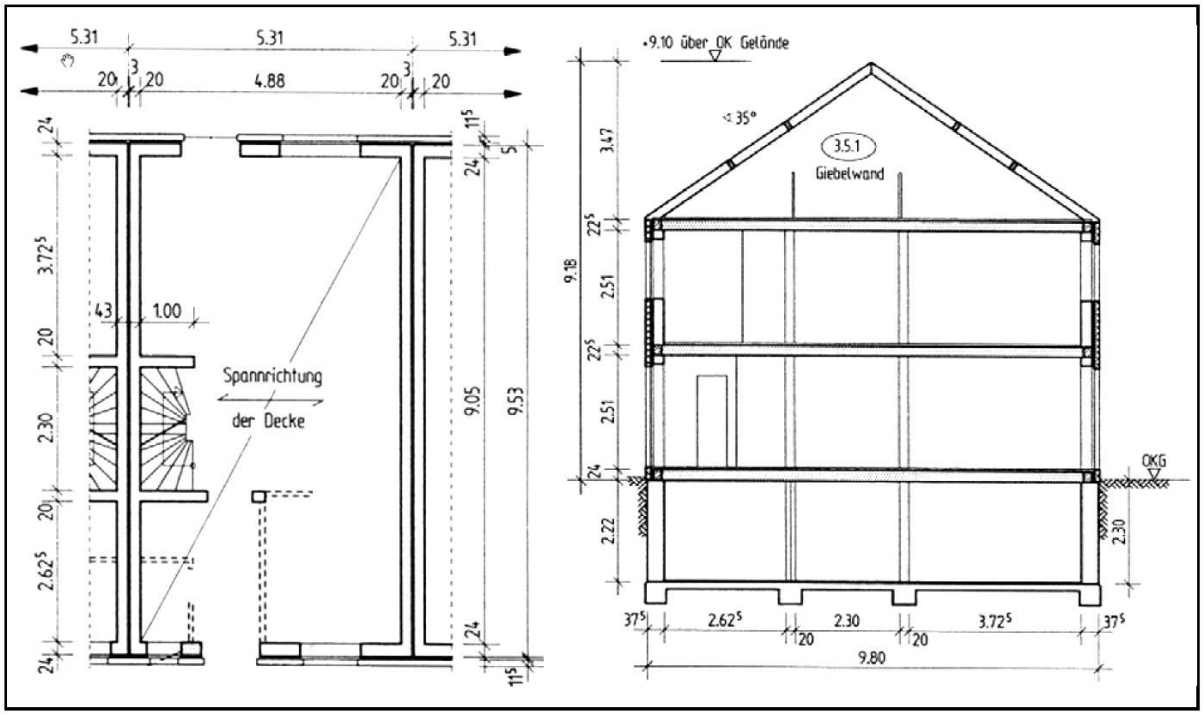

Figure 6: Plan view of the reference terraced house-structure [Deliverable 8.1]

In this numerical model, the wall in the ground floor is represented by a special two-node element, which connects the behaviour (displacements, rotations and forces resp. moments) of the real tested structure and the FE-model.

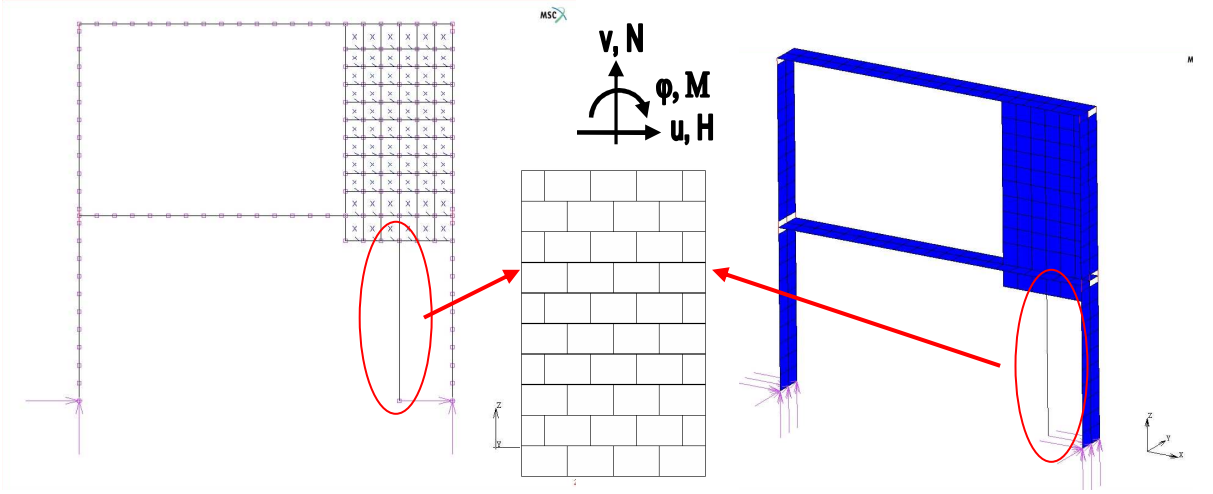

Figure 7: representative finite-element model of the two storey terrace house (e.g. model for the tests of specimen Clay03)

The geometry resp. the stiffness of the slabs and the remaining walls for the simplified finite element model, was taken from the JRC-Specimens described in WP 8 (Deliverable 8.1). Also the vertical loading of the system is calculated based on the data of the JRC.

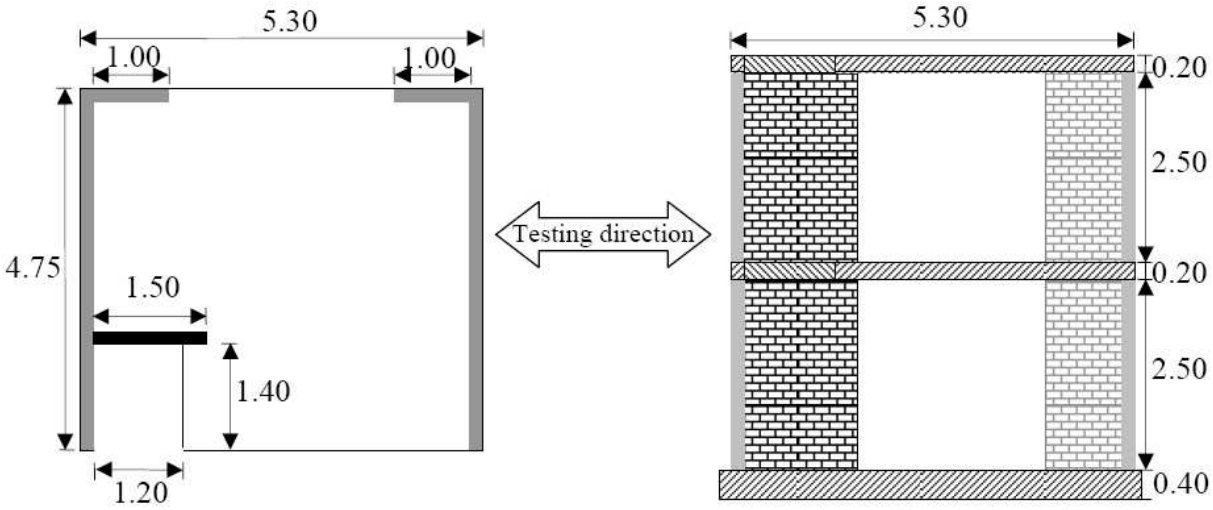

Figure 8: ground plan and elevation of the specimen which were tested at the JRC in Ispra [Deliverable 8.1]

Furthermore, for the tests on specimen LAC02 and LAC04 the geometry of the model was changed to represent a three-storey frame, to get some information of the behaviour of the tested masonry walls under a higher vertical normal stress state and the influence of the modified resonance frequency of the building. Based on the characteristics (masses, stiffness and vertical loads) of the two-storey model, the additional masses and vertical loads of the third storey were calculated.

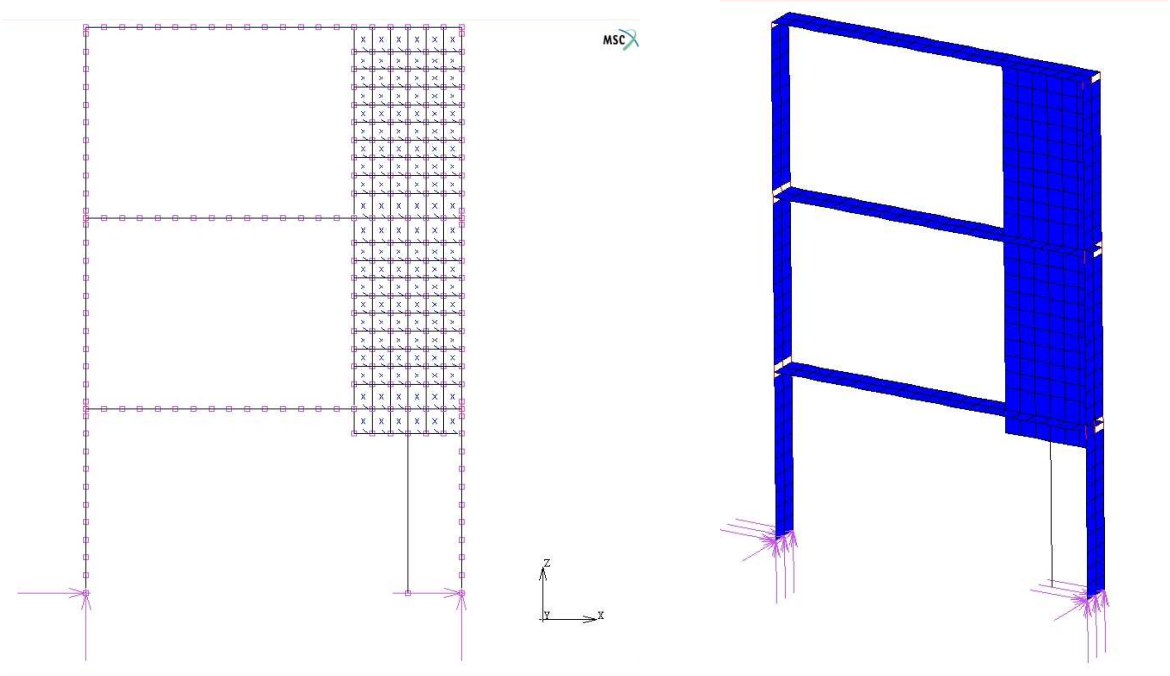

Figure 9: representative finite-element model of the three storey terrace house (e.g. model for the tests of specimen LAC02)

3.2. Test set-up and measurements

The test set-up developed in work-package 6 was used also for the execution of the pseudo dynamic tests. Details of the positioning of the hydraulic jacks and measurement equipment– especially the position of the LVDT's – of each wall can be found in the annex.

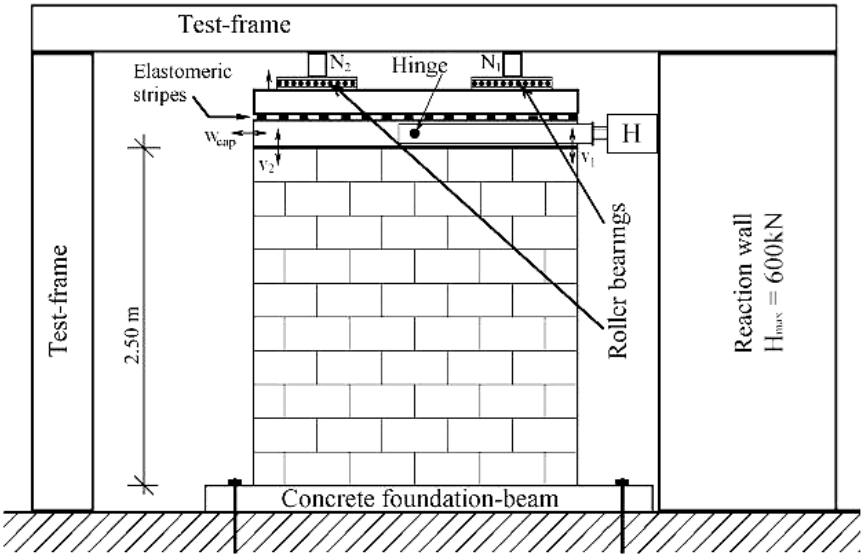

Figure 10: Test set-up used for the pseudo dynamic tests at the TU Munich [Deliverable 6]

3.3. Overview

The Pseudo dynamic tests were performed on twelve walls constructed of calcium silicate units, clay bricks and lightweight aerated concrete blocks. The thickness of the walls was 175 mm for all specimens and also the height of 2.5 m was constant for all tests. The details of the material properties of the different kind of units and mortar can be found in deliverable 5.5. Table 1 gives an overview of the geometric dimensions, vertical normal stresses and the materials:

Table 1: Overview of the tested wall specimens under pseudodynamic loading.

Name	**l[m]**	**σ_V [MPa]**	**Unit size [mm³]**	**Reinforcement**	**Bed joints (thin layer)**	**Head joints**	**Minimum overlapping length**
CS08	1.25	0.96	248x175x248 optimised units	No	Quick mix KSK grob	unfilled	$l_{unit}/2$ = 12,5cm
CS09	2.50	diversify	248x175x248 optimised units	No	Quick mix KSK grob	unfilled	$l_{unit}/2$ = 12,5cm
CS12	1.25	0.90	498x175x498 Quadro E	vertical confinement (1+1 Ø 16)	Quick mix KSK grob	unfilled	$l_{unit}/2$ = 25cm
CS13	2.50	0.35	498x175x498 Quadro E	vertical confinement (1+1 Ø 16)	Quick mix KSK grob	unfilled	$l_{unit}/2$ = 25cm
CS14	1.25	0.82	998x175x625	Internal	WEP	filled	$l_{unit}/2$ = 50cm
CS15	2.50	0.38	998x175x625	Internal	WEP	filled	$l_{unit}/2$ = 50cm
Clay03	2.25	0.51	375x175x248 (HLZ-Plan-12/0,9-17,5) Opti 2	No	DM	unfilled	$l_{unit}/2$ = 18cm
Clay04	1.50	0.74	375x175x248 (HLZ-Plan-12/0,9-17,5) Opti 2	No	DM	unfilled	$l_{unit}/2$ = 18cm
LAC01	1.25	0.98	248x175x248 (VBL-12-2,0-6DF)	No	DM	unfilled	$l_{unit}/2$ = 12,5cm
LAC02	1.25	1.23	248x175x248 (VBL-12-2,0-6DF)	No	DM	unfilled	$l_{unit}/2$ = 12,5cm
LAC03	2.50	0.44	248x175x248 (VBL-12-2,0-6DF)	No	DM	unfilled	$l_{unit}/2$ = 12,5cm
LAC04	2.50	0.62	248x175x248 (VBL-12-2,0-6DF)	No	DM	unfilled	$l_{unit}/2$ = 12,5cm

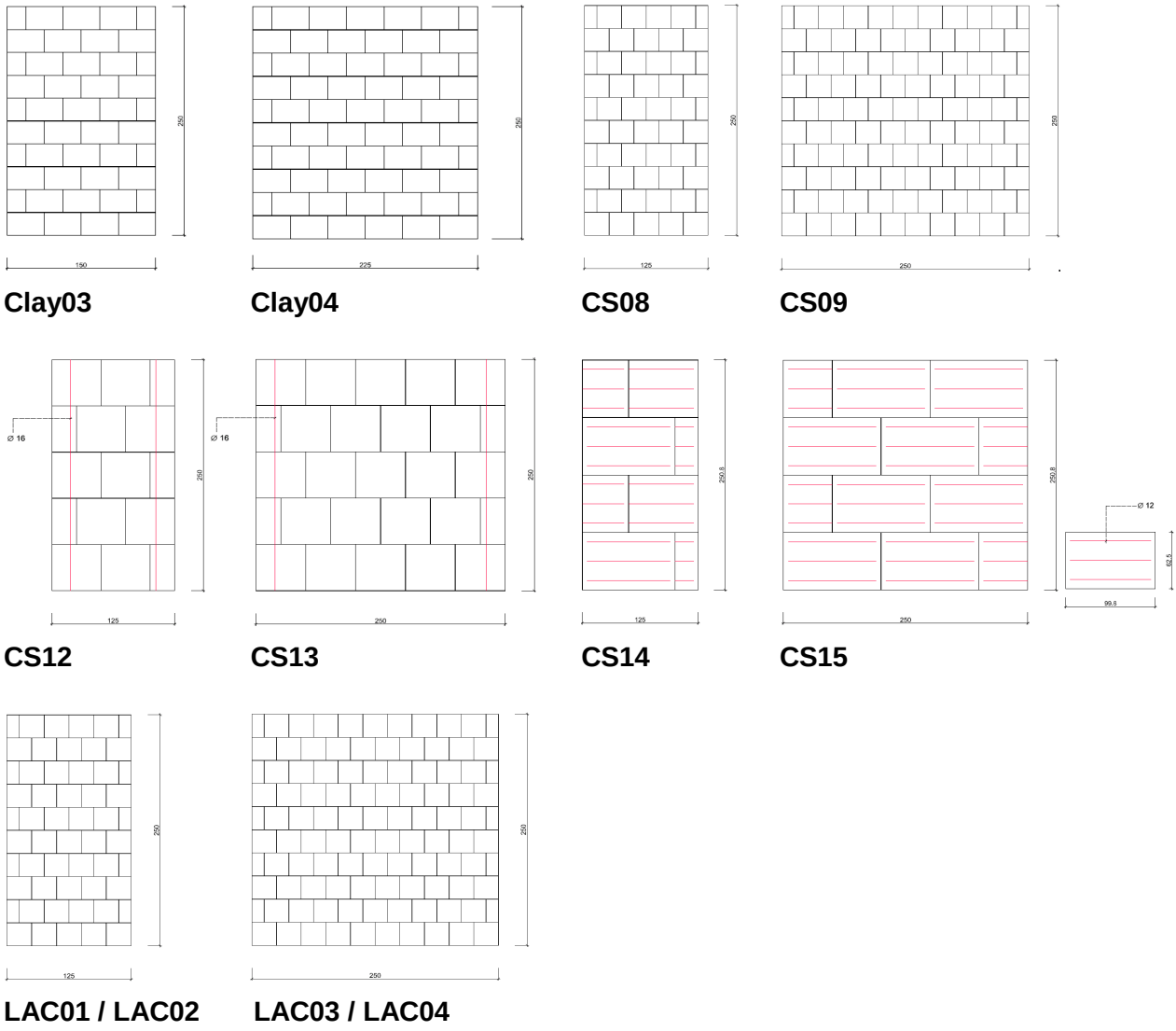

Figure 11: Overview of the wall specimen

3.4. Seismic input

The horizontal accelerogram was taken from the shaking table tests in Athens and the JRC-pseudo dynamic tests. The elastic response spectra for 5% viscous damping, for this time history, is given below. Each specimen has been tested for multiple times with different scaling factors of this time history. The scaling factors are given in the Annex for each test.
As a general rule, two pseudo dynamic test were carried out for each specimen, with a duration of about 3 to 8 hours for one test (the duration depends on the nonlinear behaviour of the specimen). The duration of the seismic acceleration was 10 seconds for all tests.

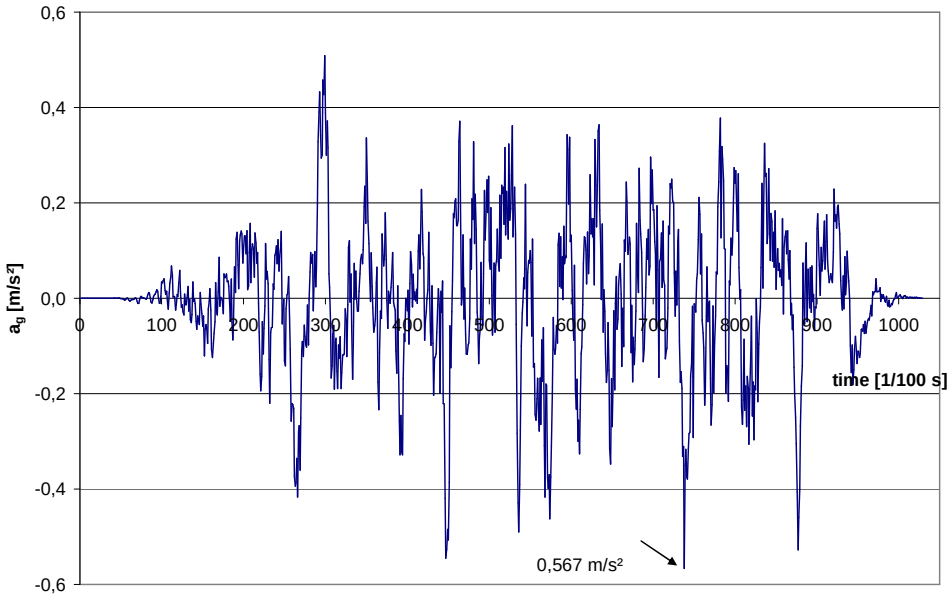

Figure 12: Used accelerogram (factorized 1.0).

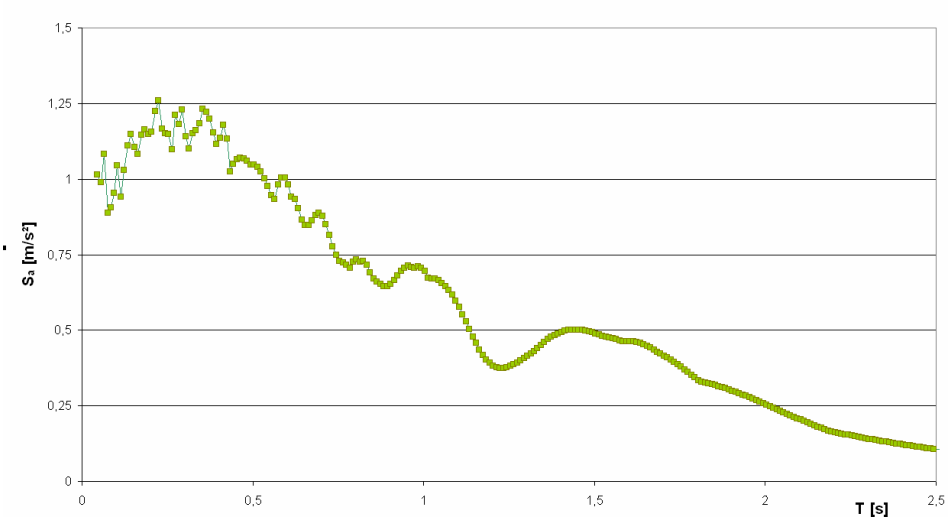

Figure 13: Elastic response spectra of the used accelerogram (factorized 1.0).

3.5. Modal mass of the structure, vertical load and restraint at the the top of the wall

The modal mass for the numerical finite element model of the two resp. three storey frames is calculated based upon the dimensions of the specimen at the JRC. The calculation of the modal masses consider the symmetry of the ground plan and the existence of additional short shear walls at the edge of the building. As a result the numerical model for the pseudo dynamic tests did not contain the whole modal mass.

To get the correct vertical loads for the simulation model (two resp. three storey frame), a spatial finite element model of the complete building structure had been calculated preliminary. The dead loads and the live loads of this numerical simulation were also based upon the loads of the Ispra-specimen.

The resulting normal force of the wall specimen depends secondary on the stiffness of itself and on the bending stiffness of the exterior walls, the slabs and the bending stiffness of the junction between the slabs and the walls. Because of several modifications of this complex detail in the numerical model, during the project, the vertical normal force for the specimen varies from 154kN to 214 kN (two storey-frame).

Usually the vertical force was calculated at the beginning of the test and then it was fixed for the whole pseudo dynamic test. This simplification was made, to make the results comparable to the static cyclic tests (Deliverable 7.1). Within the test of CS09, the normal force was also varied during the duration of the experiment. All other tests were carried out with a constant normal stress state.

In contrary to the static cyclic tests, whereas the restraint at the top of the specimen was predefined (e.g. cantilever wall), the magnitude of the counteracting moment of the slab depends on the deformation of the whole structure. As a consequence of the asymmetric ground plan, the fixation of the wall through the slab is also asymmetric. Therefore the behaviour of the wall depends on the moving direction of the structure.

Table 2: Overview of modal masses within the pseudo dynamic tests.

Name	Total modal mass [t]	N [kN]	System
CS08	44,8 t	209	Two-storey frame
CS09	44,8 t	diversify	Two-storey frame
CS12	44,8 t	197	Two-storey frame
CS13	44,8 t	154	Two-storey frame
CS14	44,8 t	179	Two-storey frame
CS15	44,8 t	165	Two-storey frame
Clay03	44,6 t	200	Two-storey frame
Clay04	44,6 t	195	Two-storey frame
Lwc01	44,8 t	214	Two-storey frame
Lwc02	70 t	270	Three-storey frame
Lwc03	44,8 t	194	Two-storey frame
Lwc04	70 t	270	Three-storey frame

3.6. Damping

The damping was covered by discrete viscous dampers in the model (applied to the node at the top of the shear-walls) and additional material damping in the remaining structure. The values were determined to achieve a total damping ration of 5% for the first and second mode. Nevertheless within the tests CS13, CS14 and CS15 the ratio was about 20%.

4. Test results

The detailed results of the different tests of all specimens can be found in the annex.

4.1. Maximum horizontal force

The results of the tests concerning the maximum horizontal load H_{max} and the maximum displacements d_{max} of the specimen are given below.

Table 3: Normal forces and maximum horizontal loads

Name	N	H_{max}	d_{max}	H/N	Geometry l/h (*)
CS08	209 kN	76 / -73 kN	7.8 / -5.3 mm	0.35	0.5
CS09	diversify (100 – 530 kN)	84 / (-126) kN	11.8 / (-1.6) mm	-	1
CS12	197 kN	90 / -72 kN	6.3 / -6.1 mm	0.41	0.5
CS13	154 kN	94 / -82 kN	10 / -12.1 mm	0.56	1
CS14	179 kN	67 / -56 kN	4.5 / -9.6 mm	0.34	0.5
CS15	165 kN	111 / -97 kN	13.8 / -8.4 mm	0.62	1
Clay03	200 kN	76 / -67 kN	8.5 / -7.4 mm	0.37	0.6
Clay04	195 kN	106 / -110 kN	11.8 / (-4.2) mm	0.55	0.9
LAC01	214 kN	82 / -79 kN	40. / -31.6 mm	0.38	0.5
LAC02	270 kN	97 / -97 kN	14.1 / -12.9 mm	0.36	0.5
LAC03	194 kN	122 / -117 kN	6.5 / -7.7 mm	0.62	1
LAC04	270 kN	150 / -138 kN	14.2 / -22 mm	0.53	1
(*) assuming rocking limitation and double fixation					

4.2. Deformation capacity and ductility

The deformation capacity of the walls is determined from the load displacement curves obtained from the test. The results are interpreted according to deliverable D7.1.

The relevant parameters were the point of the first crack (H_C and u), the maximum load H_F and the maximum deformations d_{u1} and d_{u2} on both sides. These values were taken from the data. For the calculation of the ductility, it has to be taken into account, that the bending moment at the top of the wall (due to the asymmetric ground plan) is not zero at the beginning of the test (the origin of the hysteresis is not congruent with the origin of the coordinate system).

Table 4: Overview of the deformation behaviour of the tested walls

Name	d_{u1} [mm]	d_{u2} [mm]	d_{cr1} [mm]	d_{cr2} [mm]	H_{cr1} [kN]	H_{cr2} [kN]	H_{u1} [kN]	H_{u2} [kN]	d_{e1} [mm]	d_{e2} [mm]	μ_1 [-]	μ_2 [-]
CS08	7.8	-5.3	1.0	-3.2	56	-59	76	-73	1.7	-3.7	4.5	1.4
CS09	11.8	(-1.6)	0.5	-	75	-	84	(-126)	-	-	-	-
CS12	6.3	-6.0	0.7	-2.2	50	-57	90	-72	1.8	-2.6	3.5	2.3
CS13	10.0	-12.1	0.5	-0.4	57	-34	94	-82	0.8	-0.9	12.4	14.2
CS14	4.5	-9.6	0.4	-0.6	42	-20	67	-56	0.7	-1.2	6.0	8.3
CS15	13.8	-8.4	0.6	-0.4	65	-50	111	-97	1.0	-0.8	14.0	11.2
Clay03	8.5	-7.4	1.1	-2.3	59	-42	76	-67	1.6	-3.1	5.3	2.4
Clay04	11.8	-4.2	0.6	-1.4	49	-47	106	-110	1.8	-2.8	6.5	1.5
LAC01	40.0	-31.6	1.1	-3.3	59	-66	82	-79	1.9	-3.7	20.7	8.5
LAC02	14.1	-12.9	0.9	-2.1	59	-49	97	-97	1.9	-3.4	7.5	3.8
LAC03	6.5	-7.7	0.6	-1.0	86	-42	122	-117	1.1	-1.9	6.1	4.1
LAC04	14.2	-22.0	0.4	-0.6	77	-39	150	-138	1.0	-1.5	13.6	15.0

The ductilities μ_1 and μ_2 differ from each other, because of the asymmetric ground plan of the simulated structure. Due to this asymmetry, the behaviour of the structure and also the fixation of the wall through the slab, depends on the moving direction. Therefore in most cases, the maximum displacement of the specimen is reached only in one direction.

4.3. Comparison of static cyclic with pseudo dynamic wall tests

For the static cyclic wall tests (Deliverable 7.1) some simplifications have been made. The main simplification concerns the restraint of the slab. During the static cyclic tests, the restraint moment at the top of the wall was controlled under the restriction of a zero moment in the mid height of the wall. For the pseudo dynamic tests however, the moment at the top of the wall is calculated as a reaction of the numerical model and the behaviour of the specimen. The zero point of the bending moment is therefore no longer fixed at the mid height of the wall. By the comparison of the static cyclic tests to the pseudo dynamic tests the influence of this simplification can be shown. Unfortunately there are only few specimens with the same geometry, the same material properties and almost the same level of vertical compression state, which were tested static cyclic and pseudo dynamic. Figure 14 to 17 show the comparison of the pseudo dynamic test with the static cyclic test. In Figure 14 the influence of the asymmetric fixation through the slab is observable. In the positive displacement direction, the slab acts nearly as a full restraint, comparable to the static cyclic test, in the negative direction, the fixation is considerably less. This leads to a completely different behaviour in cases where large rotations (figure 15) of the wall occur. In Figure 16, the difference between the pseudo dynamic test and the static cyclic test is not obvious. This is a conse-

quence of the only small rotations of the wall under negative displacements during the static cyclic test. The fixation of the slab therefore has no dominant influence on the hysteresis.

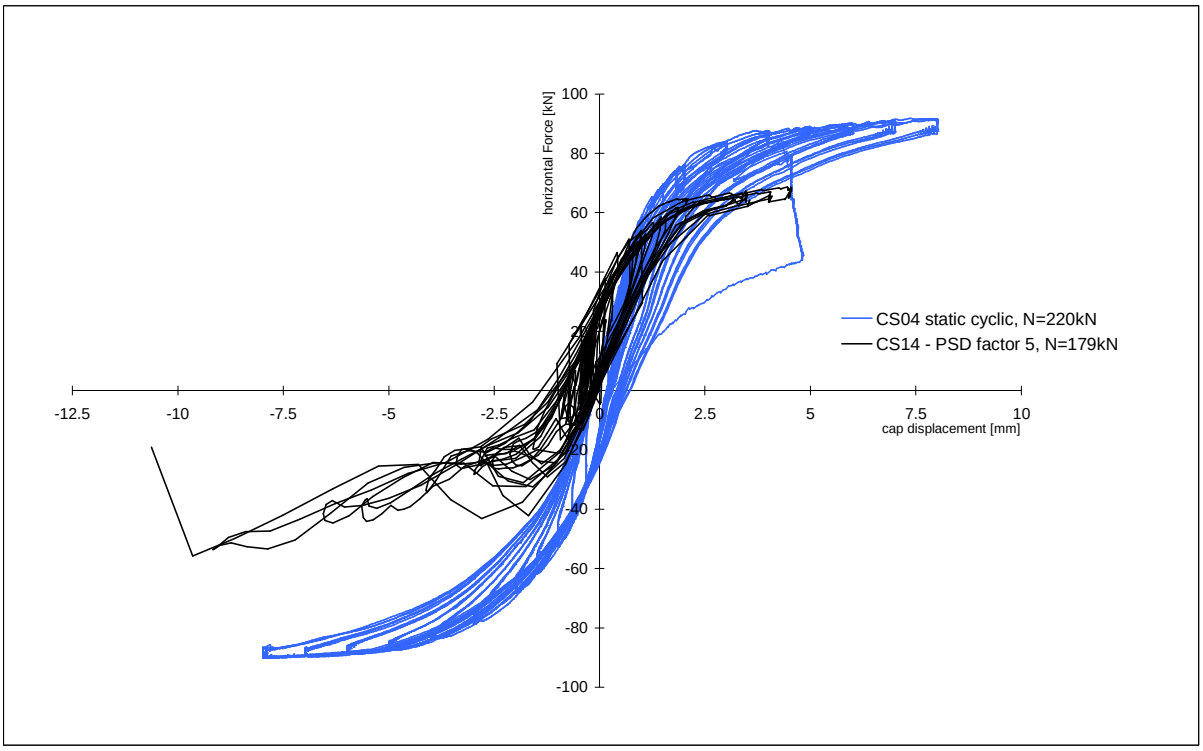

Figure 14: comparison of the hysteresis of wall CS14 (tested pseudo dynamic) and wall CS04 (tested static cyclic)

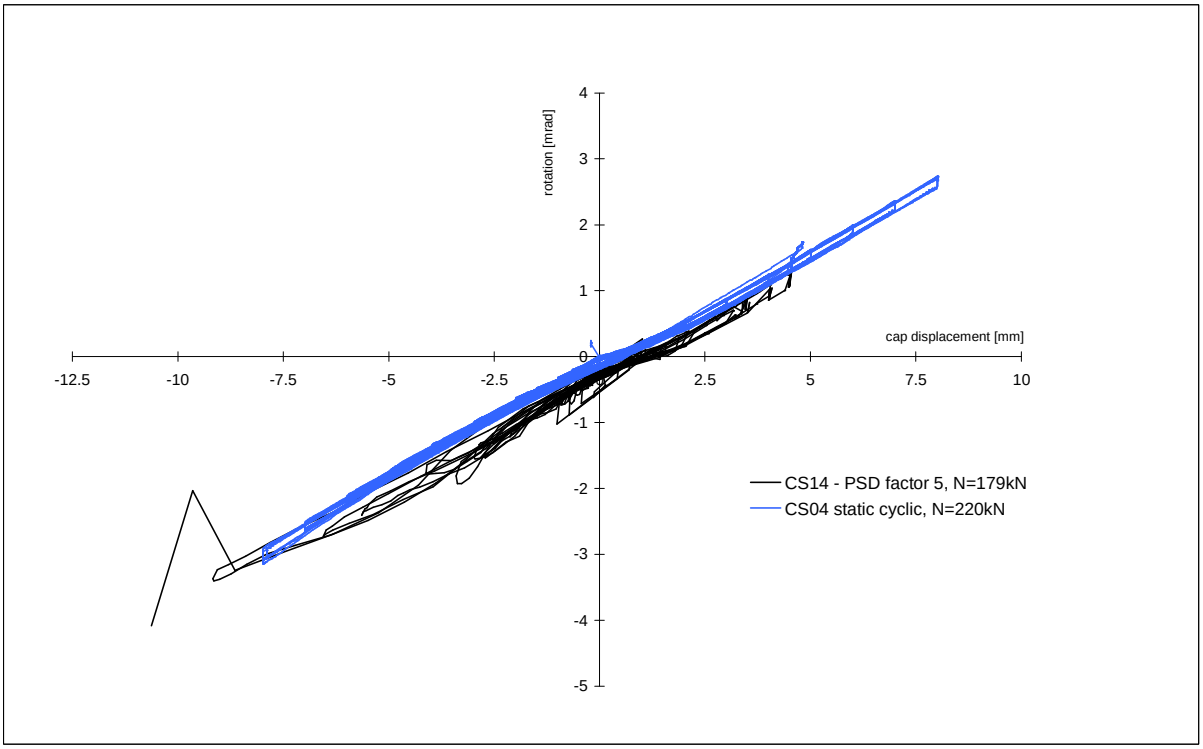

Figure 15: comparison of the rotation of wall CS14 (tested pseudo dynamic) and wall CS04 (tested static cyclic)

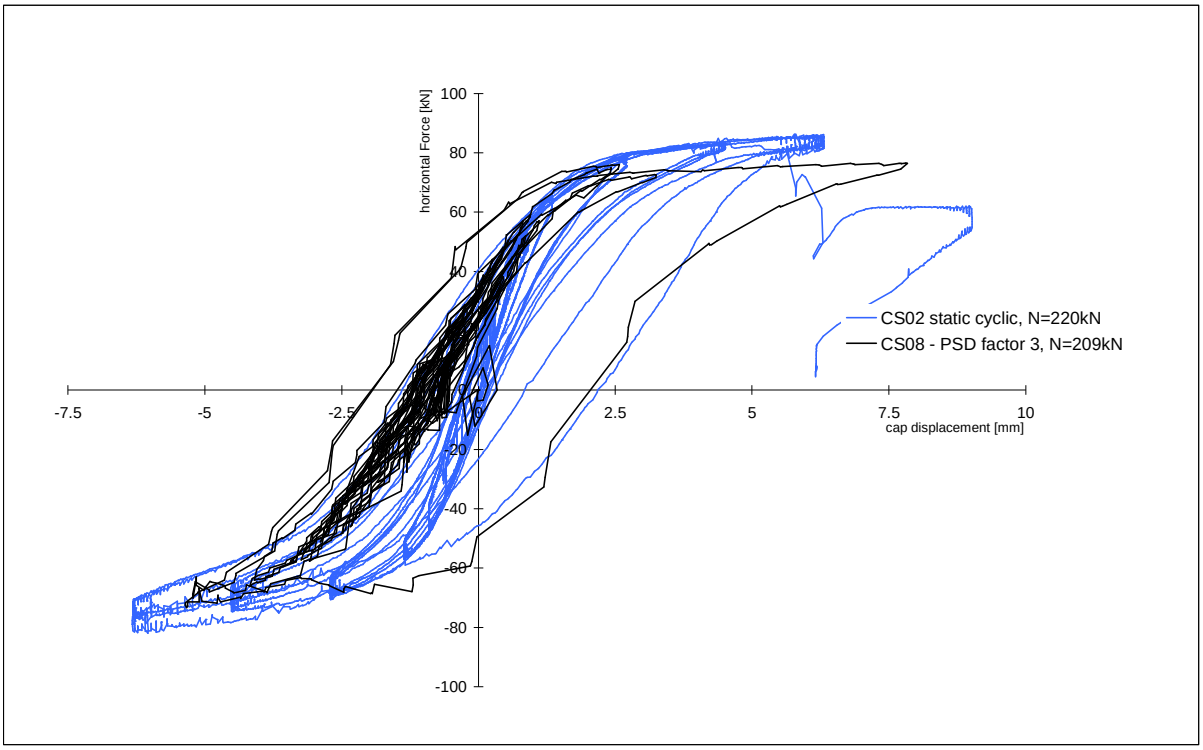

Figure 16: comparison of the hysteresis of wall CS08 (tested pseudo dynamic) and wall CS02 (tested static cyclic)

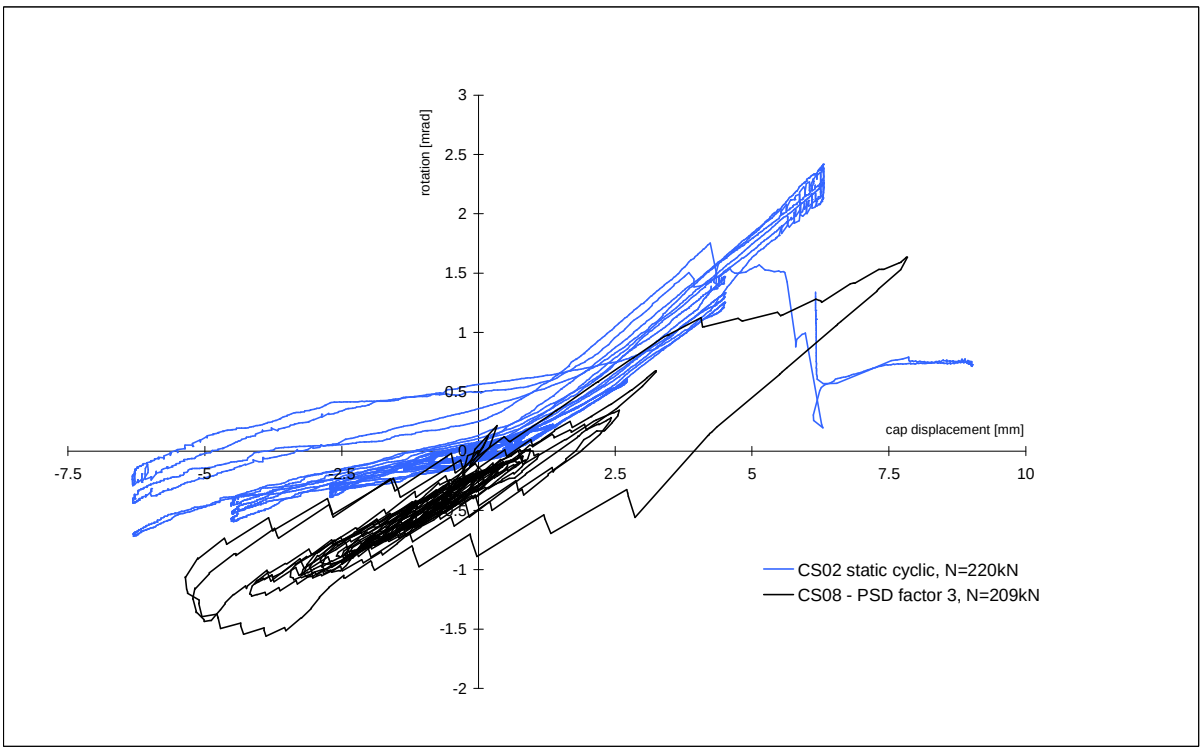

Figure 17: comparison of the rotation of wall CS08 (tested pseudo dynamic) and wall CS02 (tested static cyclic)

5. Summary

At the Technical University of Munich twelve pseudo dynamic tests on different full scale masonry walls were performed, to investigate the behaviour of masonry under seismic loading. The tested walls represent the main shear wall in the ground floor of a two storey resp. three storey height terraced house. The remaining structure has been modelled by the use of a commercial finite element program with nonlinear behaviour. The ground acceleration (artificial record), the loading and the geometry has been taken from the full scale pseudo dynamic test performed at the JRC in Ispra. The walls were tested with independent degrees of freedom for the horizontal displacement and the rotation at the top of the wall. The test setup was equal to the setup, which was used previous for the static cyclic test (Deliverable 7.1.b)
Each specimen was tested multiple times, which stepwise increased scaling factors. Totally, 24 tests with twelve specimens were carried out. Six wall specimens were built of calcium silicate units with different dimensions and material properties, two specimens was constructed with clay bricks and four specimens were built with lightweight aerated concrete bricks. Chapter 2 gives a detailed overview of the materials and the geometric dimensions of the specimen.
The results show, that the maximum horizontal forces and displacements are asymmetric, due to the asymmetric ground floor of the simulated building. Therefore also the calculated ductility depends on the moving direction of the specimen. In comparison to the static cyclic tests, the pseudo dynamic tests displayed an evident influence of the fixation of the wall through the slab. Further work will be dedicated to understand the complex failure mechanism of the masonry walls and to implement these knowledge into the numerical model for the building structure. Also the influence of the loading rate on the masonry walls has to be investigated.

6. References

[1] Anthoine, A.: Definition and design of the test specimen; Technical report of the collective research project ESECMaSE, deliverable D8.1, 2007

[2] Fehling, E.; Stürz, J.: Theoretical Investigation on Stress States of Masonry Structures Subjected to Static and Dynamic Shear Loads (Lateral Loads), Analysis of Terraced House; Technical report of the collective research project ESECMaSE, deliverable D3.1, 2005

[3] Fehling, E.; Stürz, J.; Schermer, D.: Theoretical Investigation on Shear Test Methods, Construction of test setup for shear tests for validation of proposed method; Technical report of the collective Research project ESECMaSE, 2006

[4] Fehling, E.; Stürz, J.; Schermer, D.: Theoretical Investigation on Shear Tests Methods, Series of shear test for validation; Technical report of the collective Research project ESECMaSE, 2006

[5] Grabowski, S.: Material properties for the tests in WP7 and 8 and the verification of the design model of WP4. Technical report of the collective Research project ESECMaSE, 2005

[6] Grabowski, S.: Tests on the relevant material properties on improved clay units; Technical report of the collective Research project ESECMaSE, 2006

[7] MARC. Version 2005r3. MSC.Software Corporation. Santa Ana: 2001.

[8] Ötes, A.; Löring, S.: Tastversuche zur Identifizierung des Verhaltensfaktors von Mauerwerksbauten für den Erdbebennachweis; Abschlussbericht; Universität Dortmund; Lehrstuhl für Tragwerkskonstruktionen; 2003

[9] Schermer, D.: Verhalten von unbewehrtem Mauerwerk unter Erdbebenbeanspruchung; Dissertation; TU München, Institut für Baustoffe und Konstruktion, Lehrstuhl für Massivbau; 2004

[10] Schermer, D.: Theoretical Investigation on Stress States of Masonry Structures Subjected to Static and Dynamic Shear Loads (Lateral Loads); Analysis of Apartment House; Technical report of the collective Research project ESECMaSE, 2005

[11] Thiele, K.: Pseudodynamische Versuche an Tragwerken mit großen Steifigkeitsänderungen und mehreren Freiheitsgraden; Dissertation; Zürich; 2000

[12] Carydis, P.: Test results on the earthquake resistance on improved masonry materials by shaking table tests; Technical report of the collective research project ESECMaSE, deliverable D7.2c, 2008

[13] Zilch, K.; Finckh, W.; Grabowski, S.; Schermer, D.; Scheufler, W.: Test results on the behaviour of masonry under static (monotonic and cyclic) in plane lateral loads; Technical report of the collective research project ESECMaSE, deliverable D7.1b, 2008

7. ANNEX

7.1. CS08

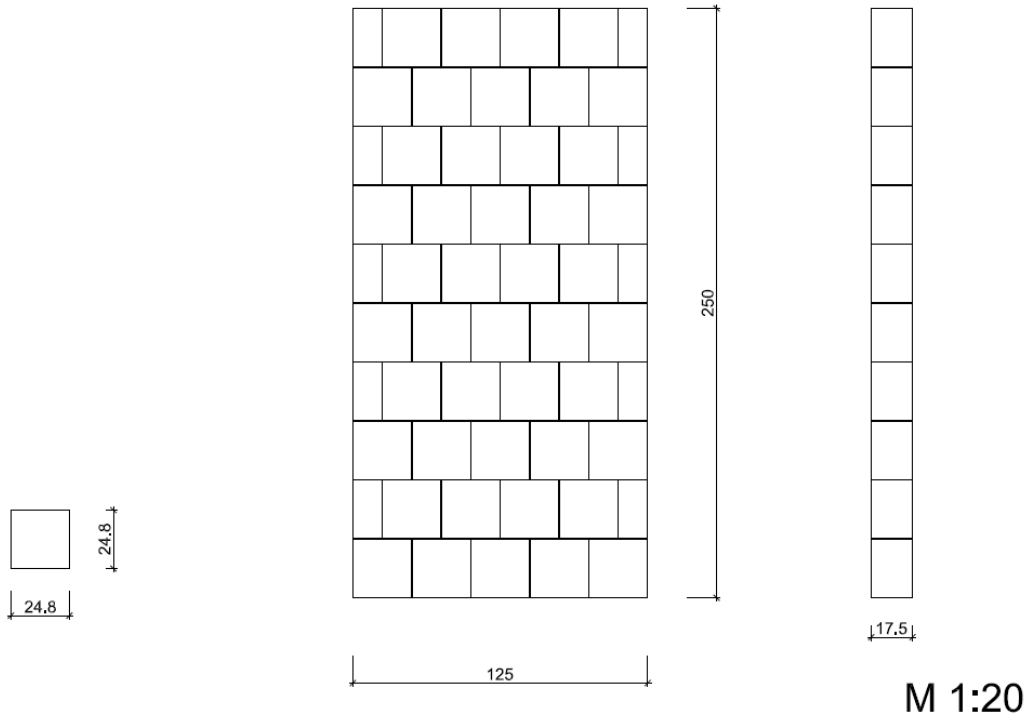

Figure 18: Dimension of the test specimen CS08

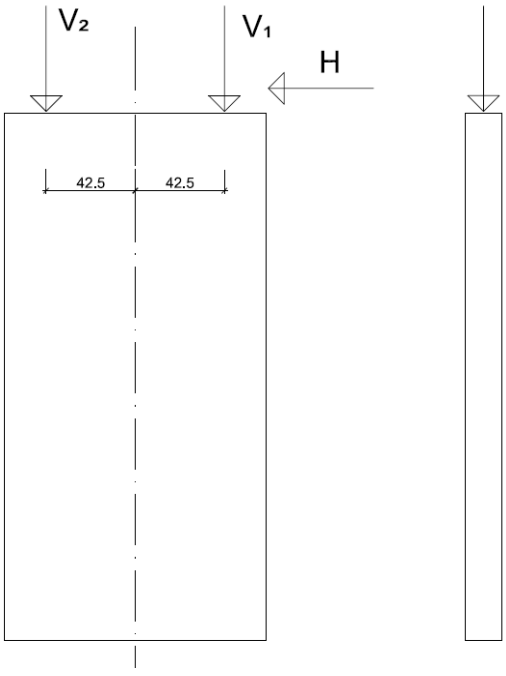

Figure 19: Position of the hydraulic actuators at test specimen CS08

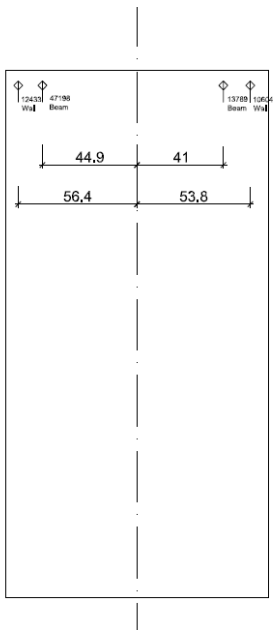

Figure 20: Position of the LVDTs at test specimen CS08

7.1.1. Scale factor 2 (max 0,12g)

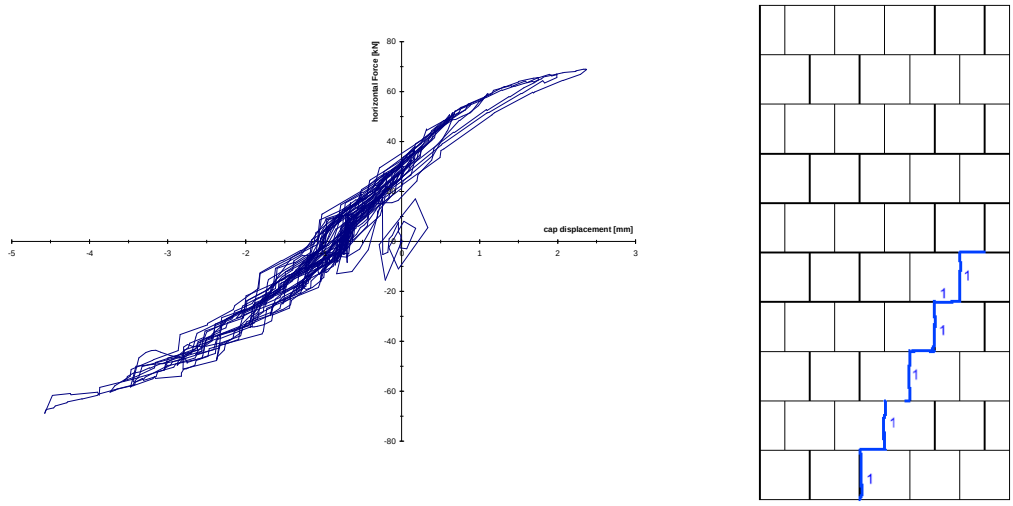

Figure 21: Load-displacement curve (hysteresis) and crack pattern of the test specimen CS08

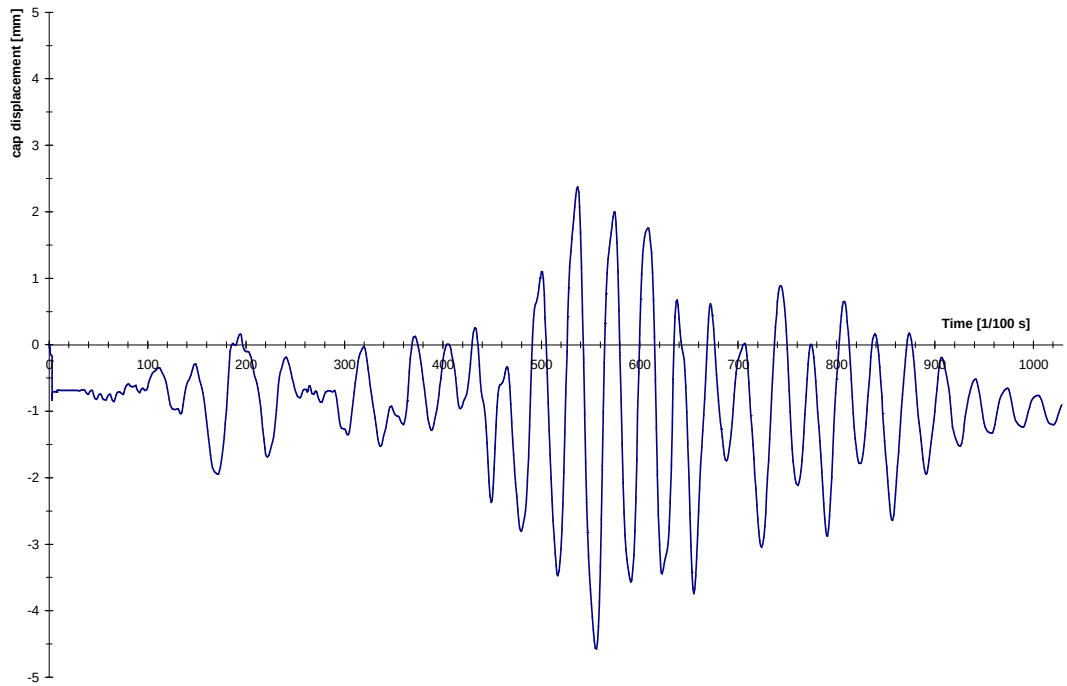

Figure 22: displacement history (earthquake time) CS08

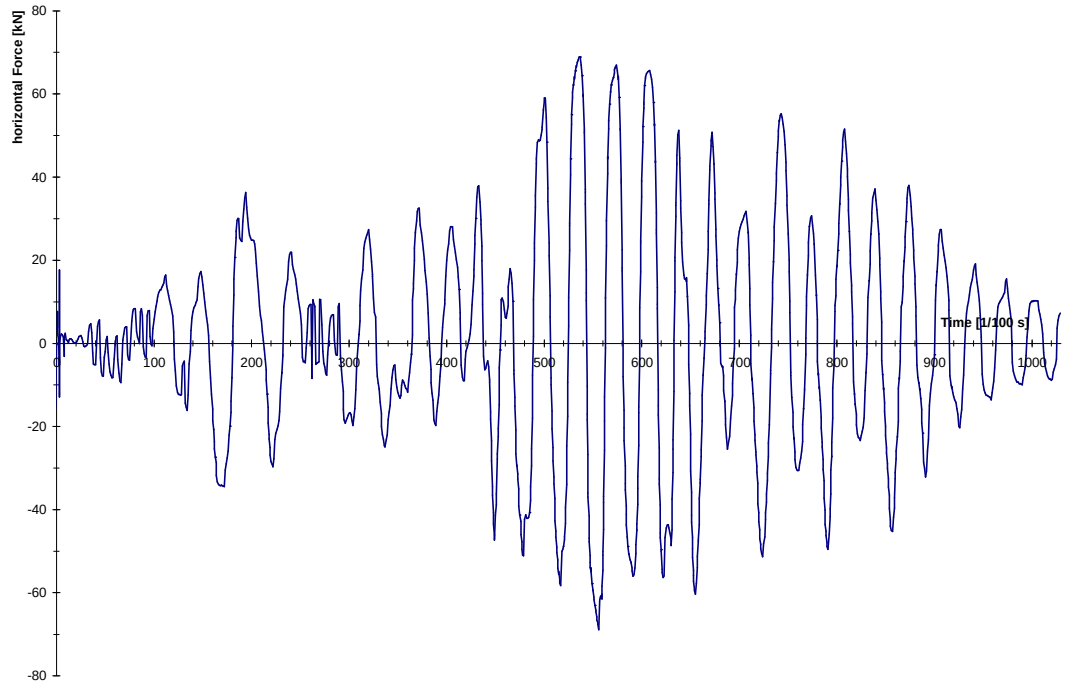

Figure 23: horizontal load history (earthquake time) CS08

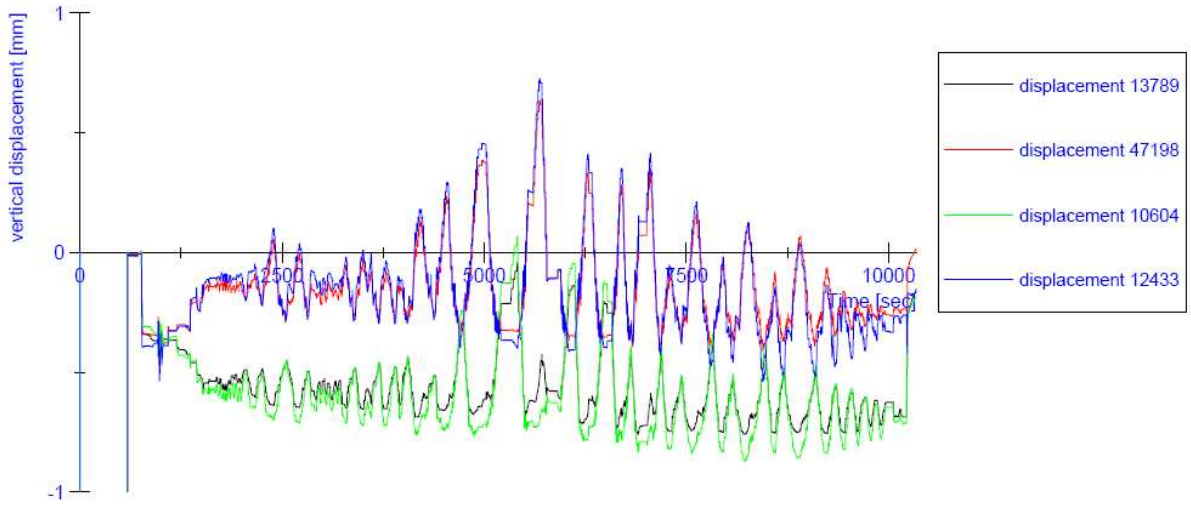

Figure 24: Progress of the vertical displacements (testing time) CS08

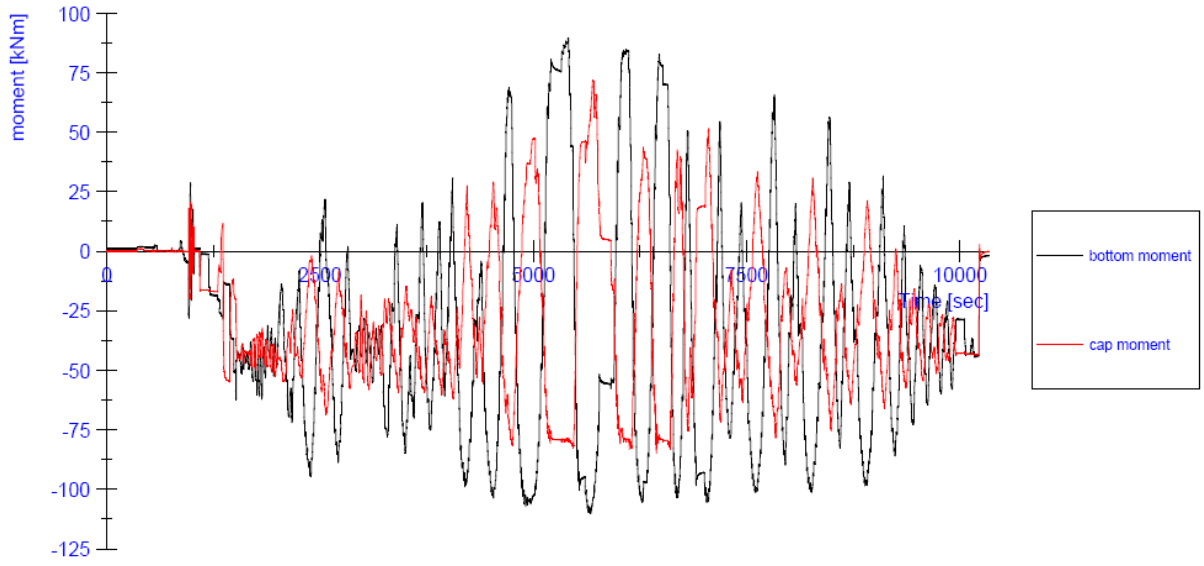

Figure 25: Progress of the in-plane bending moments at the top and at the bottom of the wall (testing time) CS08

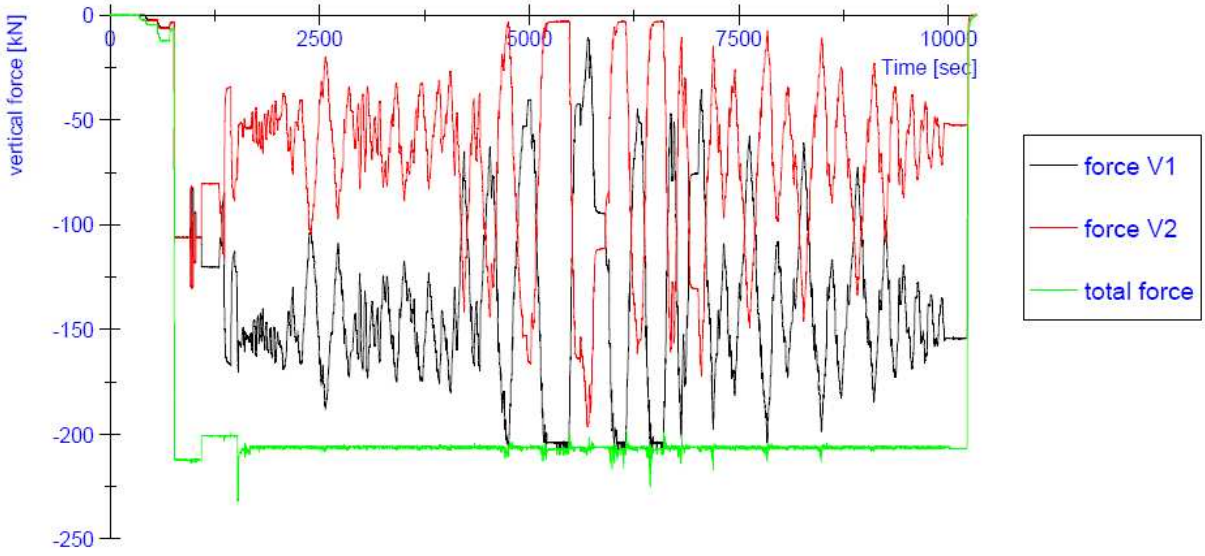

Figure 26: Progress of the vertical forces V1 and V2 (testing time) CS08

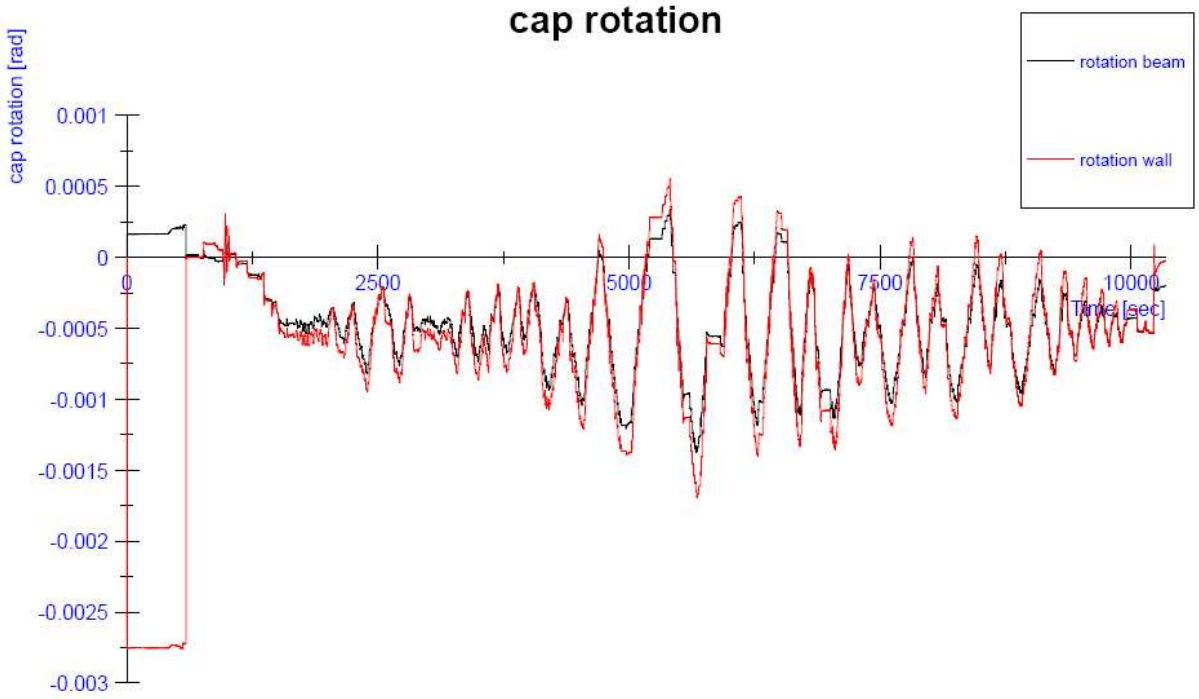

Figure 27: Progress of the in-plane rotation at the top of the wall (testing time) CS08

7.1.2. Scale factor 3 (max 0,17g)

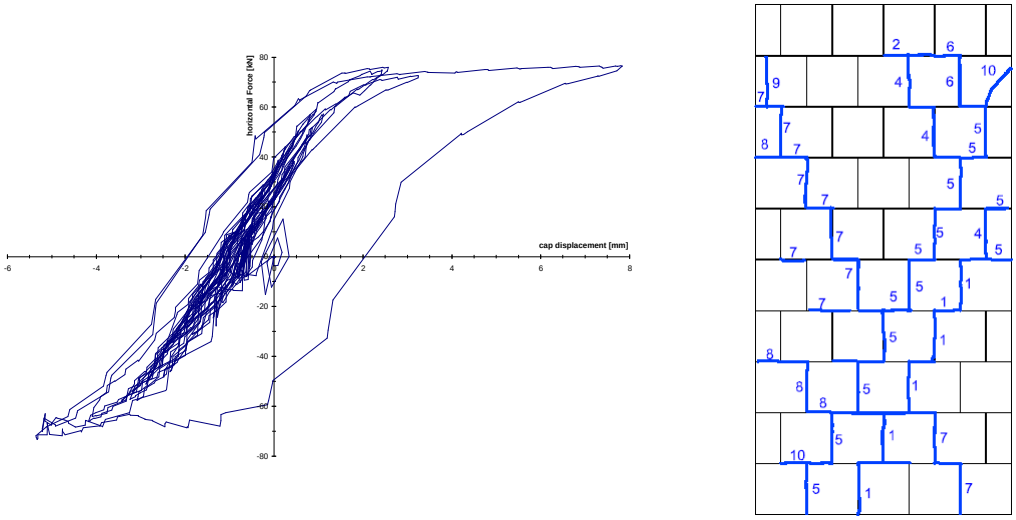

Figure 28: Load-displacement curve (hysteresis) and crack pattern of the test specimen CS08

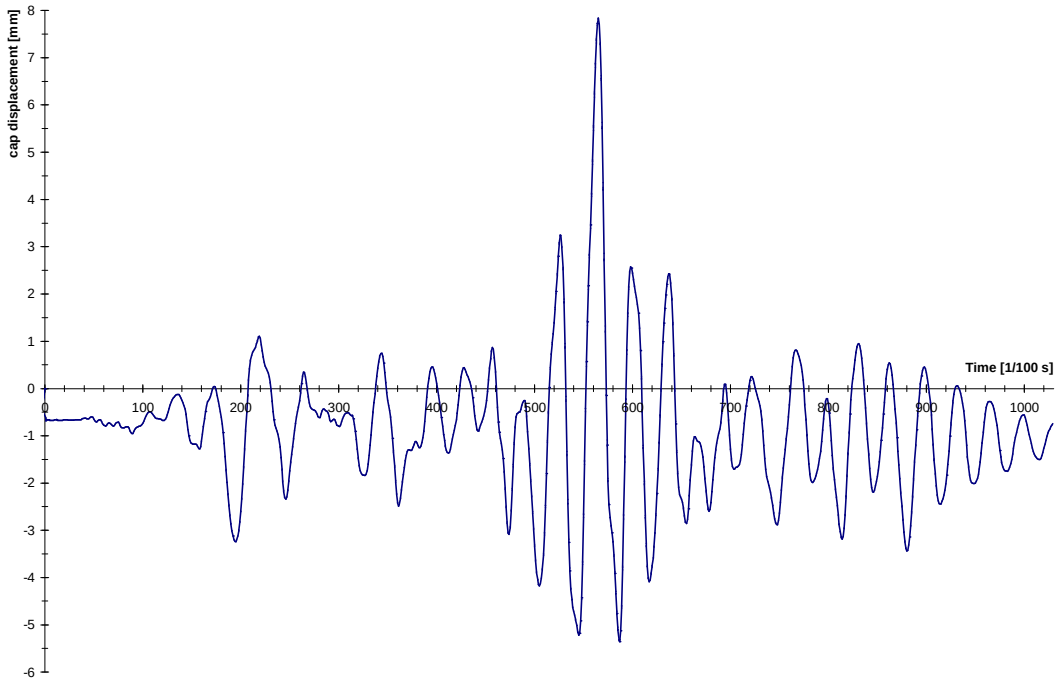

Figure 29: displacement history (earthquake time) CS08

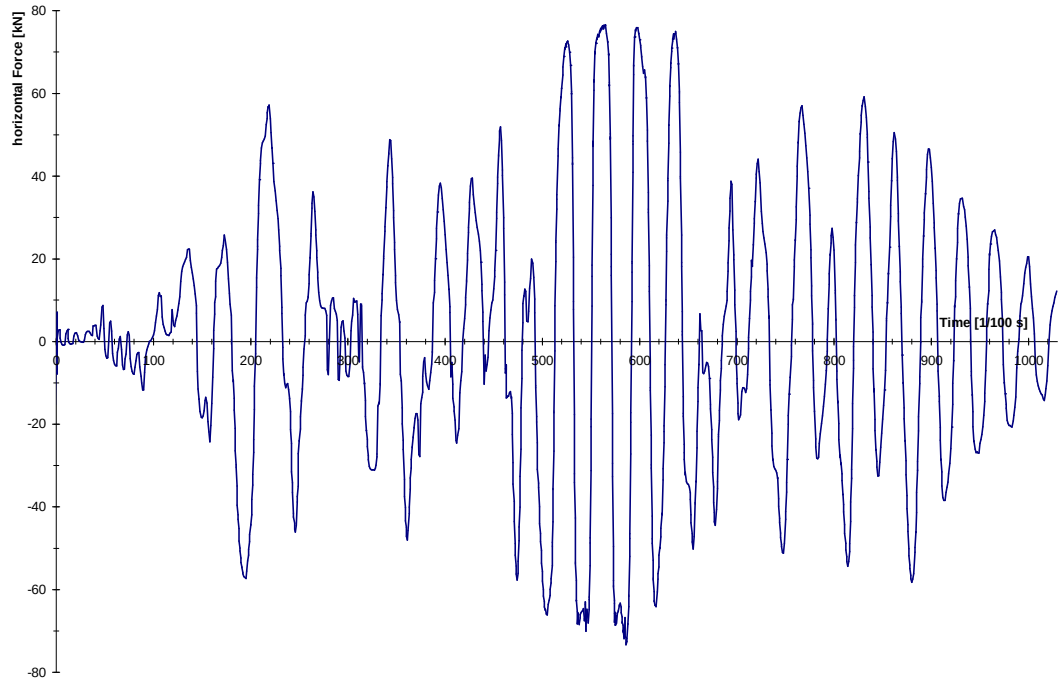

Figure 30: horizontal load history (earthquake time) CS08

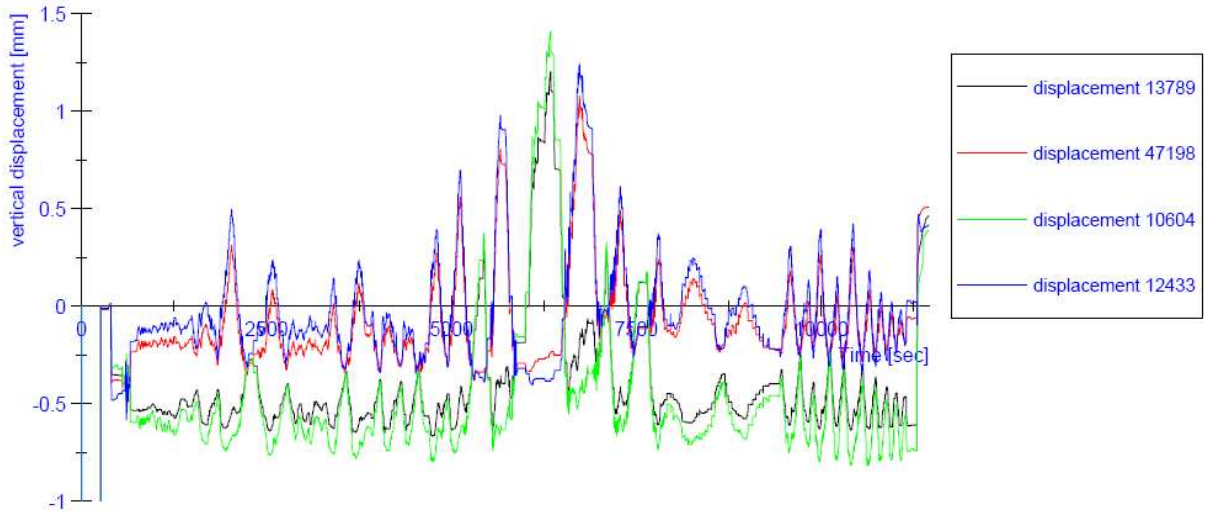

Figure 31: Progress of the vertical displacements (testing time) CS08

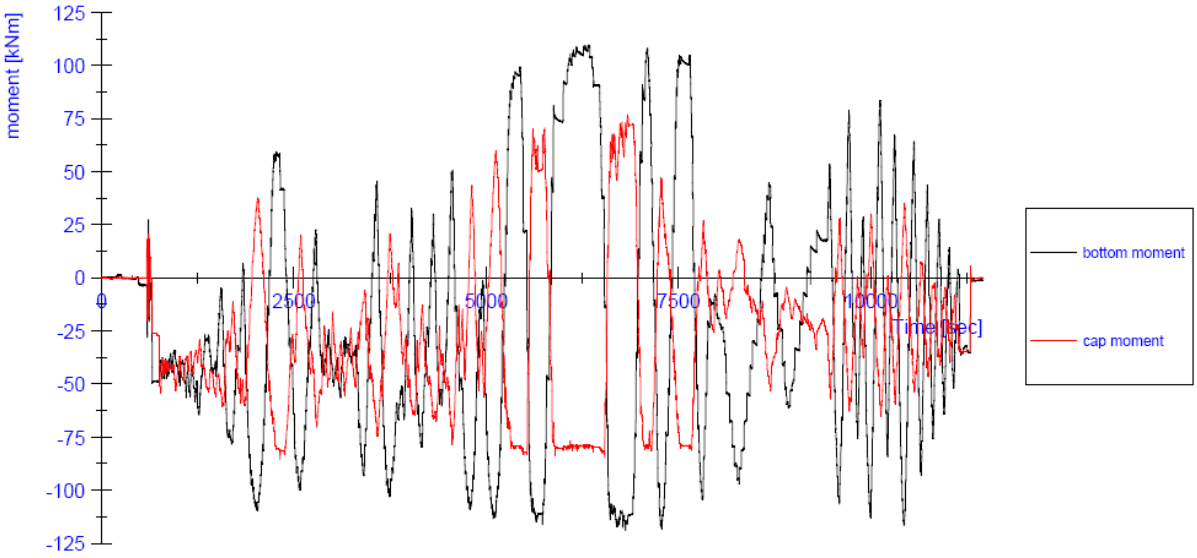

Figure 32: Progress of the in-plane bending moments at the top and at the bottom of the wall (testing time) CS08

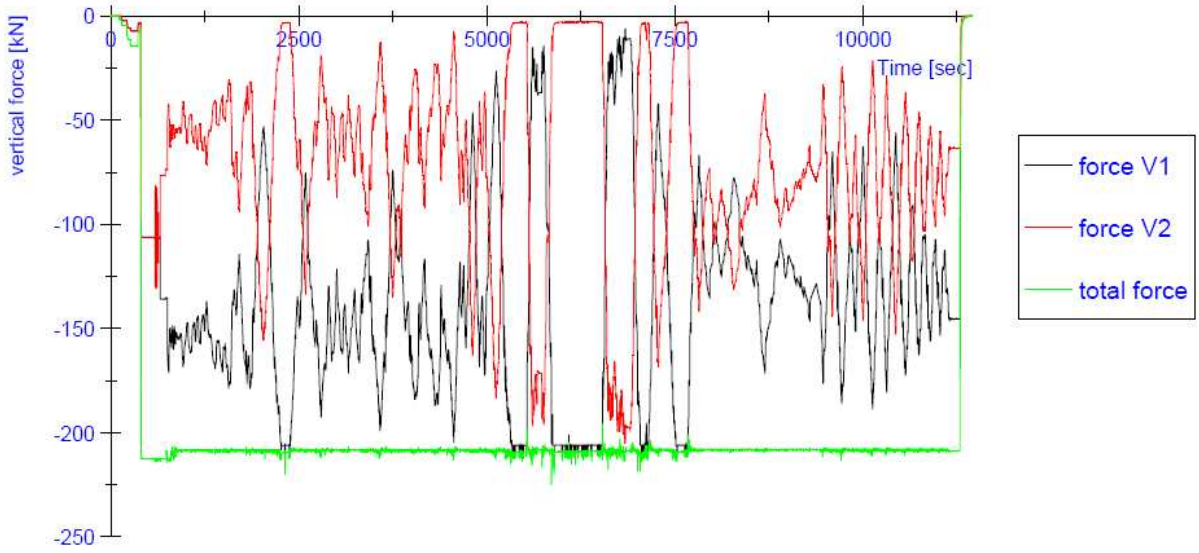

Figure 33: Progress of the vertical forces V1 and V2 (testing time) CS08

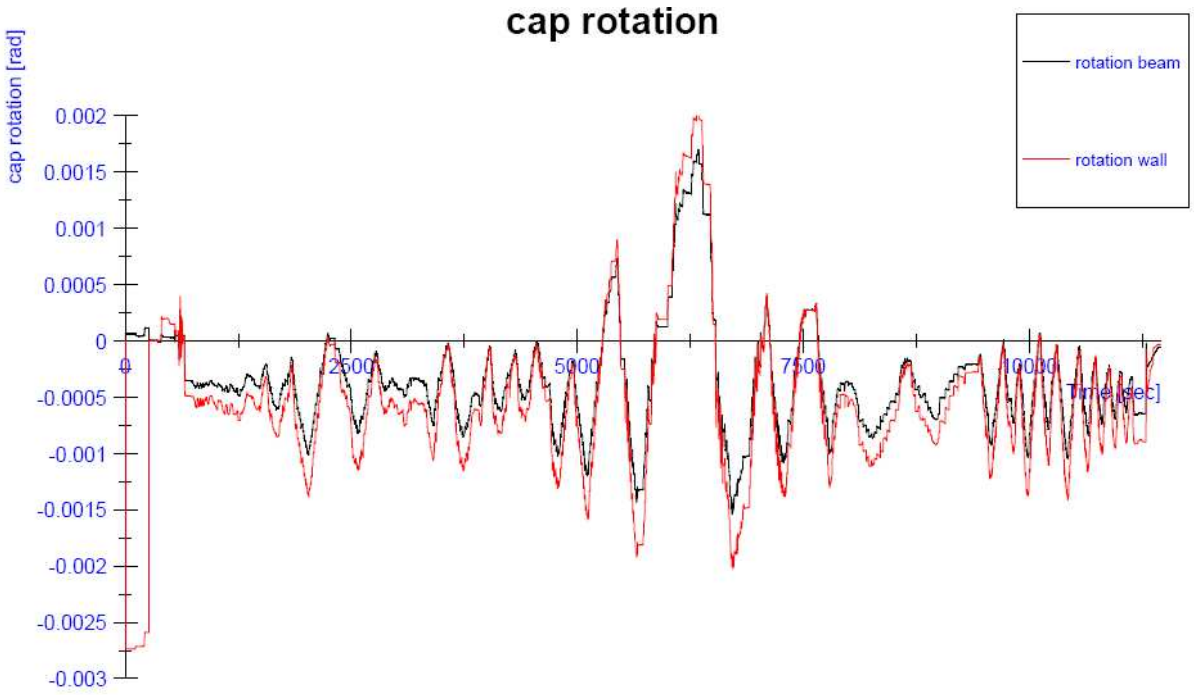

Figure 34: Progress of the in-plane rotation at the top of the wall (testing time) CS08

Figure 35: Crack pattern CS08

7.2. CS09

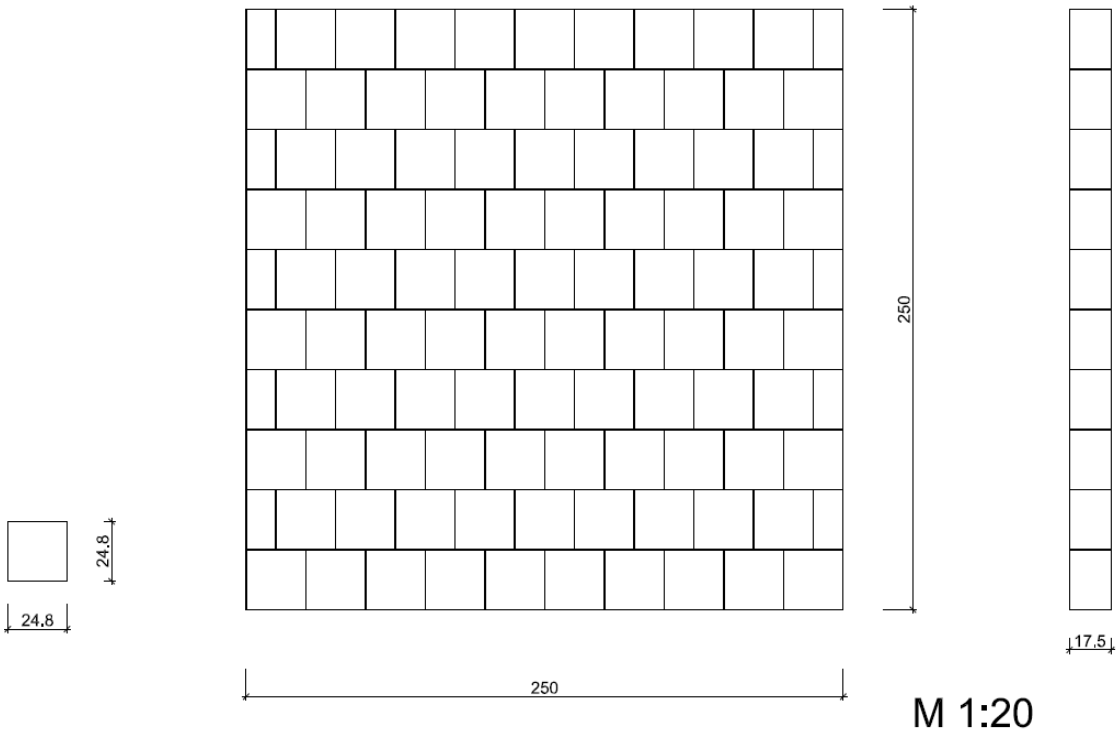

Figure 36: Dimension of the test specimen CS09

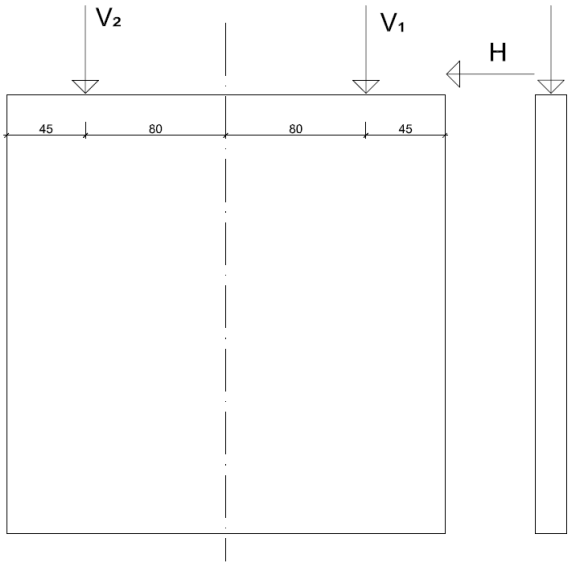

Figure 37: Position of the hydraulic actuators at test specimen CS09

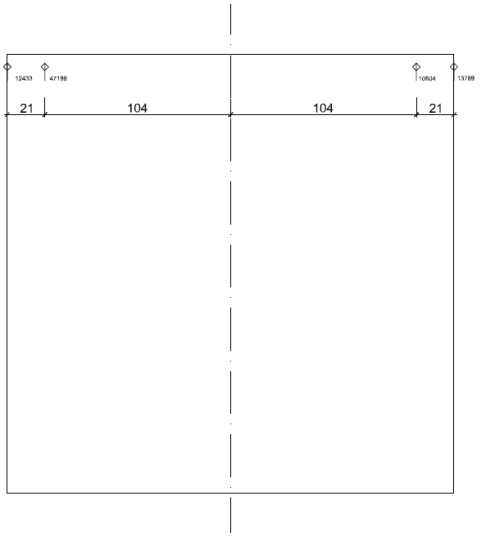

Figure 38: Position of the LVDTs at test specimen CS09

7.2.1. Scale factor 1 (max 0.06 g)

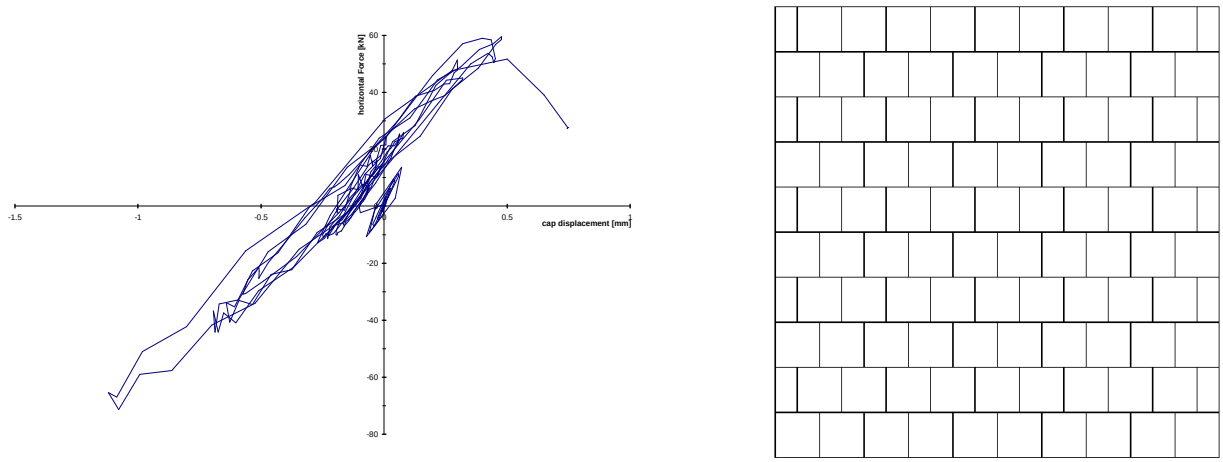

Figure 39: Load-displacement curve (hysteresis) and crack pattern of the test specimen CS09

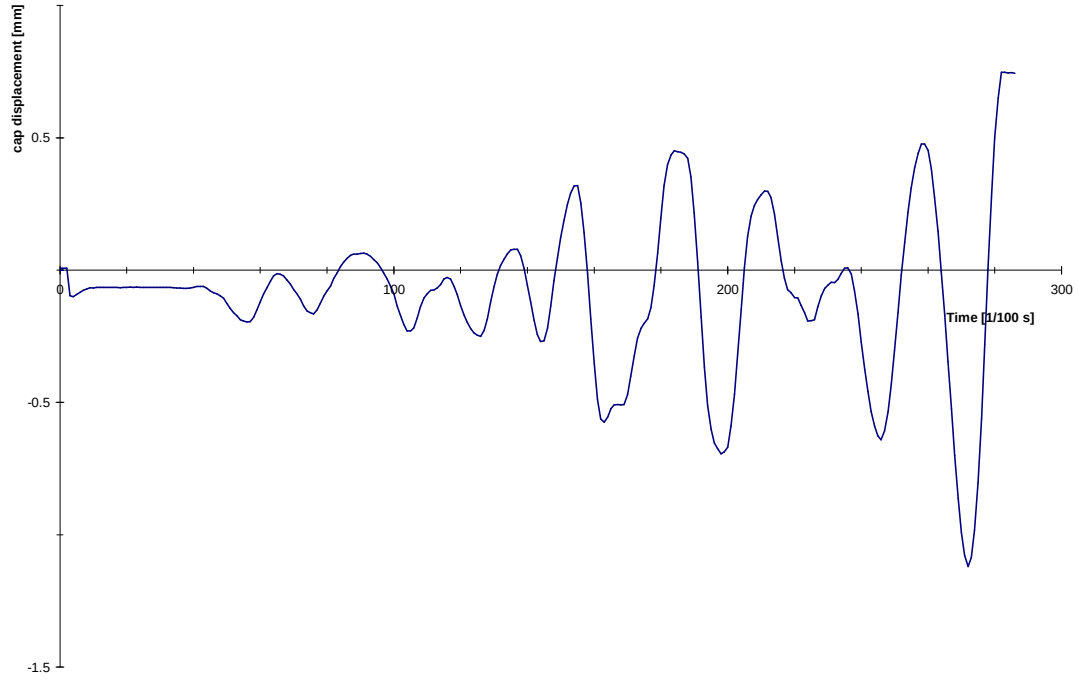

Figure 40: displacement history (earthquake time) CS09

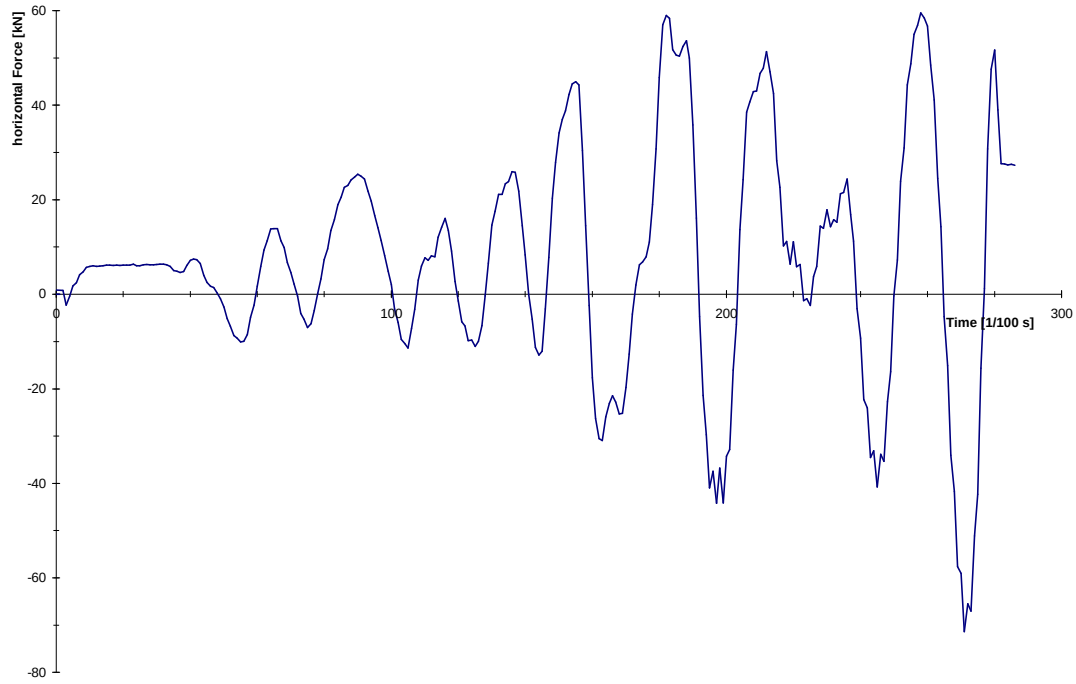

Figure 41: horizontal load history (earthquake time) CS09

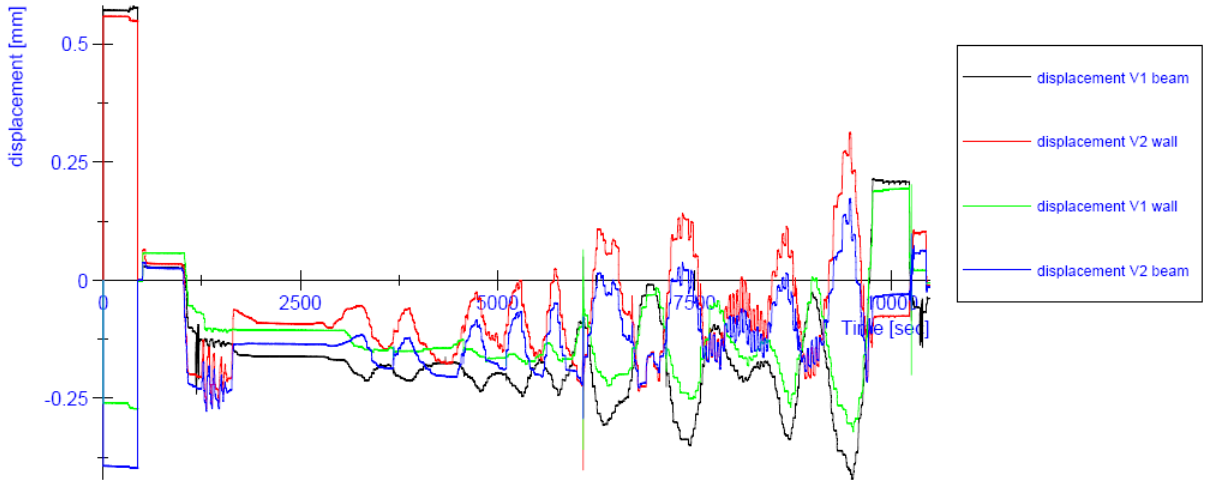

Figure 42: Progress of the vertical displacements (testing time) CS09

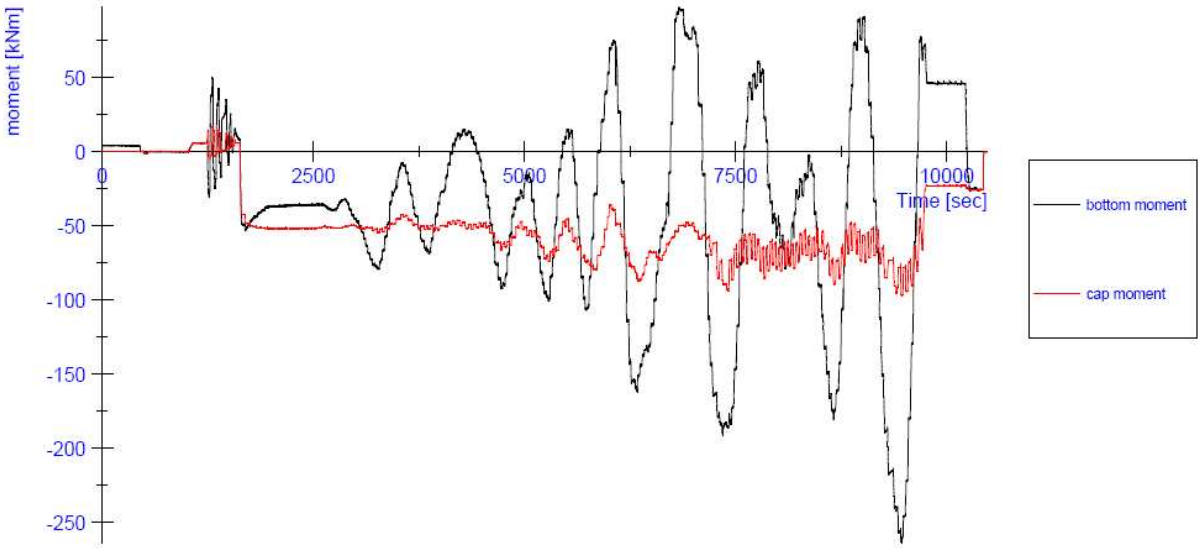

Figure 43: Progress of the in-plane bending moments at the top and at the bottom of the wall (testing time) CS09

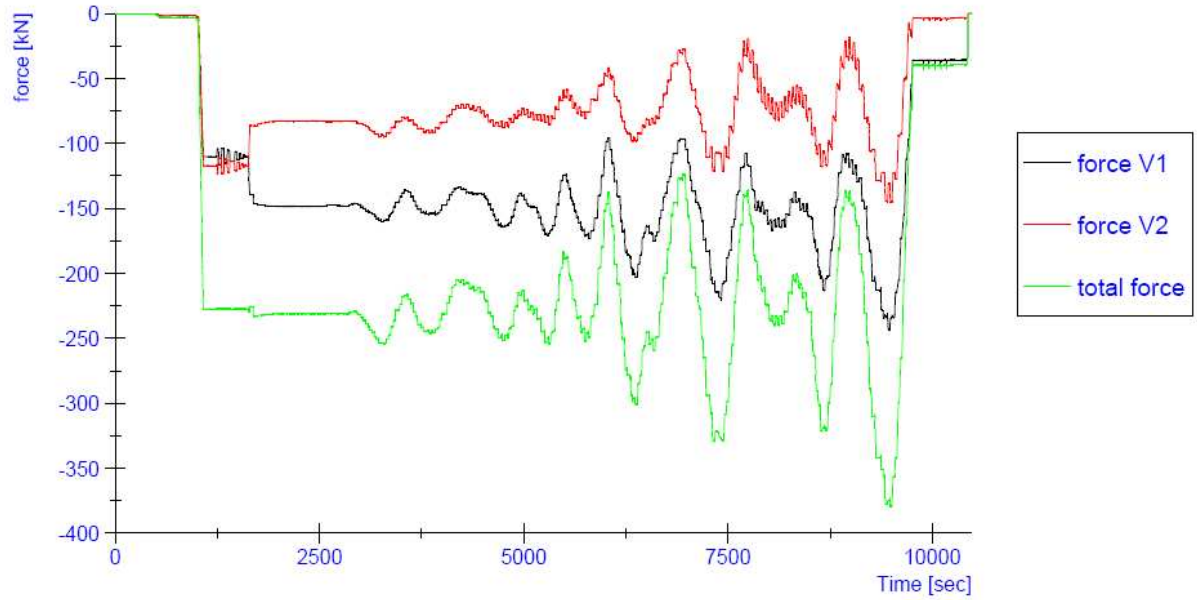

Figure 44: Progress of the vertical forces V1 and V2 (testing time) CS09

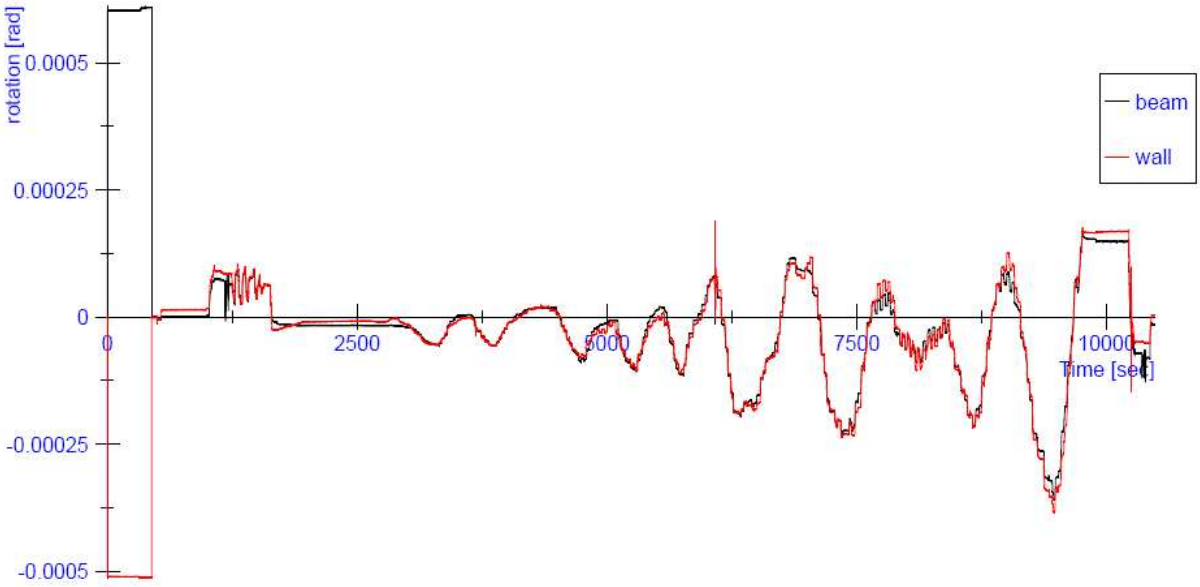

Figure 45: Progress of the in-plane rotation at the top of the wall (testing time) CS09

7.2.2. Scale factor 2.5 (max 0.14 g)

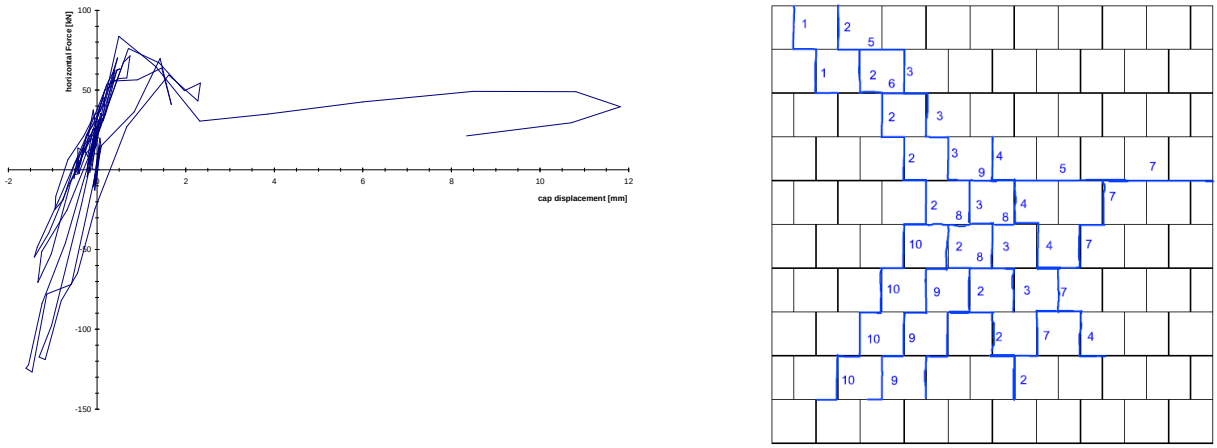

Figure 46: Load-displacement curve (hysteresis) and crack pattern of the test specimen CS09

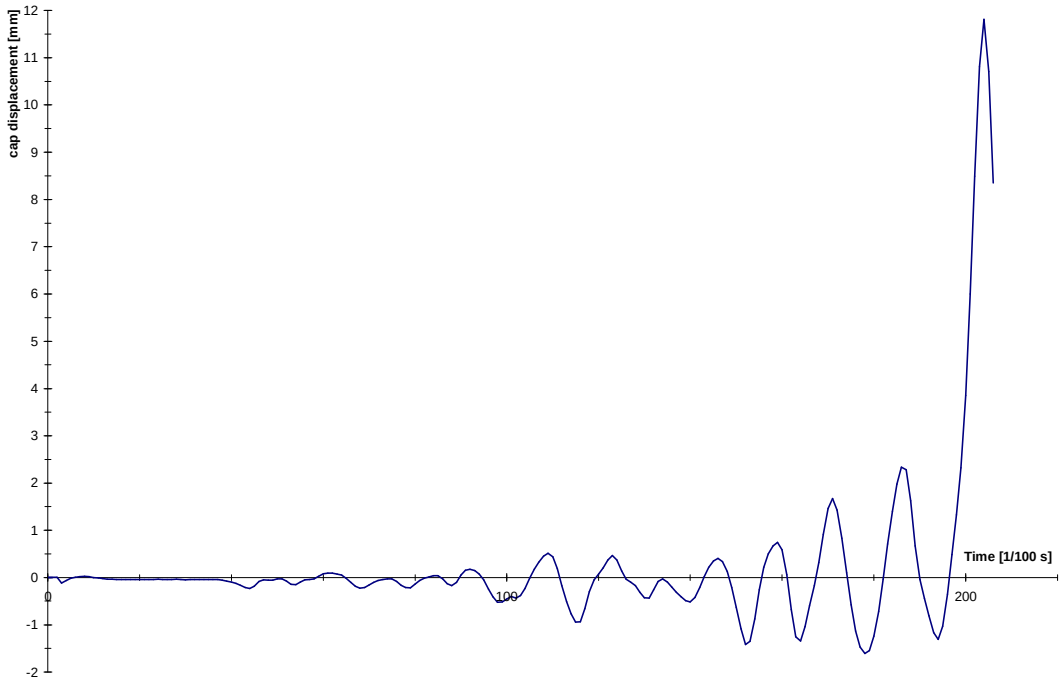

Figure 47: displacement history (earthquake time) CS09

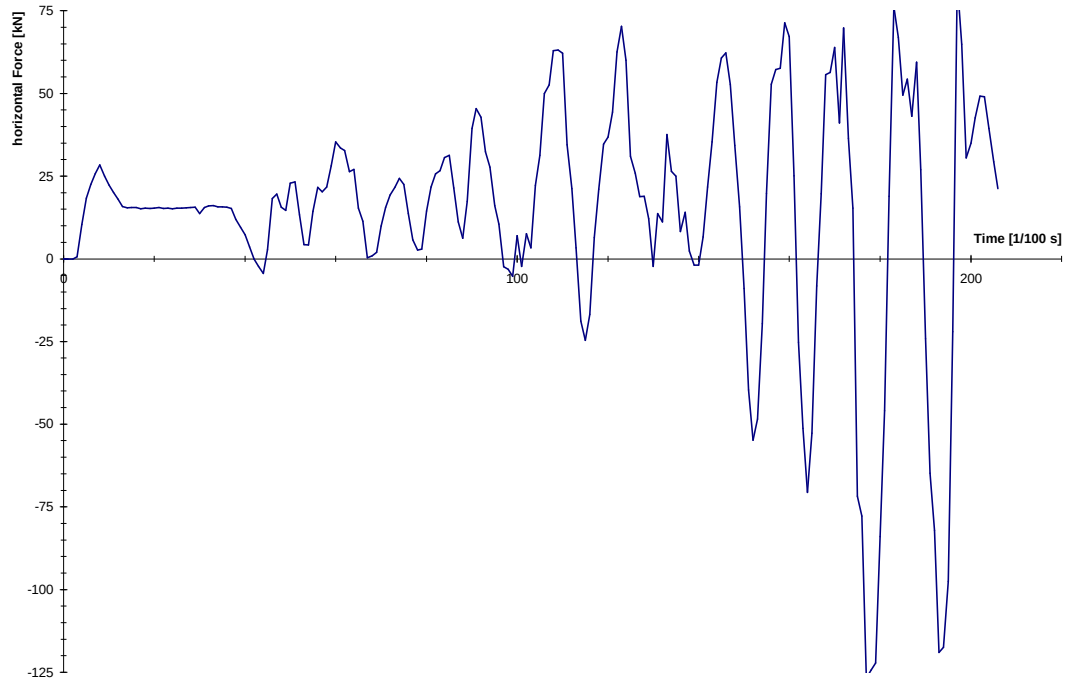

Figure 48: horizontal load history (earthquake time) CS09

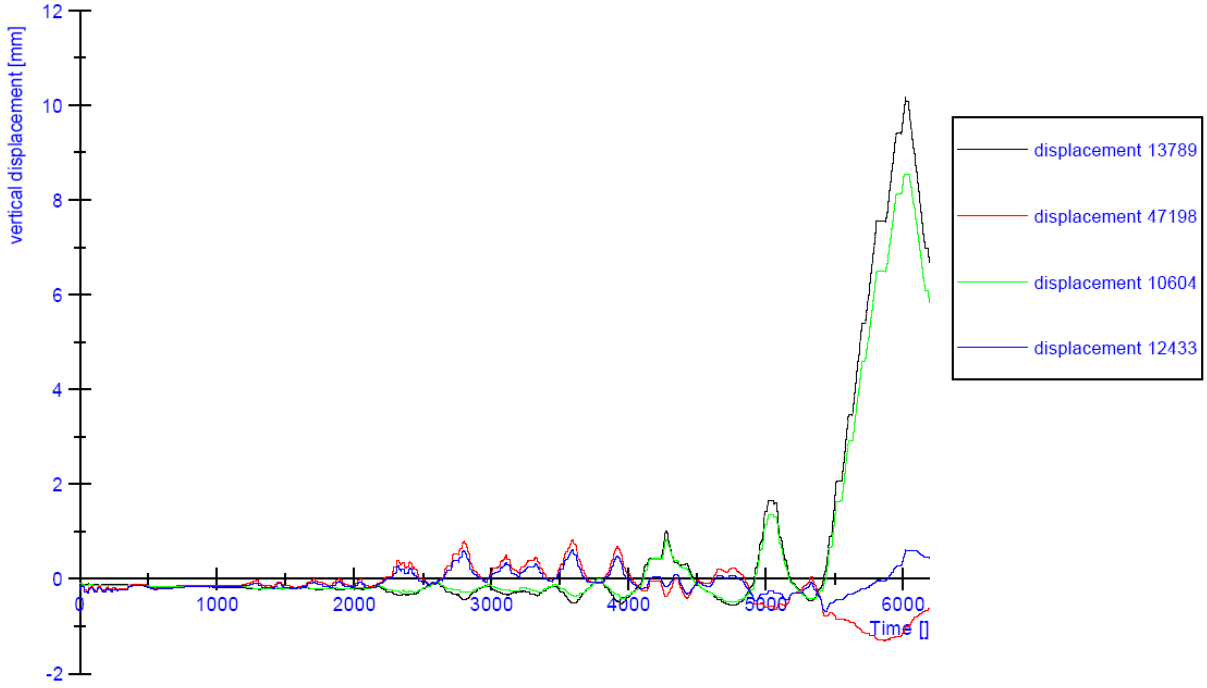

Figure 49: Progress of the vertical displacements (testing time) CS09

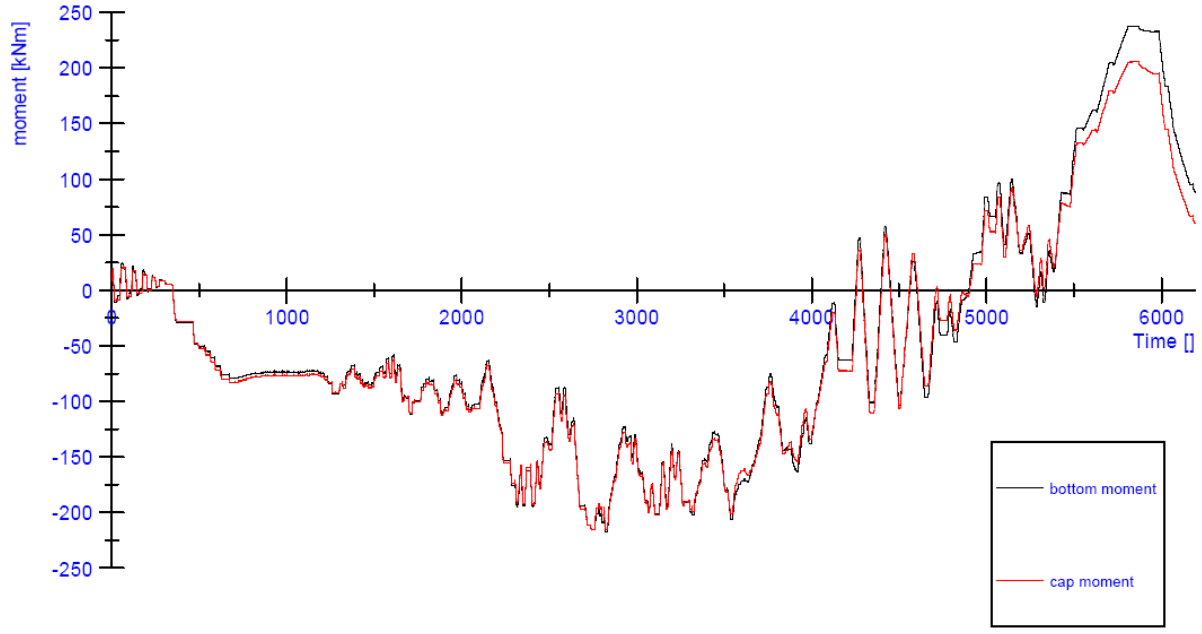

Figure 50: Progress of the in-plane bending moments at the top and at the bottom of the wall (testing time) CS09

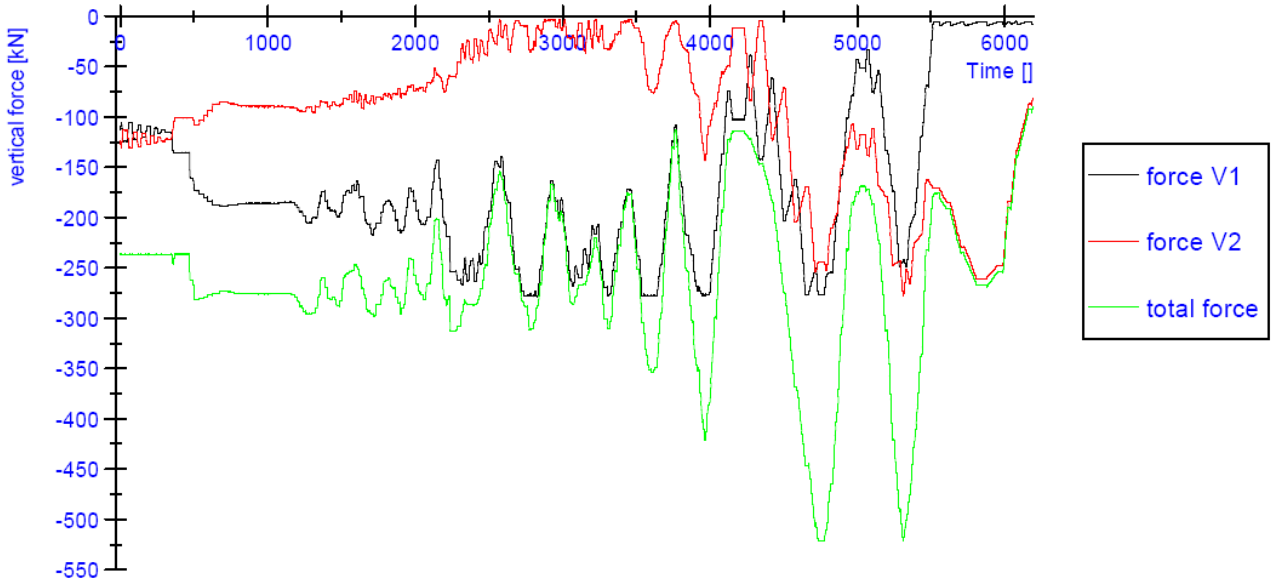

Figure 51: Progress of the vertical forces V1 and V2 (testing time) CS09

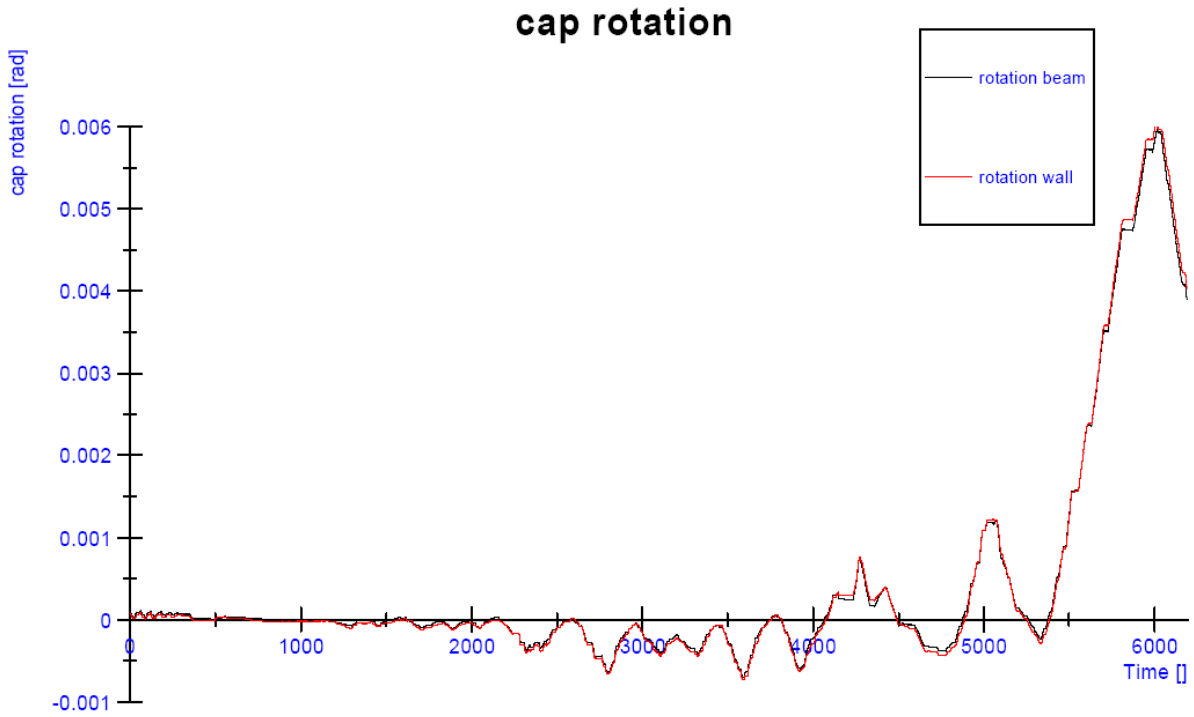

Figure 52: Progress of the in-plane rotation at the top of the wall (testing time) CS09

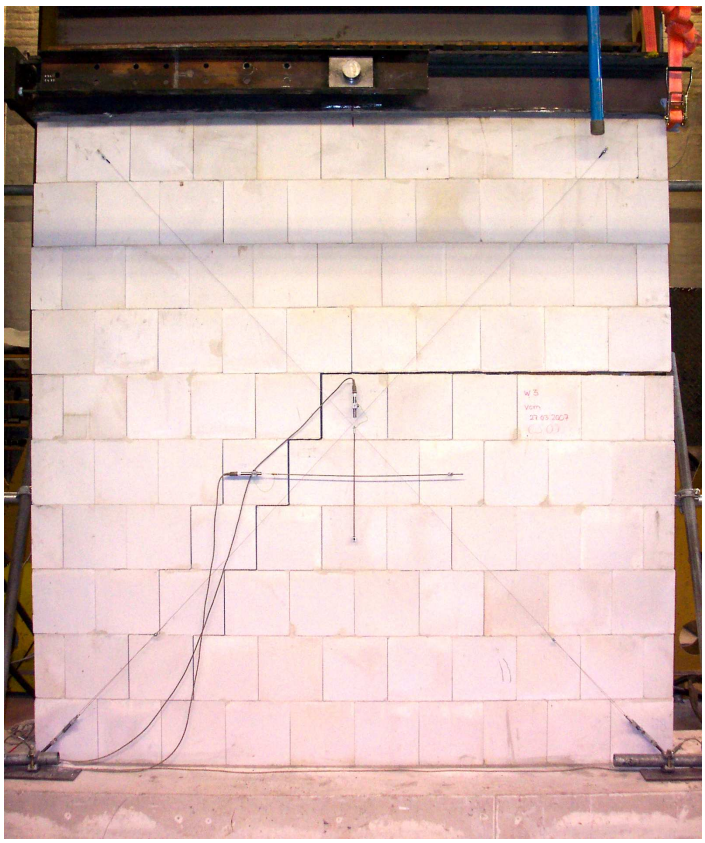

Figure 53: Crack pattern CS09

7.3. CS12

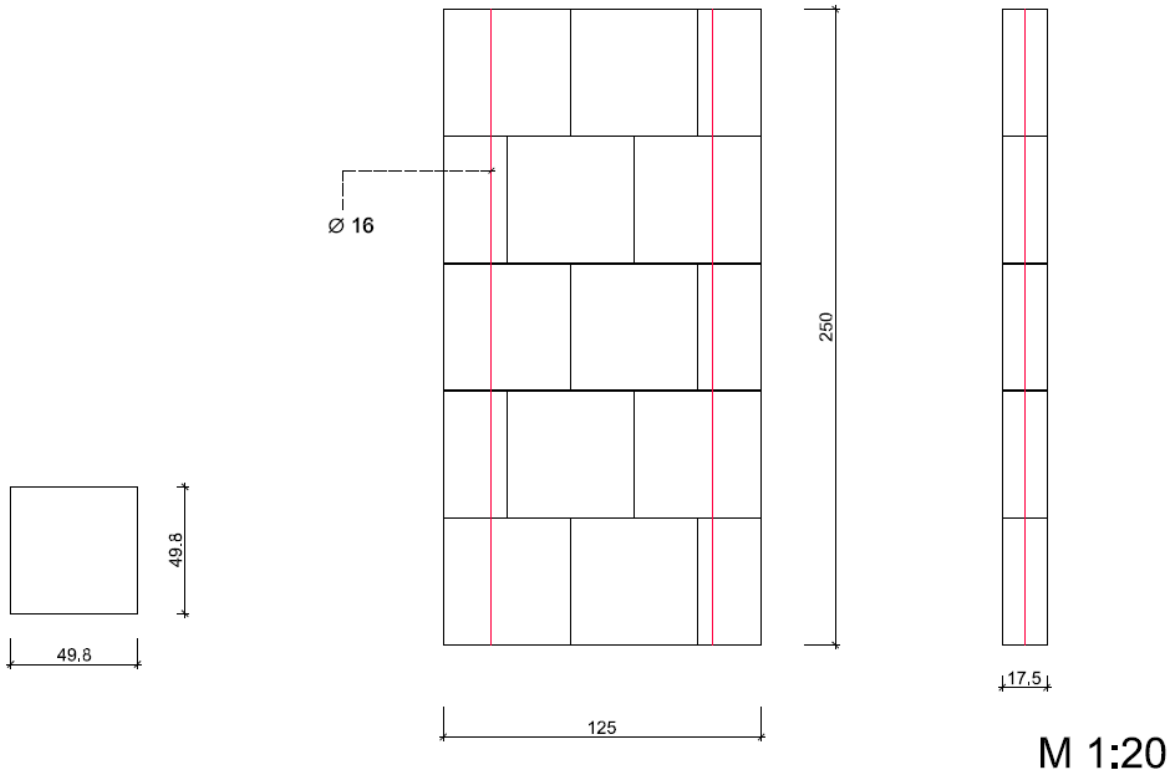

Figure 54: Dimension of the test specimen CS12

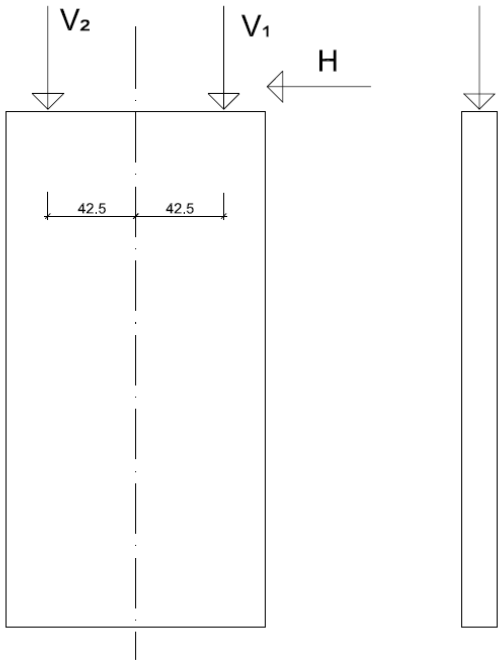

Figure 55: Position of the hydraulic actuators at test specimen CS12

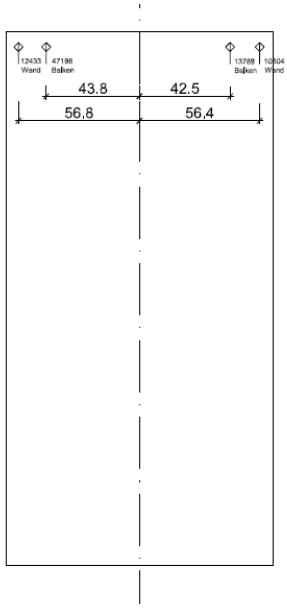

Figure 56: Position of the LVDTs at test specimen CS12

7.3.1. Scale factor 2 (max 0.12 g)

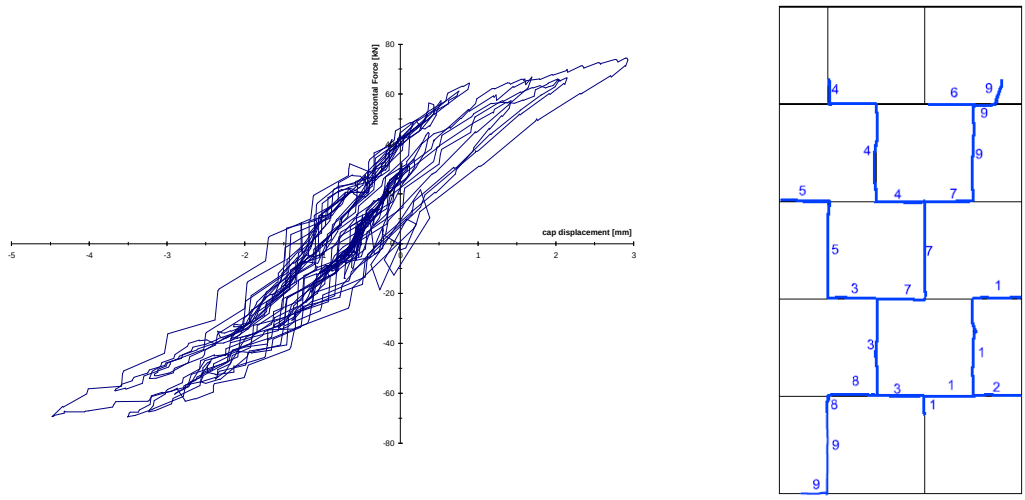

Figure 57: Load-displacement curve (hysteresis) and crack pattern of the test specimen CS12

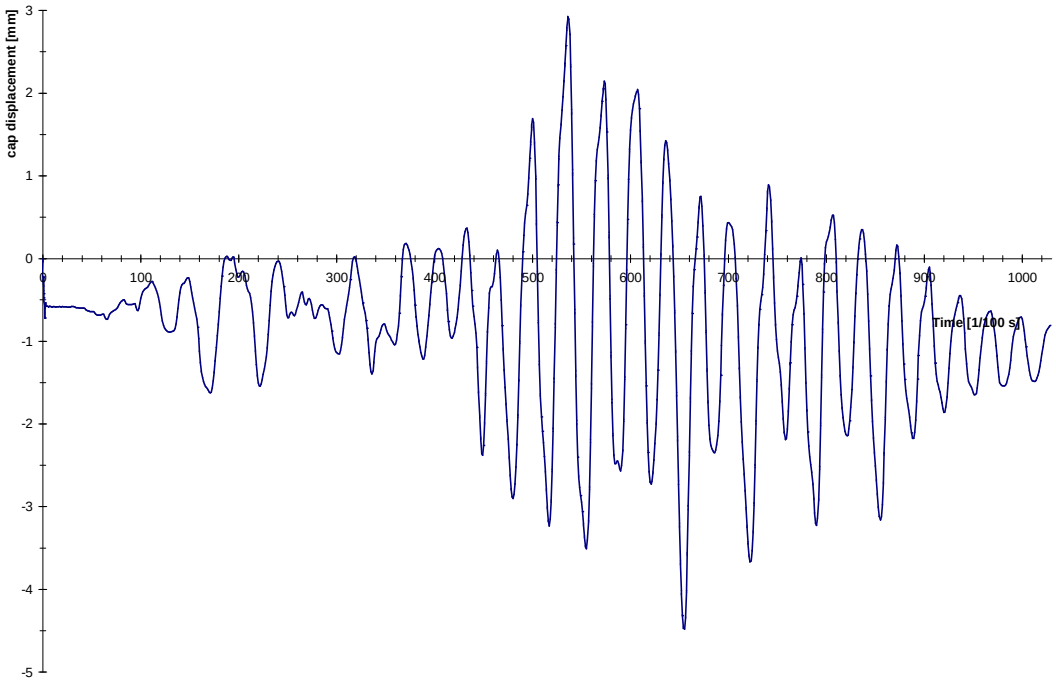

Figure 58: displacement history (earthquake time) CS12

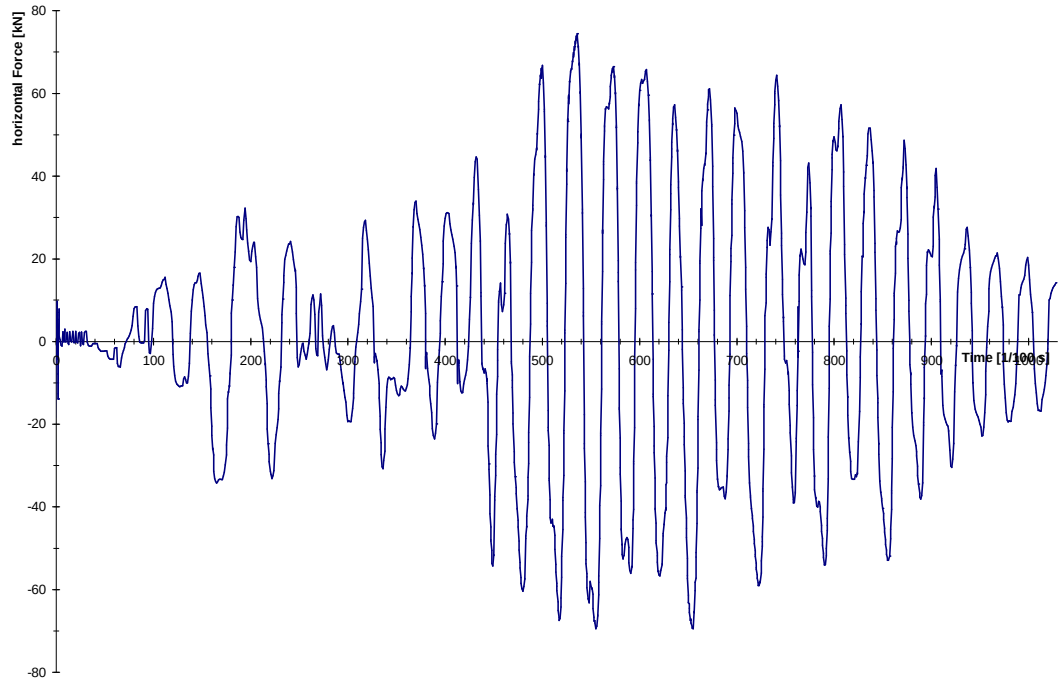

Figure 59: horizontal load history (earthquake time) CS12

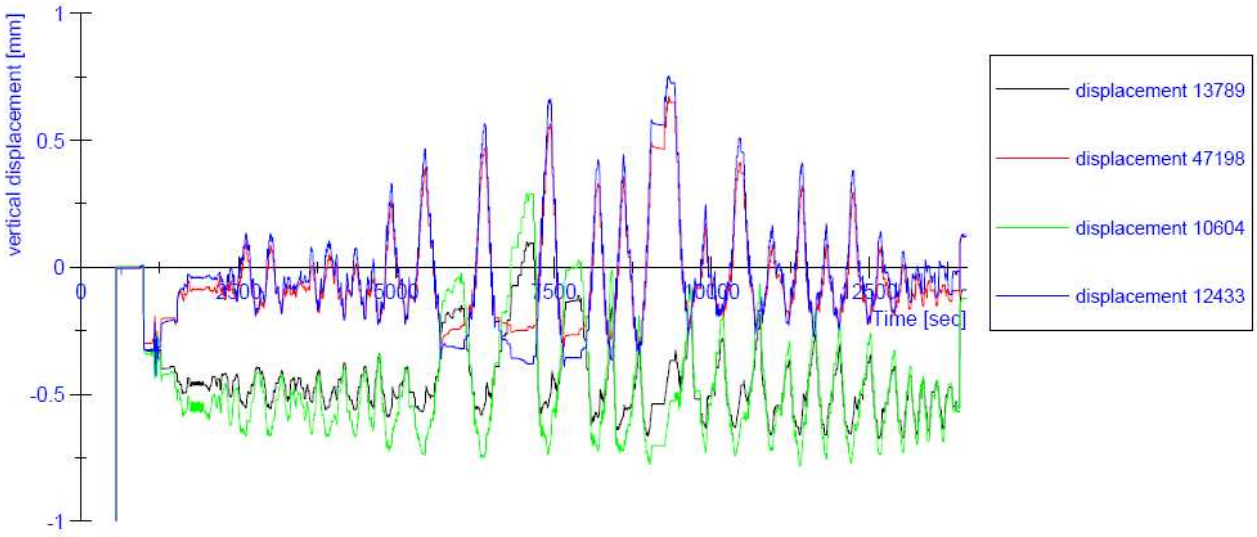

Figure 60: Progress of the vertical displacements (testing time) CS12

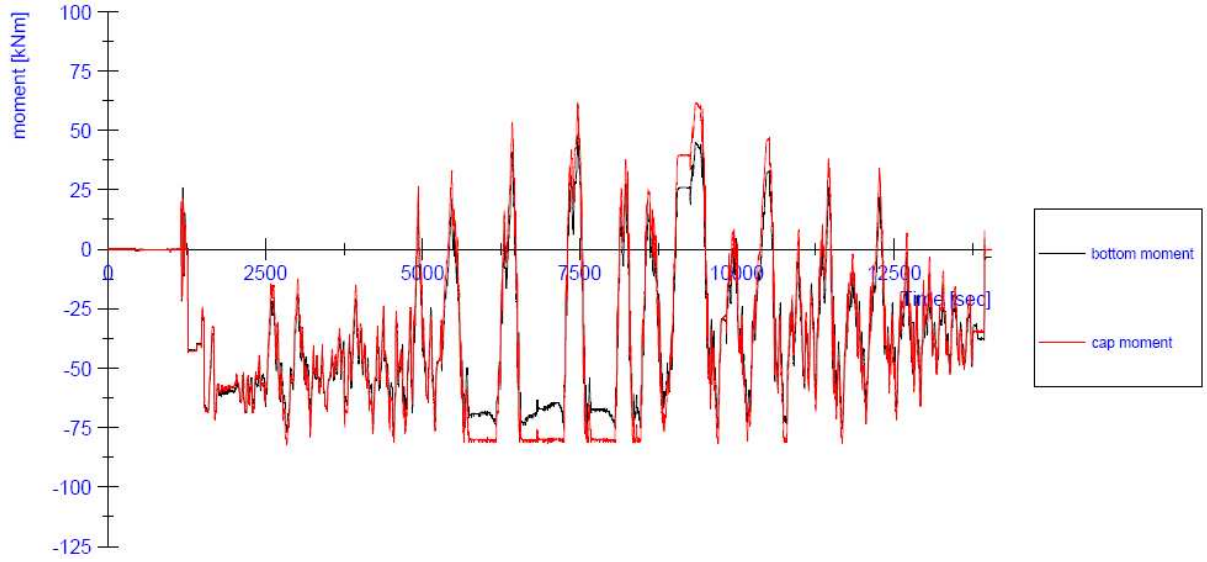

Figure 61: Progress of the in-plane bending moments at the top and at the bottom of the wall (testing time) CS12

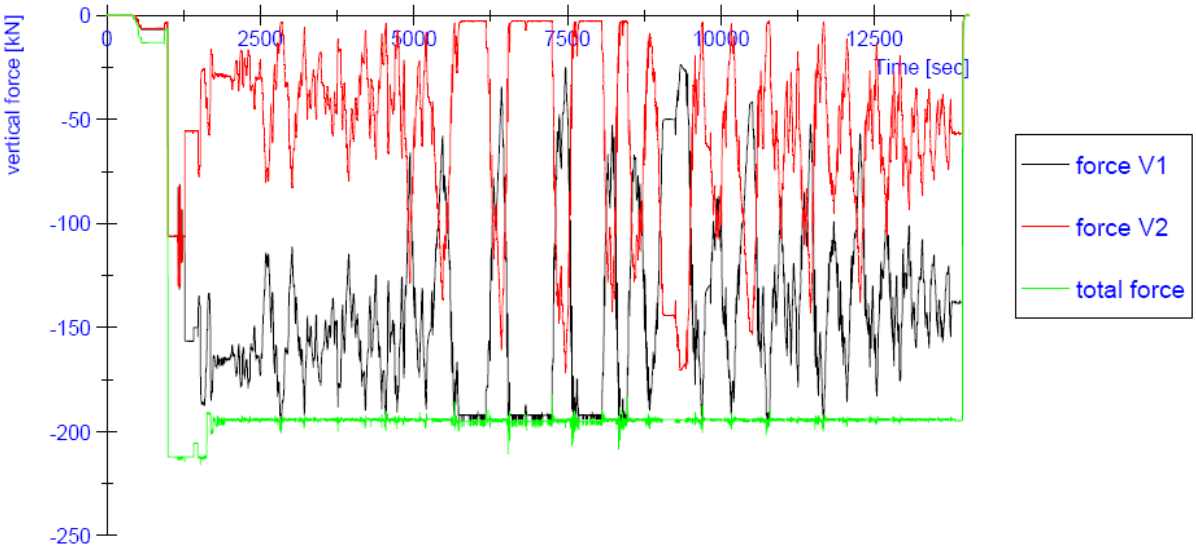

Figure 62: Progress of the vertical forces V1 and V2 (testing time) CS12

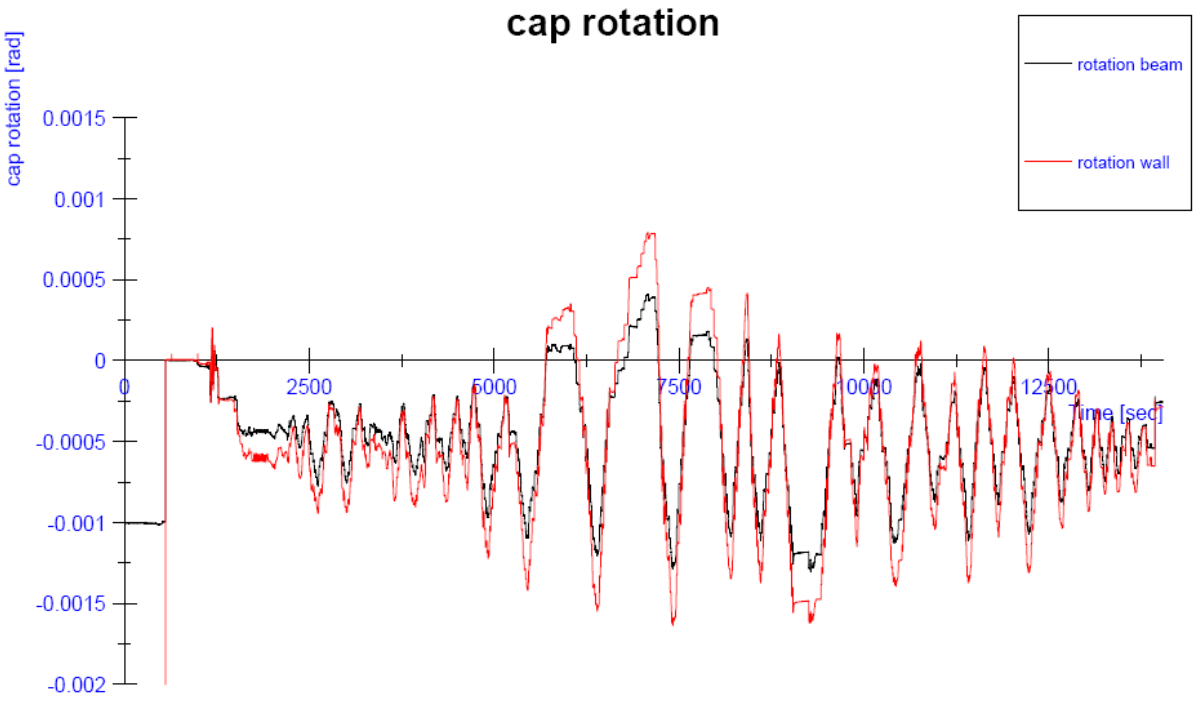

Figure 63: Progress of the in-plane rotation at the top of the wall (testing time) CS12

7.3.2. Scale factor 3 (max 0.17 g)

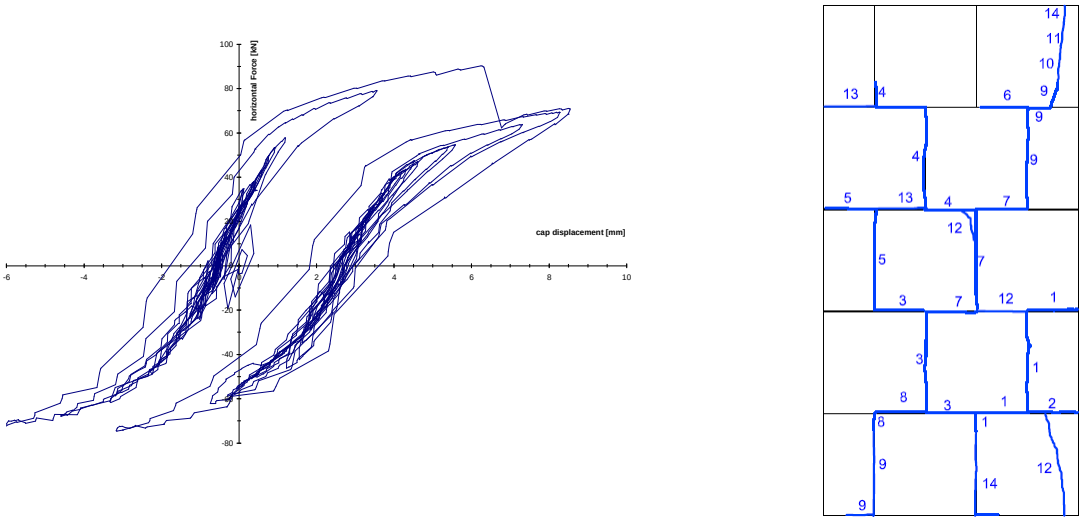

Figure 64: Load-displacement curve (hysteresis) and crack pattern of the test specimen CS12

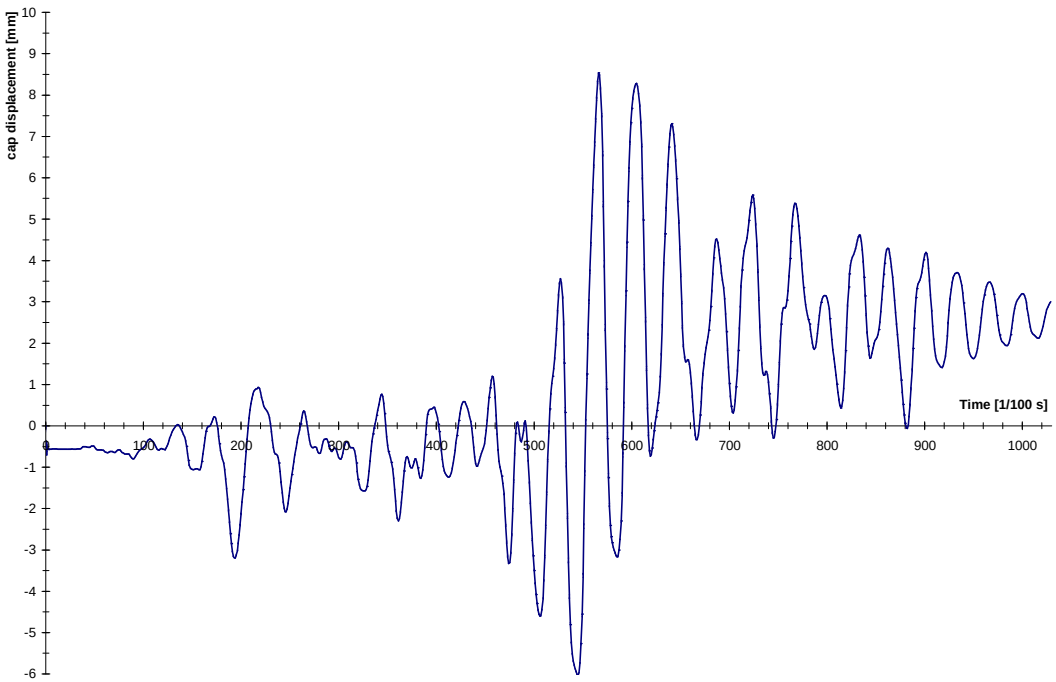

Figure 65: displacement history (earthquake time) CS12

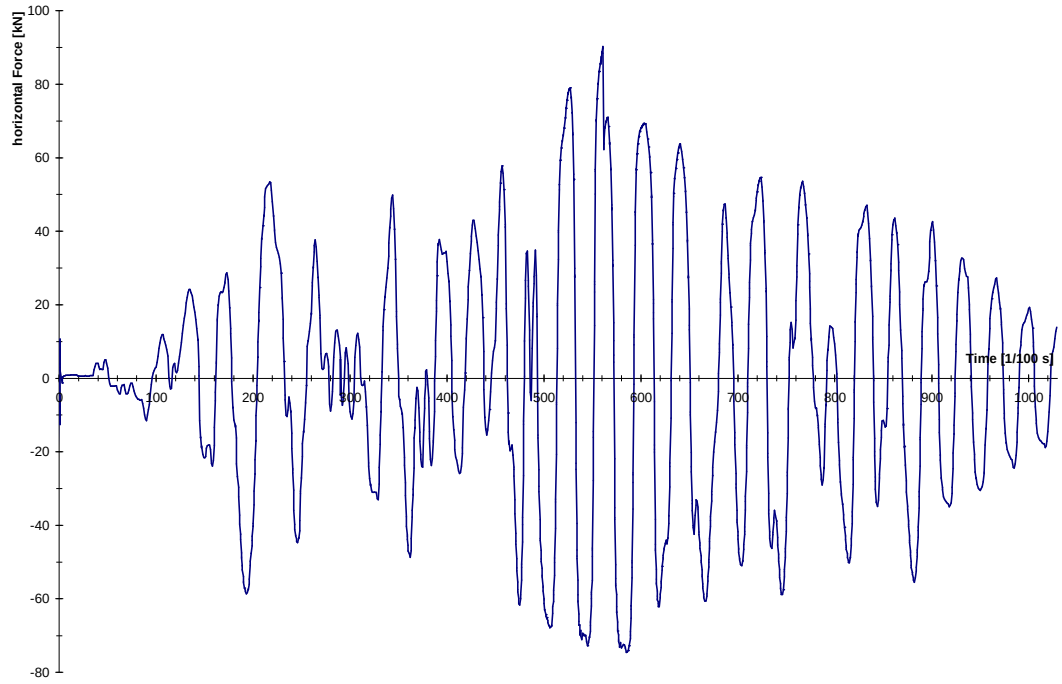

Figure 66: horizontal load history (earthquake time) CS12

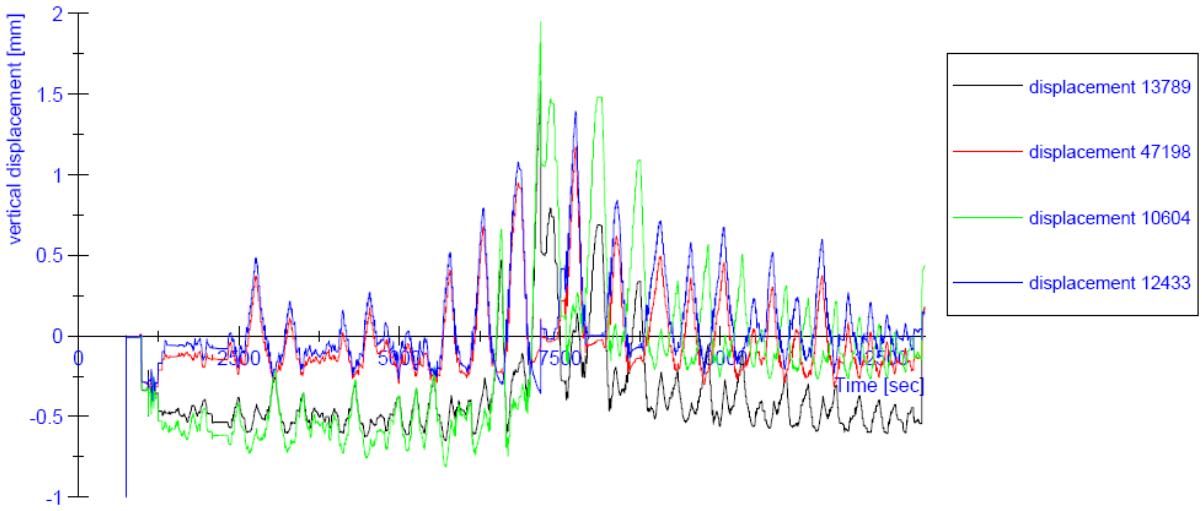

Figure 67: Progress of the vertical displacements (testing time) CS12

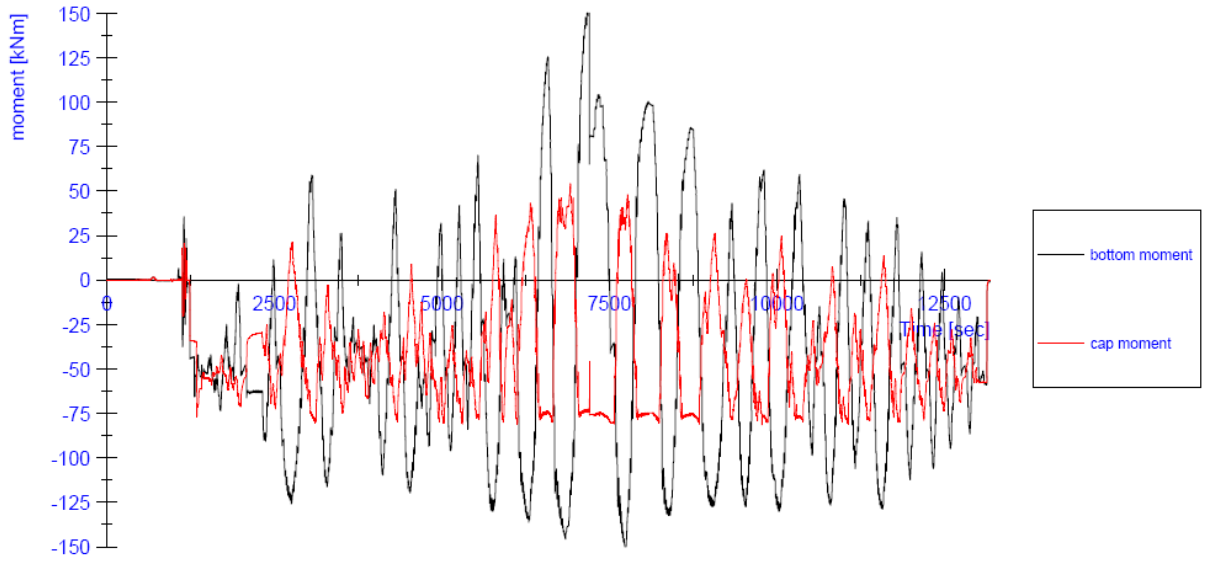

Figure 68: Progress of the in-plane bending moments at the top and at the bottom of the wall (testing time) CS12

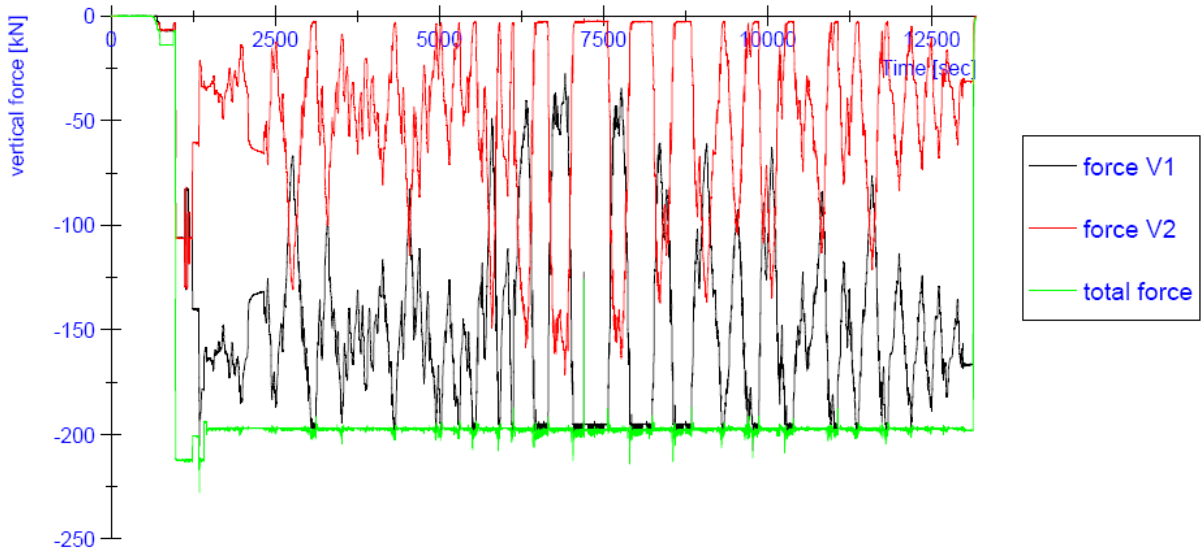

Figure 69: Progress of the vertical forces V1 and V2 (testing time) CS12

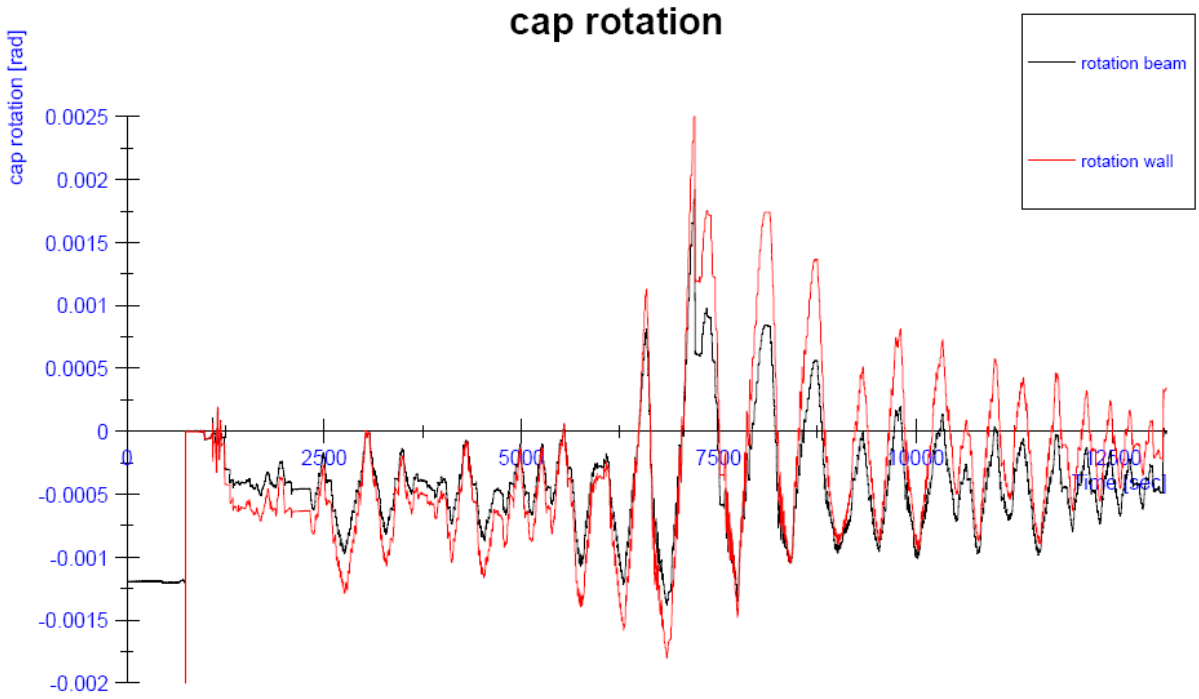

Figure 70: Progress of the in-plane rotation at the top of the wall (testing time) CS12

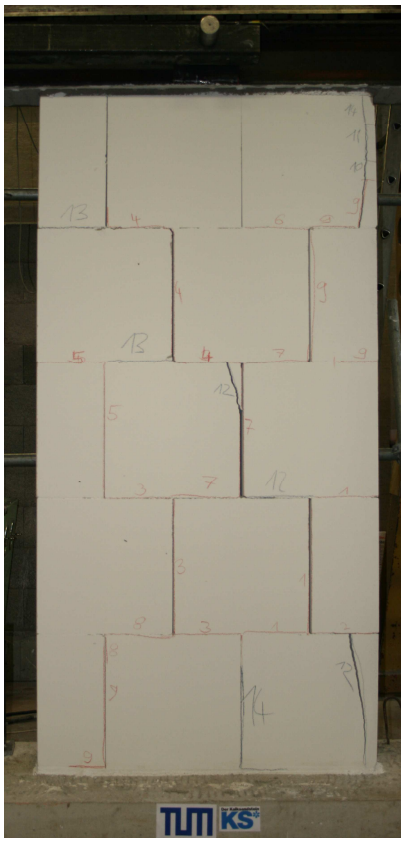

Figure 71: Crack pattern CS12

7.4. CS13

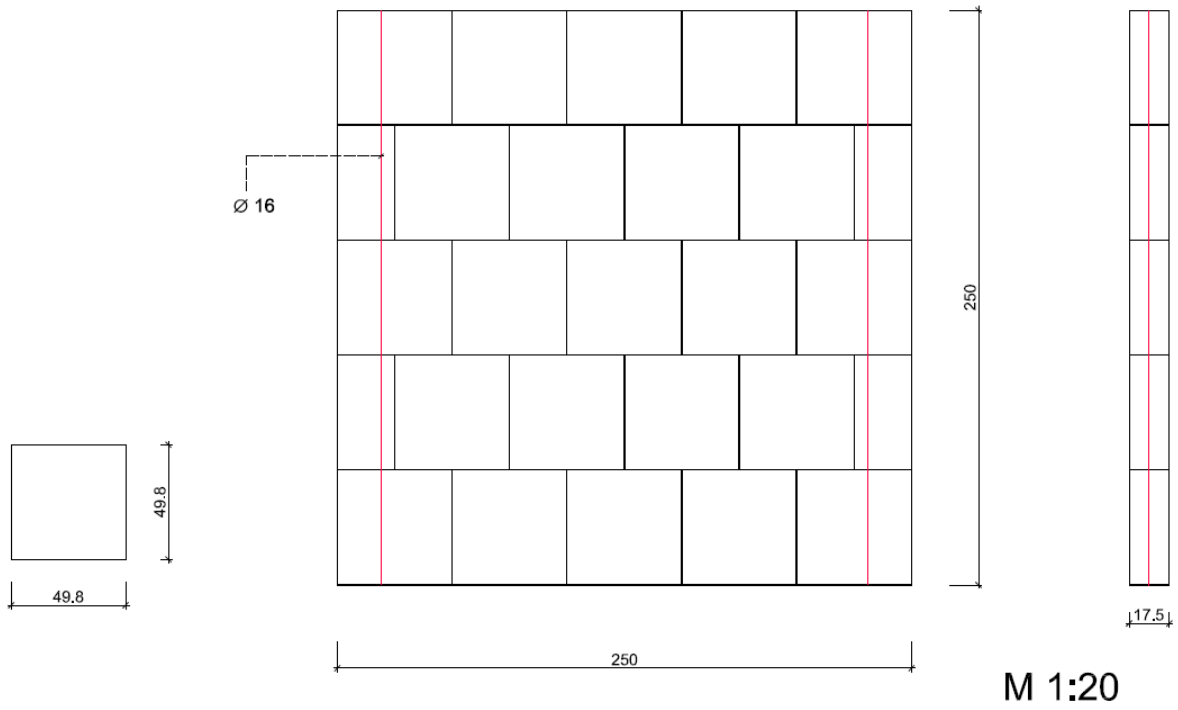

Figure 72: Dimension of the test specimen CS13

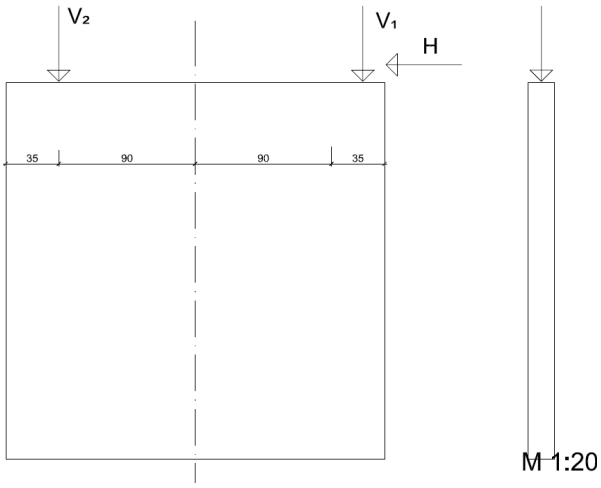

Figure 73: Position of the hydraulic actuators at test specimen CS13

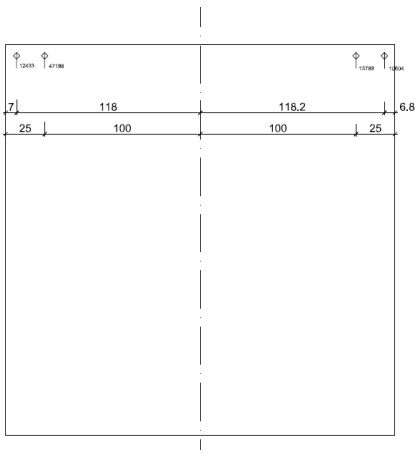

Figure 74: Position of the LVDTs at test specimen CS13

7.4.1. Scale factor 5 (max 0.29 g, damping ratio ~ 20%)

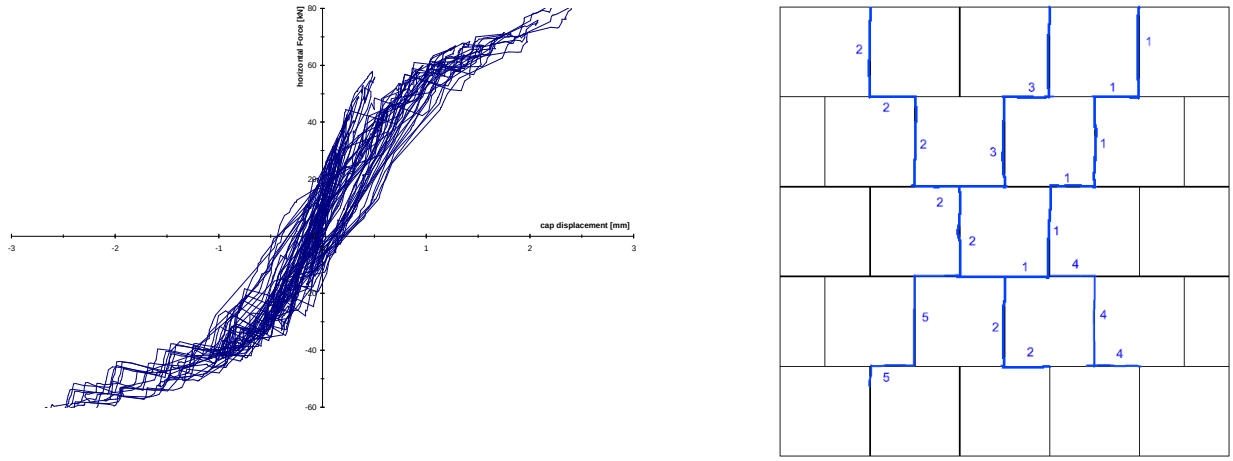

Figure 75: Load-displacement curve (hysteresis) and crack pattern of the test specimen CS13

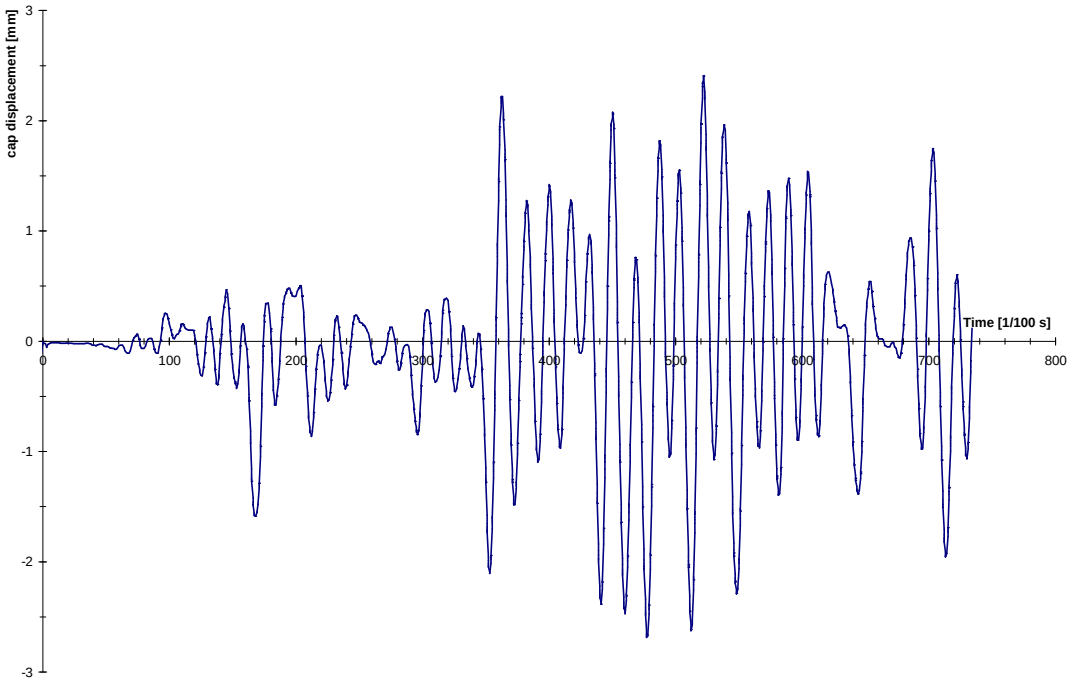

Figure 76: displacement history (earthquake time) CS13

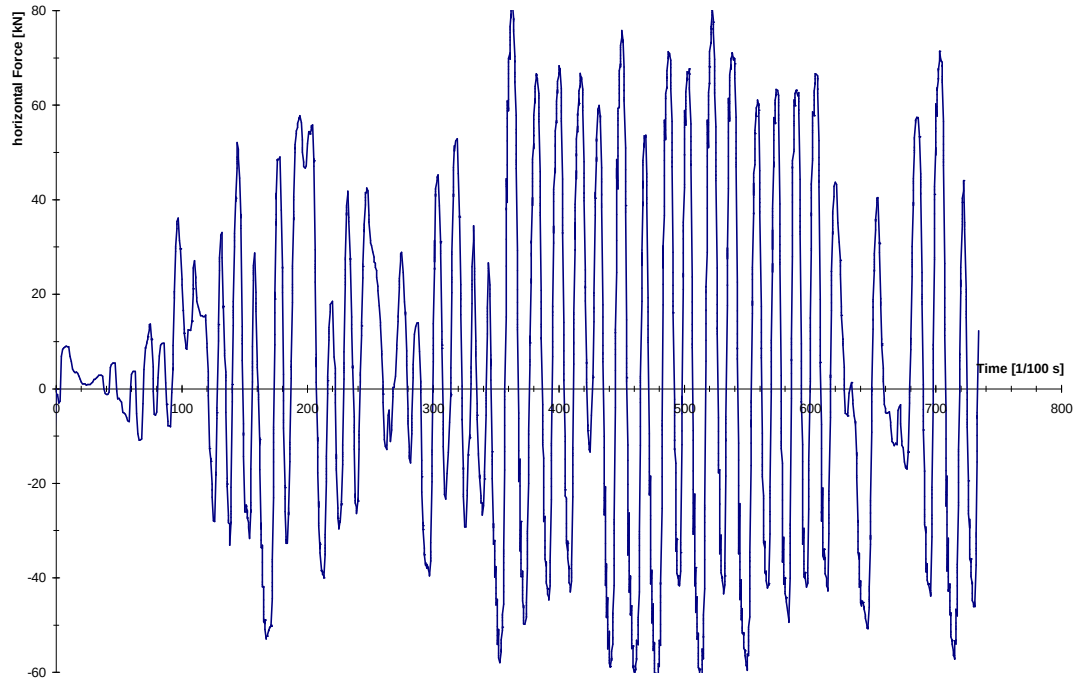

Figure 77: horizontal load history (earthquake time) CS13

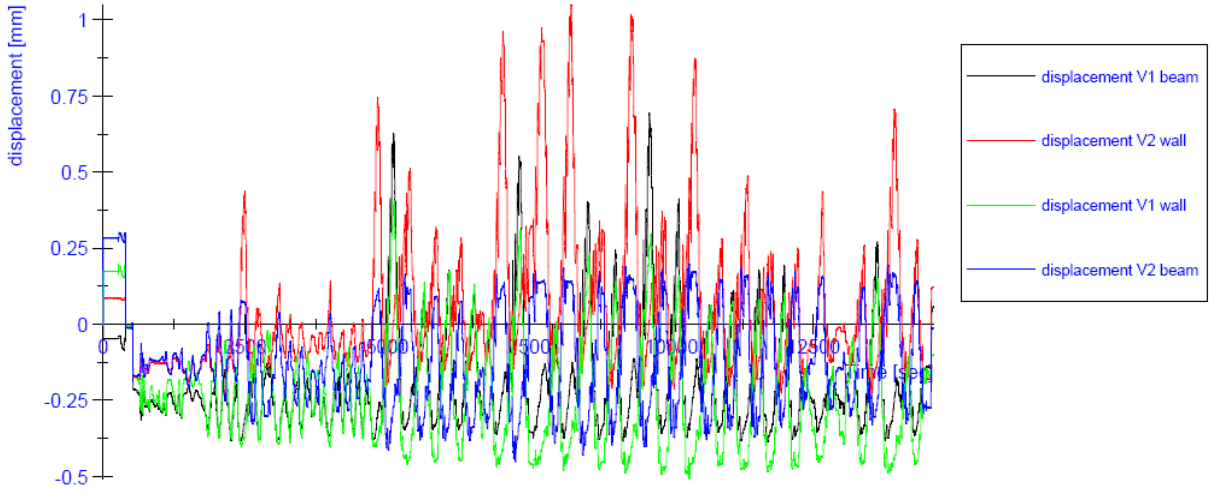

Figure 78: Progress of the vertical displacements (testing time) CS13

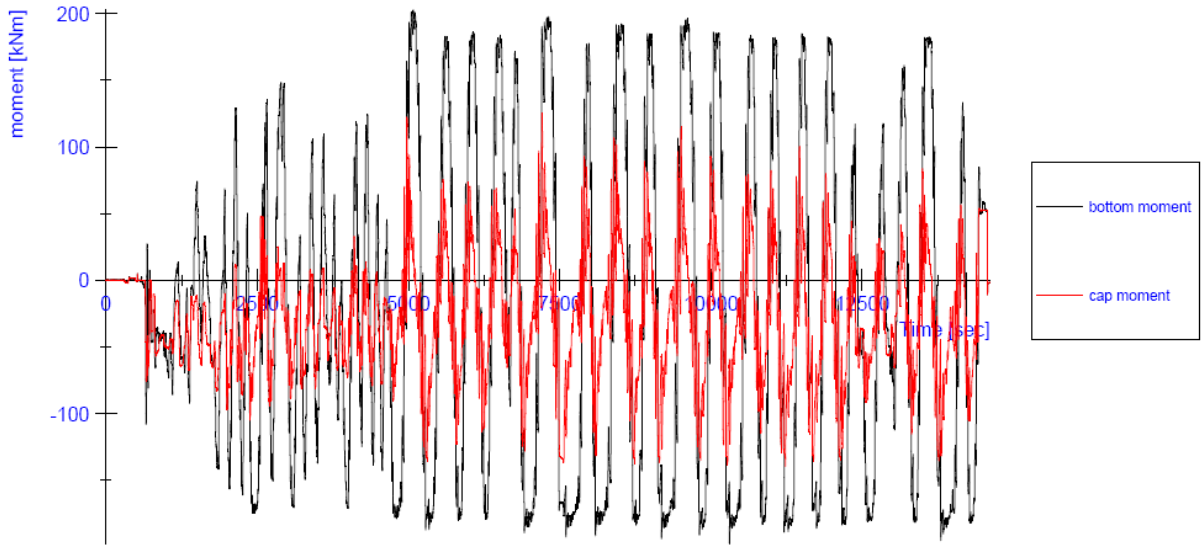

Figure 79: Progress of the in-plane bending moments at the top and at the bottom of the wall (testing time) CS13

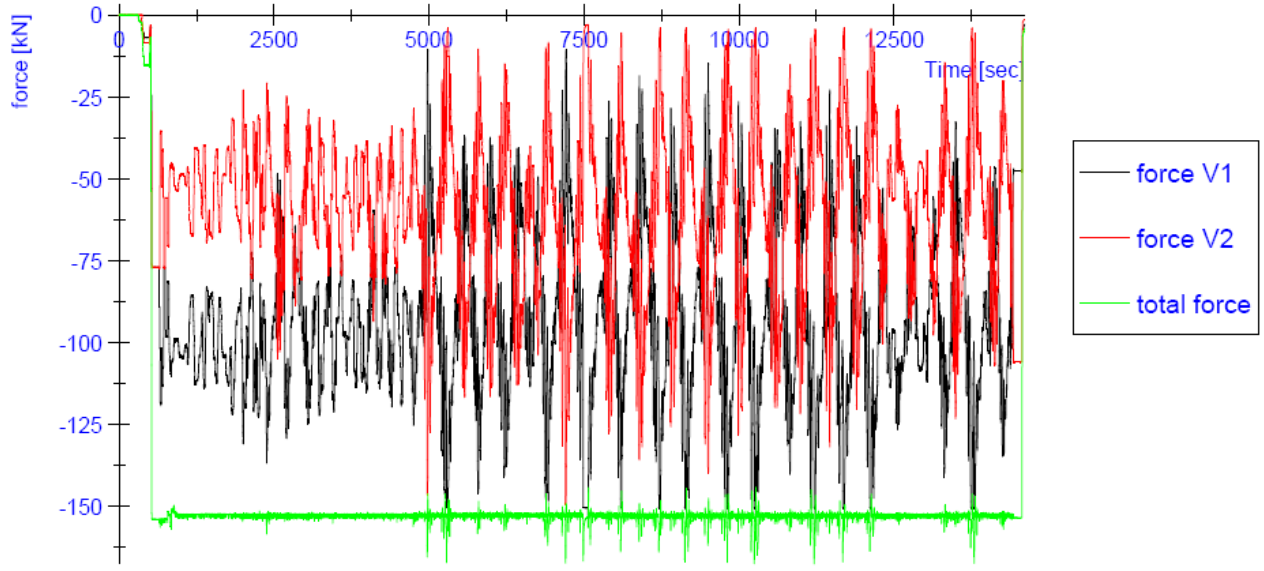

Figure 80: Progress of the vertical forces V1 and V2 (testing time) CS13

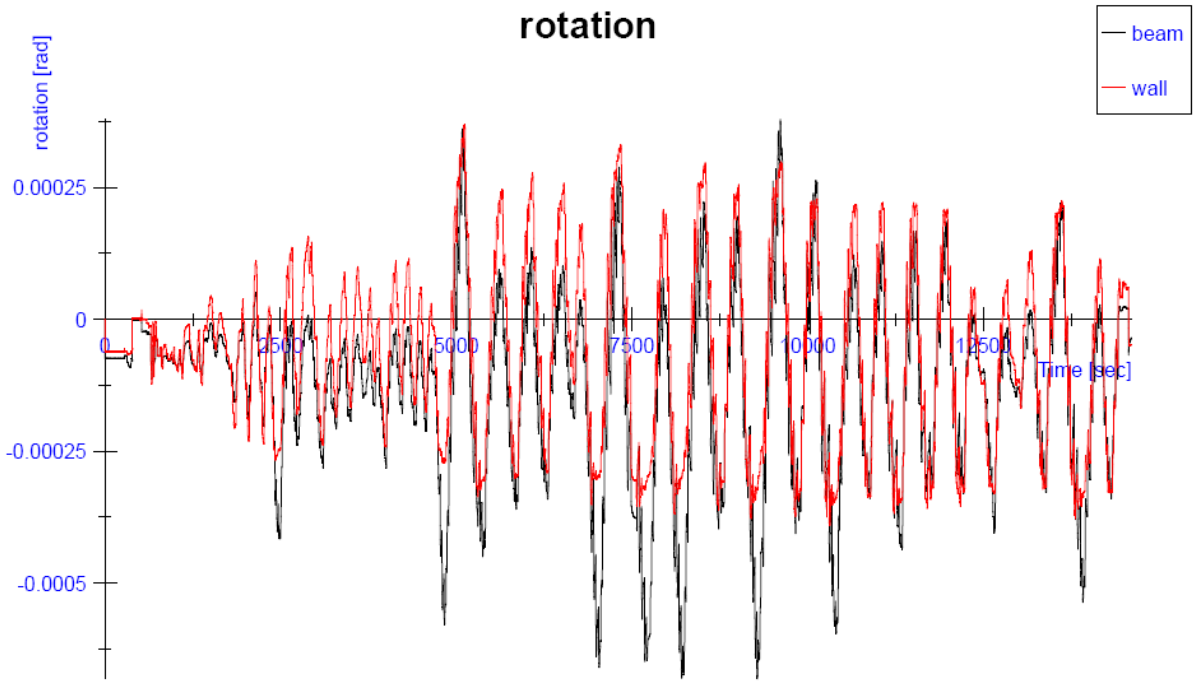

Figure 81: Progress of the in-plane rotation at the top of the wall (testing time) CS13

7.4.2. Scale factor 10 (max 0.58 g, damping ratio ~ 20%)

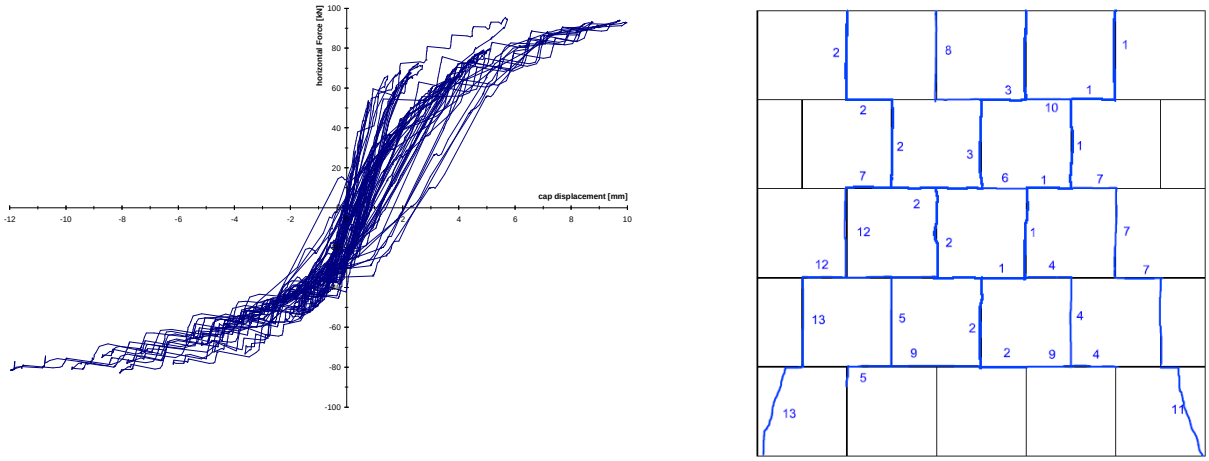

Figure 82: Load-displacement curve (hysteresis) and crack pattern of the test specimen CS13

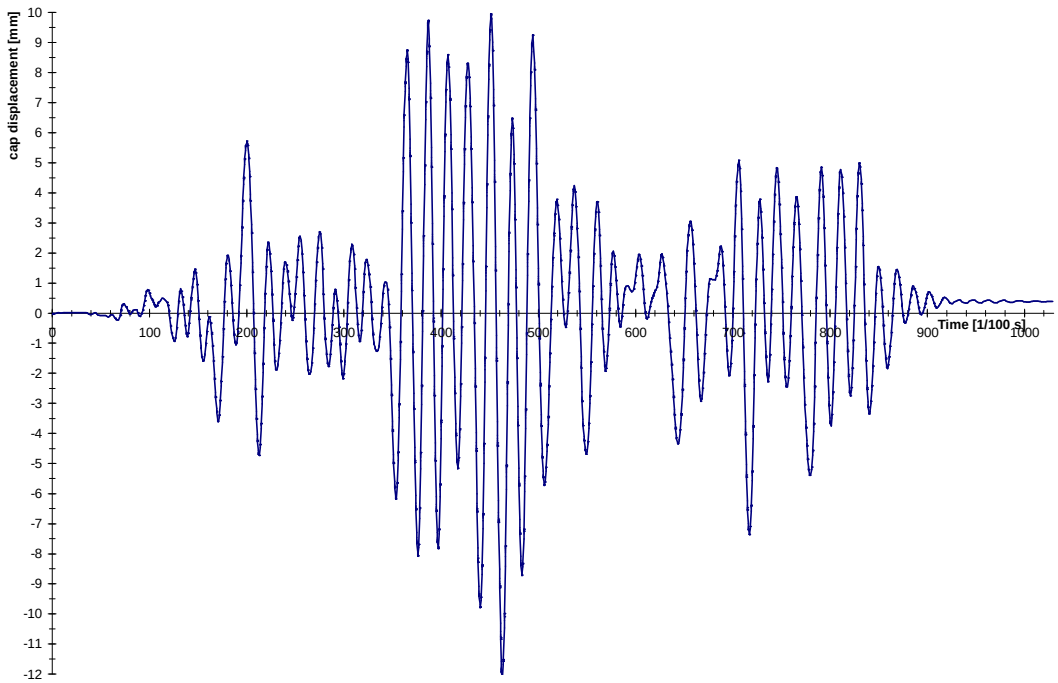

Figure 83: displacement history (earthquake time) CS13

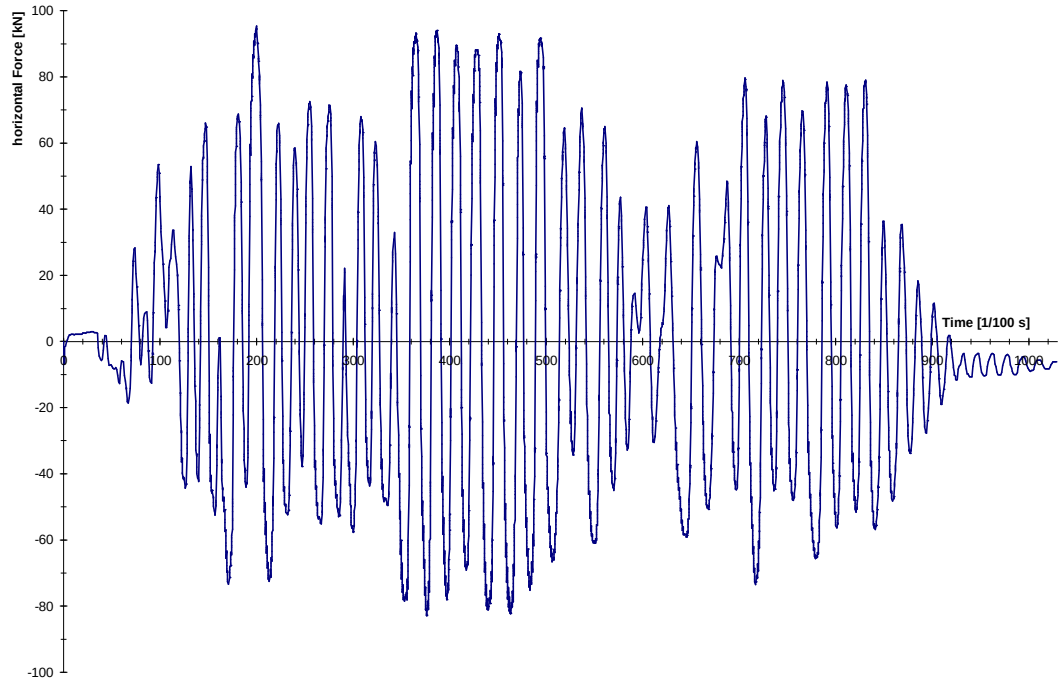

Figure 84: horizontal load history (earthquake time) CS13

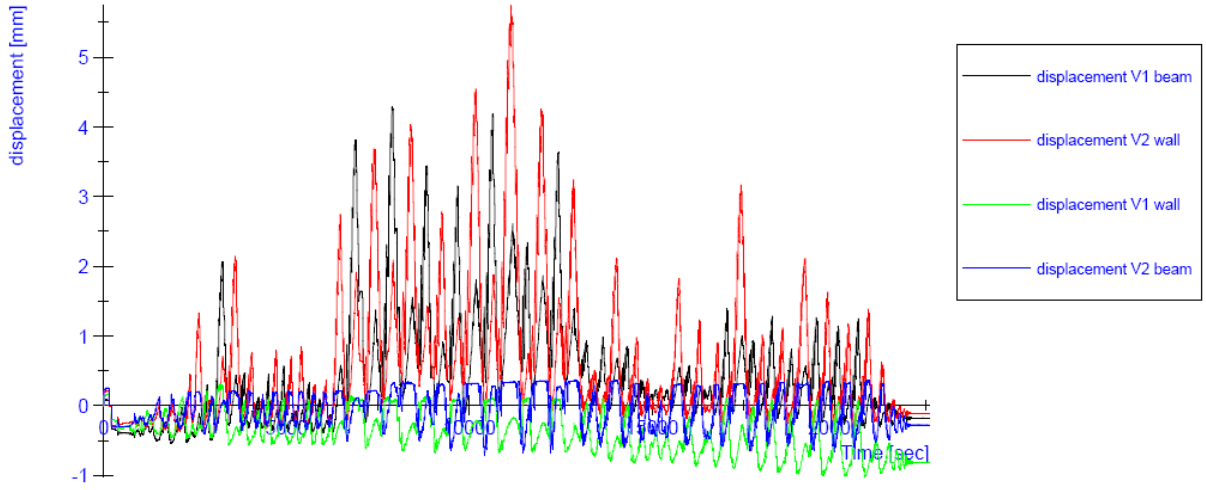

Figure 85: Progress of the vertical displacements (testing time) CS13

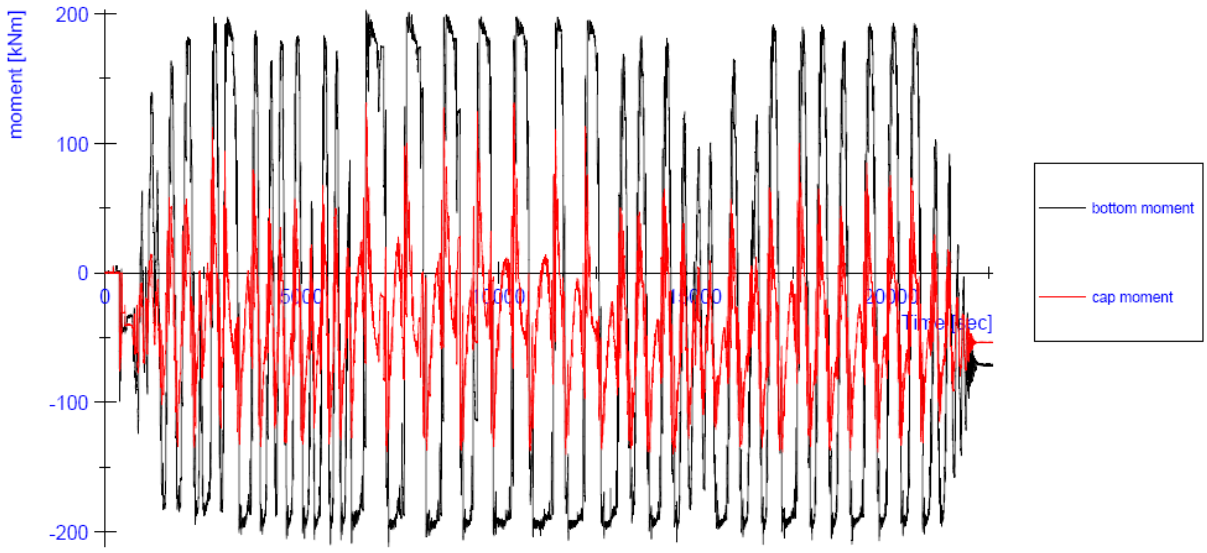

Figure 86: Progress of the in-plane bending moments at the top and at the bottom of the wall (testing time) CS13

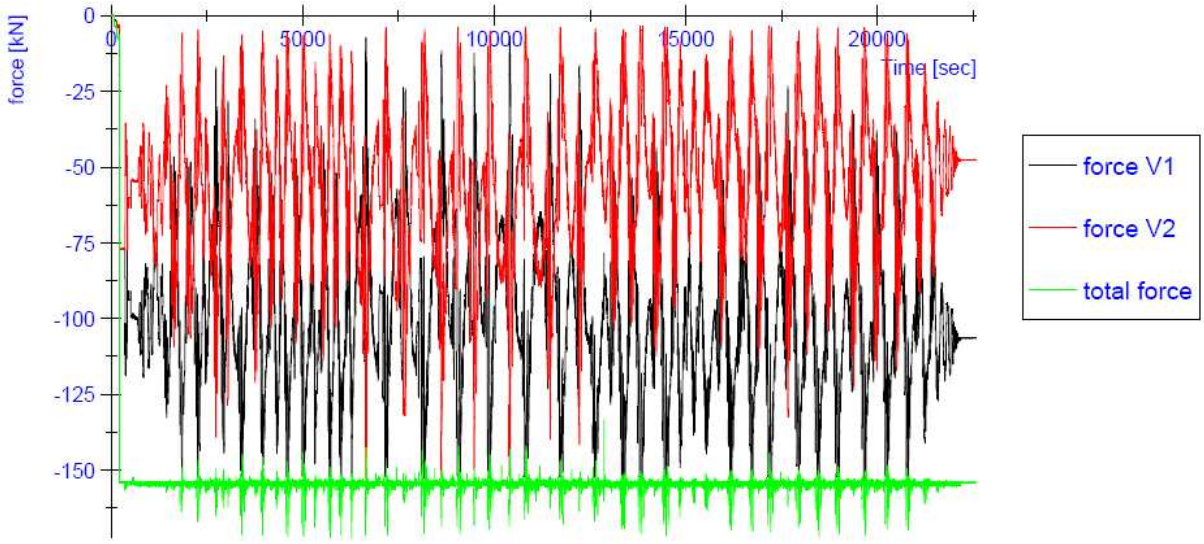

Figure 87: Progress of the vertical forces V1 and V2 (testing time) CS13

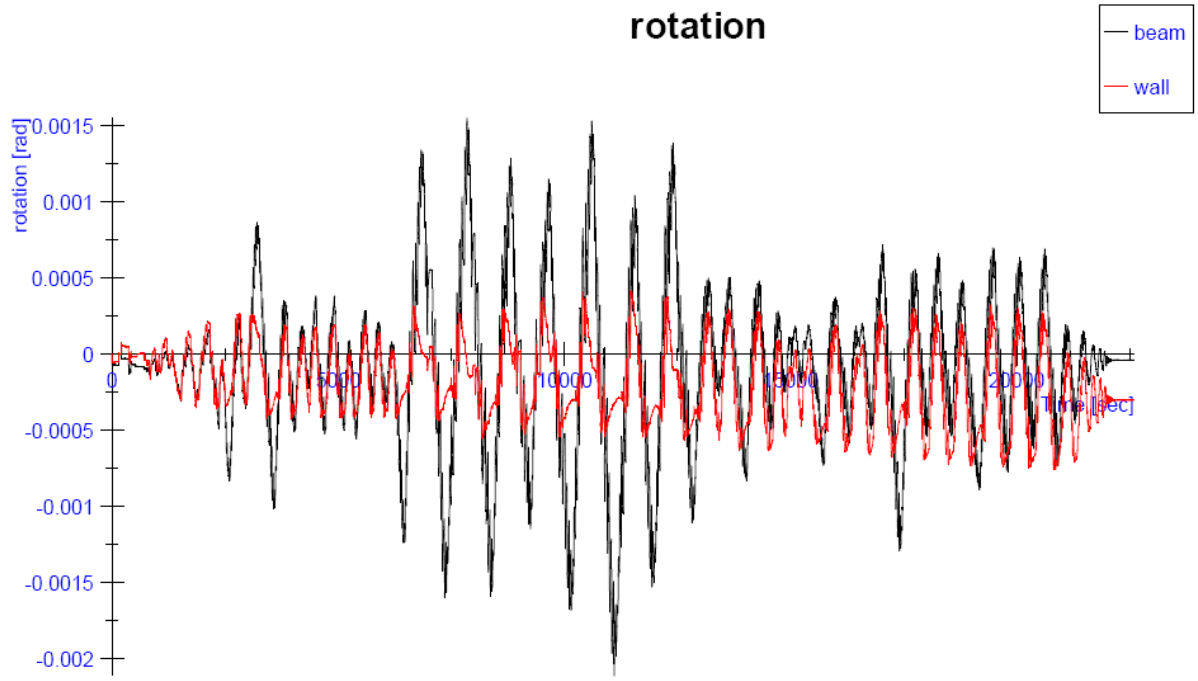

Figure 88: Progress of the in-plane rotation at the top of the wall (testing time) CS13

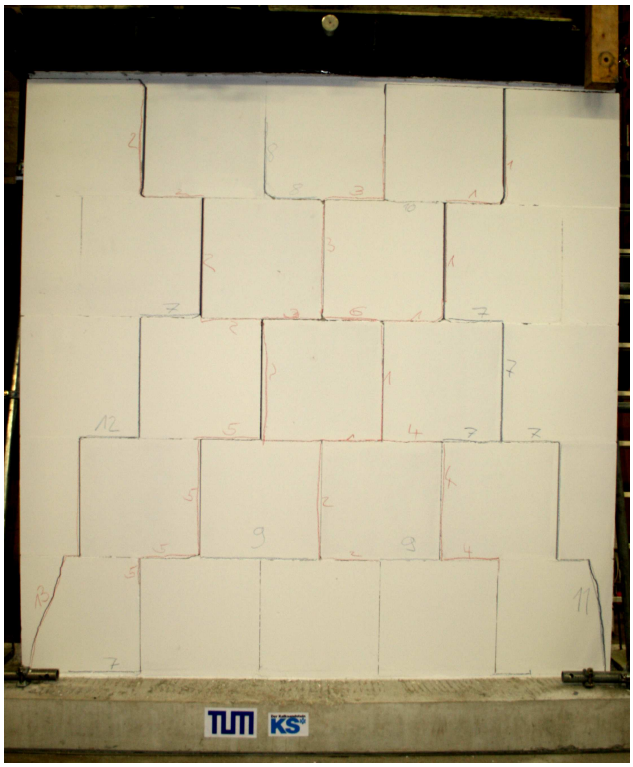

Figure 89: Crack pattern CS13

7.5. CS14

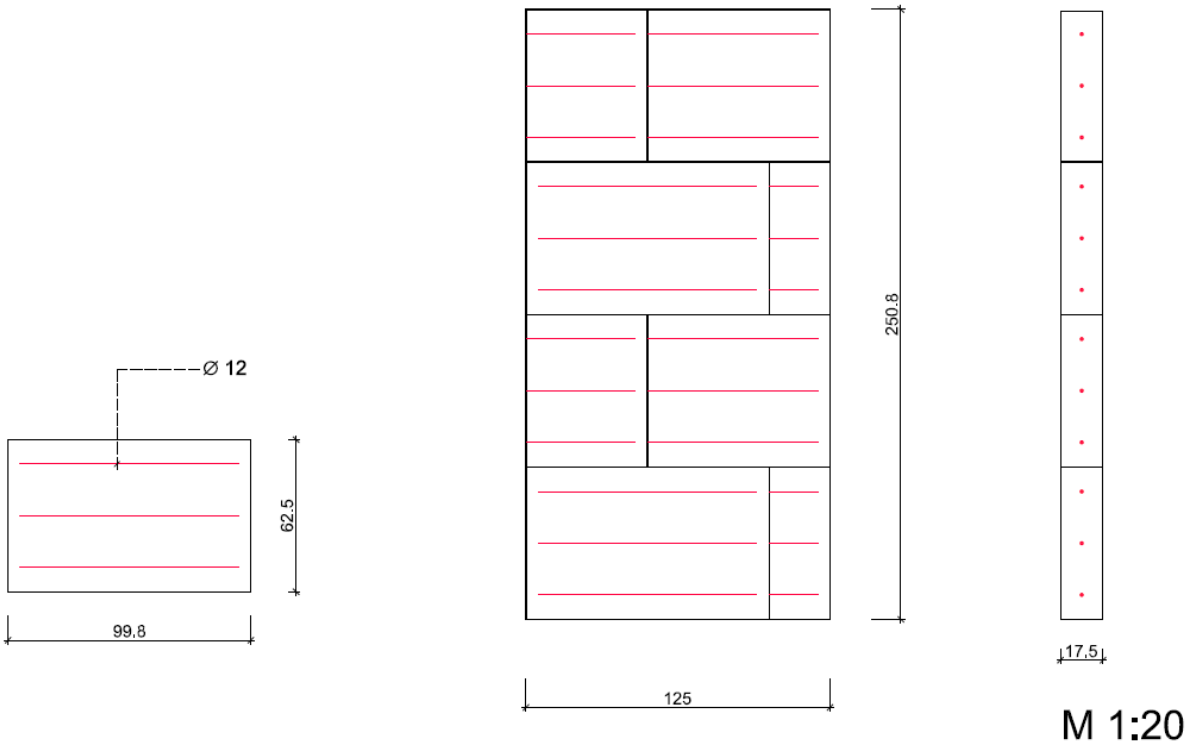

Figure 90: Dimension of the test specimen CS14

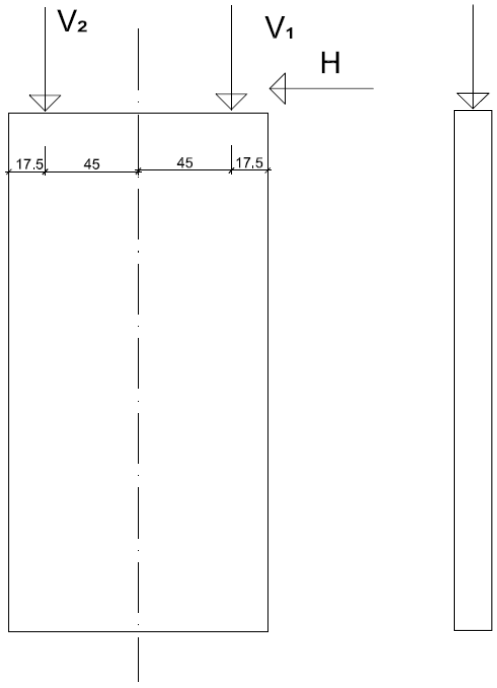

Figure 91: Position of the hydraulic actuators at test specimen CS14

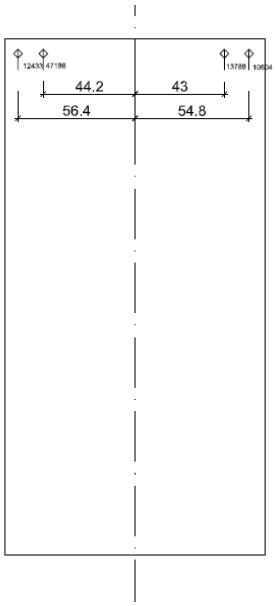

Figure 92: Position of the LVDTs at test specimen CS14

7.5.1. Scale factor 5 (max 0.29 g, damping ratio ~ 20%)

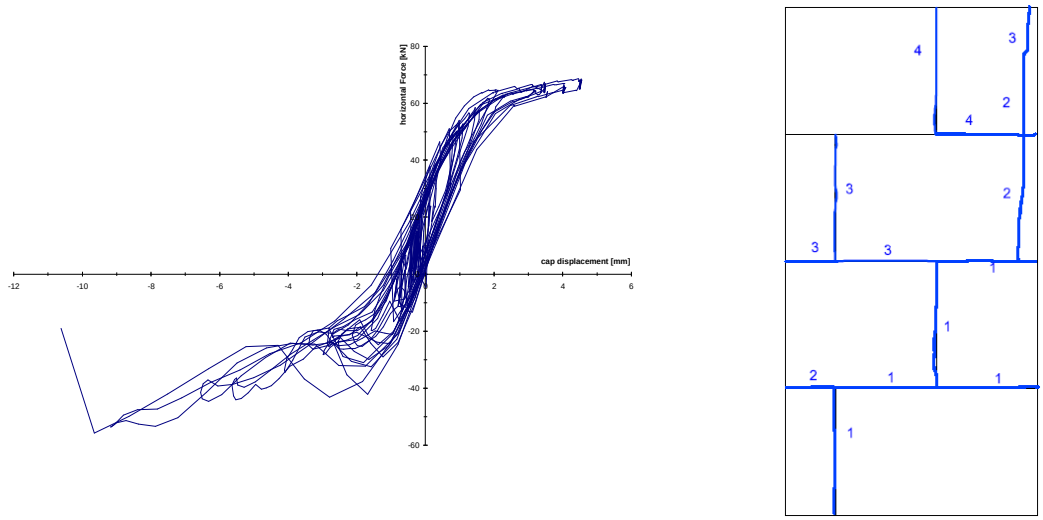

Figure 93: Load-displacement curve (hysteresis) and crack pattern of the test specimen CS14

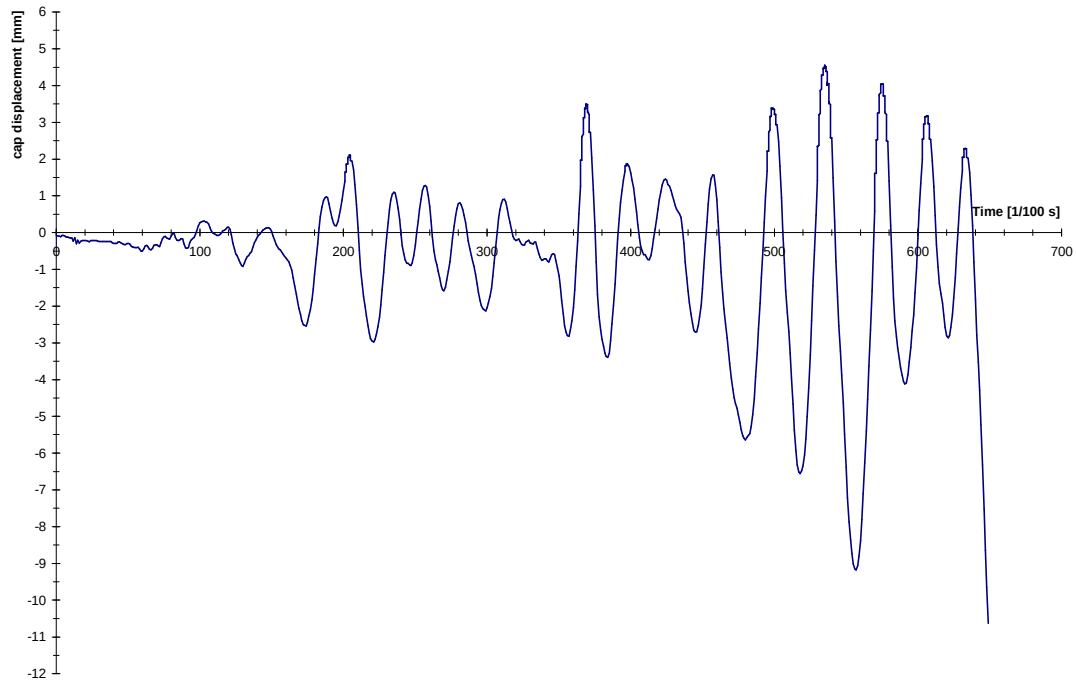

Figure 94: displacement history (earthquake time) CS14

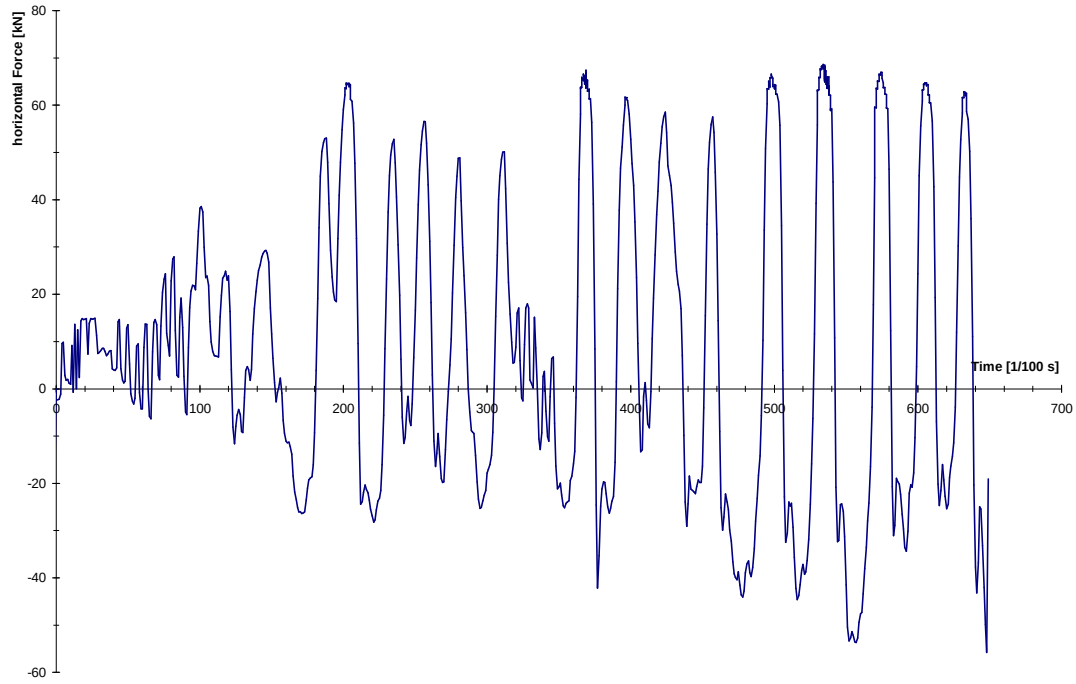

Figure 95: horizontal load history (earthquake time) CS14

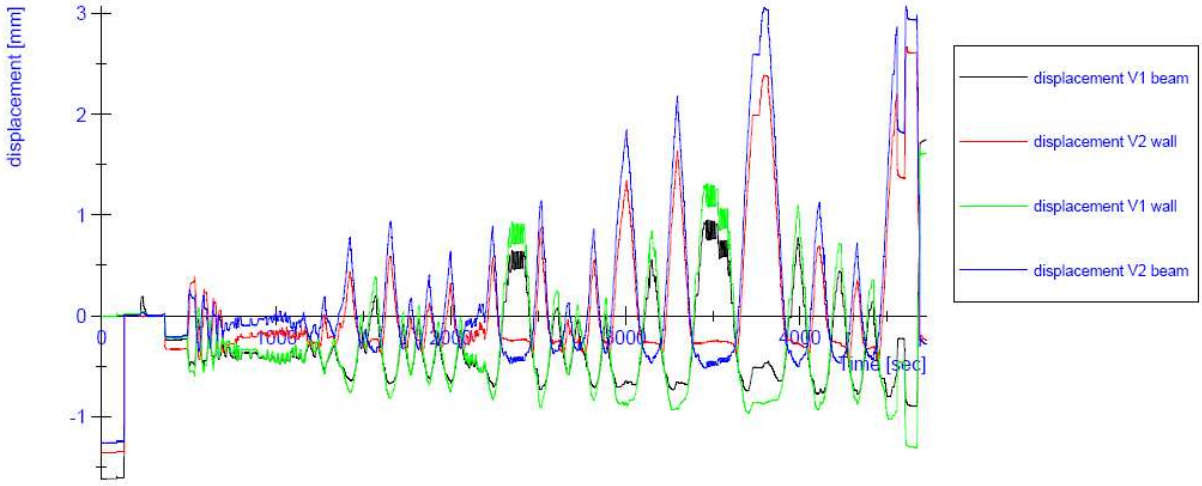

Figure 96: Progress of the vertical displacements (testing time) CS14

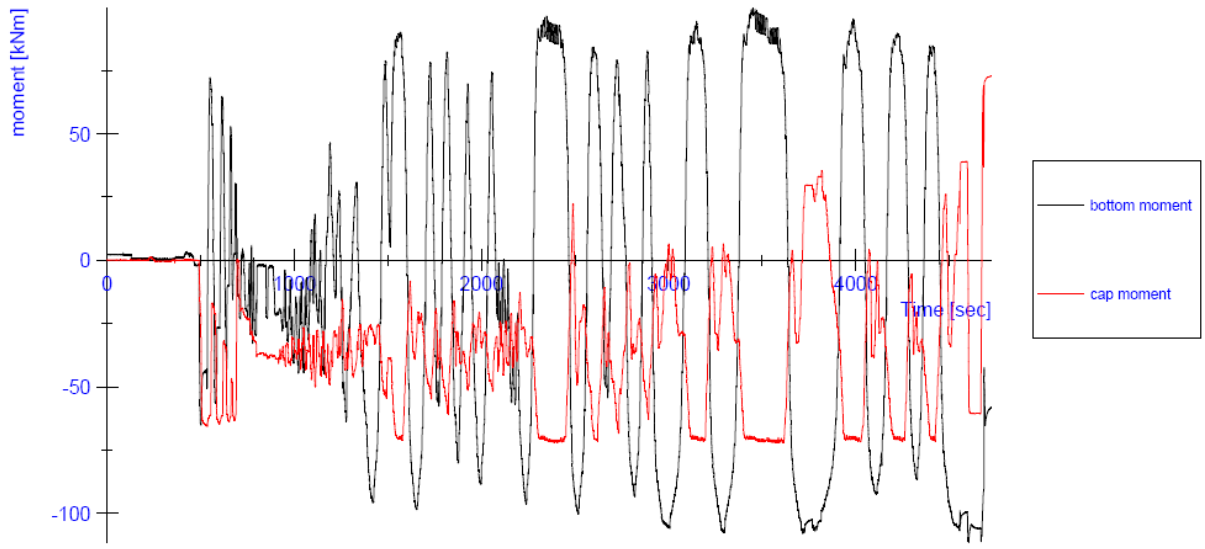

Figure 97: Progress of the in-plane bending moments at the top and at the bottom of the wall (testing time) CS14

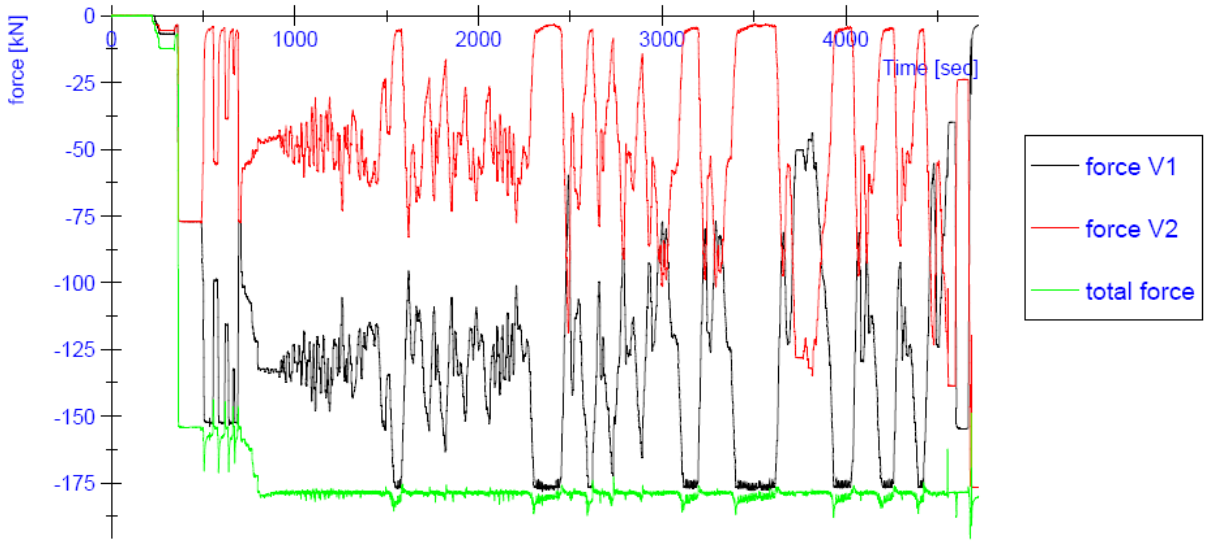

Figure 98: Progress of the vertical forces V1 and V2 (testing time) CS14

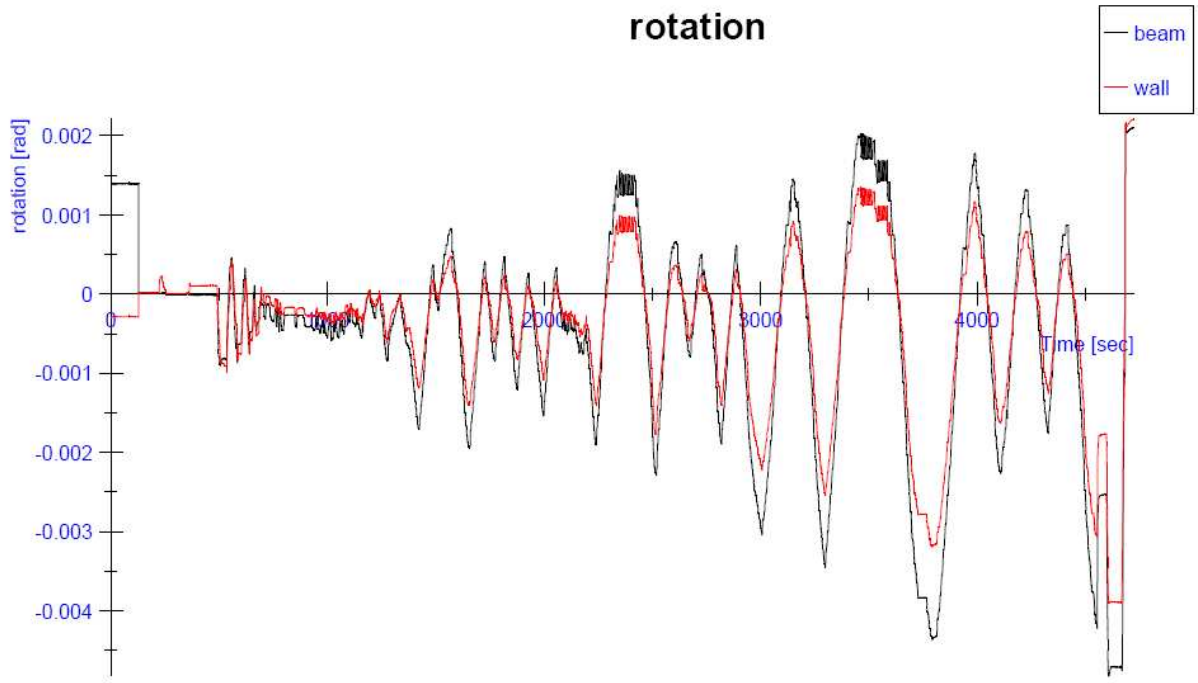

Figure 99: Progress of the in-plane rotation at the top of the wall (testing time) CS14

Figure 100: Crack pattern CS14

7.6. CS15

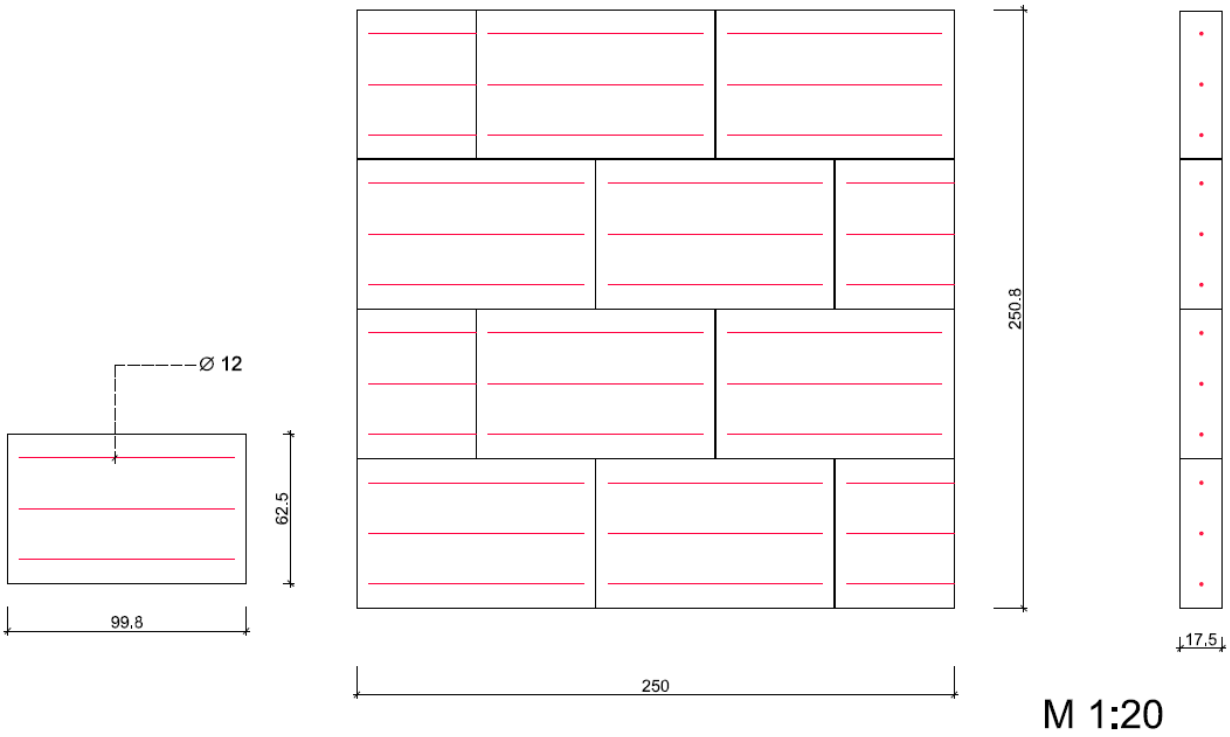

Figure 101: Dimension of the test specimen CS15

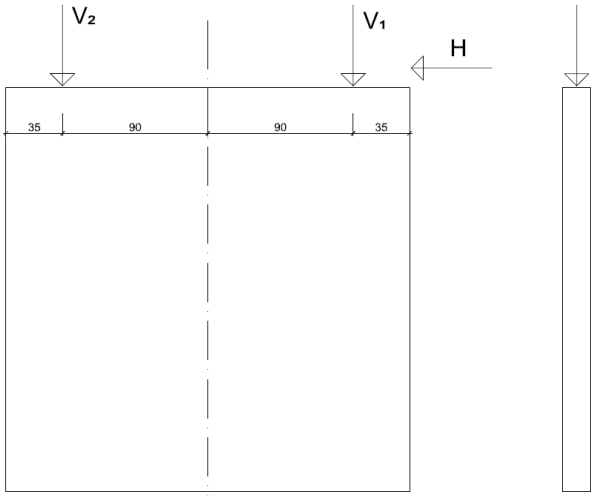

Figure 102: Position of the hydraulic actuators at test specimen CS15

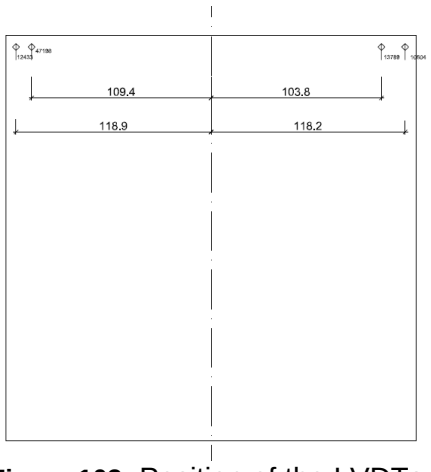

Figure 103: Position of the LVDTs at test specimen CS15

7.6.1. Scale factor 5 (max 0.29 g, damping ratio ~ 20%))

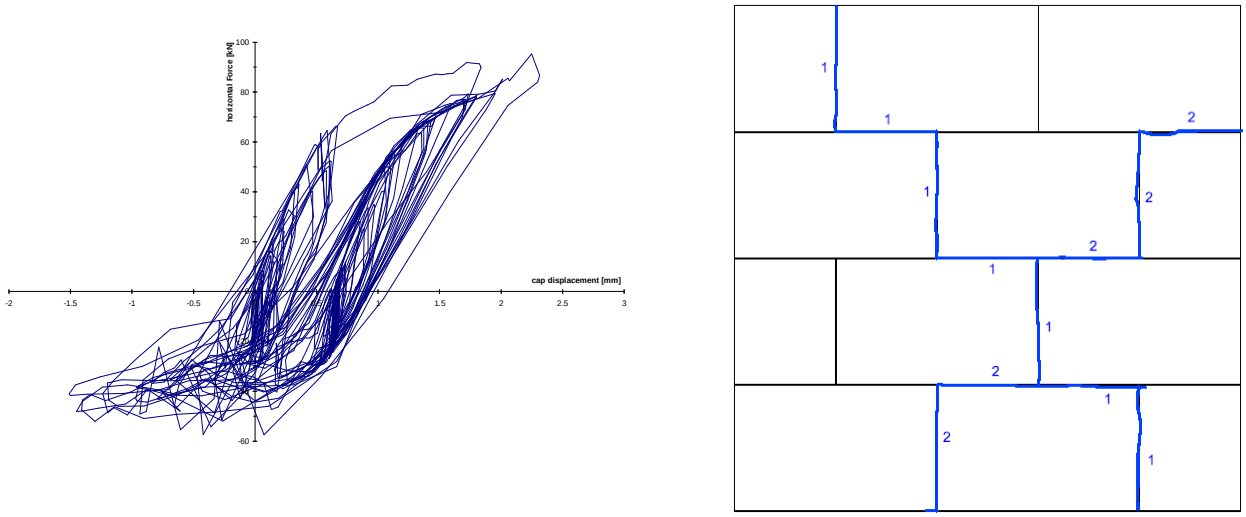

Figure 104: Load-displacement curve (hysteresis) and crack pattern of the test specimen CS15

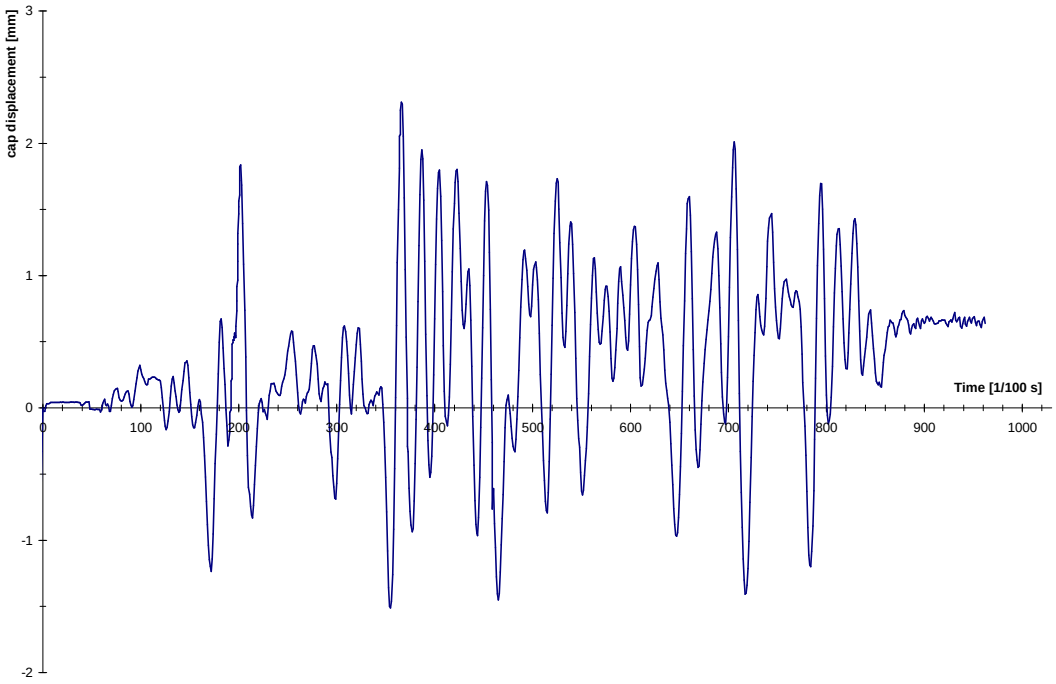

Figure 105: displacement history (earthquake time) CS15

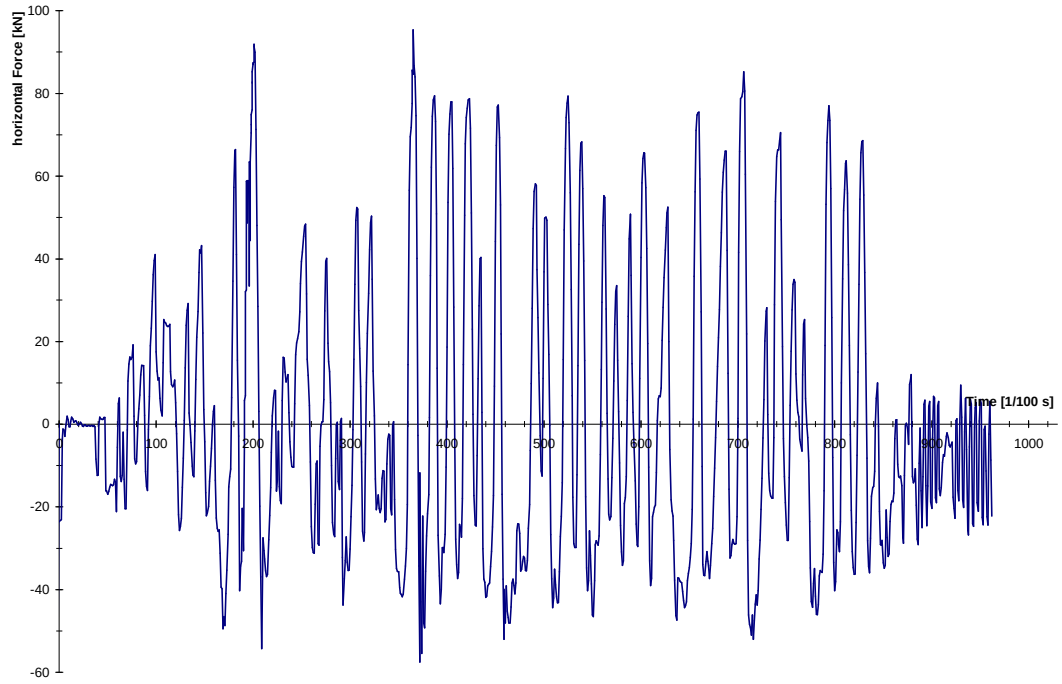

Figure 106: horizontal load history (earthquake time) CS15

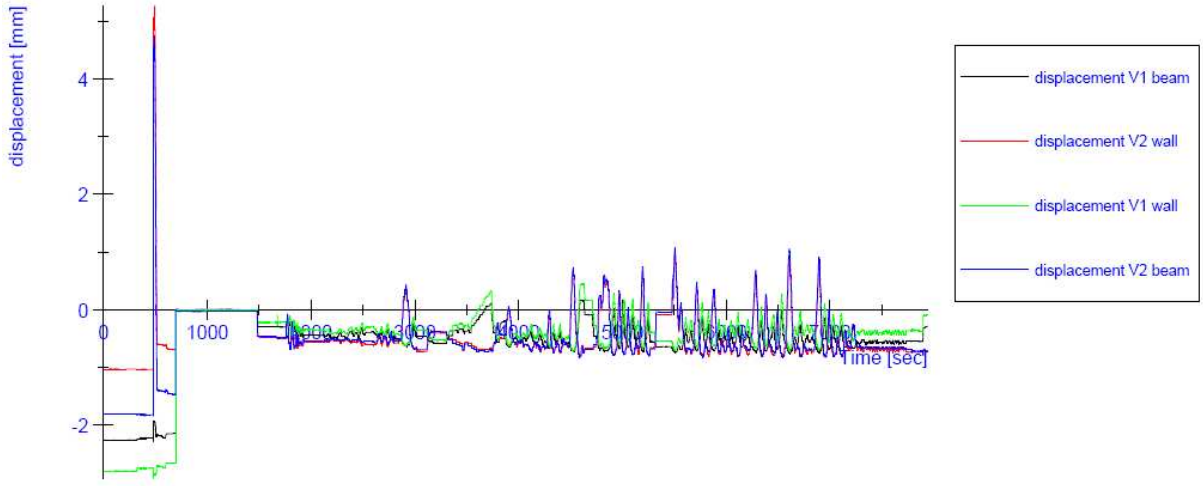

Figure 107: Progress of the vertical displacements (testing time) CS15

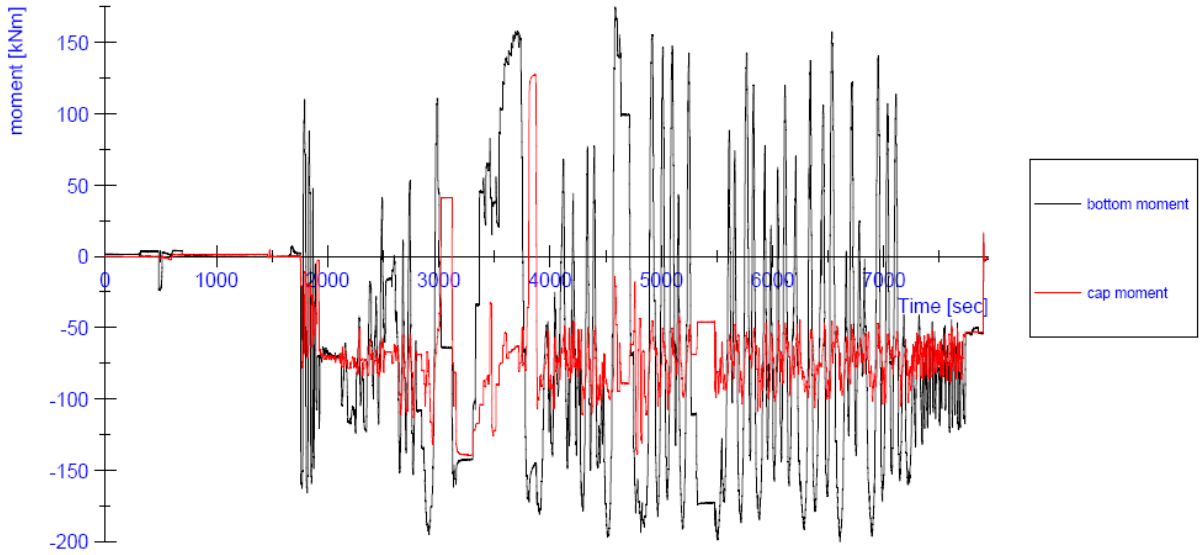

Figure 108: Progress of the in-plane bending moments at the top and at the bottom of the wall (testing time) CS15

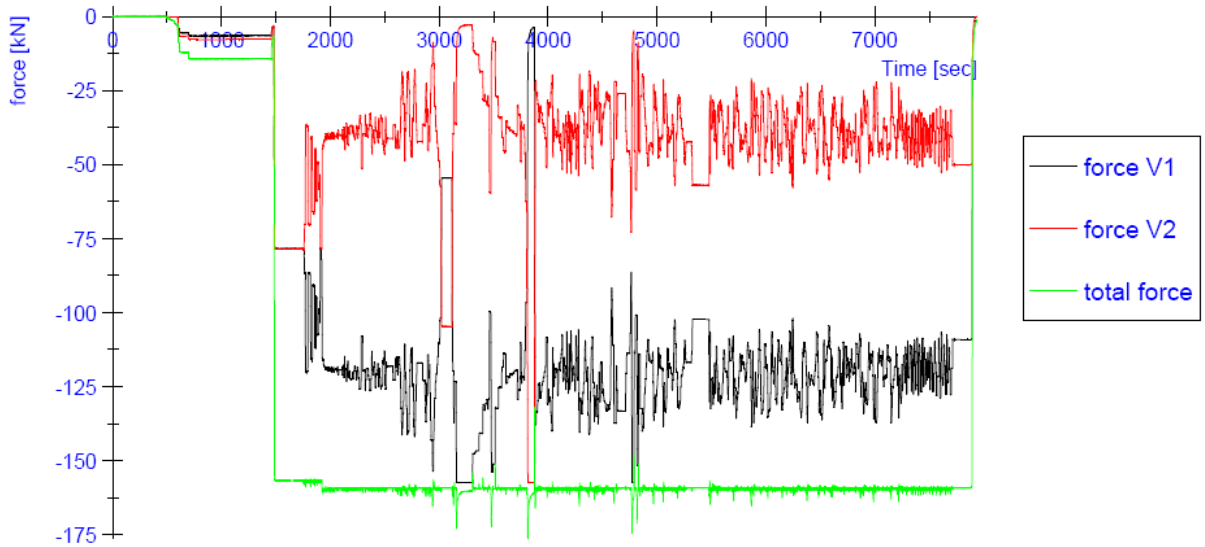

Figure 109: Progress of the vertical forces V1 and V2 (testing time) CS15

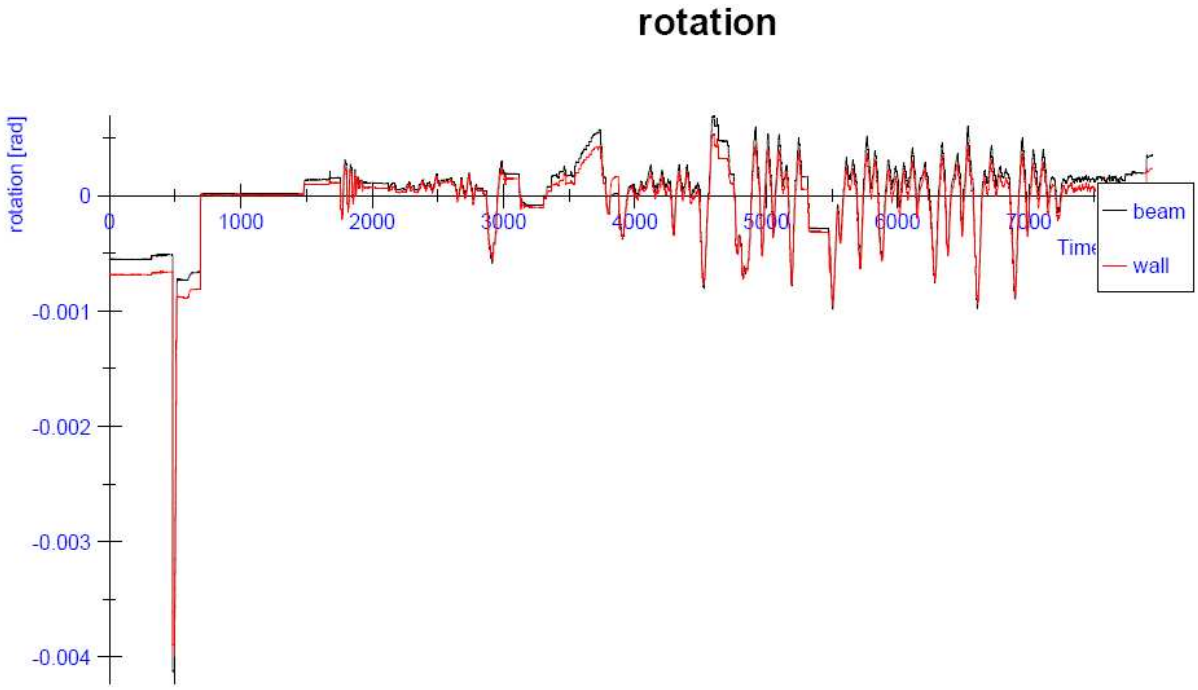

Figure 110: Progress of the in-plane rotation at the top of the wall (testing time) CS15

7.6.2. Scale factor 10 (max 0.58 g, damping ratio ~ 20%)

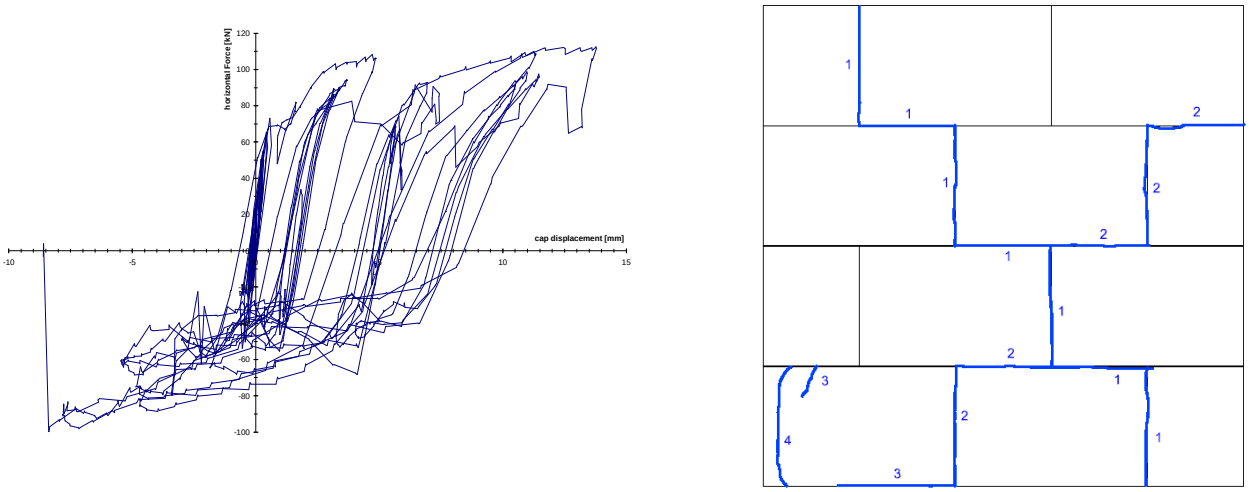

Figure 111: Load-displacement curve (hysteresis) and crack pattern of the test specimen CS15

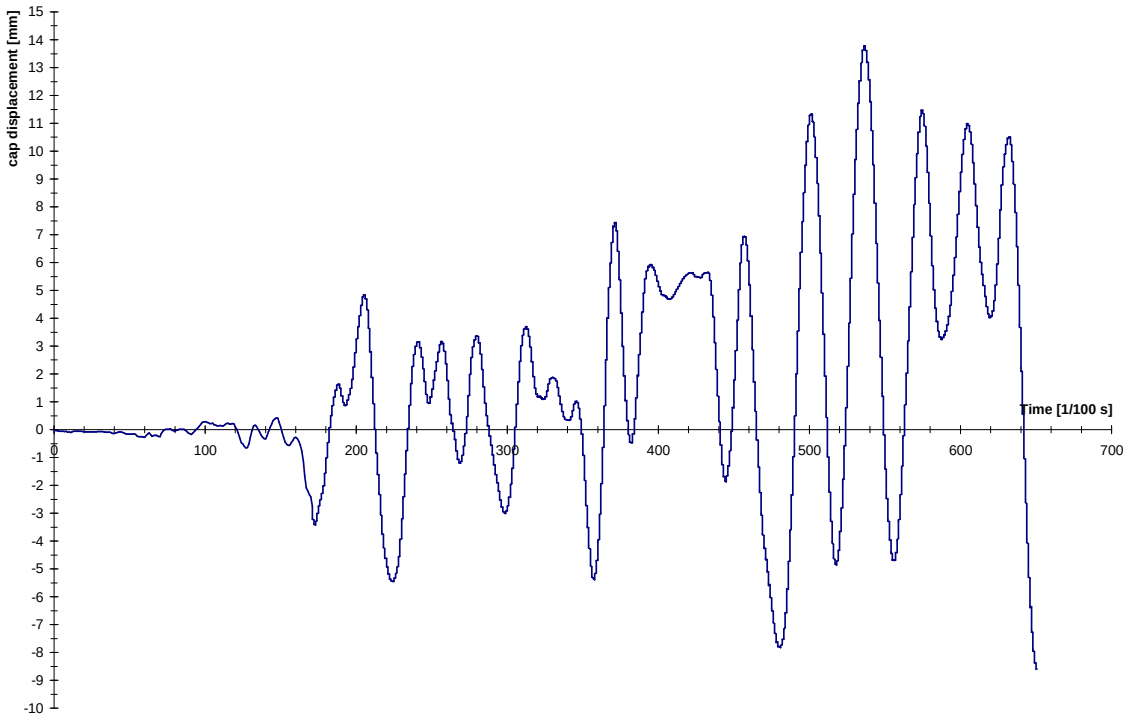

Figure 112: displacement history (earthquake time) CS15

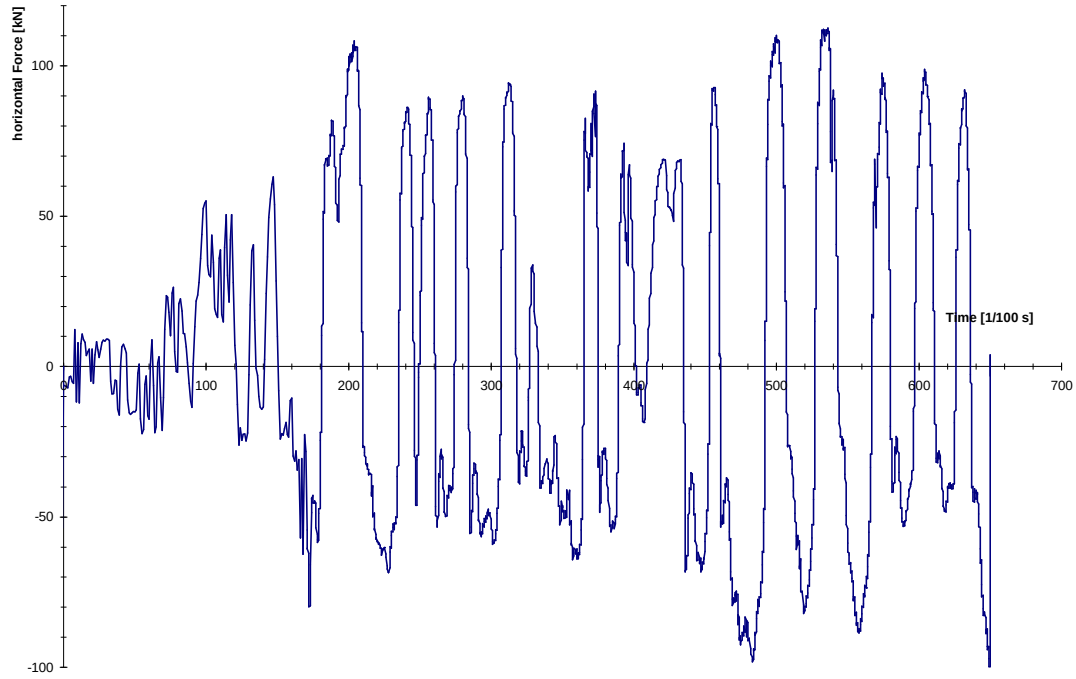

Figure 113: horizontal load history (earthquake time) CS15

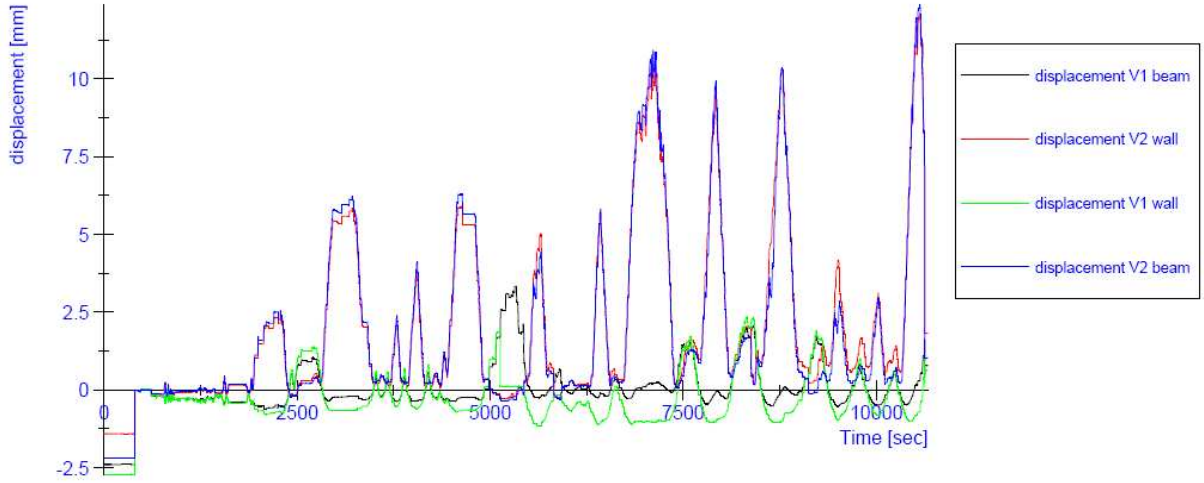

Figure 114: Progress of the vertical displacements (testing time) CS15

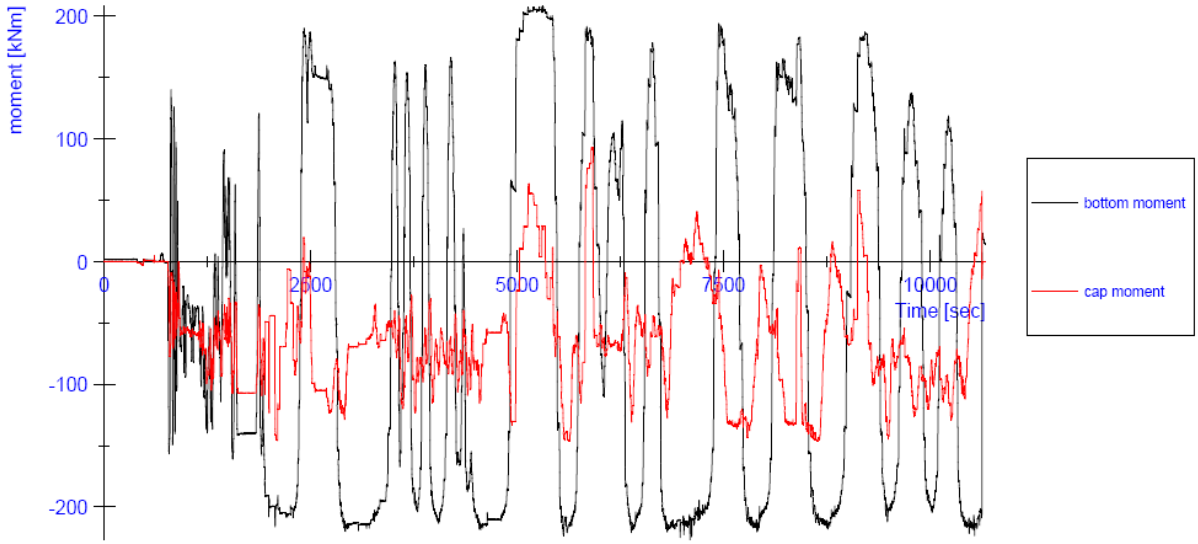

Figure 115: Progress of the in-plane bending moments at the top and at the bottom of the wall (testing time) CS15

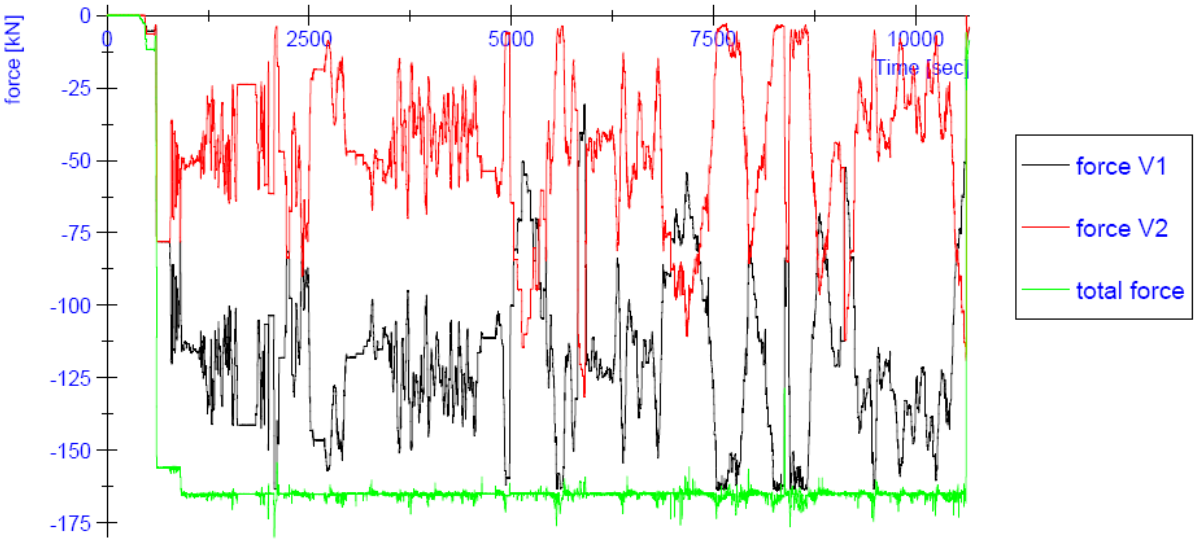

Figure 116: Progress of the vertical forces V1 and V2 (testing time) CS15

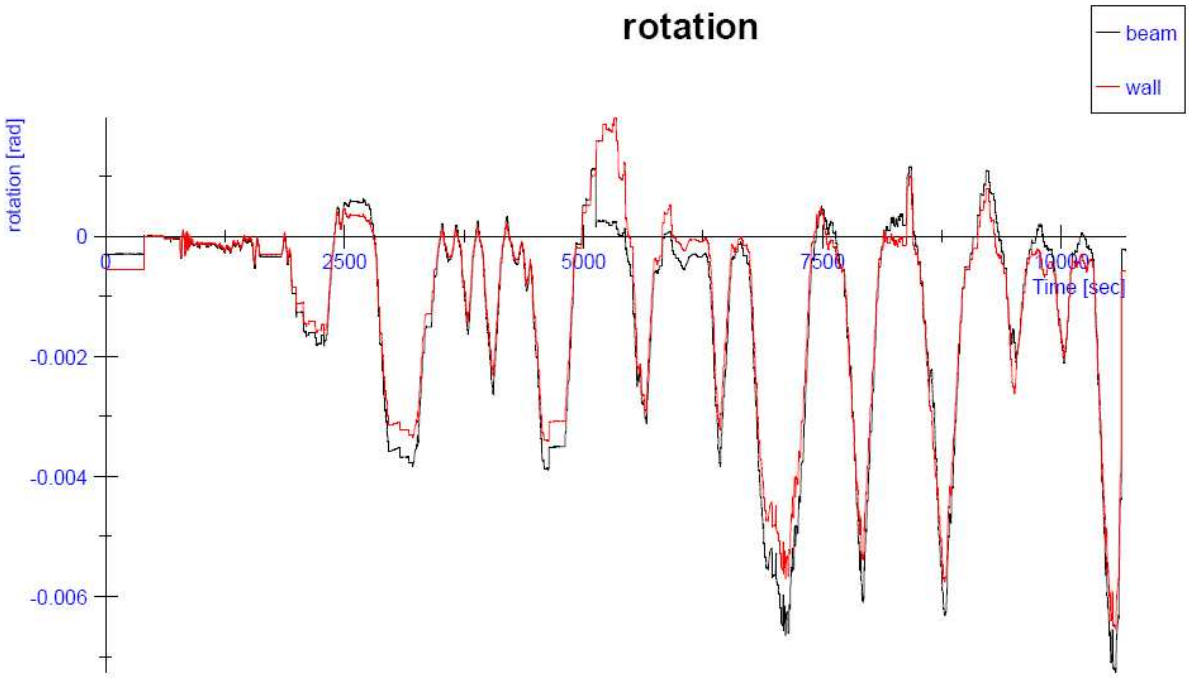

Figure 117: Progress of the in-plane rotation at the top of the wall (testing time) CS15

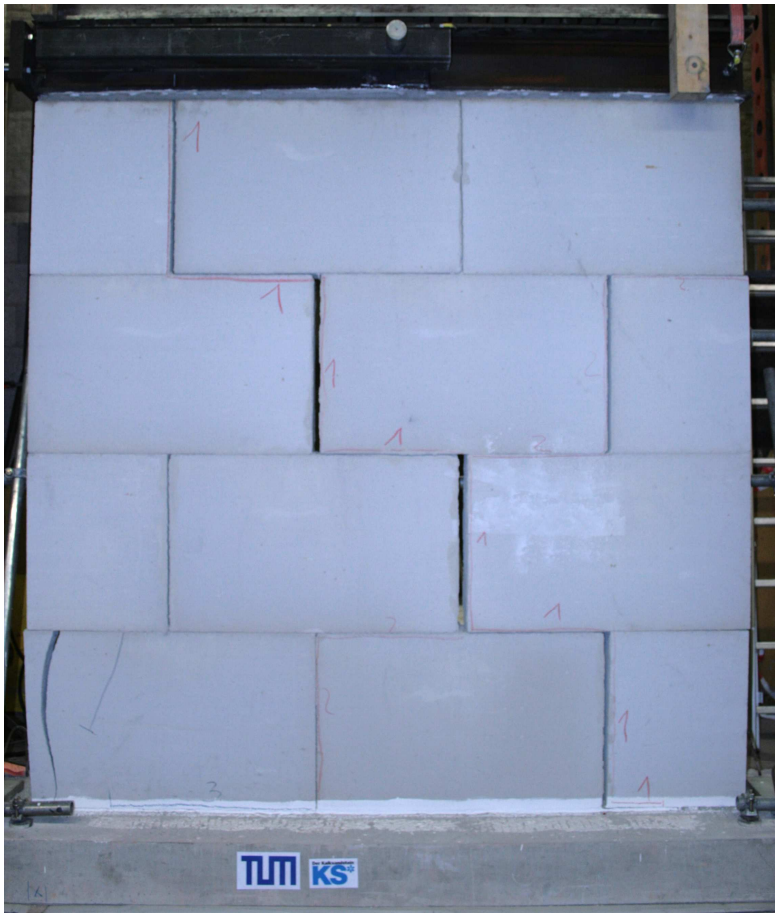

Figure 118: Crack pattern CS15

7.7. LAC01

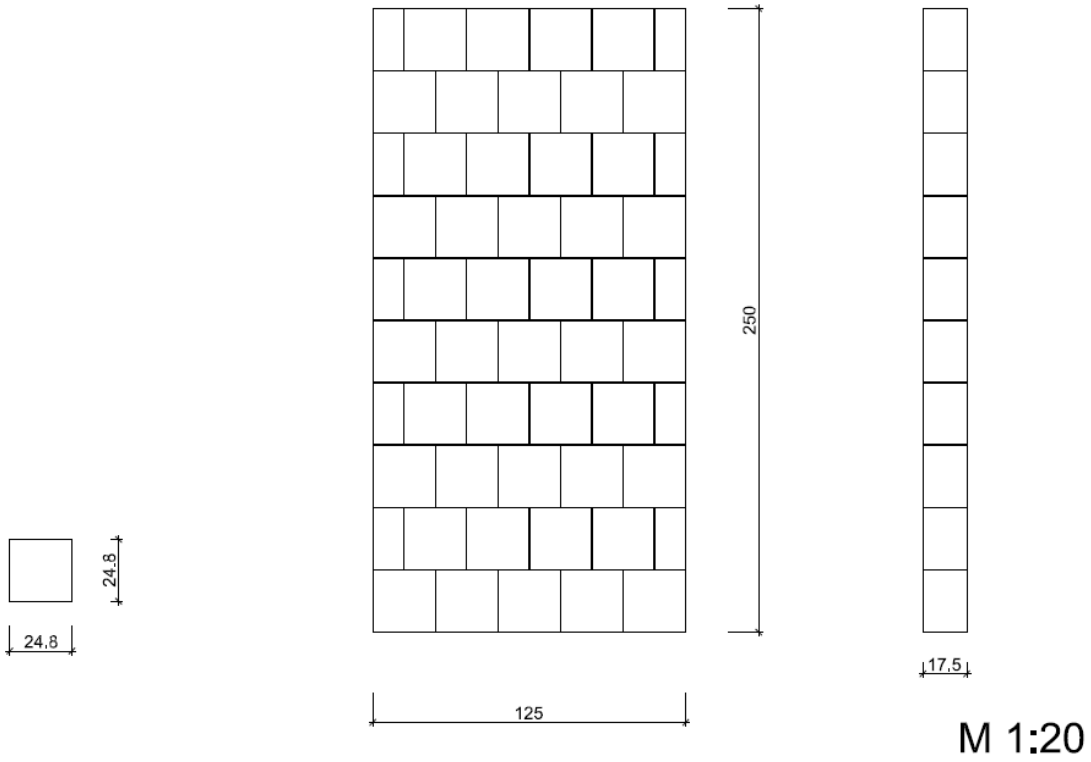

Figure 119: Dimension of the test specimen LAC01

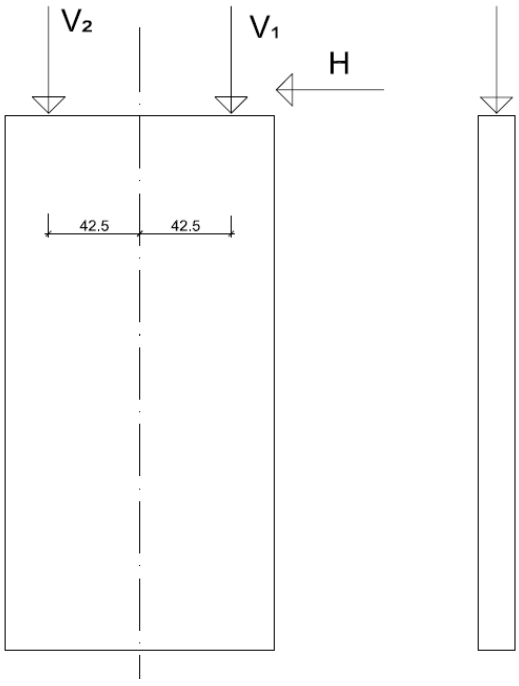

Figure 120: Position of the hydraulic actuators at test specimen LAC01

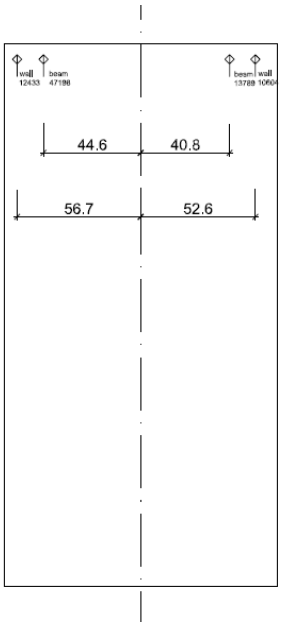

Figure 121: Position of the LVDTs at test specimen LAC01

7.7.1. Scale factor 2 (max 0.12 g)

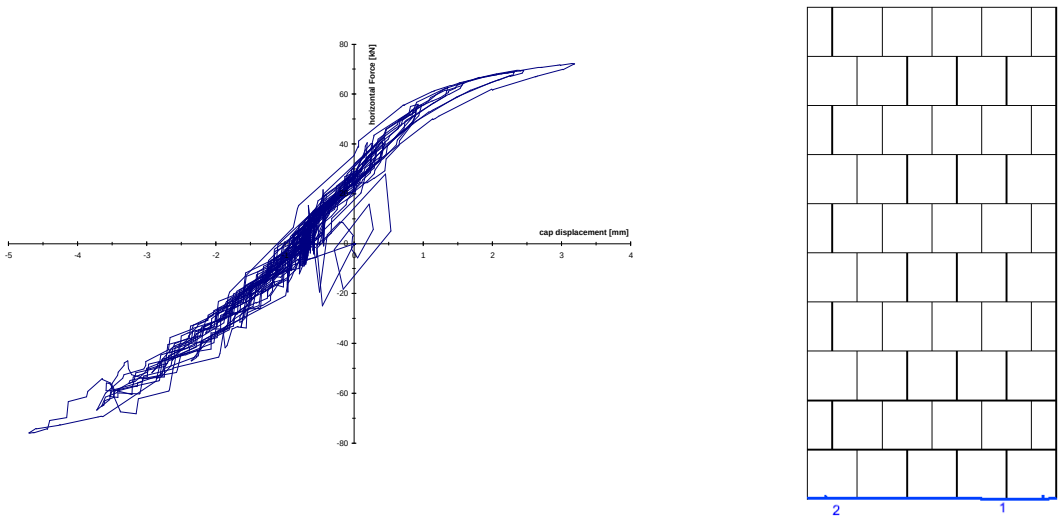

Figure 122: Load-displacement curve (hysteresis) and crack pattern of the test specimen LAC01

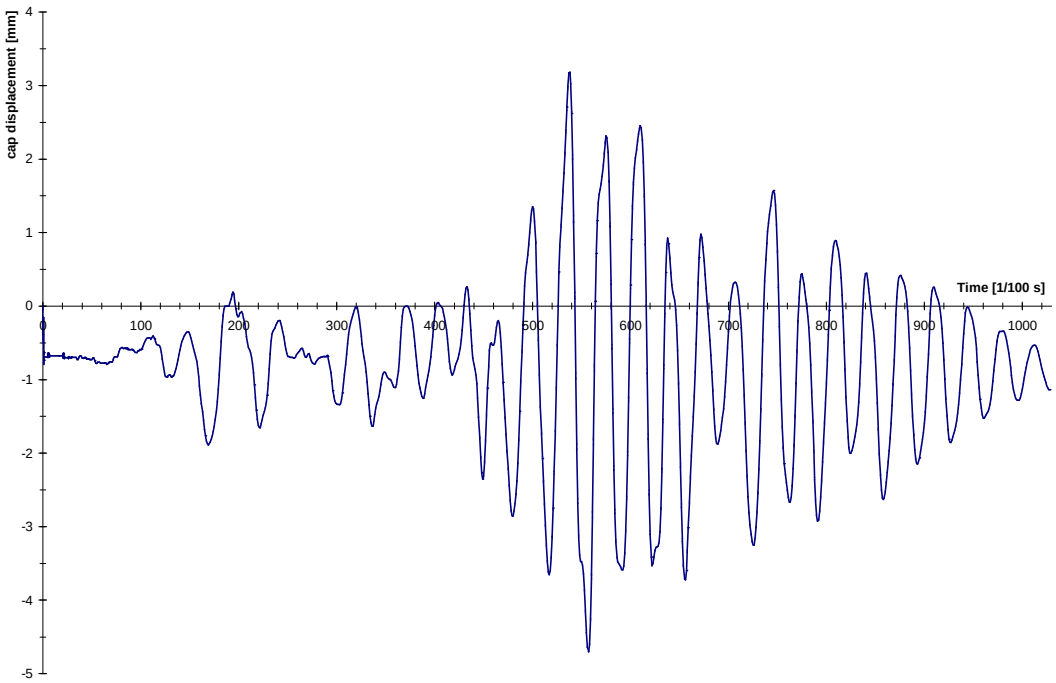

Figure 123: displacement history (earthquake time) LAC01

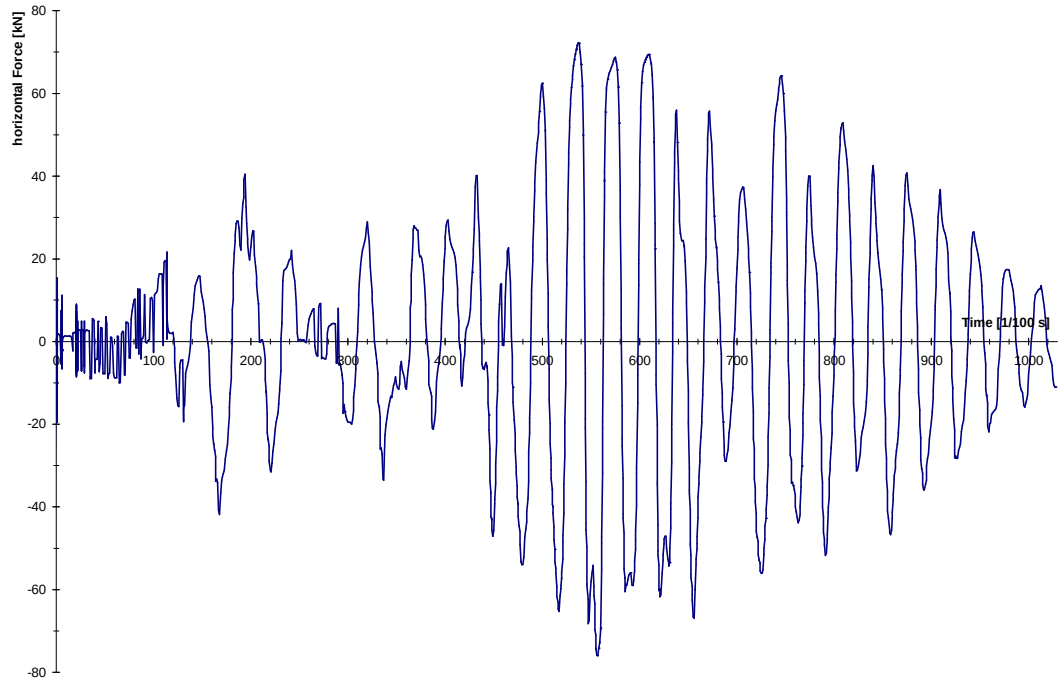

Figure 124: horizontal load history (earthquake time) LAC01

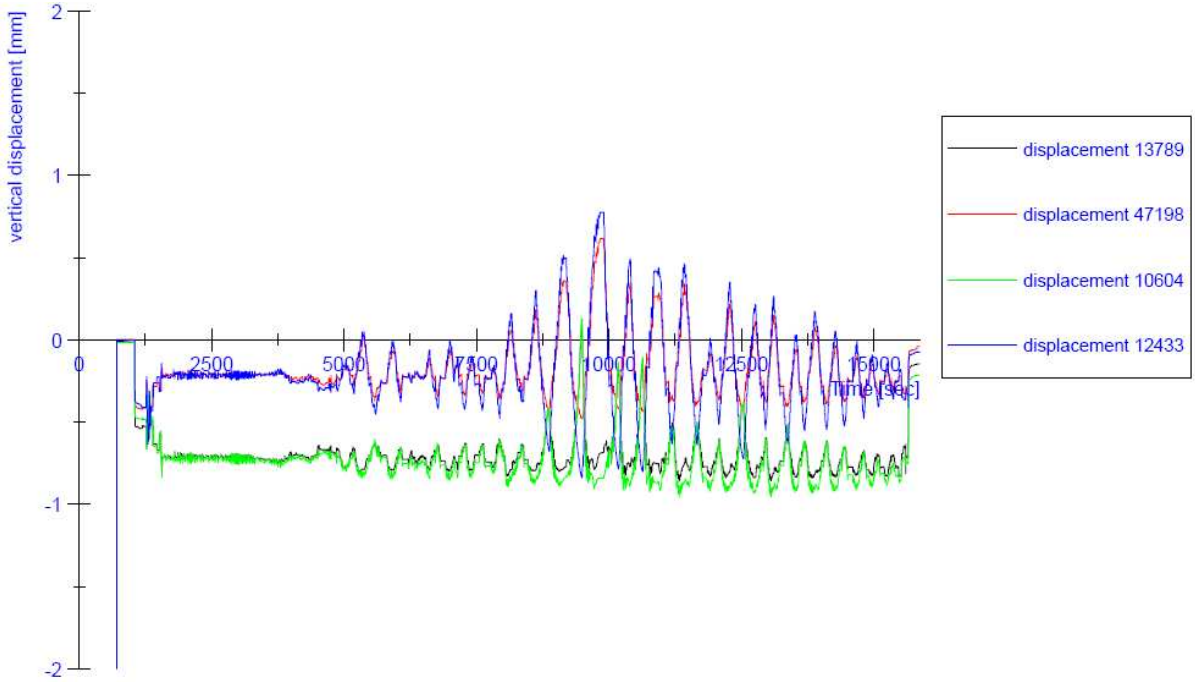

Figure 125: Progress of the vertical displacements (testing time) LAC01

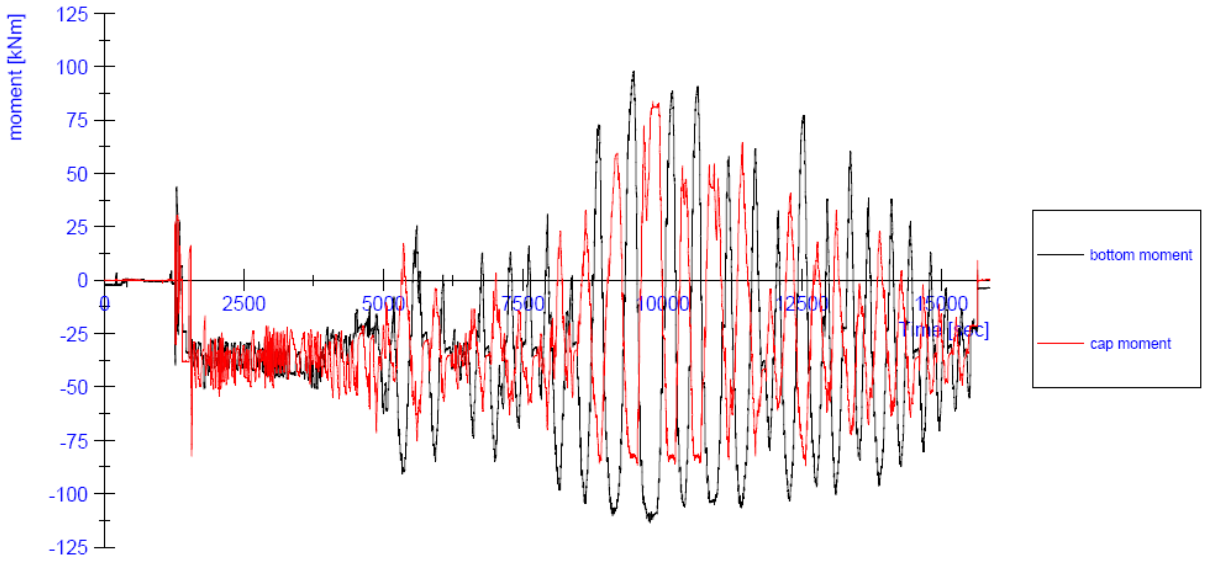

Figure 126: Progress of the in-plane bending moments at the top and at the bottom of the wall (testing time) LAC01

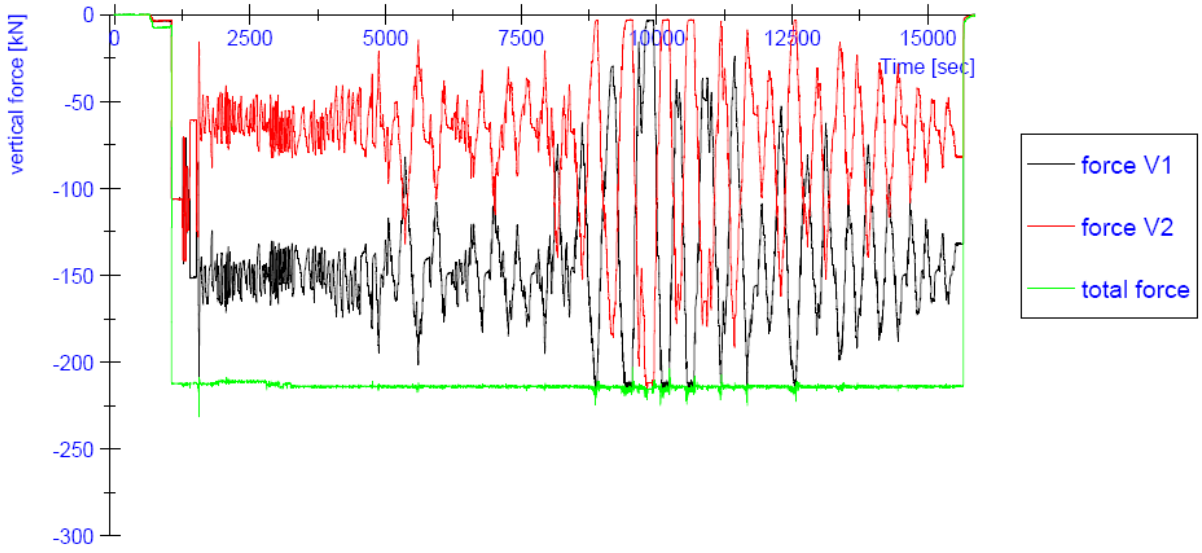

Figure 127: Progress of the vertical forces V1 and V2 (testing time) LAC01

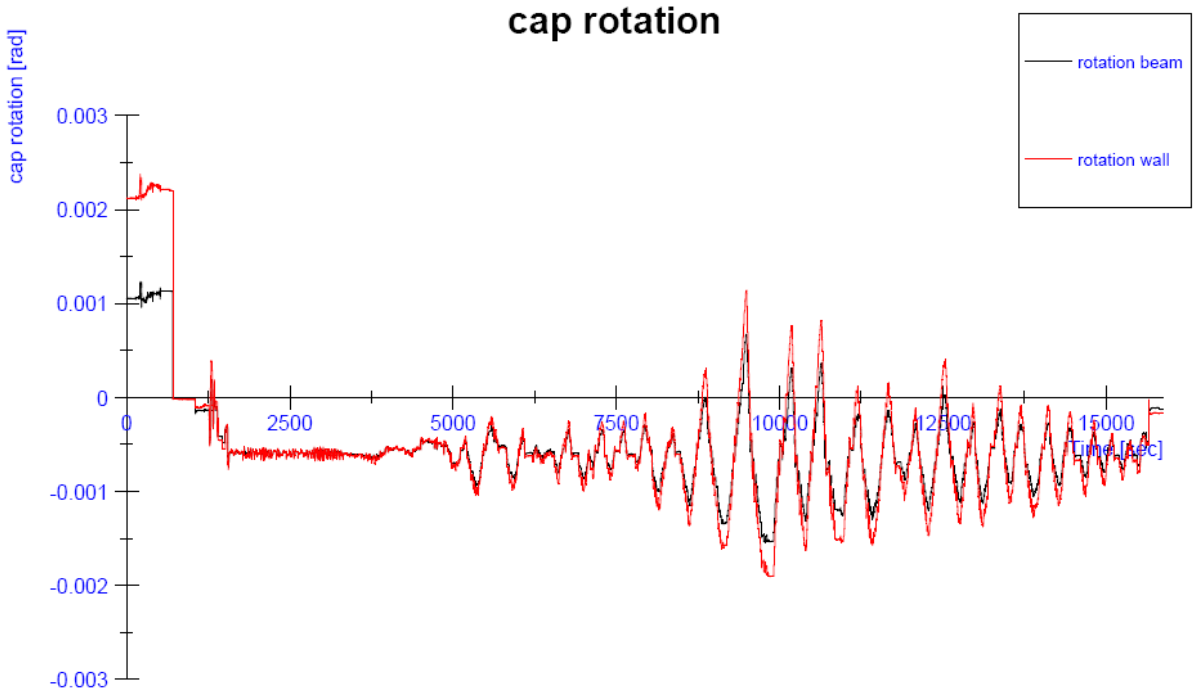

Figure 128: Progress of the in-plane rotation at the top of the wall (testing time) LAC01

Figure 129: Crack pattern LAC01

7.7.2. Scale factor 3 (max 0.17 g)

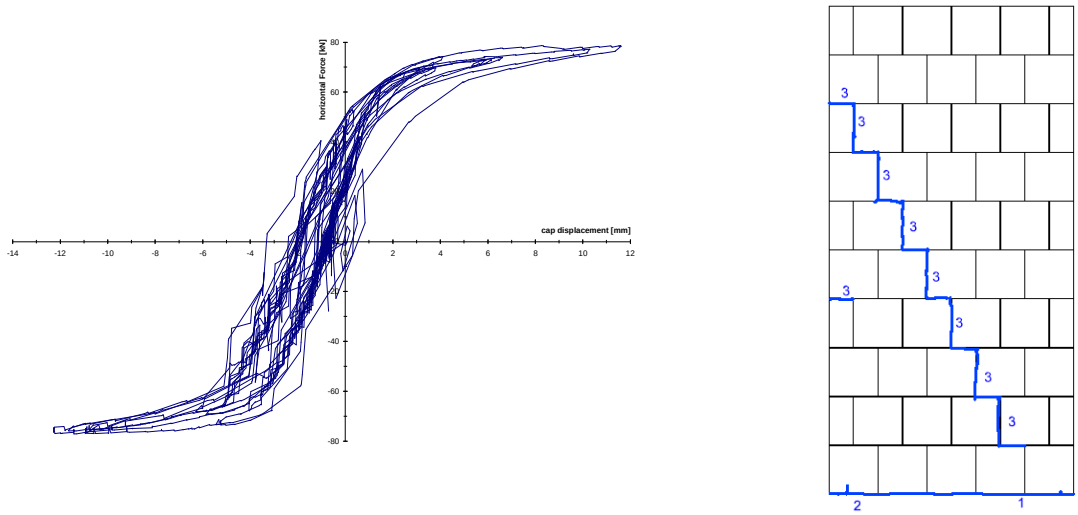

Figure 130: Load-displacement curve (hysteresis) and crack pattern of the test specimen LAC01

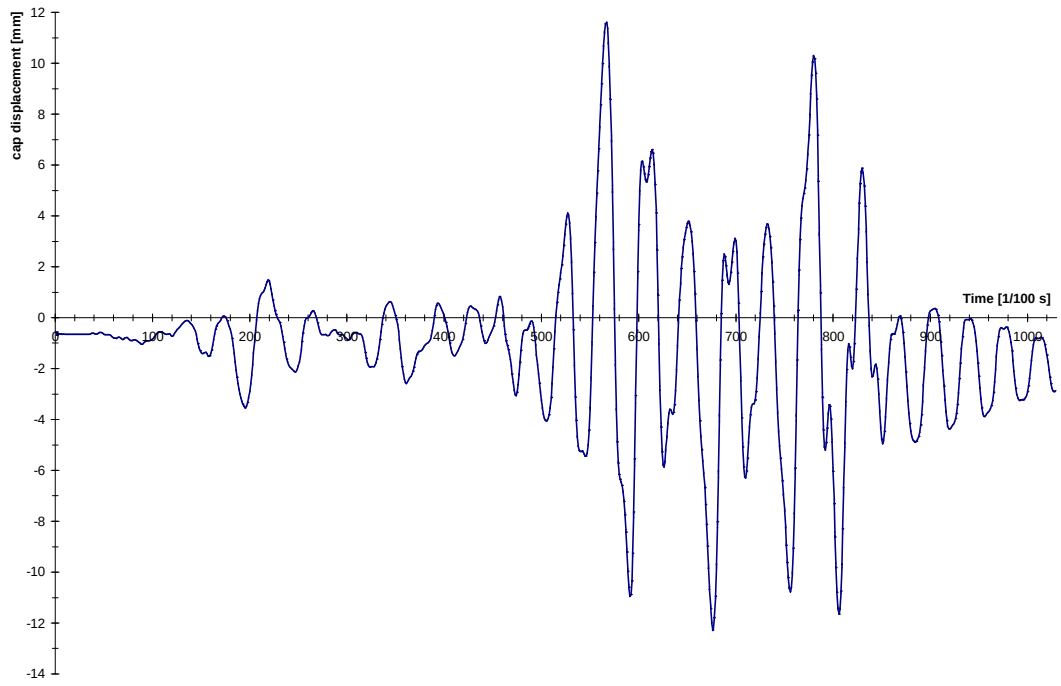

Figure 131: displacement history (earthquake time) LAC01

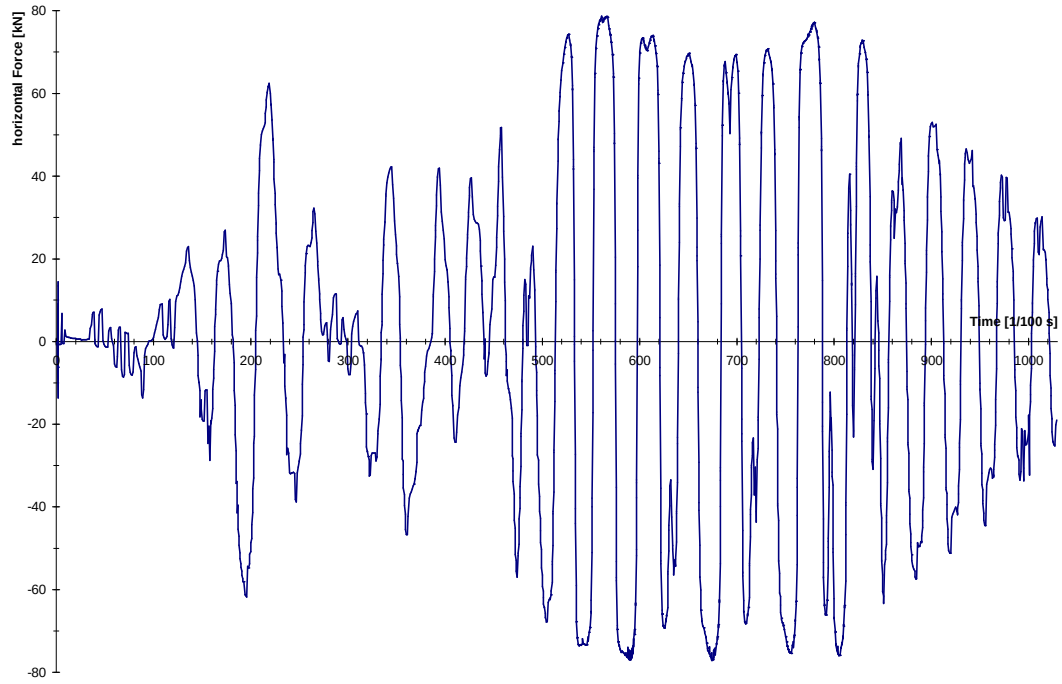

Figure 132: horizontal load history (earthquake time) LAC01

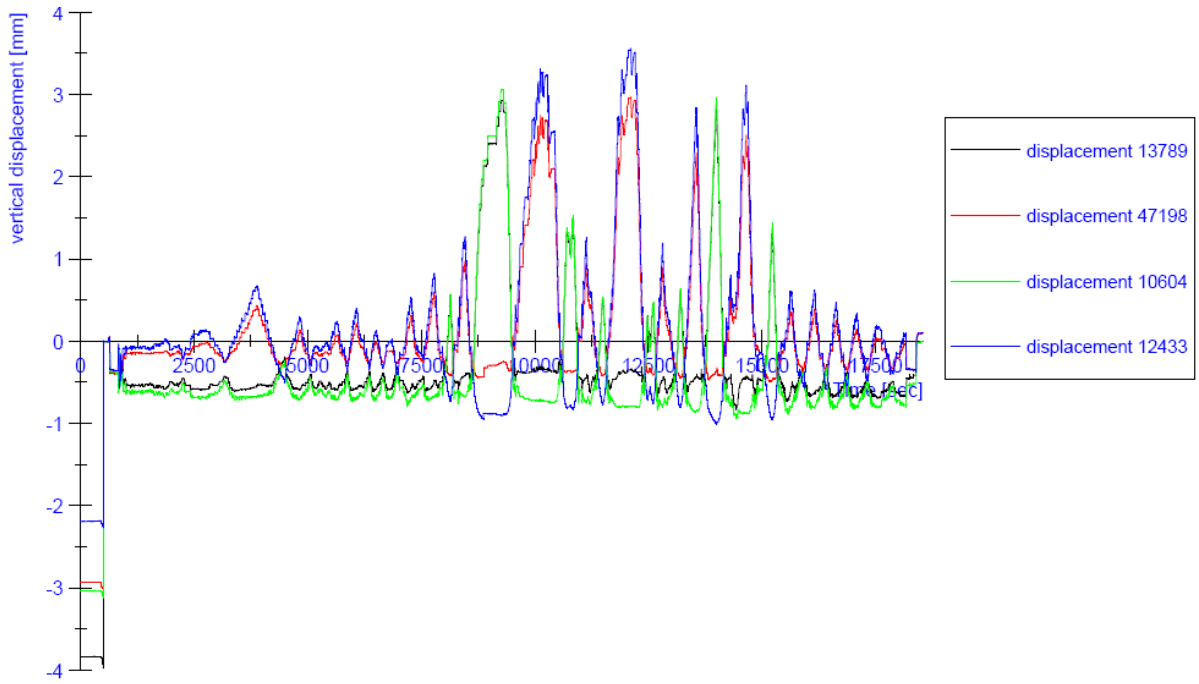

Figure 133: Progress of the vertical displacements (testing time) LAC01

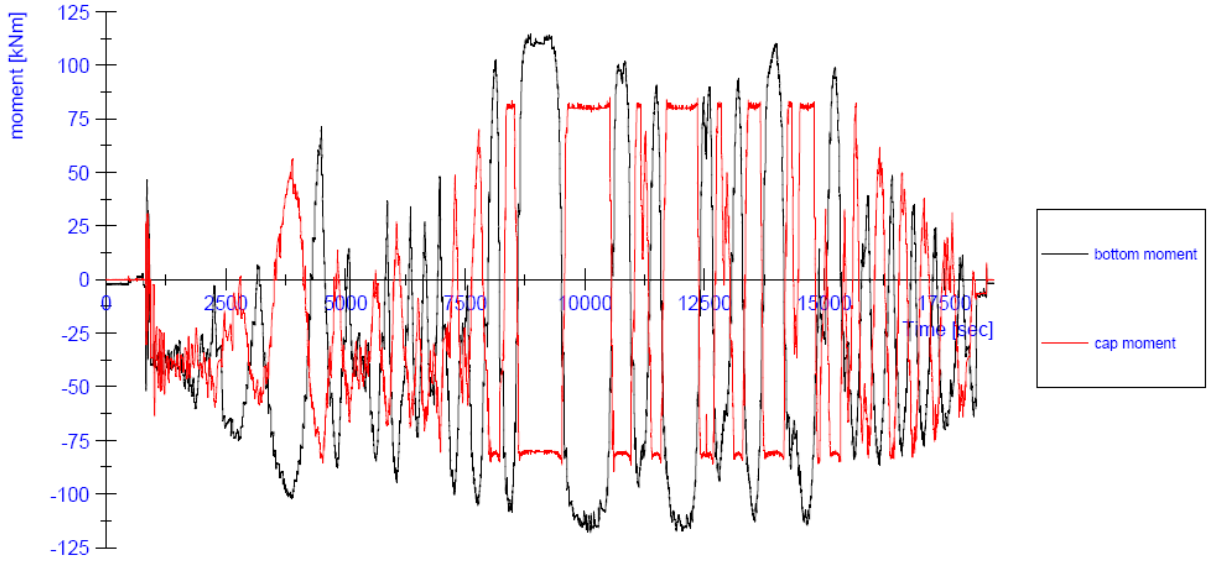

Figure 134: Progress of the in-plane bending moments at the top and at the bottom of the wall (testing time) LAC01

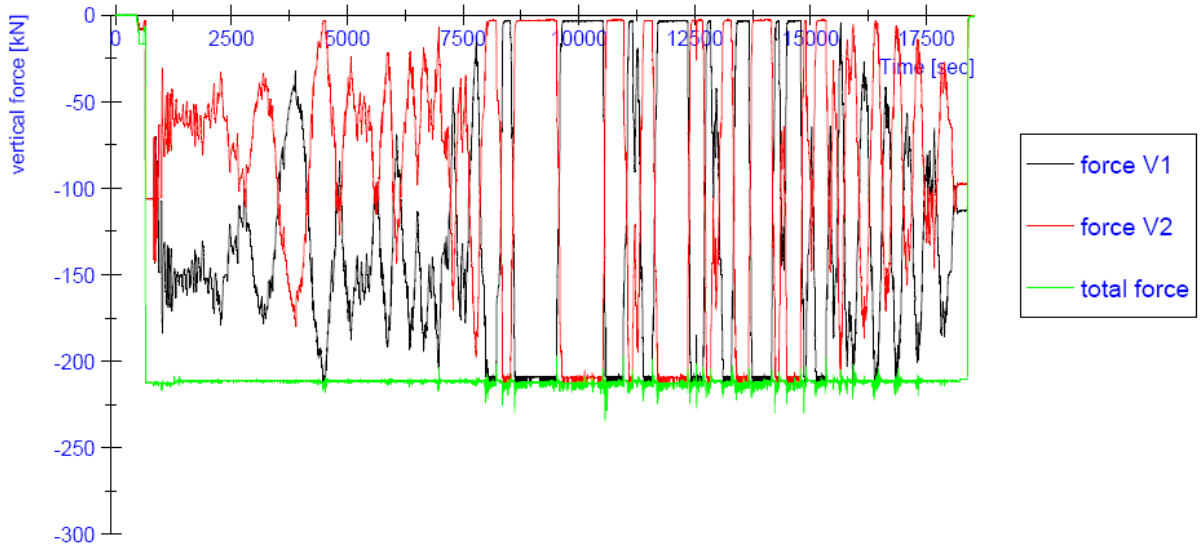

Figure 135: Progress of the vertical forces V1 and V2 (testing time) LAC01

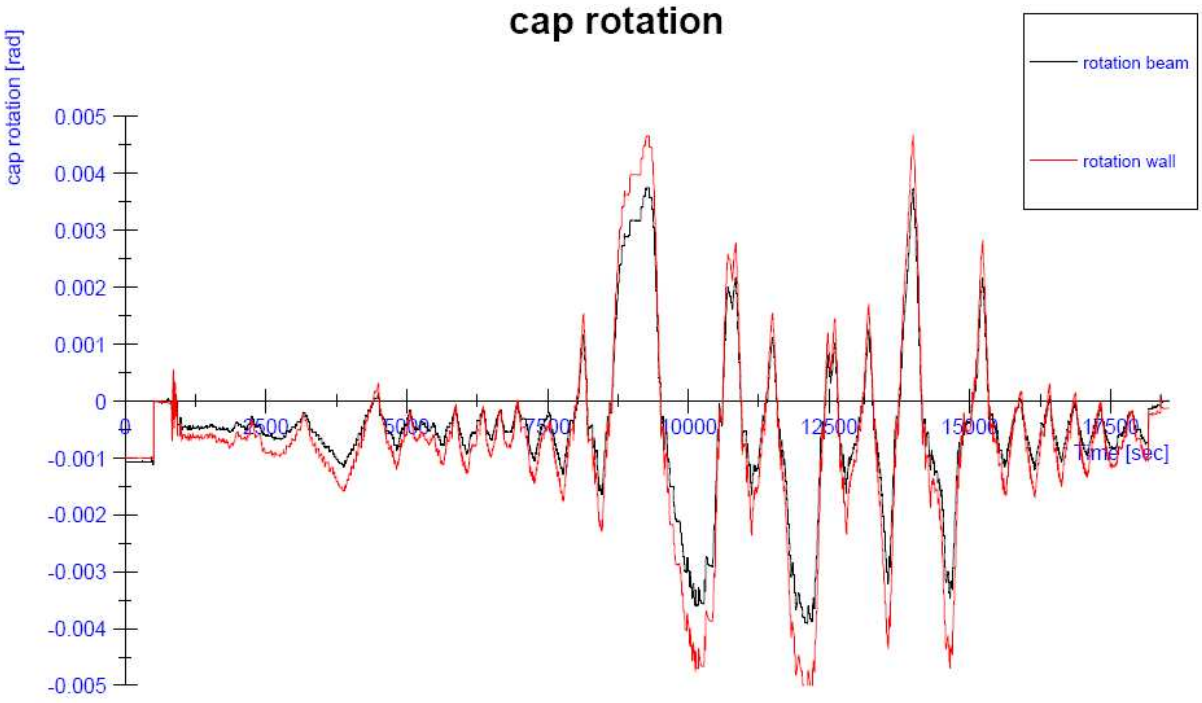

Figure 136: Progress of the in-plane rotation at the top of the wall (testing time) LAC01

7.7.3. Scale factor 5 (max 0.29 g)

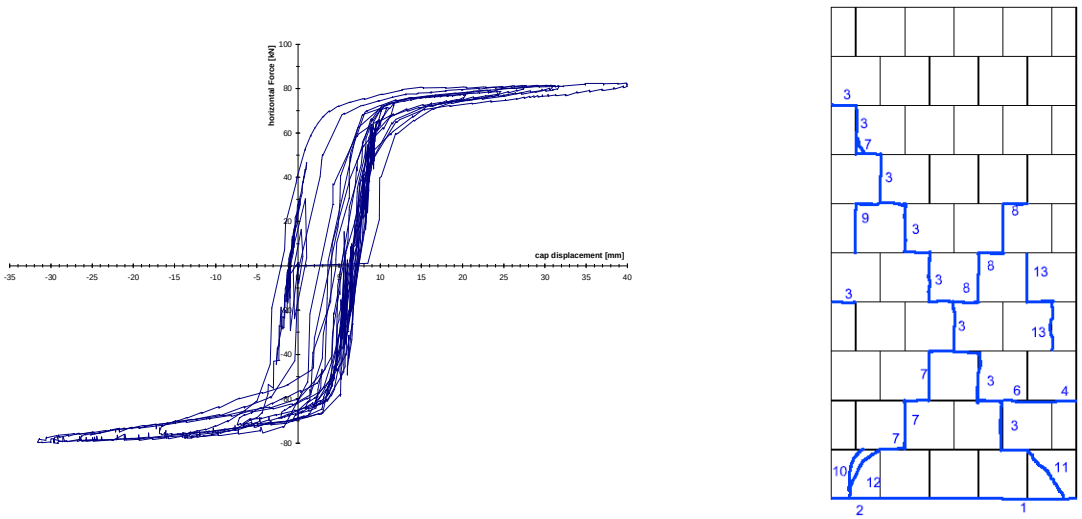

Figure 137: Load-displacement curve (hysteresis) and crack pattern of the test specimen LAC01

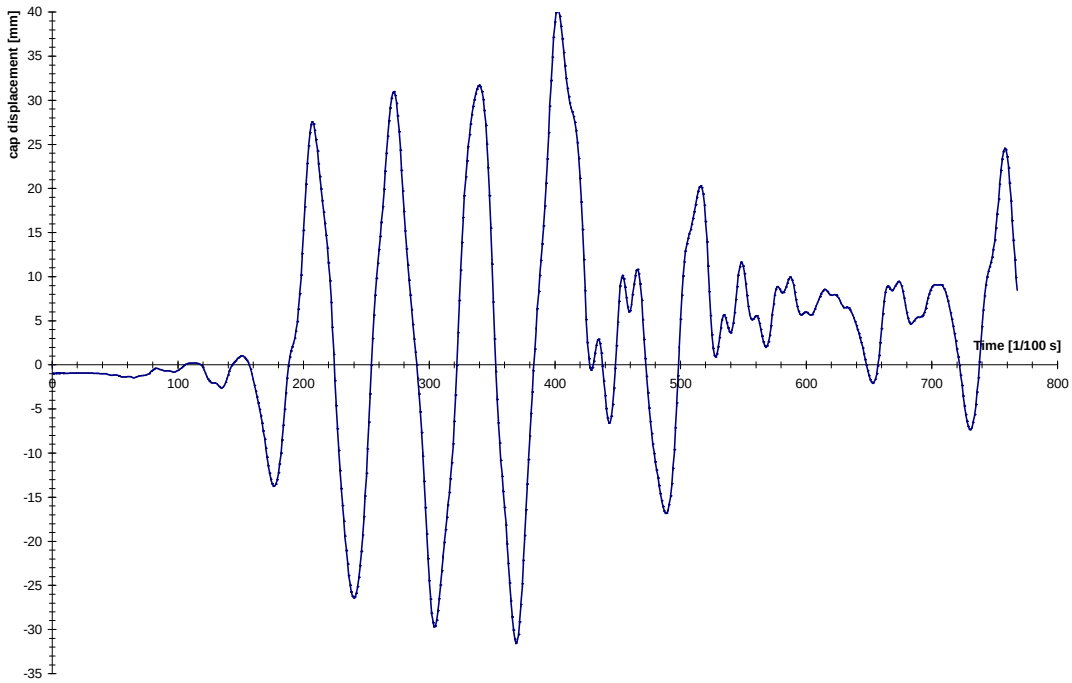

Figure 138: displacement history (earthquake time) LAC01

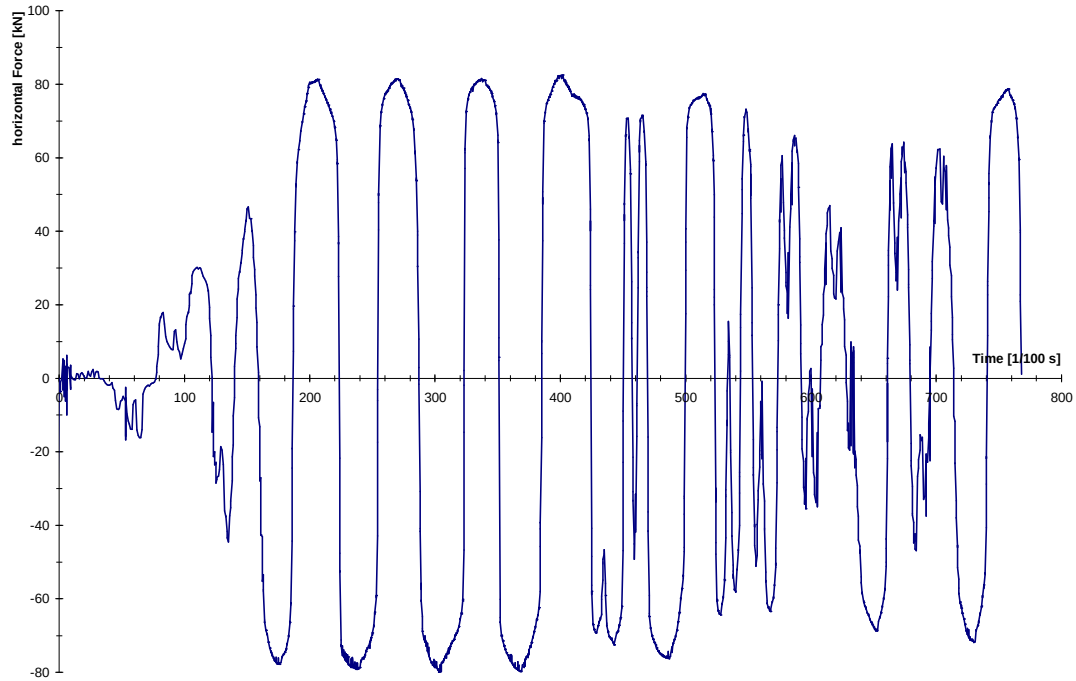

Figure 139: horizontal load history (earthquake time) LAC01

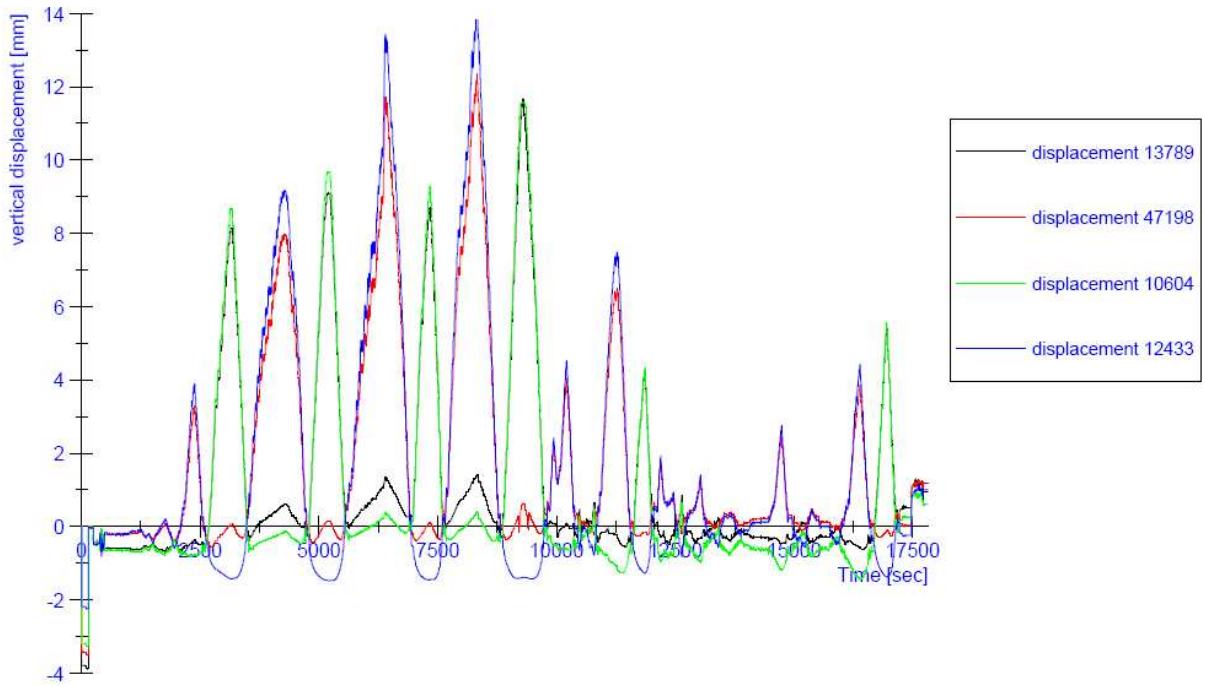

Figure 140: Progress of the vertical displacements (testing time) LAC01

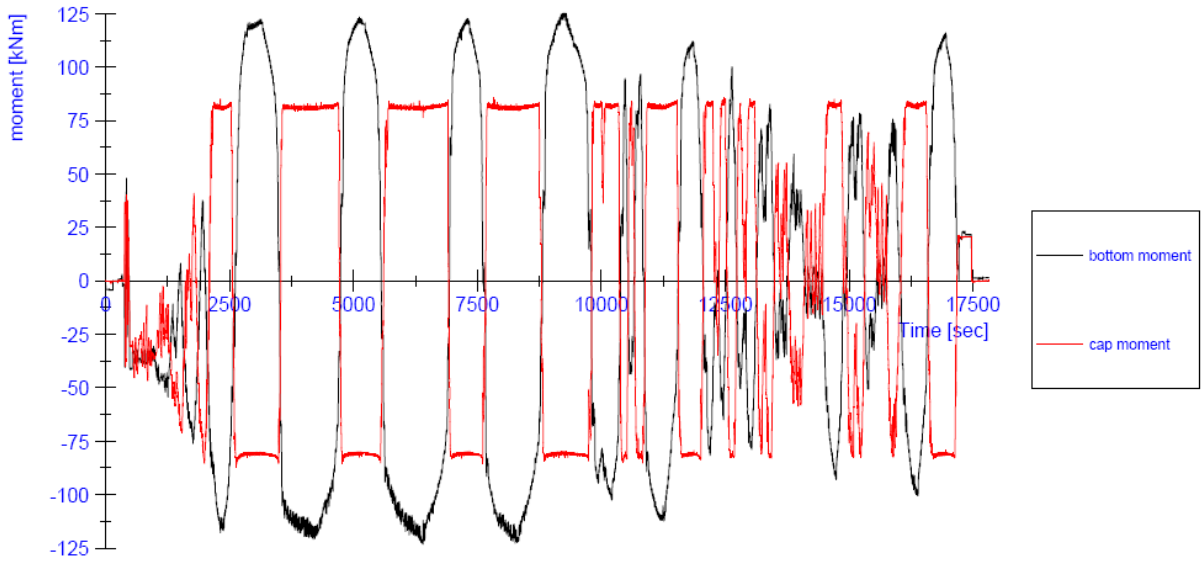

Figure 141: Progress of the in-plane bending moments at the top and at the bottom of the wall (testing time) LAC01

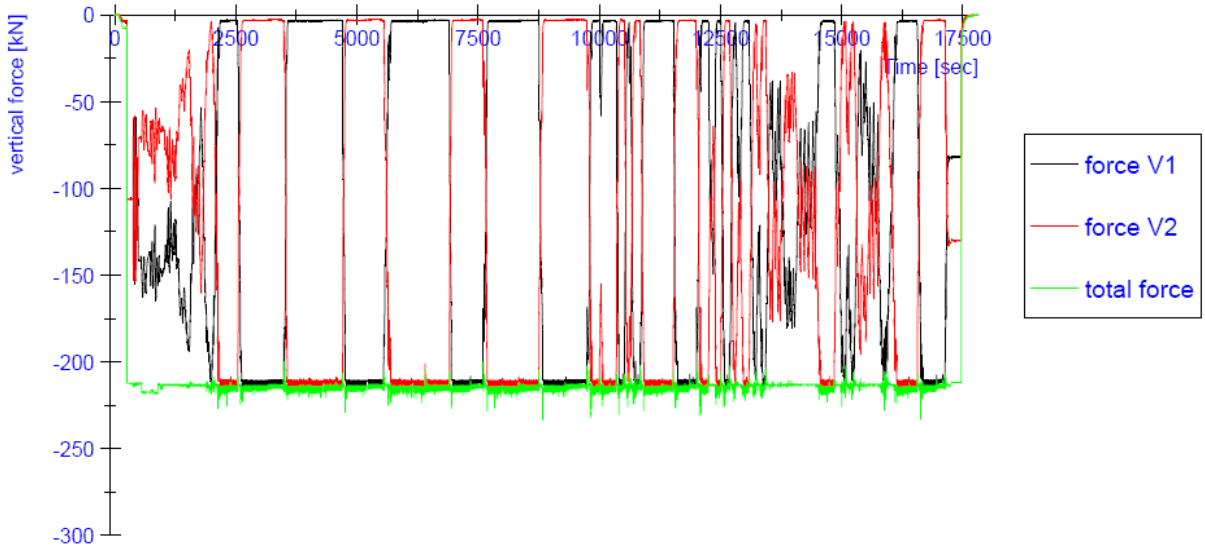

Figure 142: Progress of the vertical forces V1 and V2 (testing time) LAC01

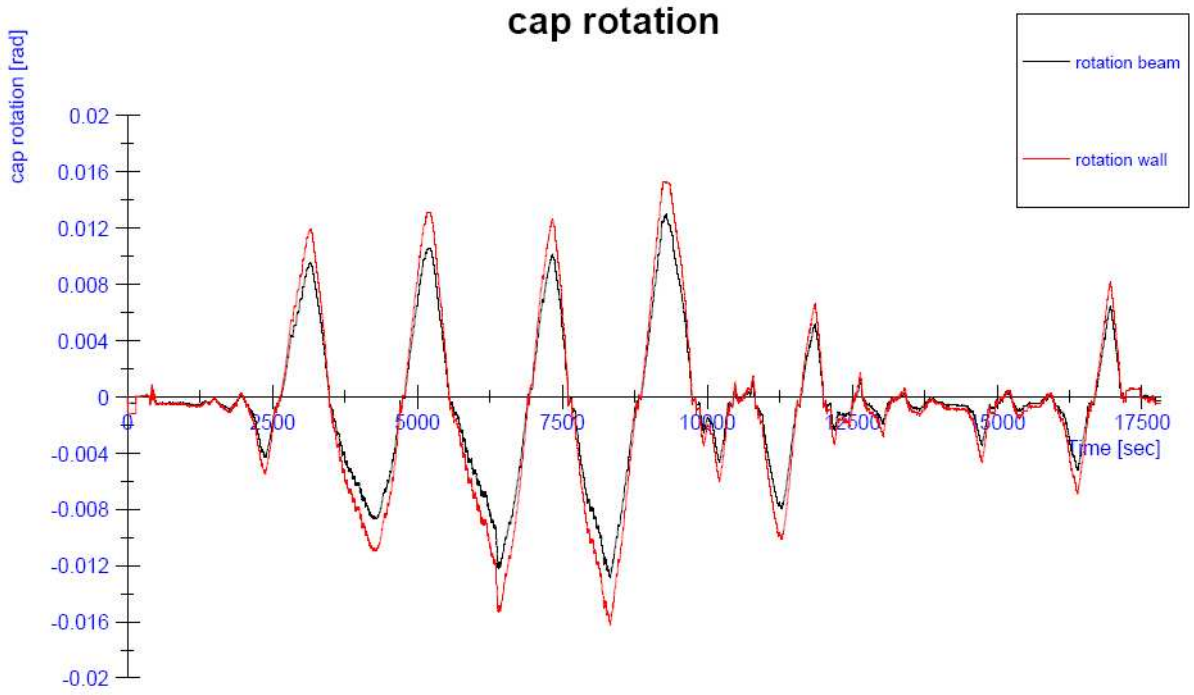

Figure 143: Progress of the in-plane rotation at the top of the wall (testing time) LAC01

Figure 144: Crack pattern LAC01

7.8. LAC02

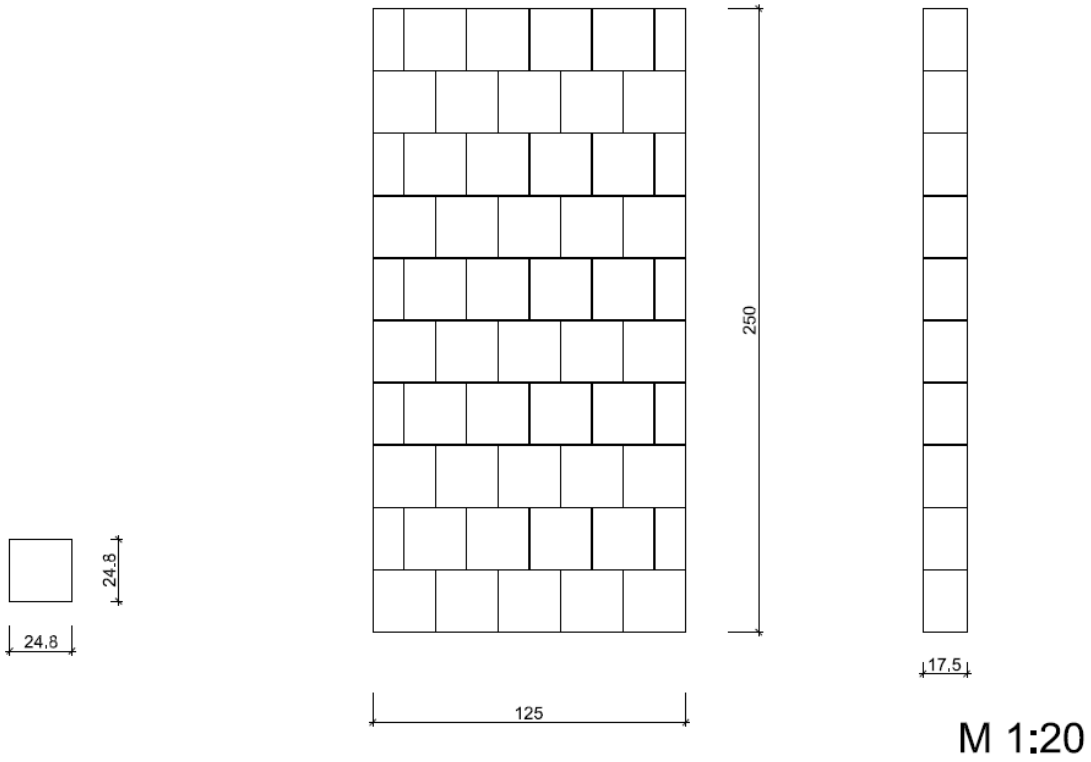

Figure 145: Dimension of the test specimen LAC02

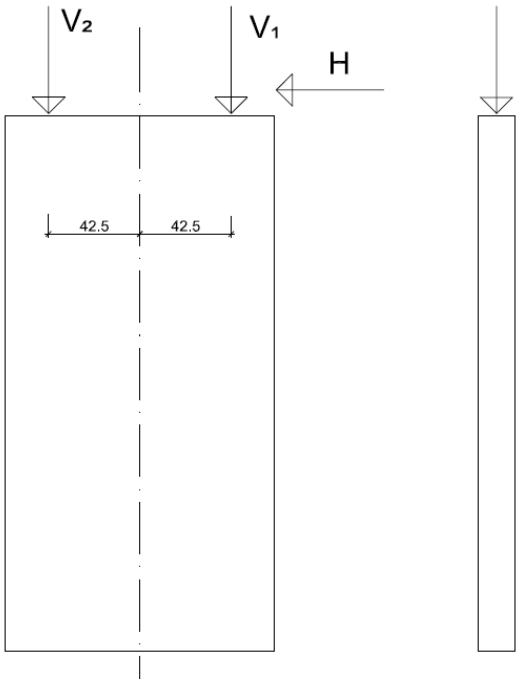

Figure 146: Position of the hydraulic actuators at test specimen LAC02

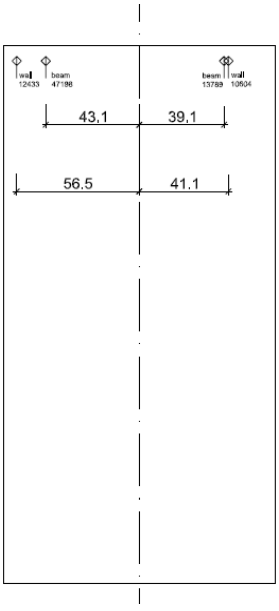

Figure 147: Position of the LVDTs at test specimen LAC02

7.8.1. Scale factor 2.5 (max 0.14 g)

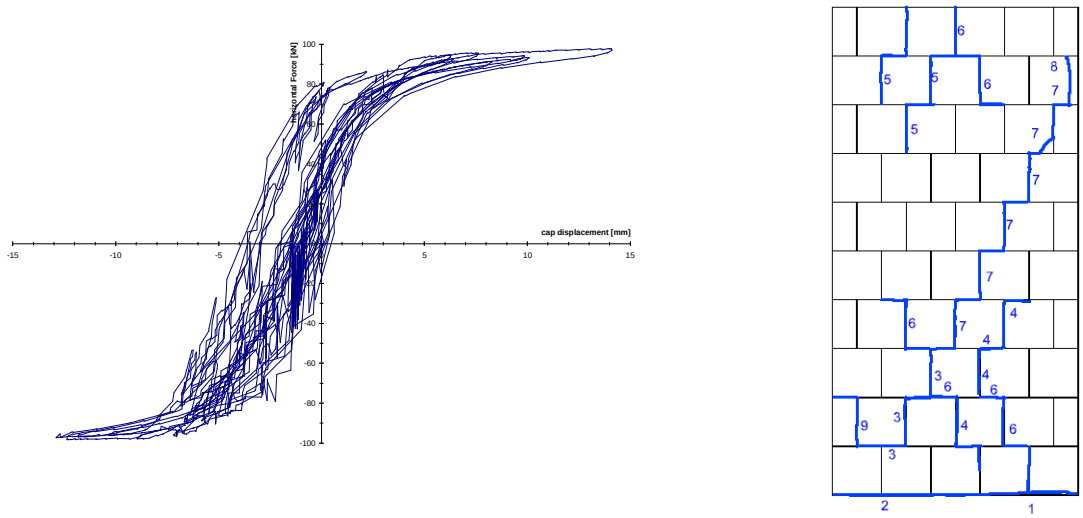

Figure 148: Load-displacement curve (hysteresis) and crack pattern of the test specimen LAC02

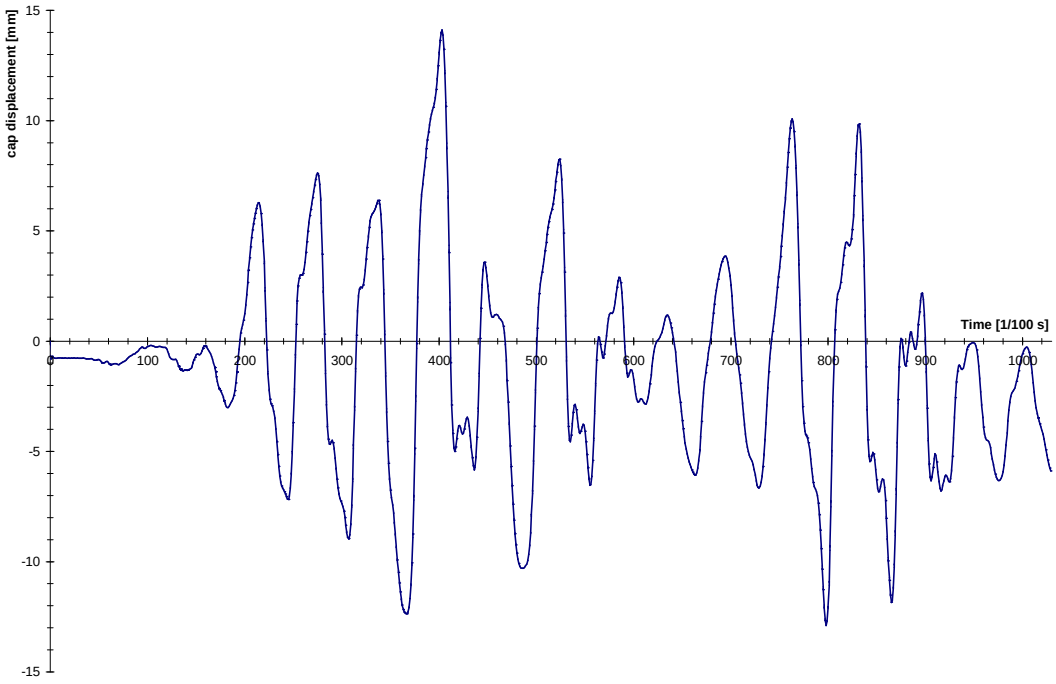

Figure 149: displacement history (earthquake time) LAC02

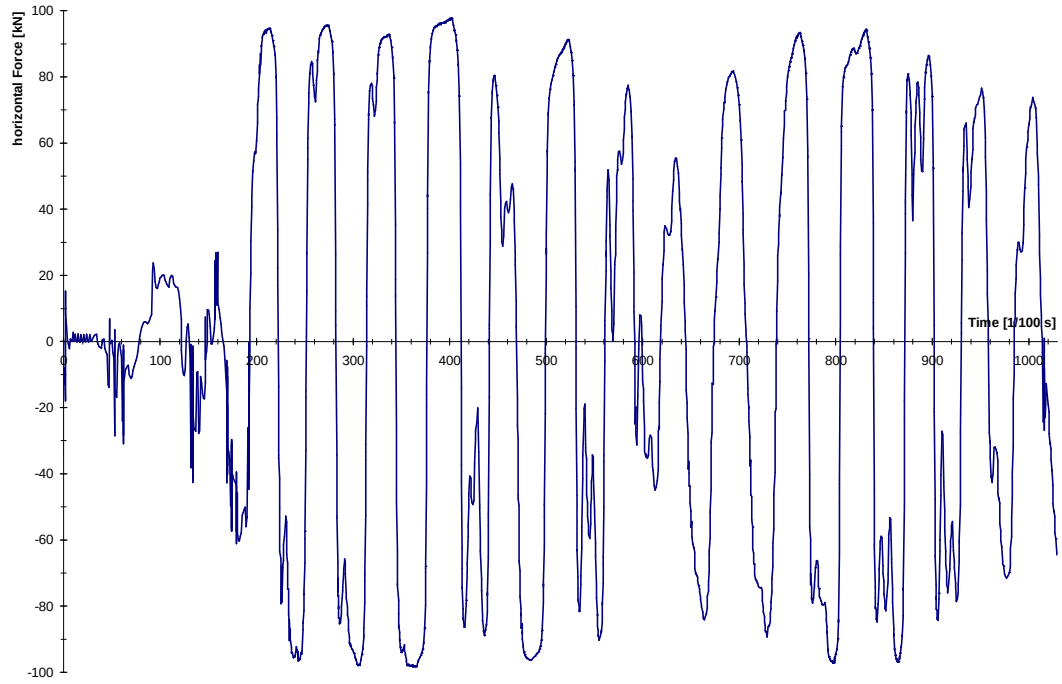

Figure 150: horizontal load history (earthquake time) LAC02

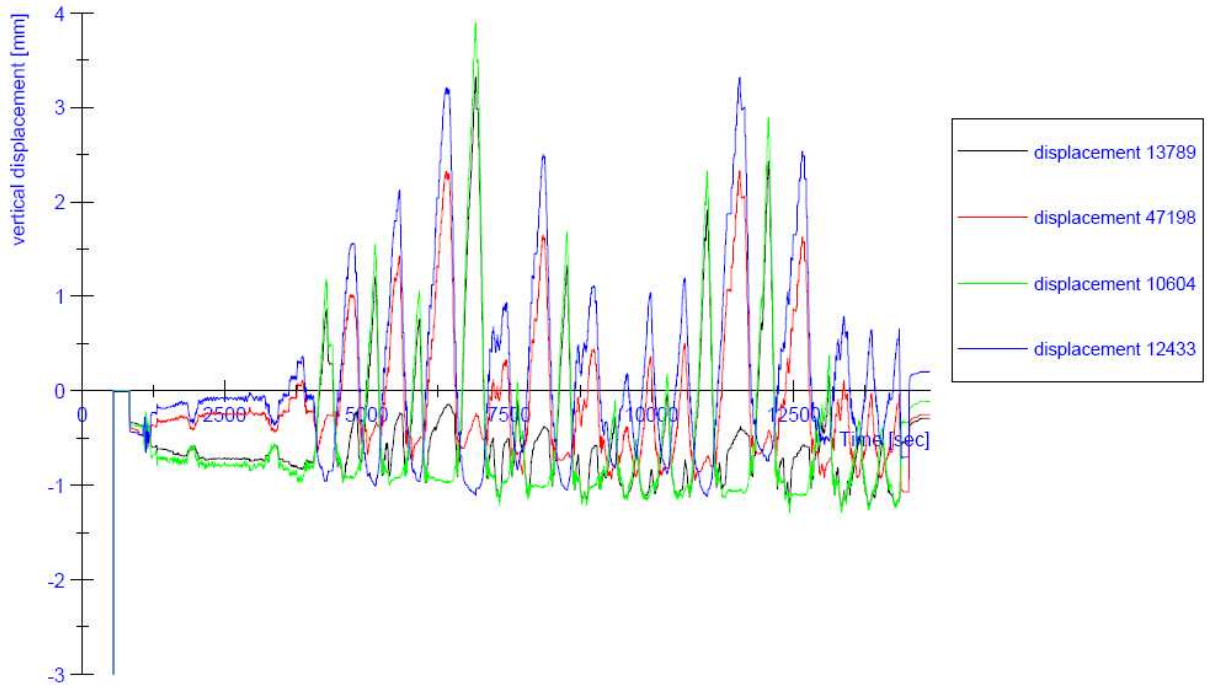

Figure 151: Progress of the vertical displacements (testing time) LAC02

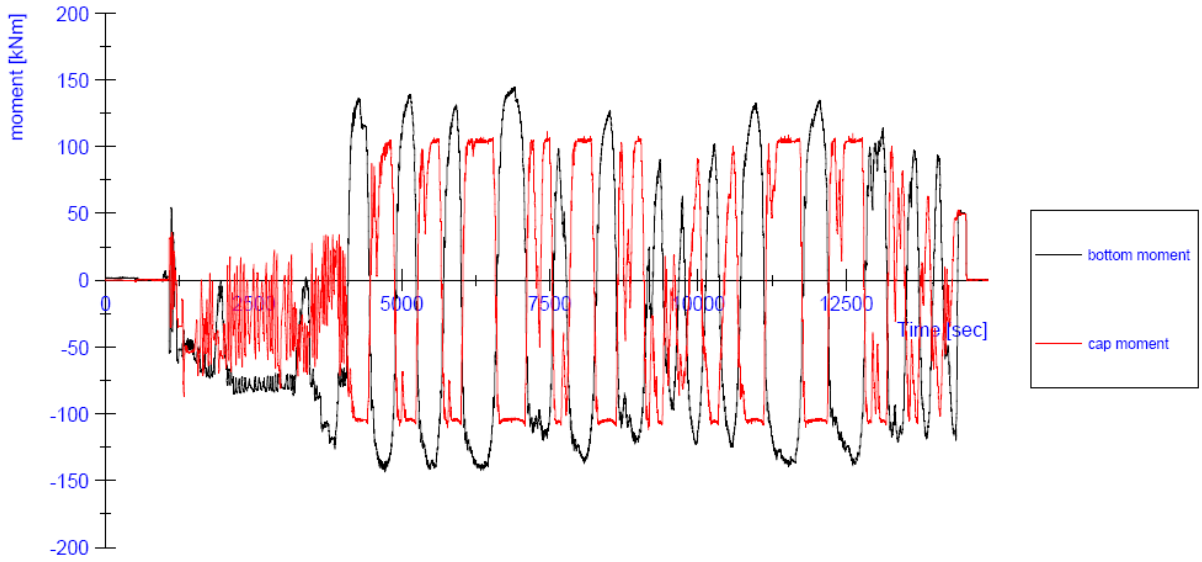

Figure 152: Progress of the in-plane bending moments at the top and at the bottom of the wall (testing time) LAC02

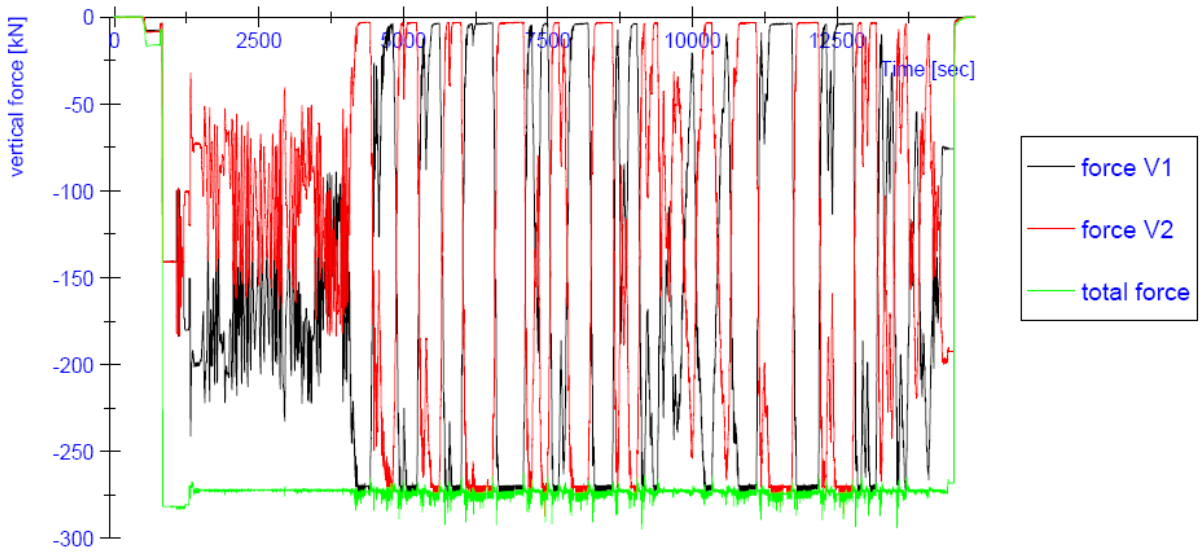

Figure 153: Progress of the vertical forces V1 and V2 (testing time) LAC02

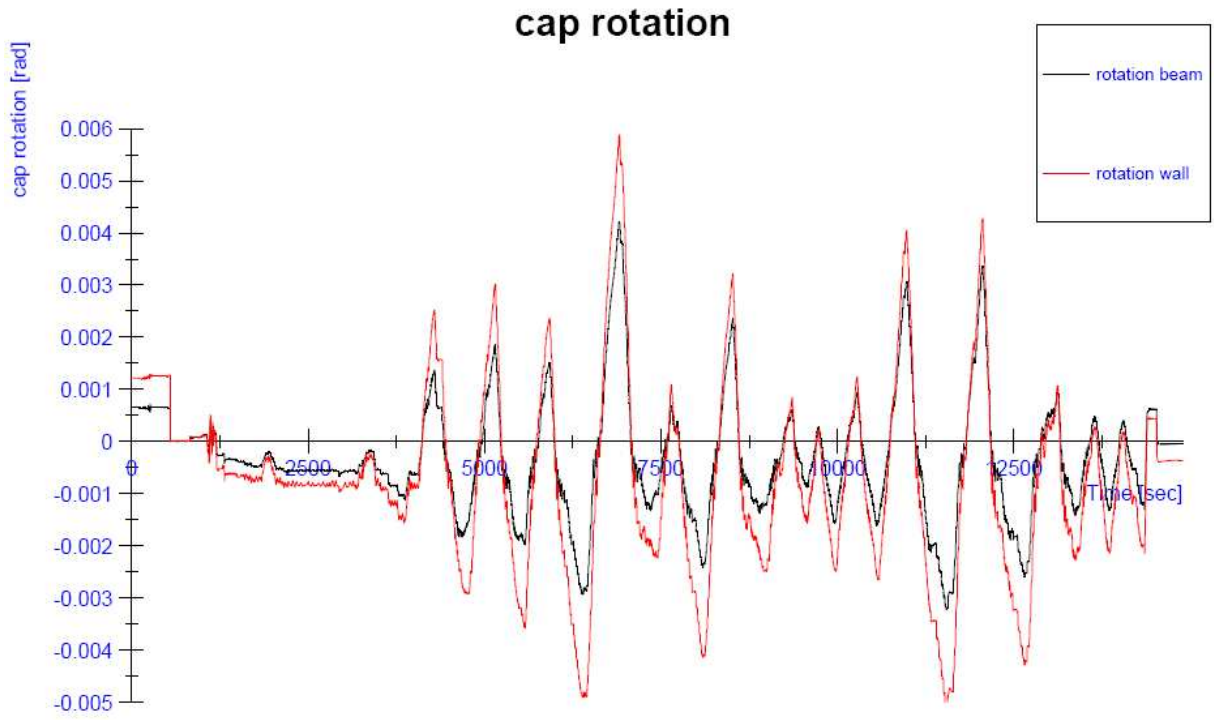

Figure 154: Progress of the in-plane rotation at the top of the wall (testing time) LAC02

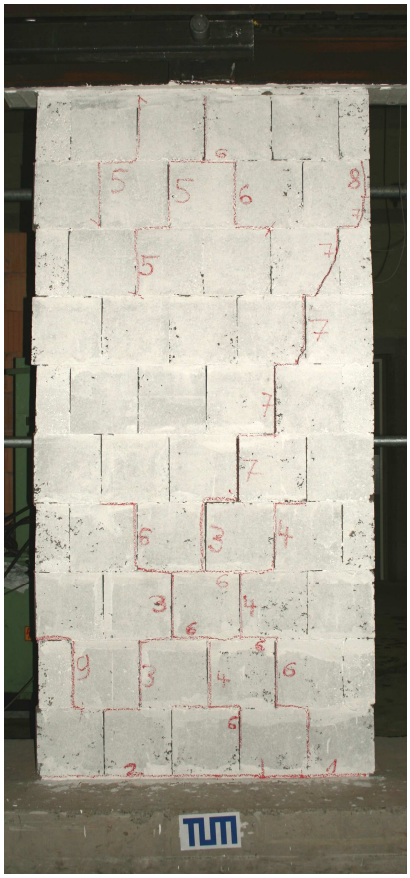

Figure 155: Crack pattern LAC02

7.9. LAC03

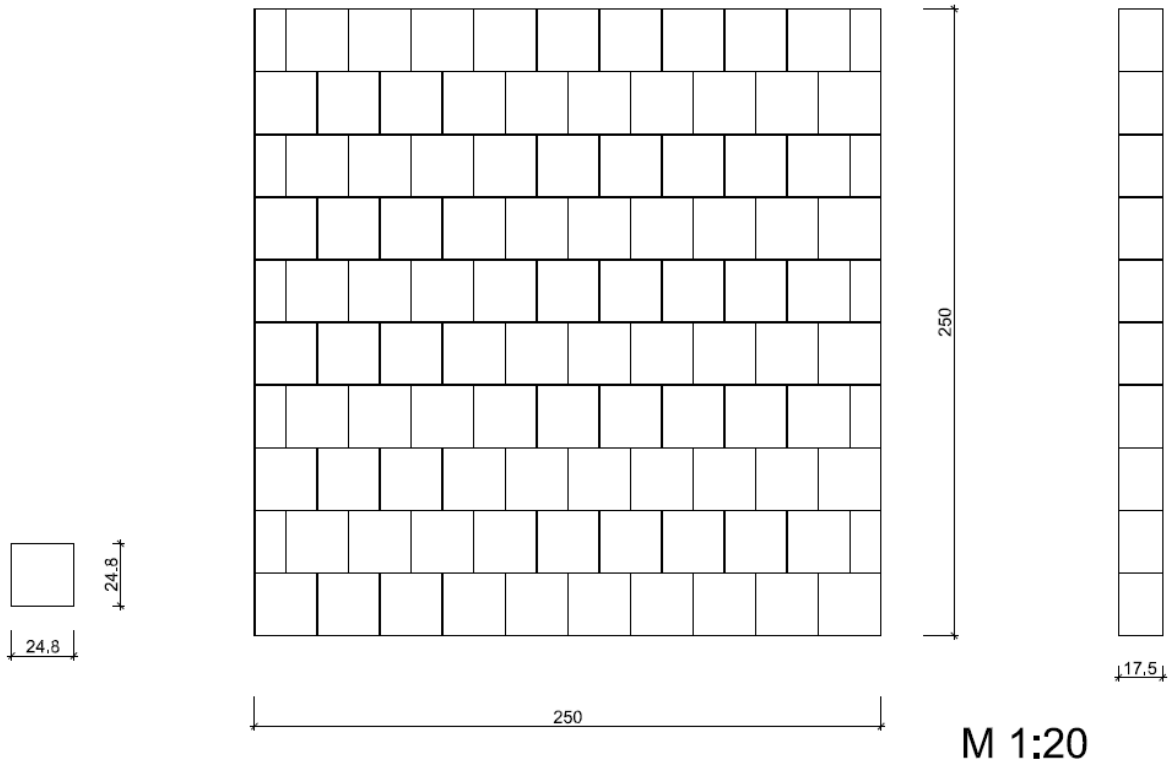

Figure 156: Dimension of the test specimen LAC03

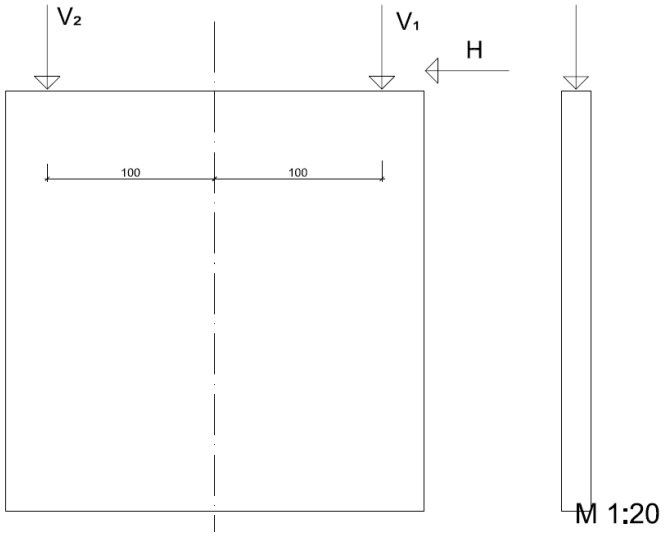

Figure 157: Position of the hydraulic actuators at test specimen LAC03

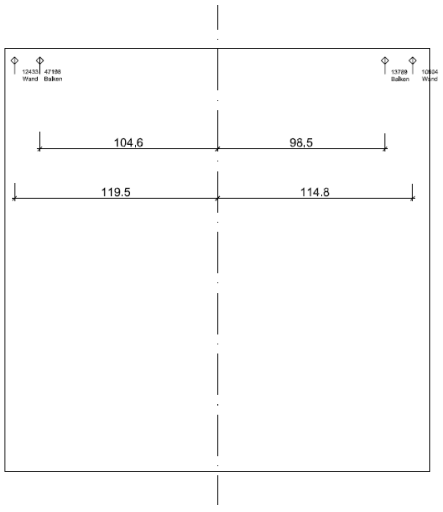

Figure 158: Position of the LVDTs at test specimen LAC03

7.9.1. Scale factor 2.5 (max 0.14 g)

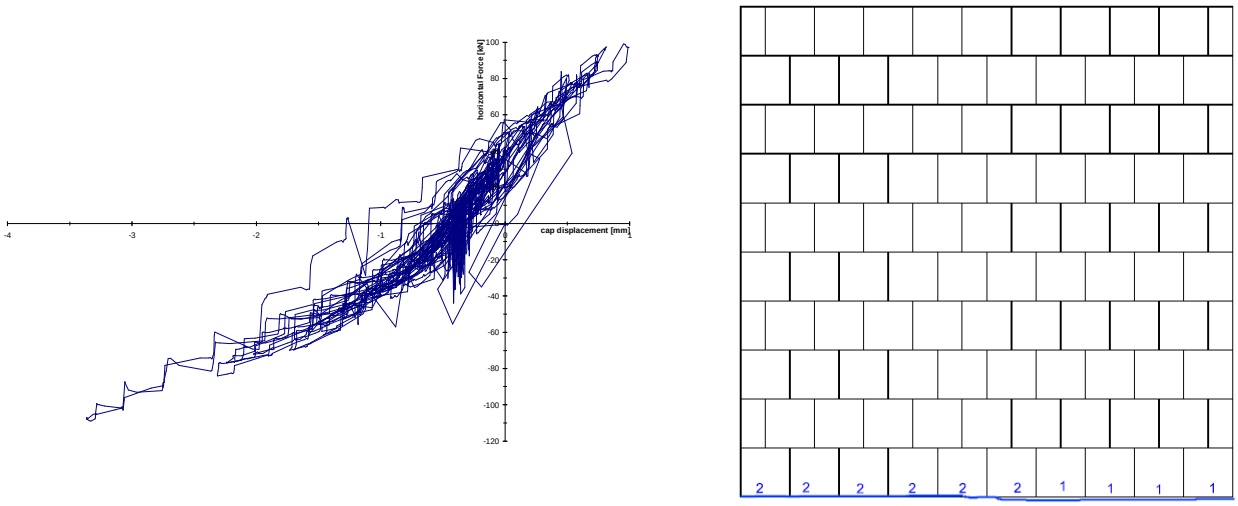

Figure 159: Load-displacement curve (hysteresis) and crack pattern of the test specimen LAC03

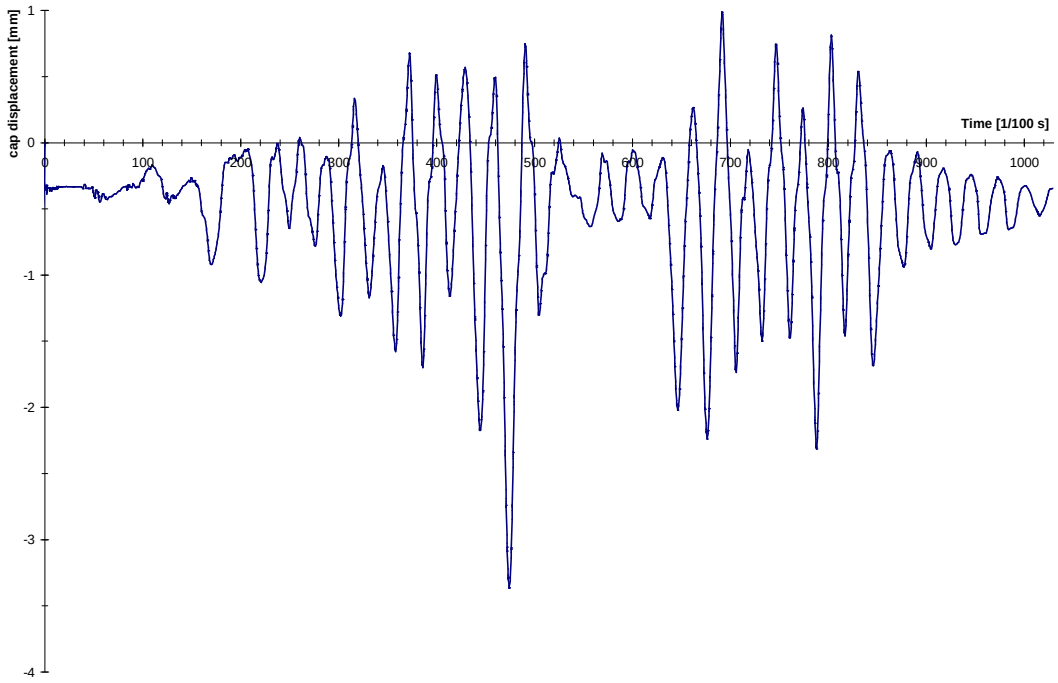

Figure 160: displacement history (earthquake time) LAC03

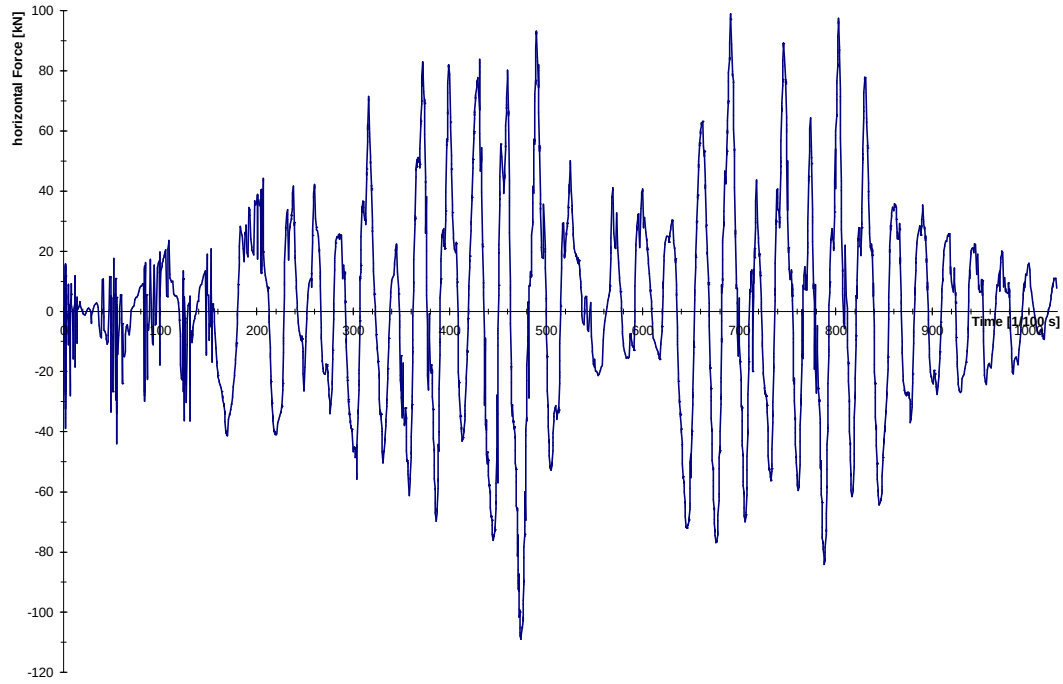

Figure 161: horizontal load history (earthquake time) LAC03

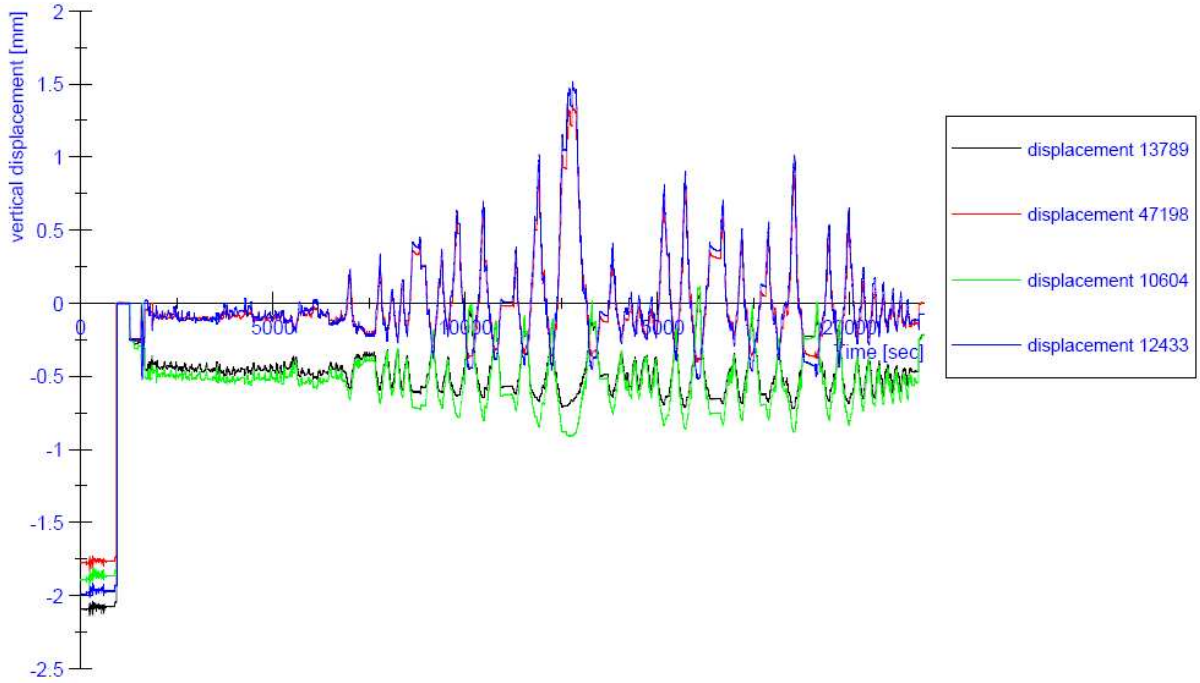

Figure 162: Progress of the vertical displacements (testing time) LAC03

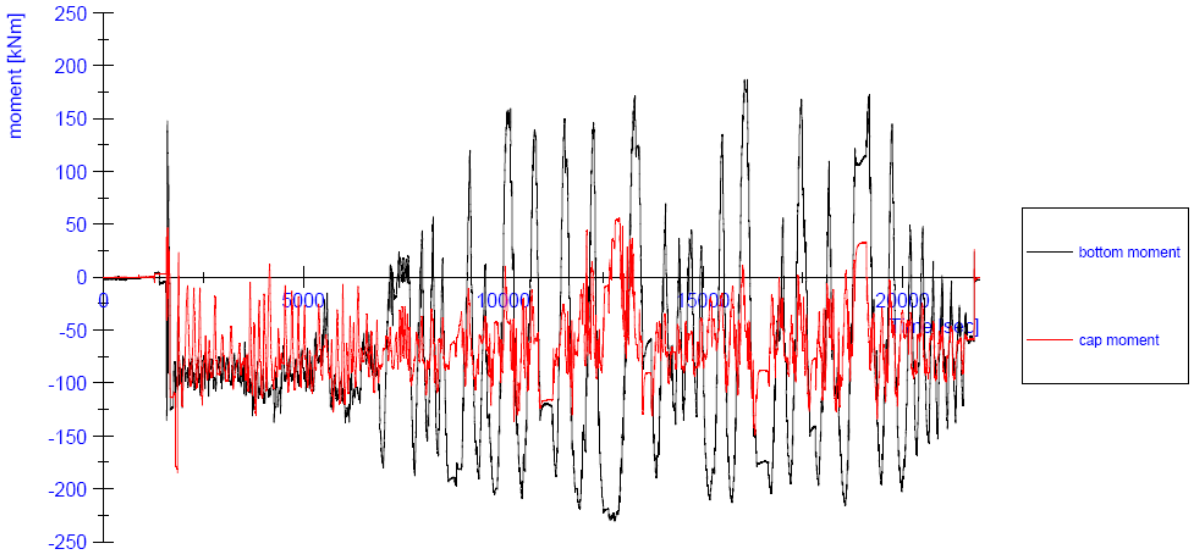

Figure 163: Progress of the in-plane bending moments at the top and at the bottom of the wall (testing time) LAC03

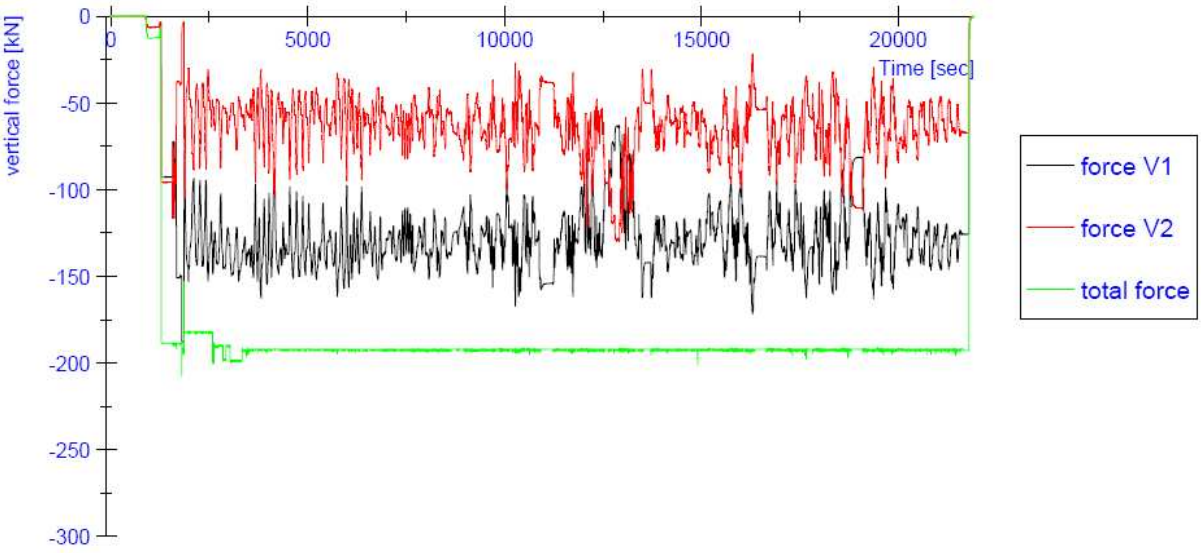

Figure 164: Progress of the vertical forces V1 and V2 (testing time) LAC03

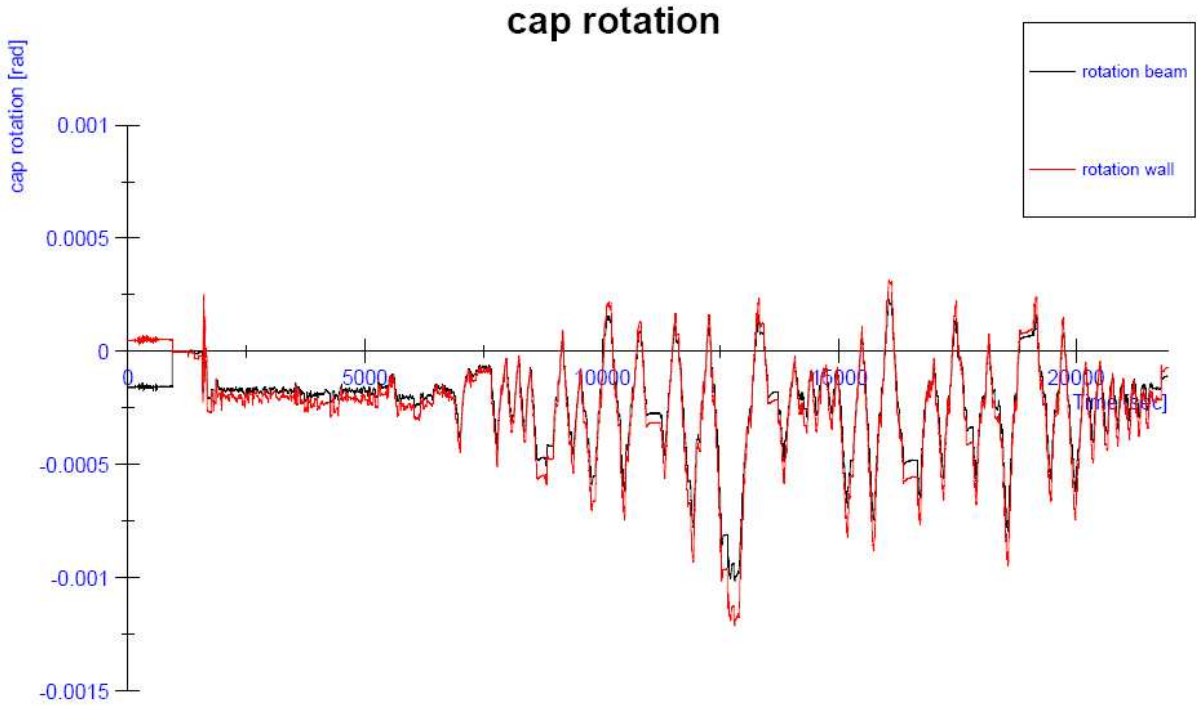

Figure 165: Progress of the in-plane rotation at the top of the wall (testing time) LAC03

7.9.2. Scale factor 4 (max 0.23 g)

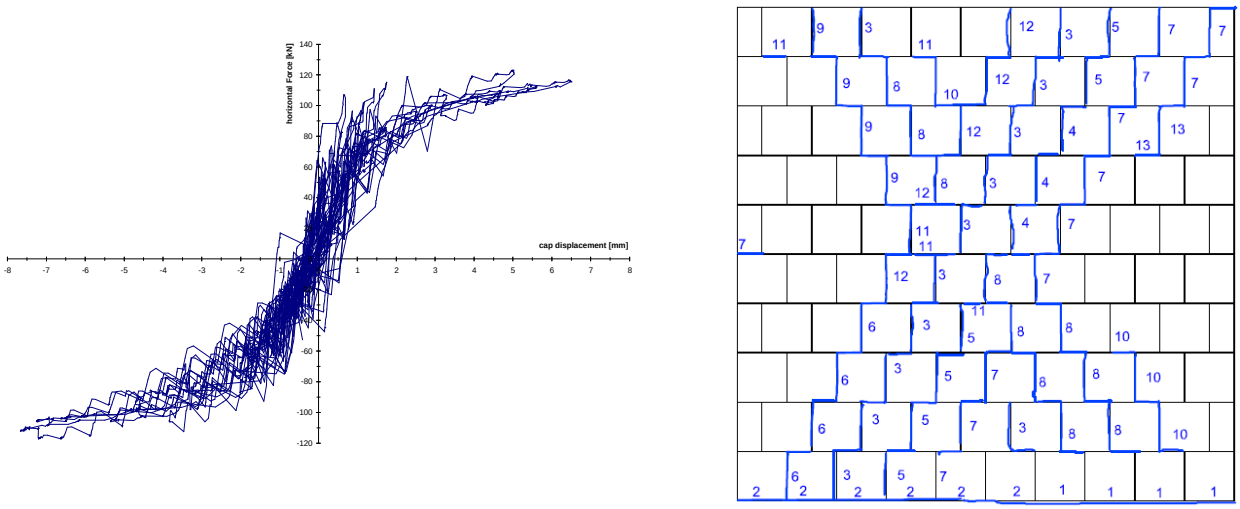

Figure 166: Load-displacement curve (hysteresis) and crack pattern of the test specimen LAC03

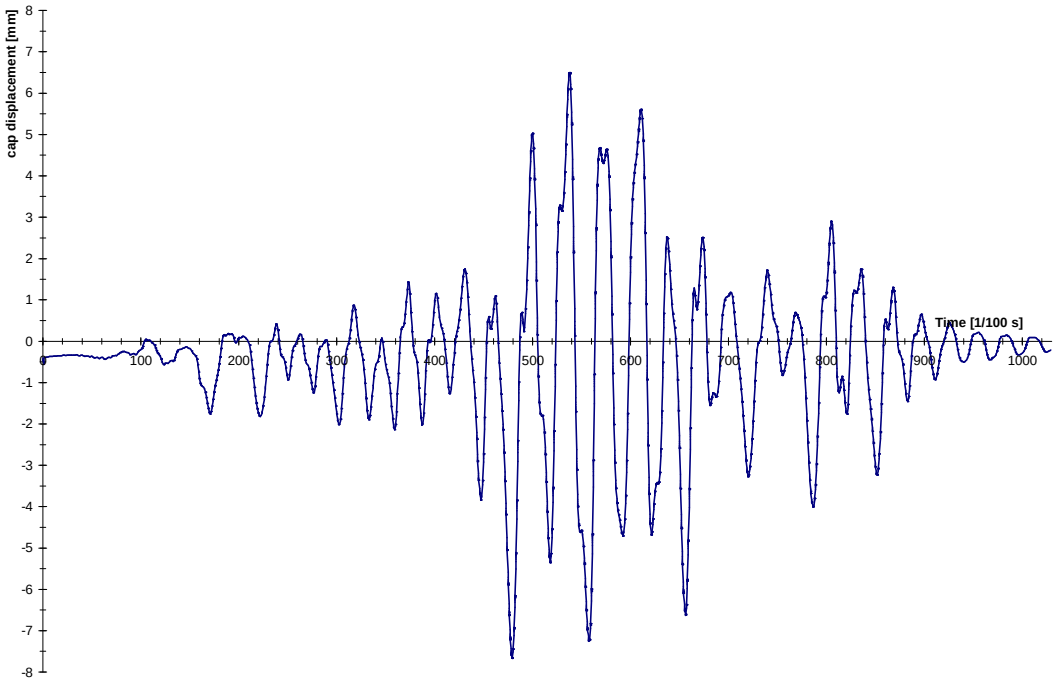

Figure 167: displacement history (earthquake time) LAC03

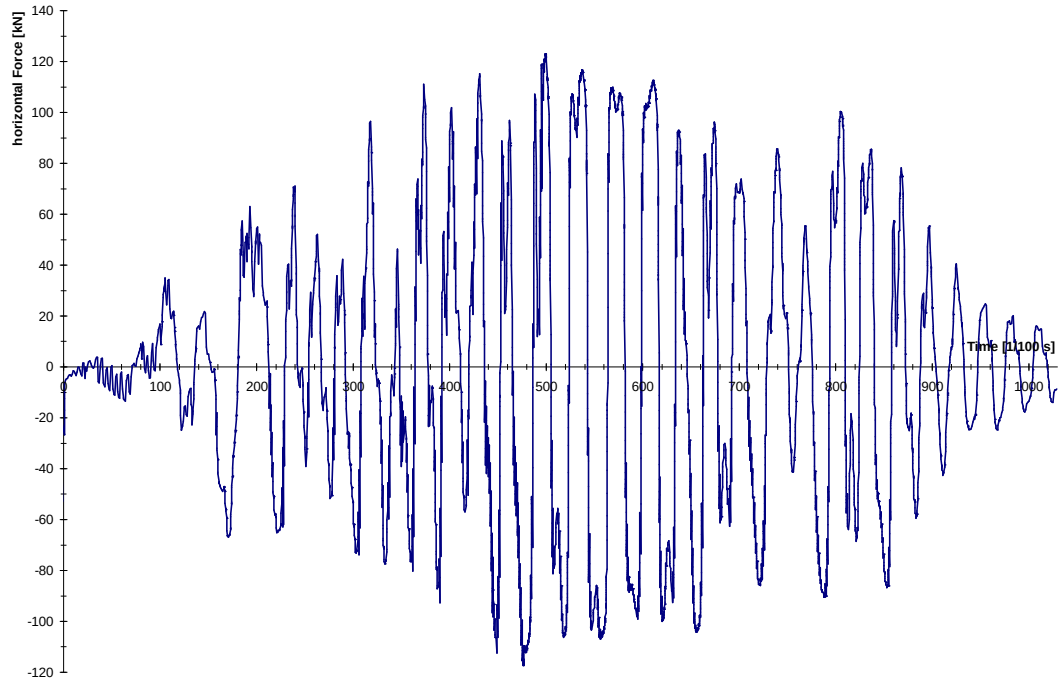

Figure 168: horizontal load history (earthquake time) LAC03

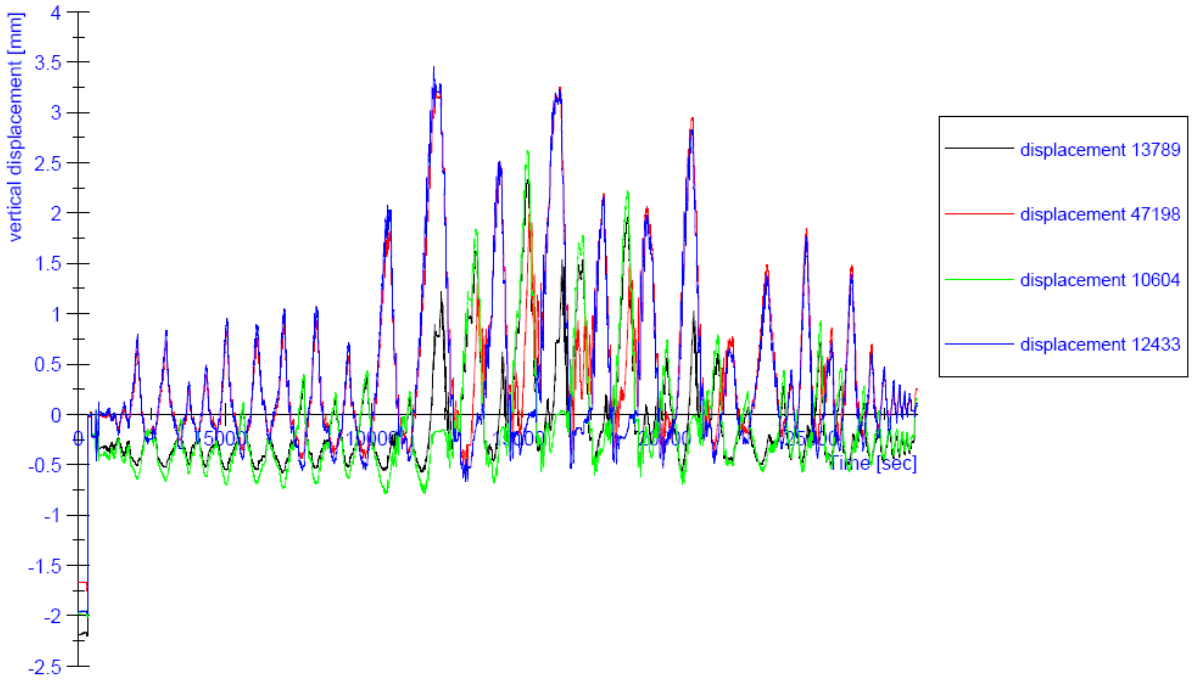

Figure 169: Progress of the vertical displacements (testing time) LAC03

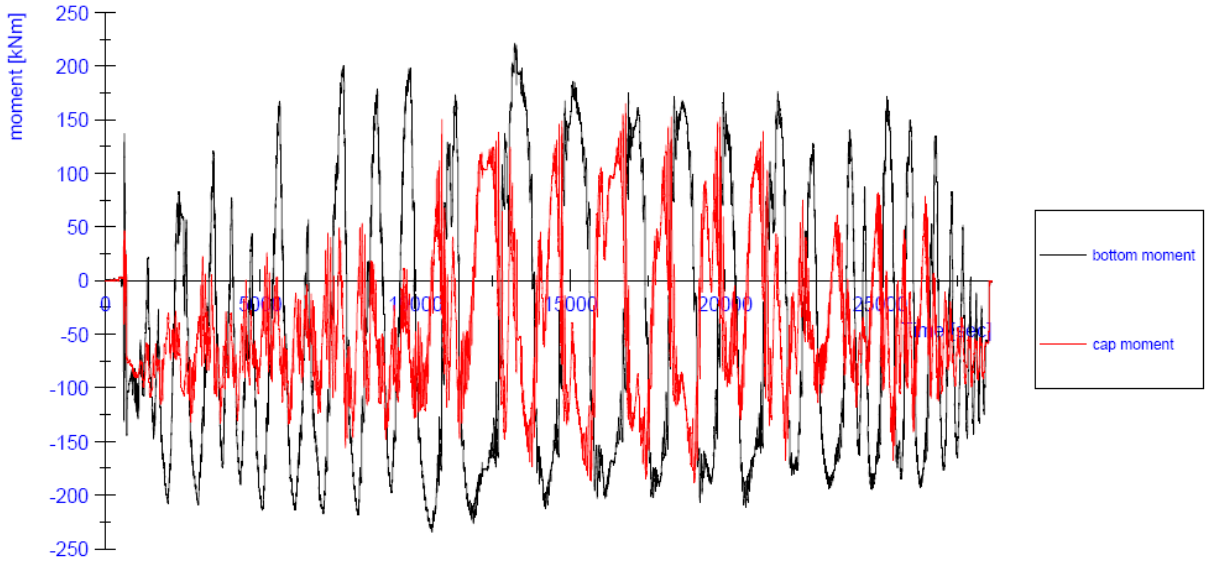

Figure 170: Progress of the in-plane bending moments at the top and at the bottom of the wall (testing time) LAC03

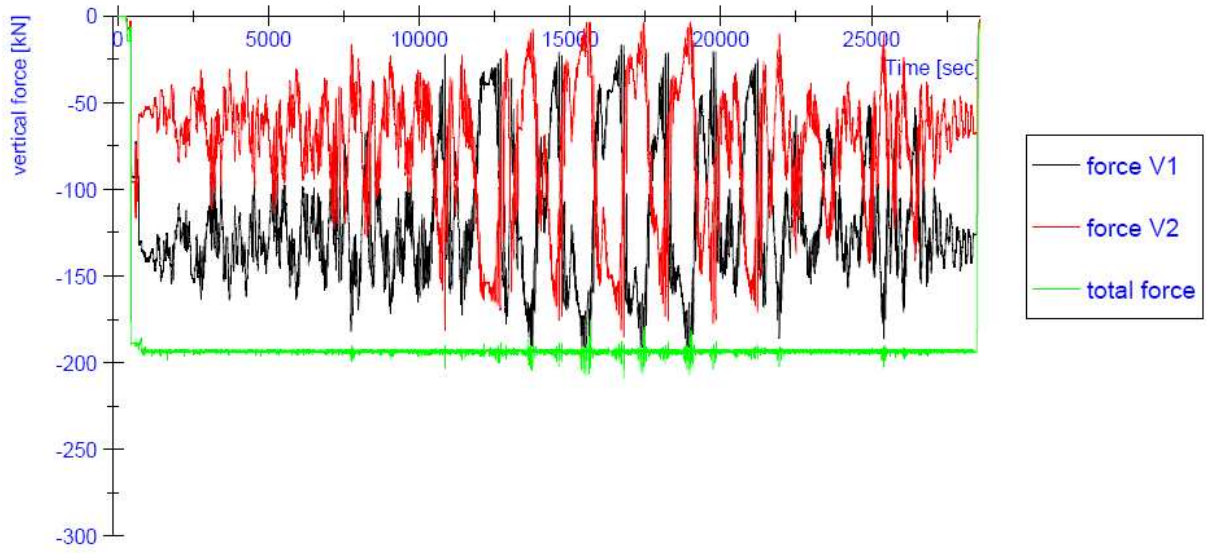

Figure 171: Progress of the vertical forces V1 and V2 (testing time) LAC03

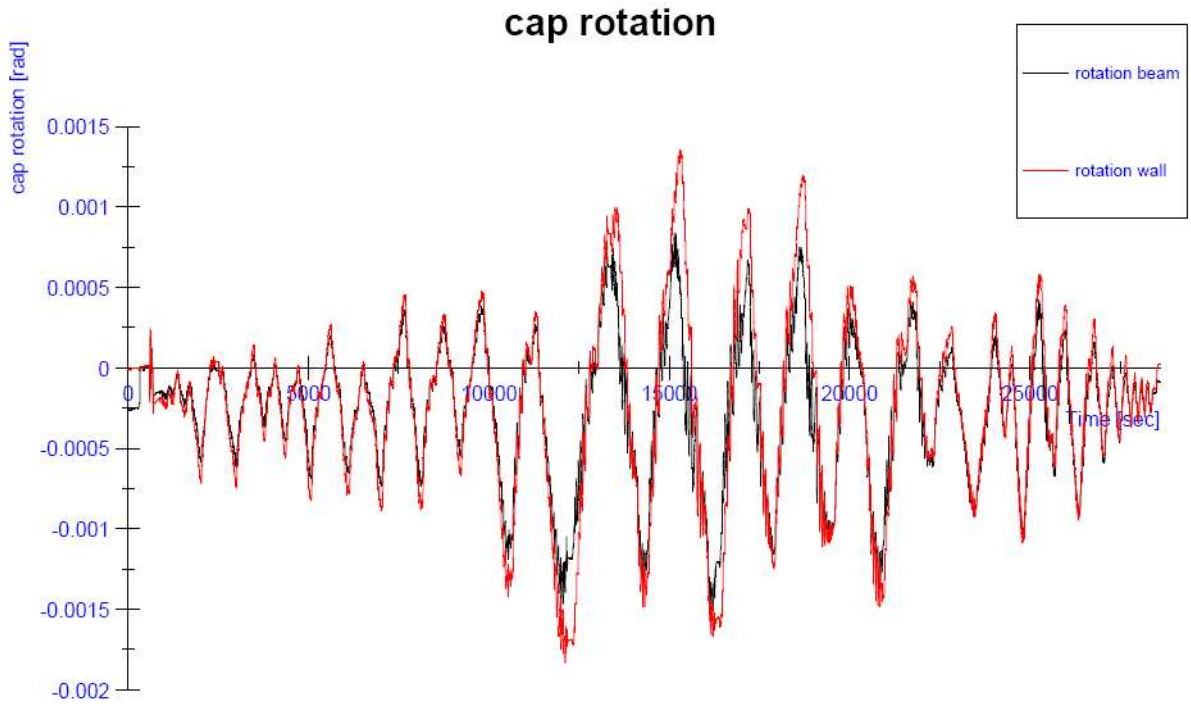

Figure 172: Progress of the in-plane rotation at the top of the wall (testing time) LAC03

Figure 173: Crack pattern LAC03

7.10. LAC04

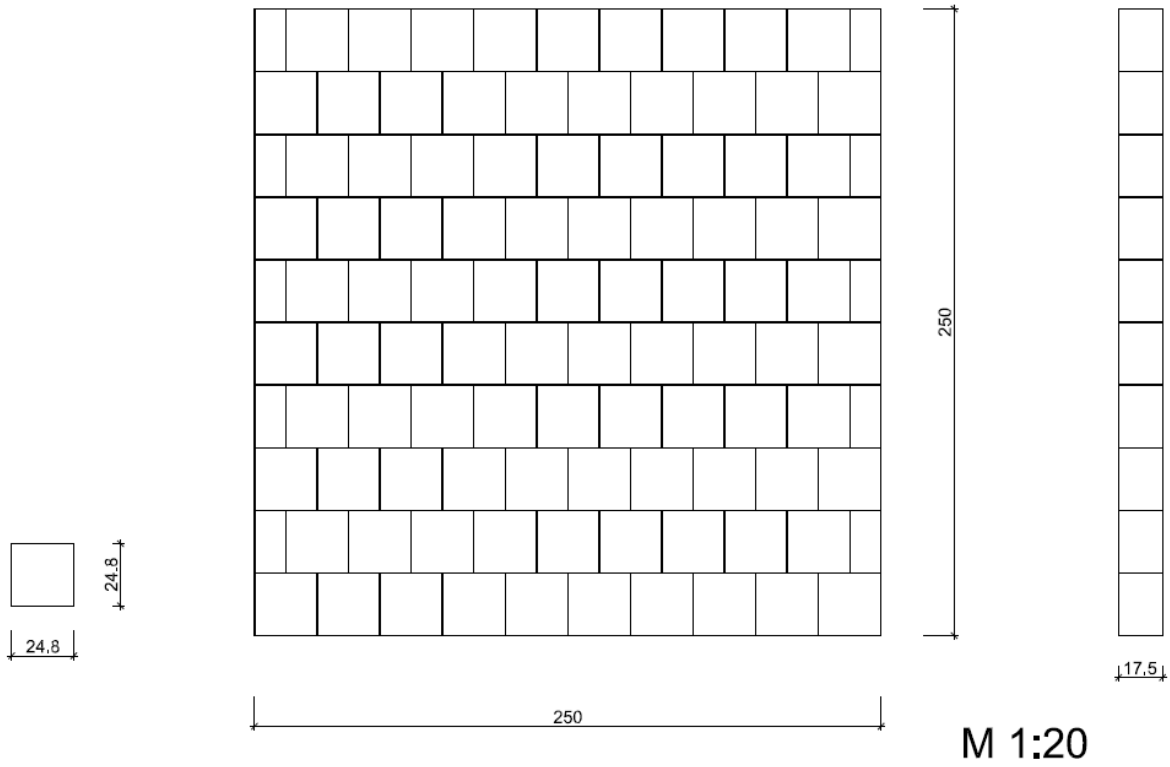

Figure 174: Dimension of the test specimen LAC04

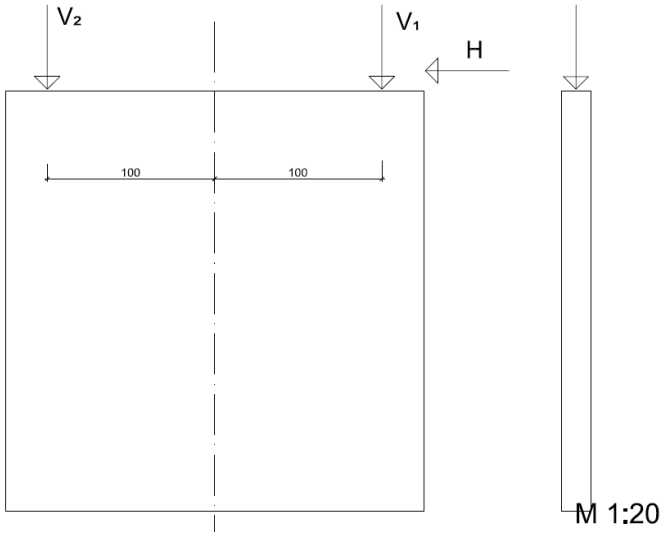

Figure 175: Position of the hydraulic actuators at test specimen LAC04

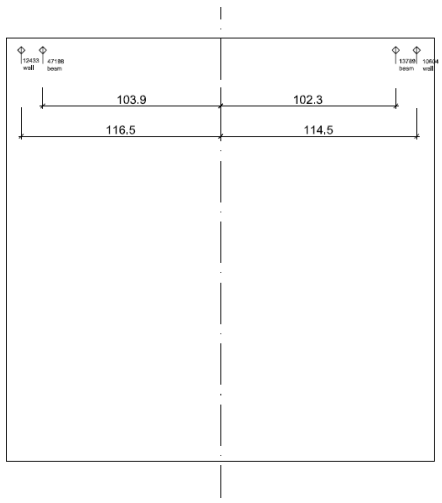

Figure 176: Position of the LVDTs at test specimen LAC04

7.10.1. Scale factor 2.5 (max 0.14 g)

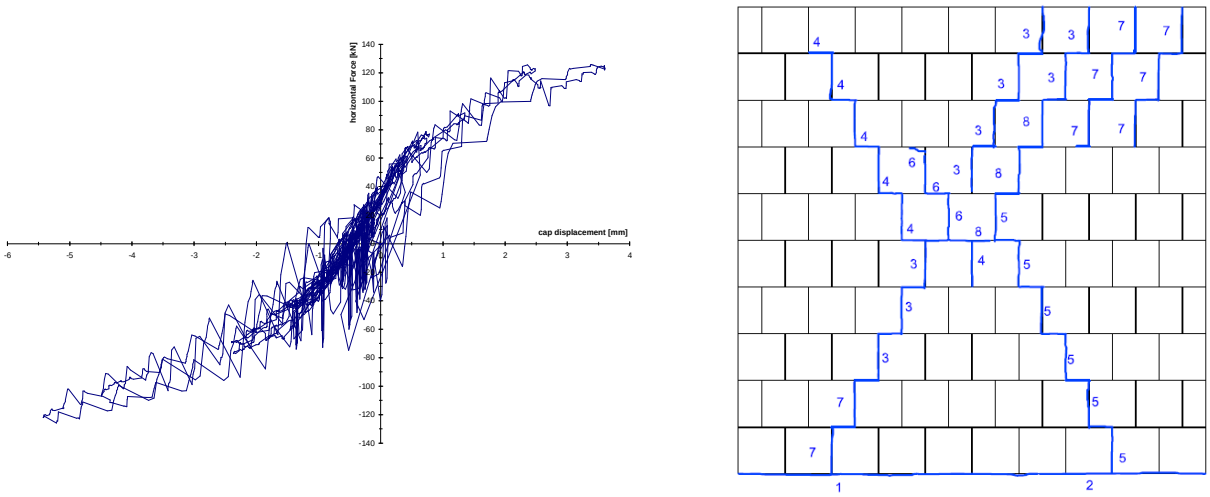

Figure 177: Load-displacement curve (hysteresis) and crack pattern of the test specimen LAC04

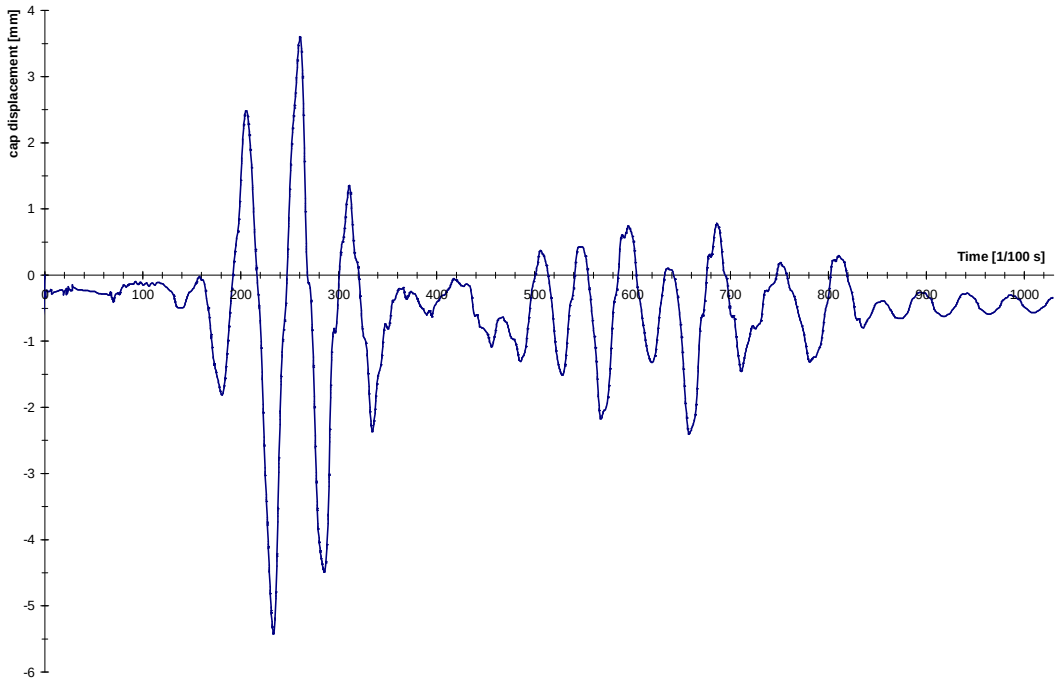

Figure 178: displacement history (earthquake time) LAC04

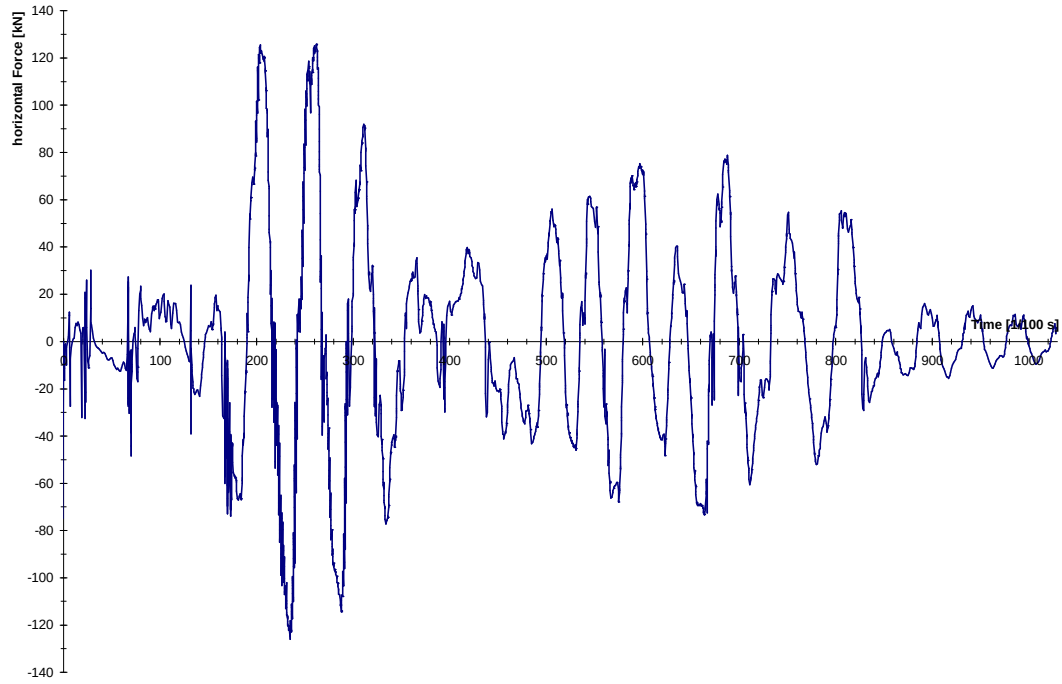

Figure 179: horizontal load history (earthquake time) LAC04

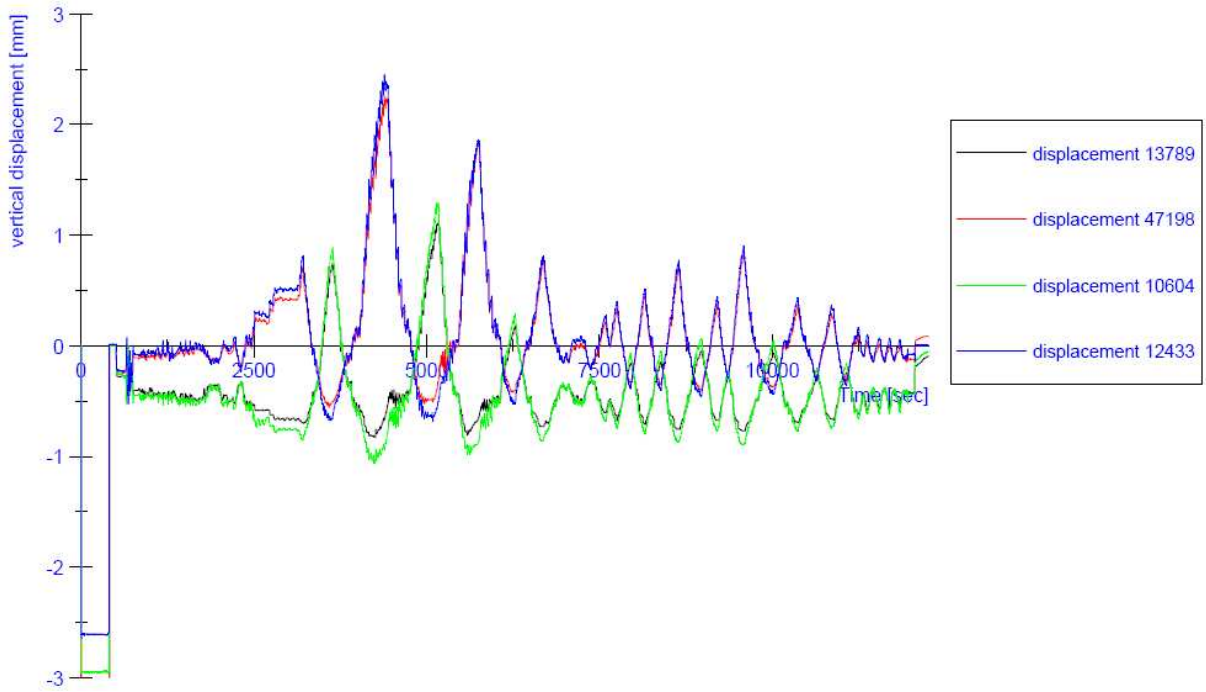

Figure 180: Progress of the vertical displacements (testing time) LAC04

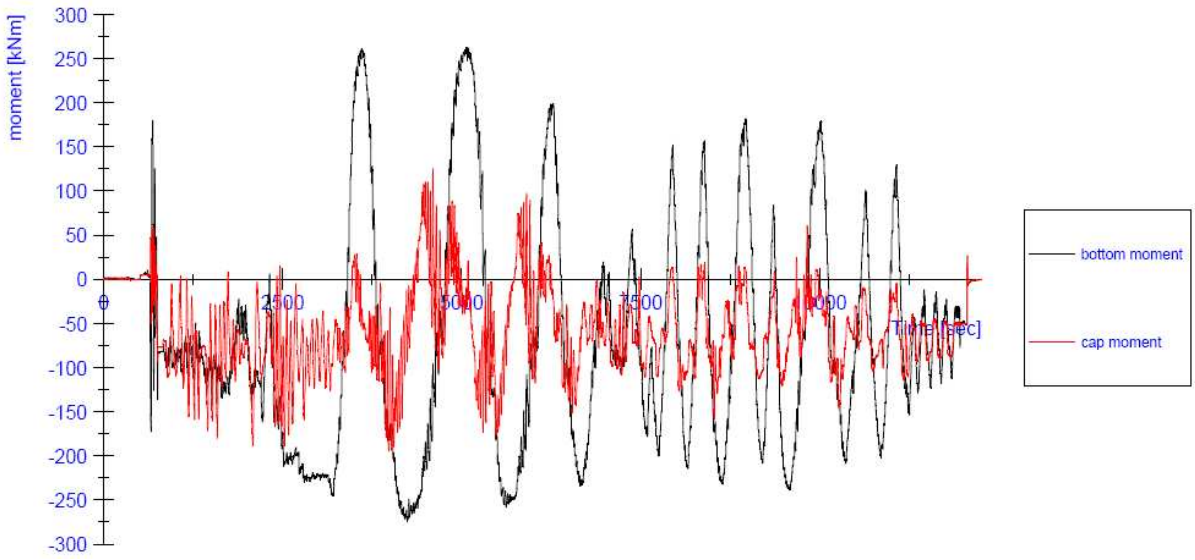

Figure 181: Progress of the in-plane bending moments at the top and at the bottom of the wall (testing time) LAC04

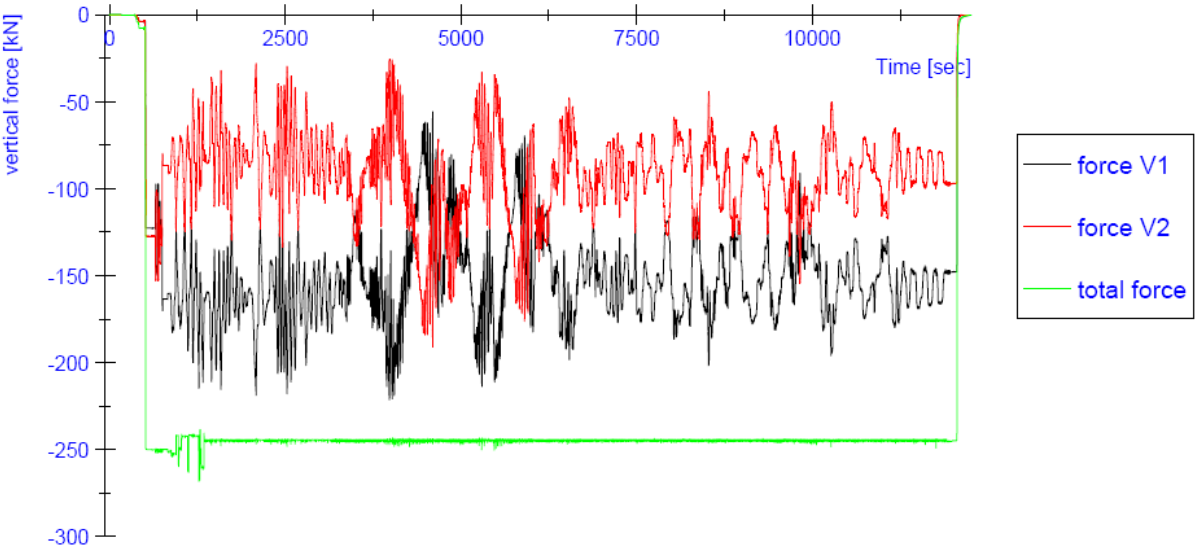

Figure 182: Progress of the vertical forces V1 and V2 (testing time) LAC04

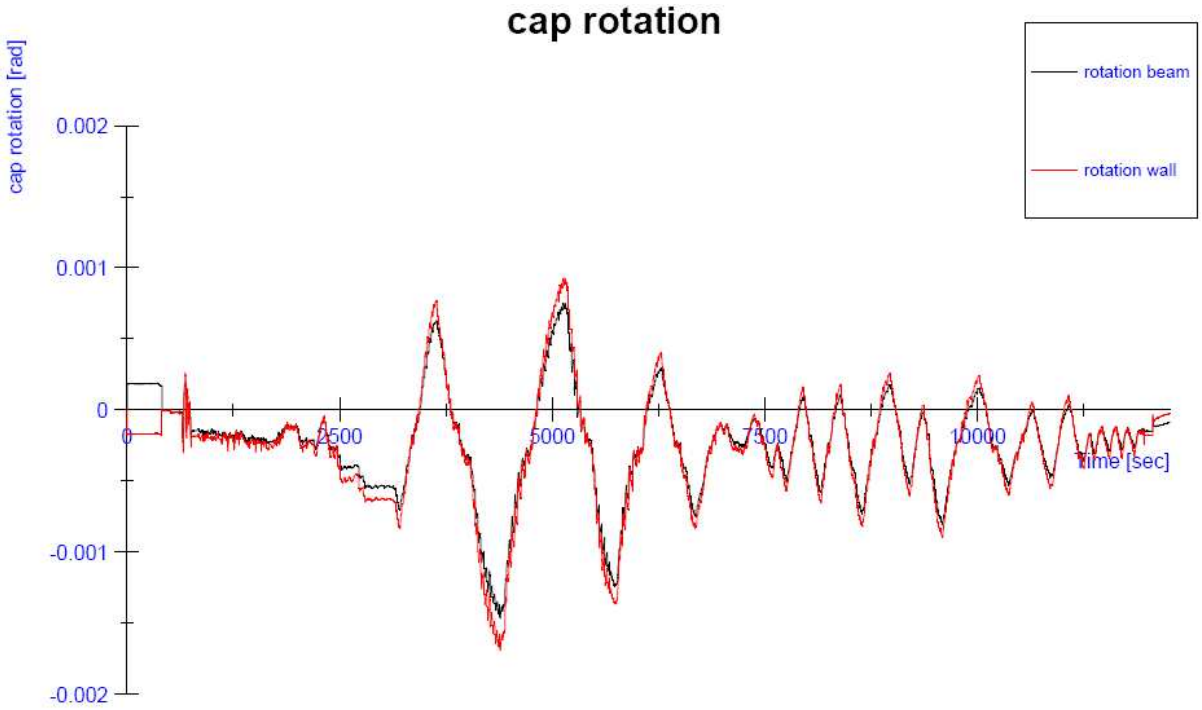

Figure 183: Progress of the in-plane rotation at the top of the wall (testing time) LAC04

Figure 184: Crack pattern LAC04

7.10.2. Scale factor 4 (max 0.23 g)

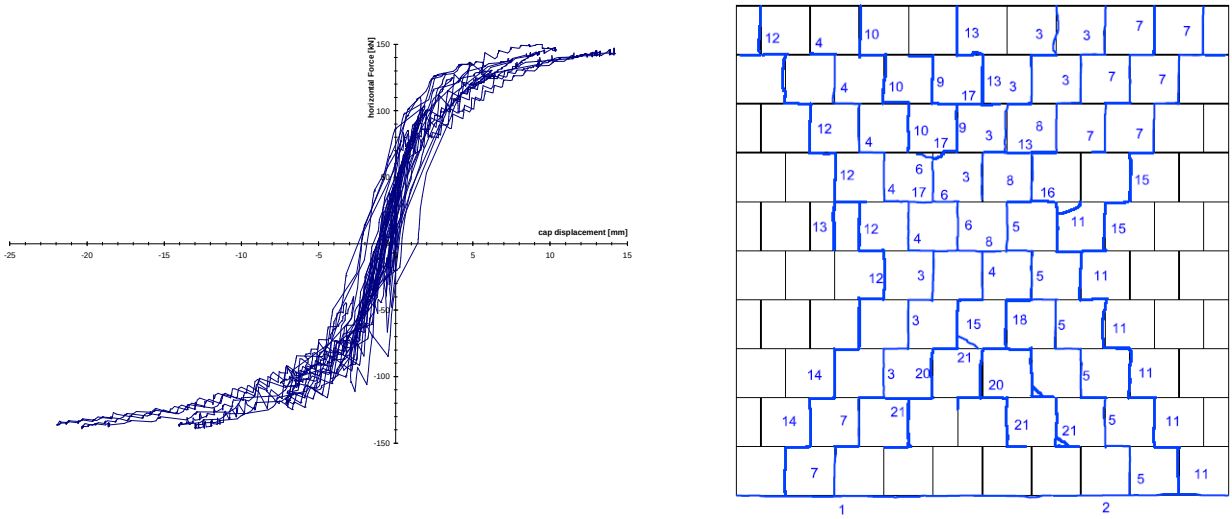

Figure 185: Load-displacement curve (hysteresis) and crack pattern of the test specimen LAC04

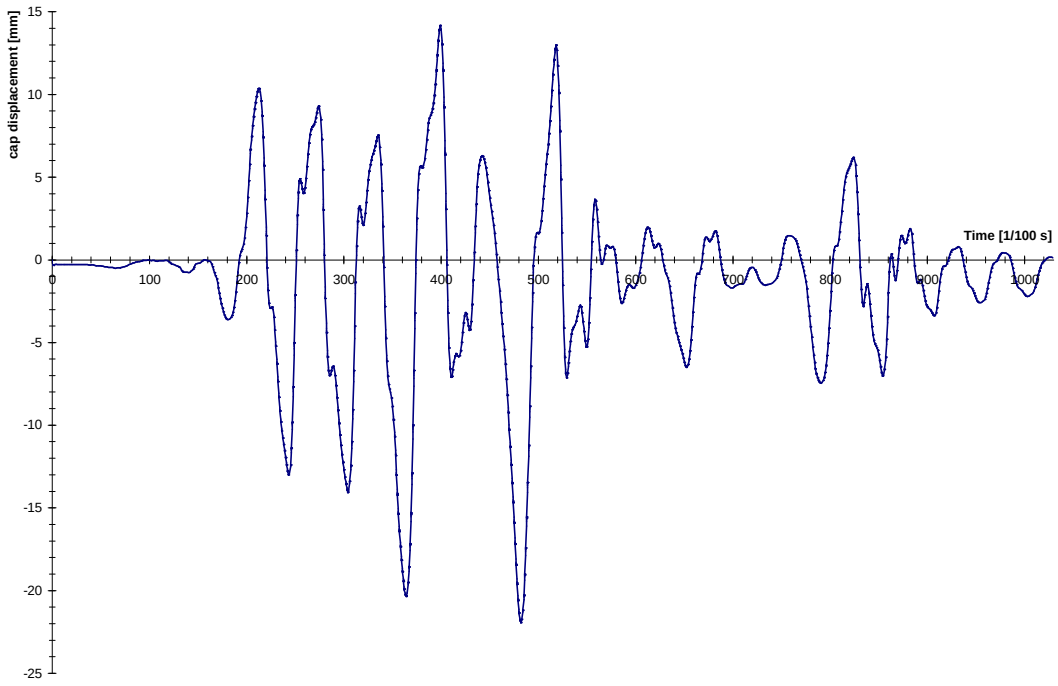

Figure 186: displacement history (earthquake time) LAC04

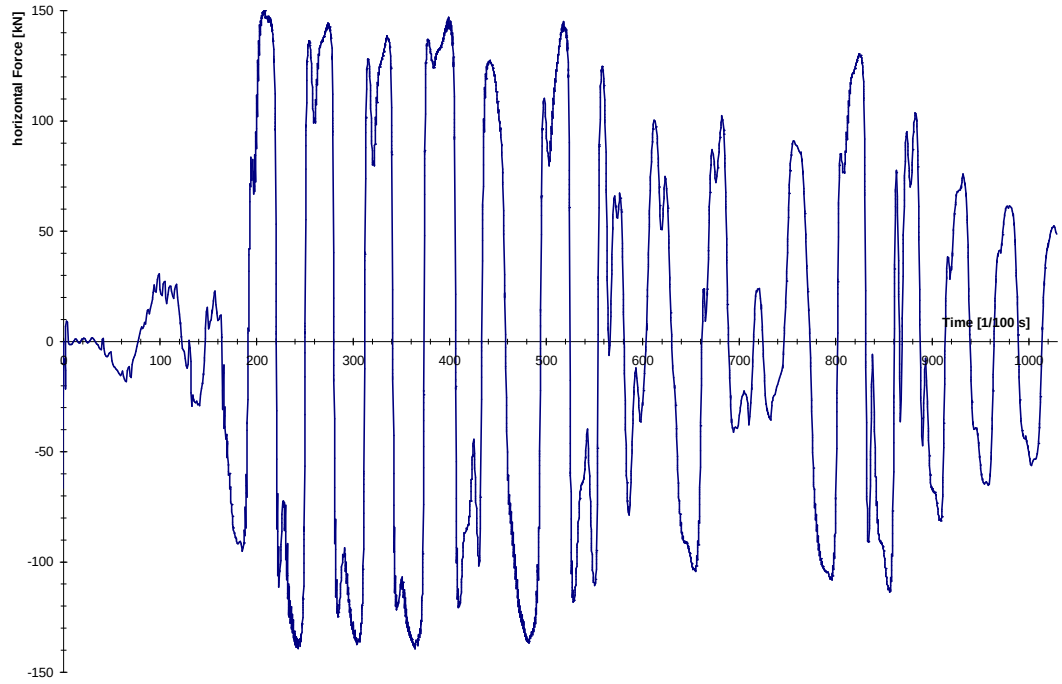

Figure 187: horizontal load history (earthquake time) LAC04

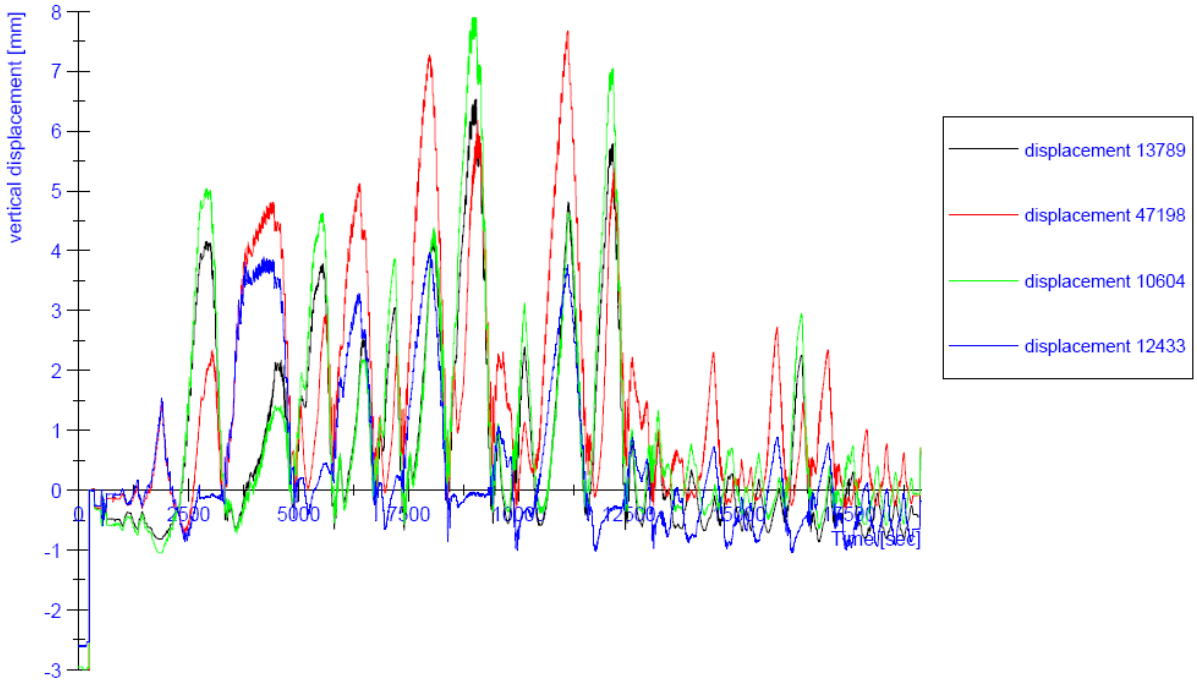

Figure 188: Progress of the vertical displacements (testing time) LAC04

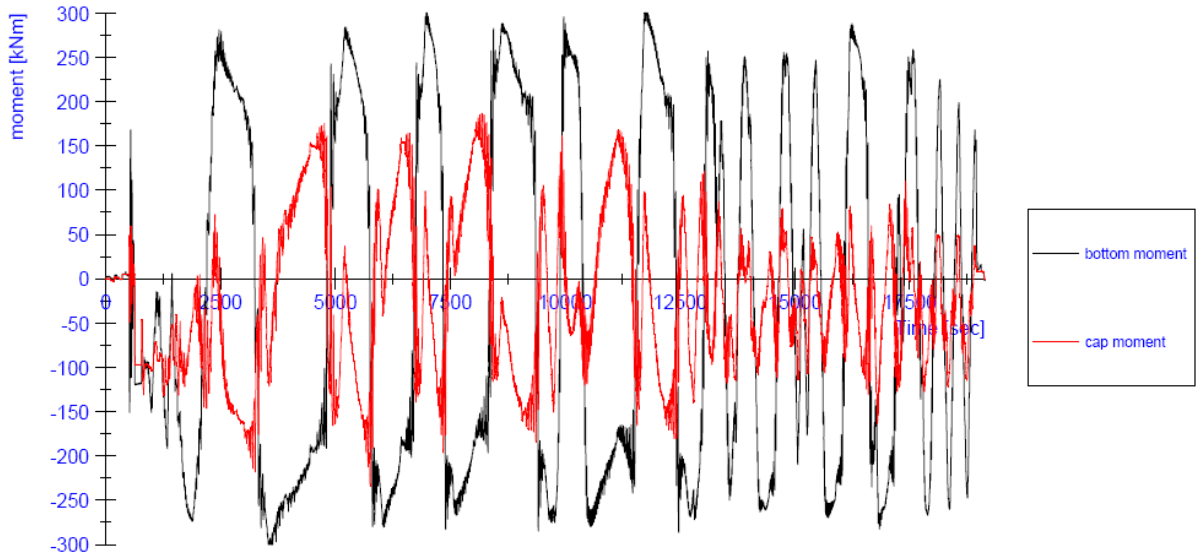

Figure 189: Progress of the in-plane bending moments at the top and at the bottom of the wall (testing time) LAC04

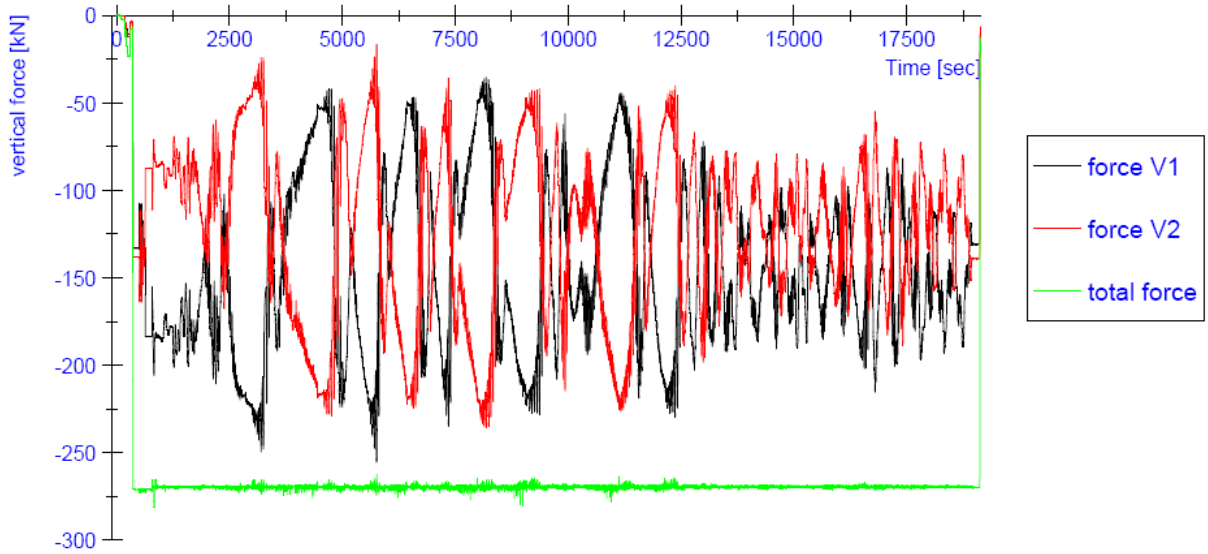

Figure 190: Progress of the vertical forces V1 and V2 (testing time) LAC04

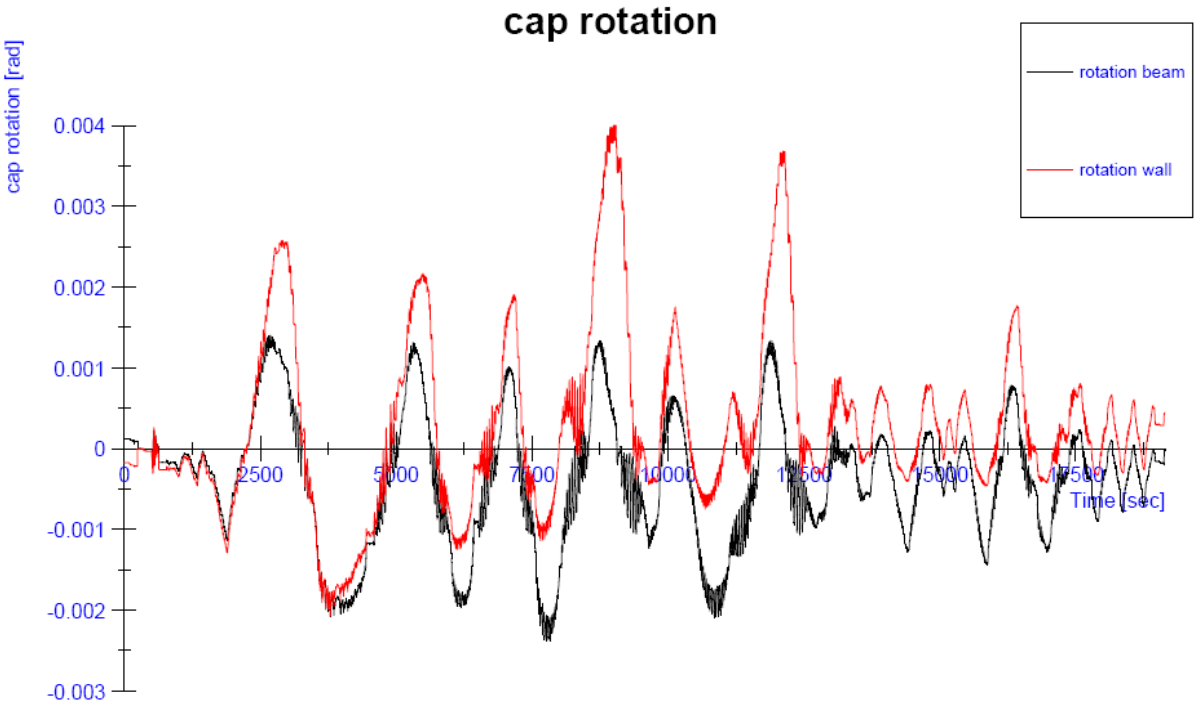

Figure 191: Progress of the in-plane rotation at the top of the wall (testing time) LAC04

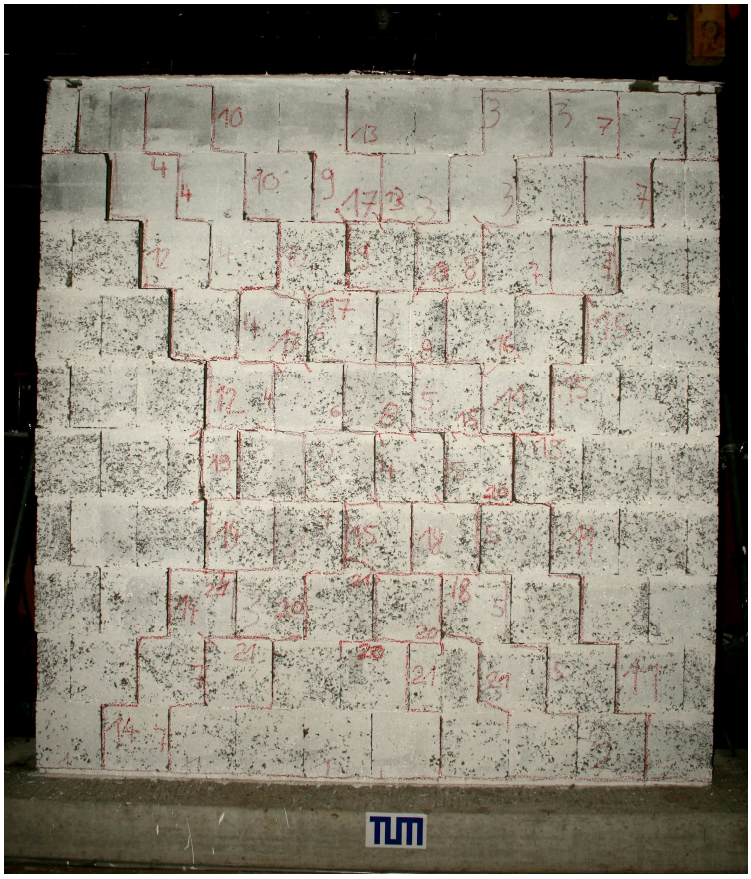

Figure 192: Crack pattern LAC04

7.11. Clay03

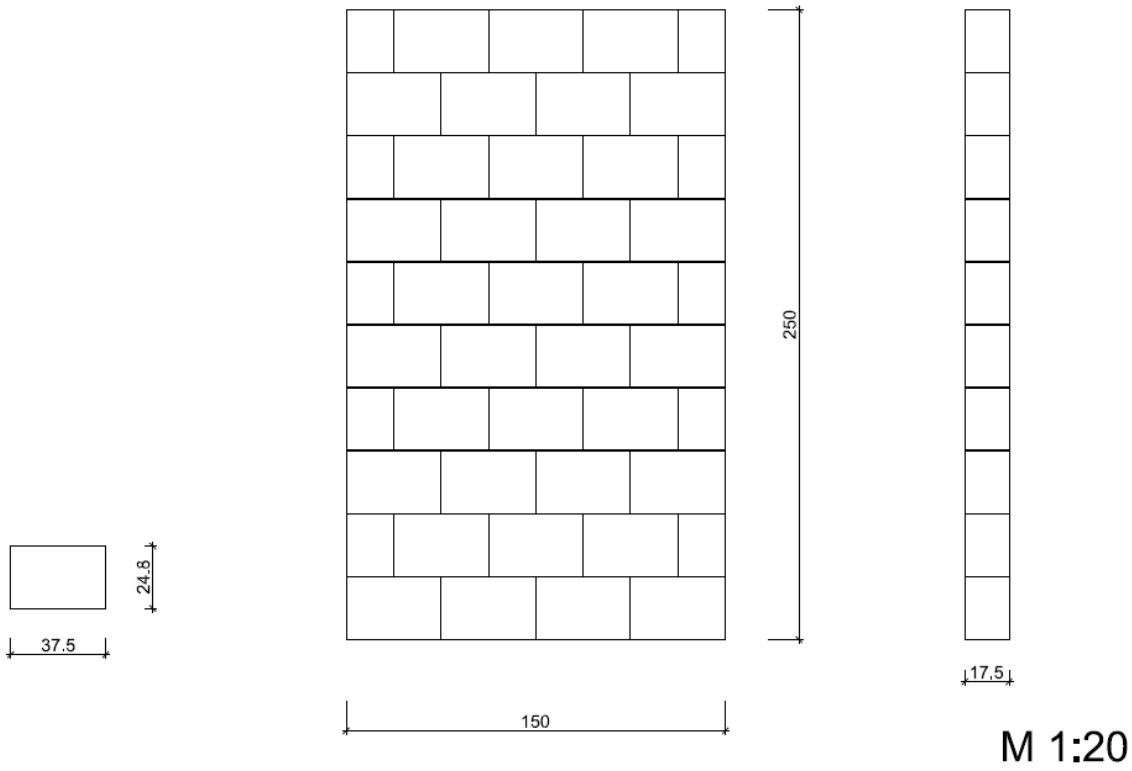

Figure 193: Dimension of the test specimen Clay03

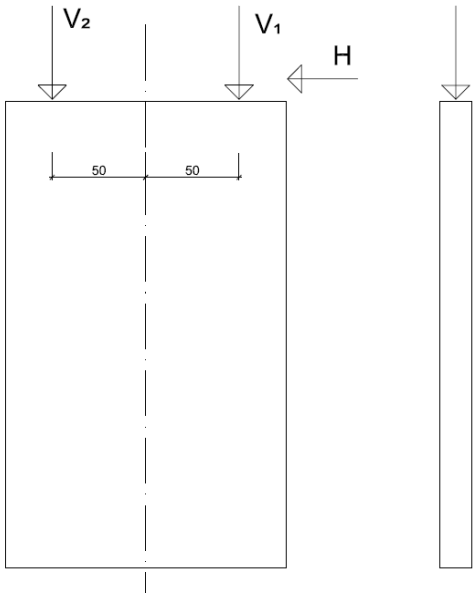

Figure 194: Position of the hydraulic actuators at test specimen Clay03

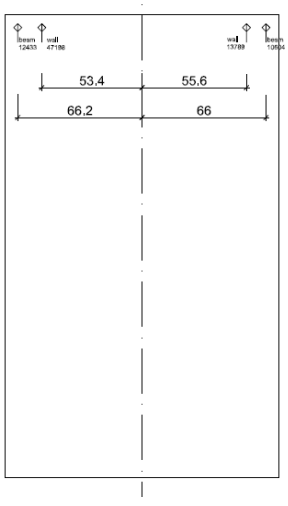

Figure 195: Position of the LVDTs at test specimen Clay03

7.11.1. Scale factor 2 (max 0.12 g)

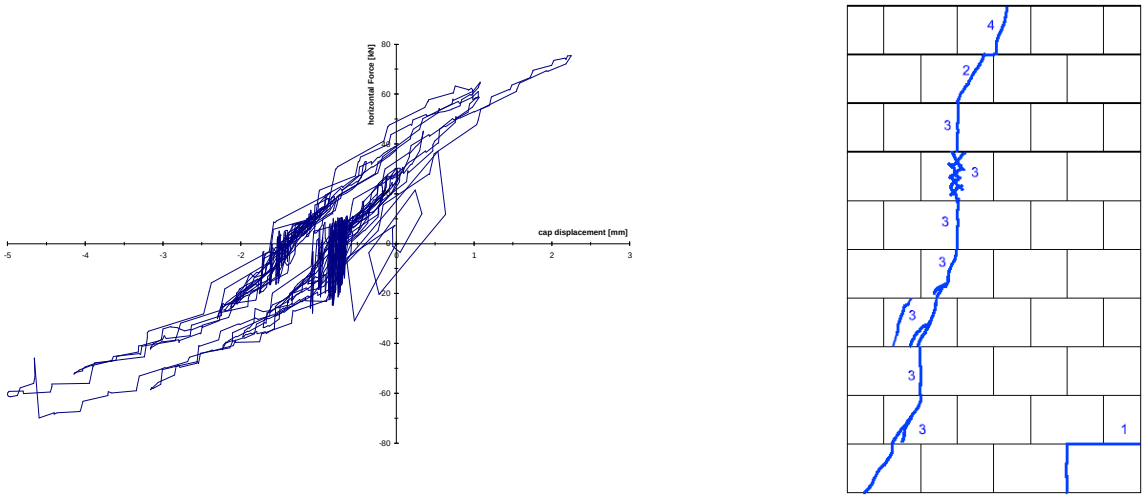

Figure 196: Load-displacement curve (hysteresis) and crack pattern of the test specimen Clay03

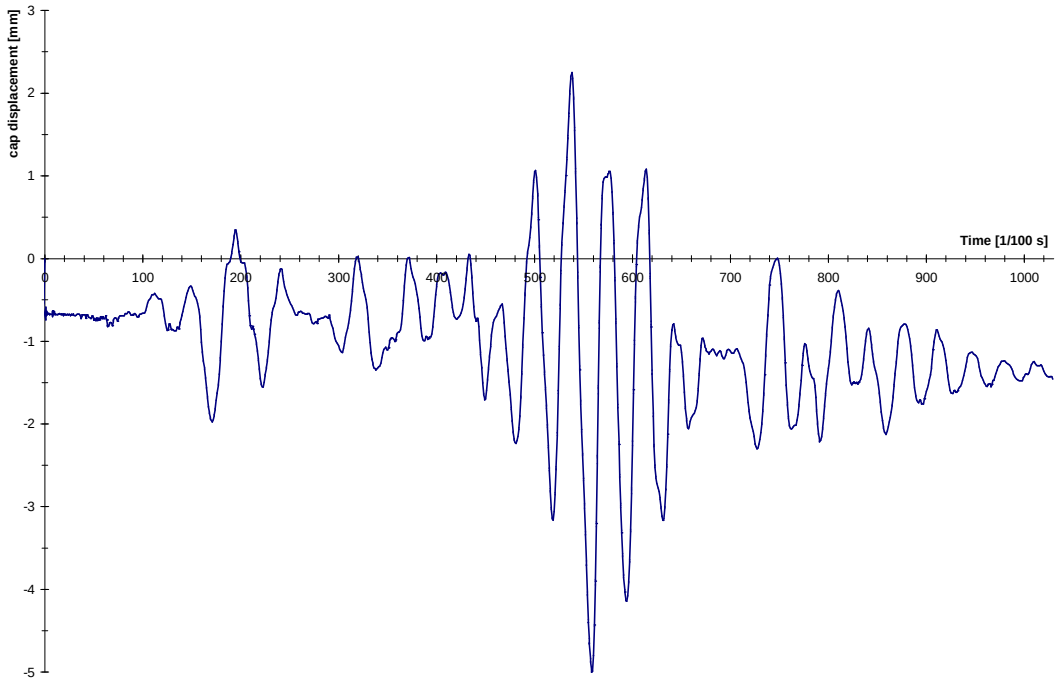

Figure 197: displacement history (earthquake time) Clay03

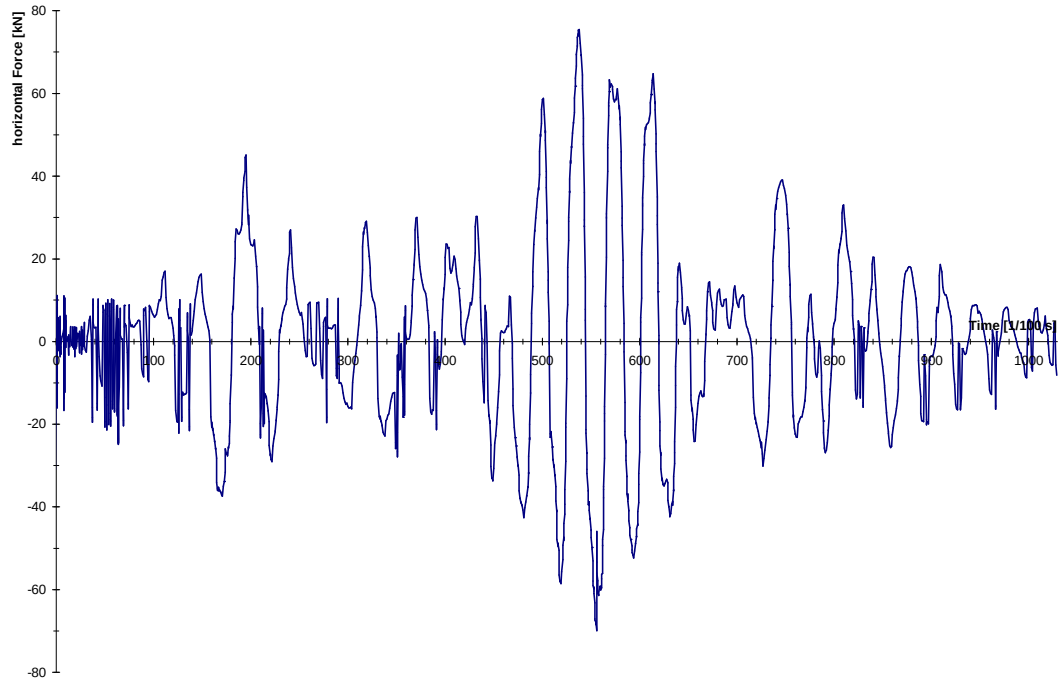

Figure 198: horizontal load history (earthquake time) Clay03

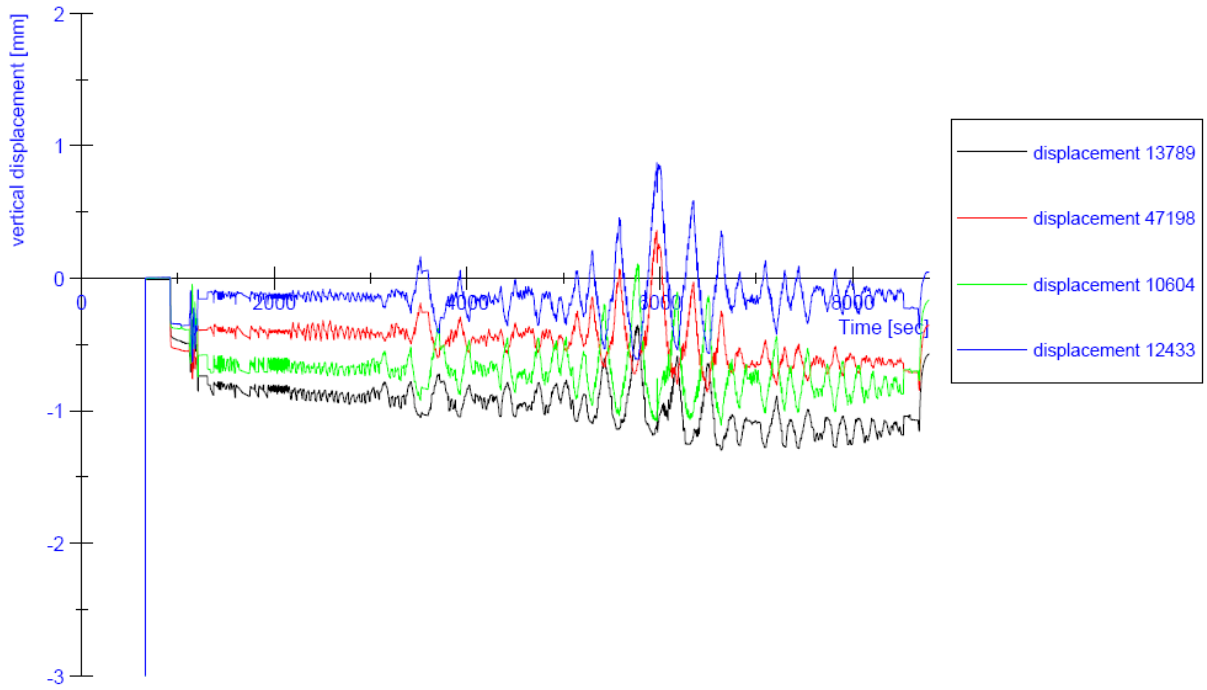

Figure 199: Progress of the vertical displacements (testing time) Clay03

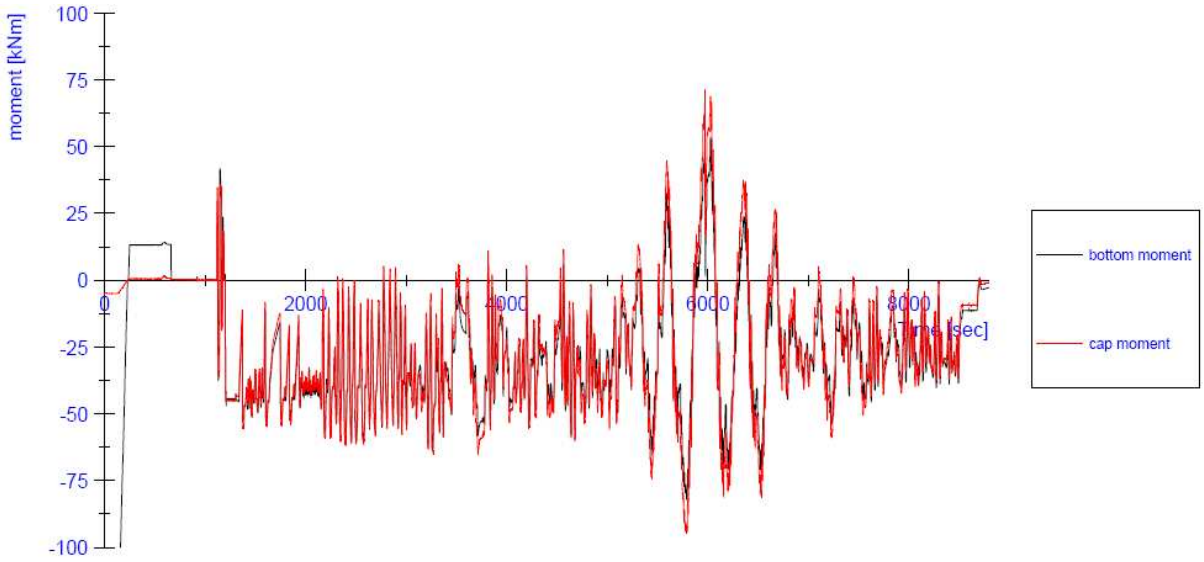

Figure 200: Progress of the in-plane bending moments at the top and at the bottom of the wall (testing time) Clay03

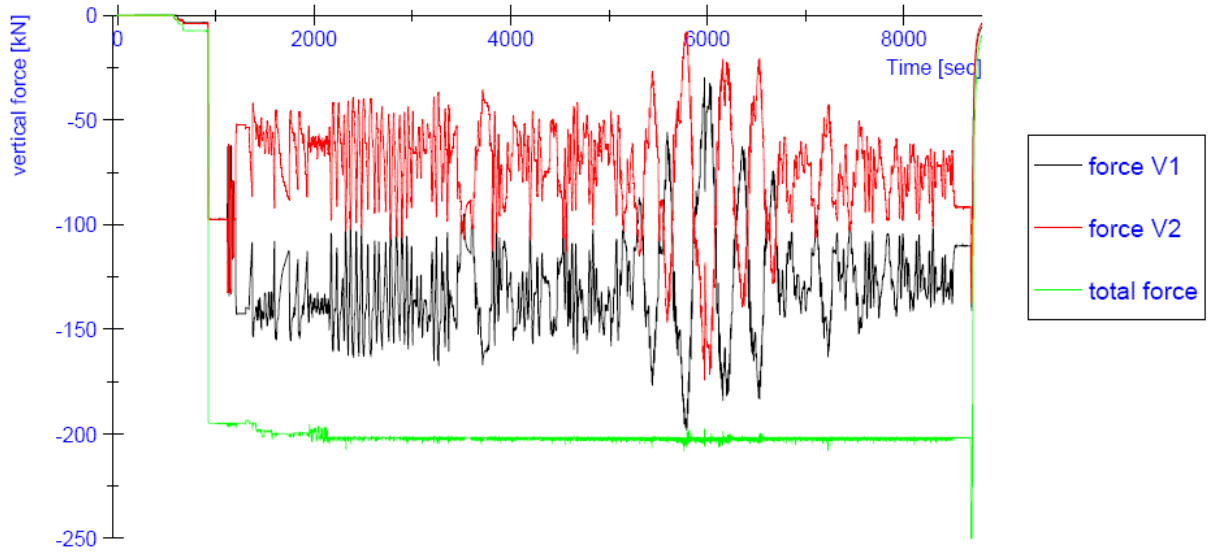

Figure 201: Progress of the vertical forces V1 and V2 (testing time) Clay03

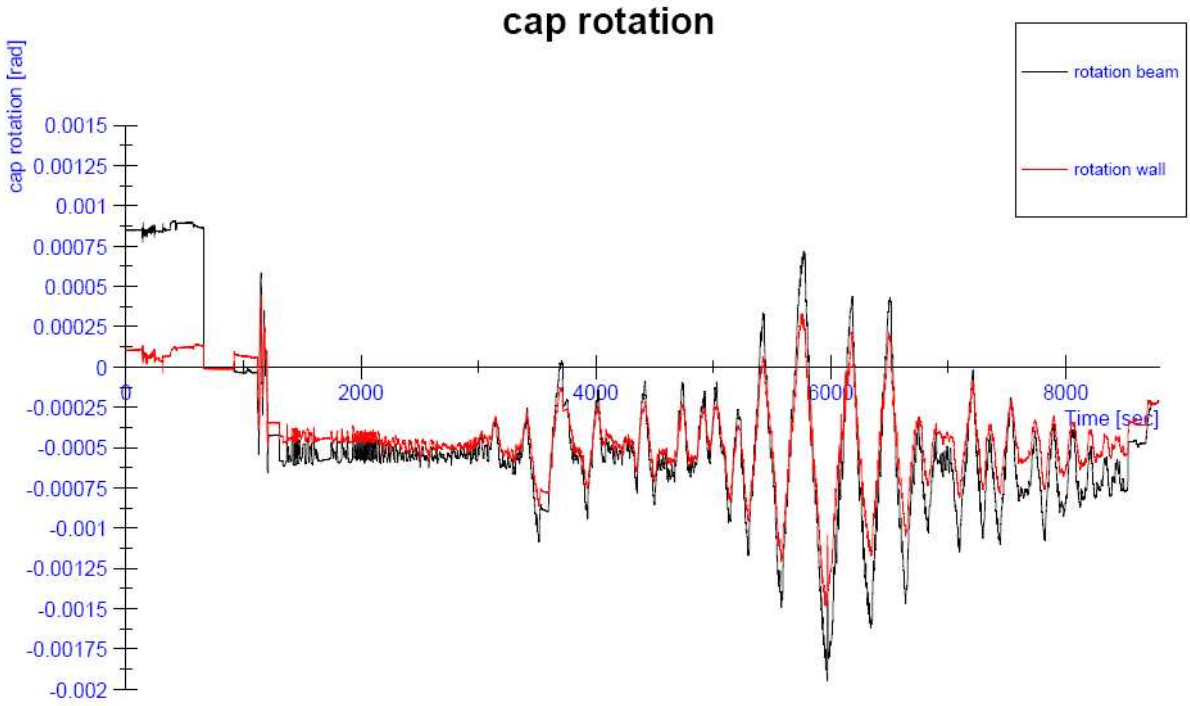

Figure 202: Progress of the in-plane rotation at the top of the wall (testing time) Clay03

7.11.2. Scale factor 3.5 (max 0.20 g)

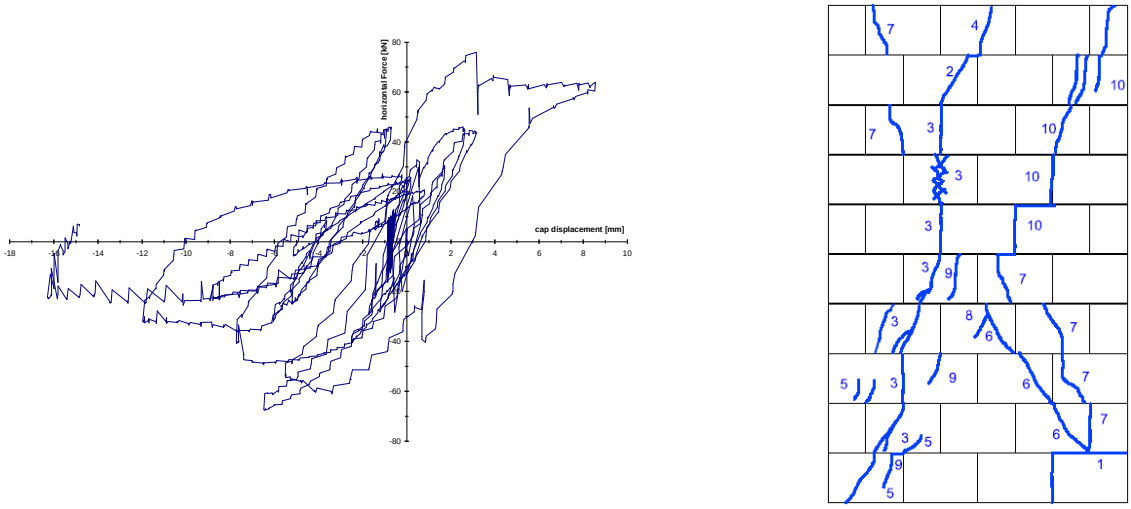

Figure 203: Load-displacement curve (hysteresis) and crack pattern of the test specimen Clay03

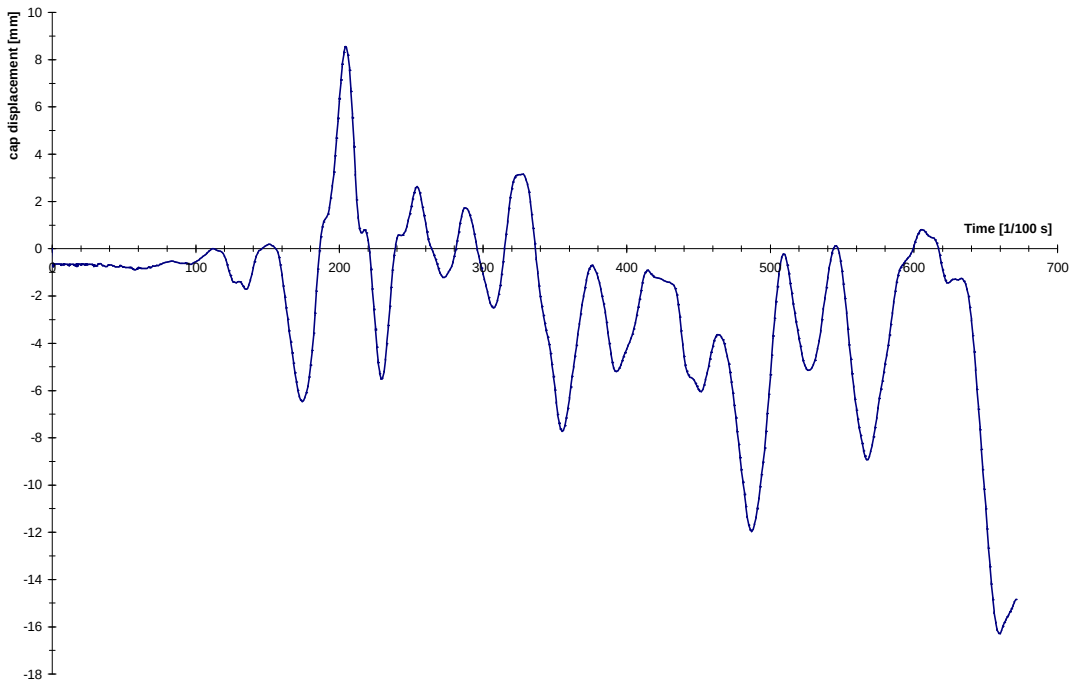

Figure 204: displacement history (earthquake time) Clay03

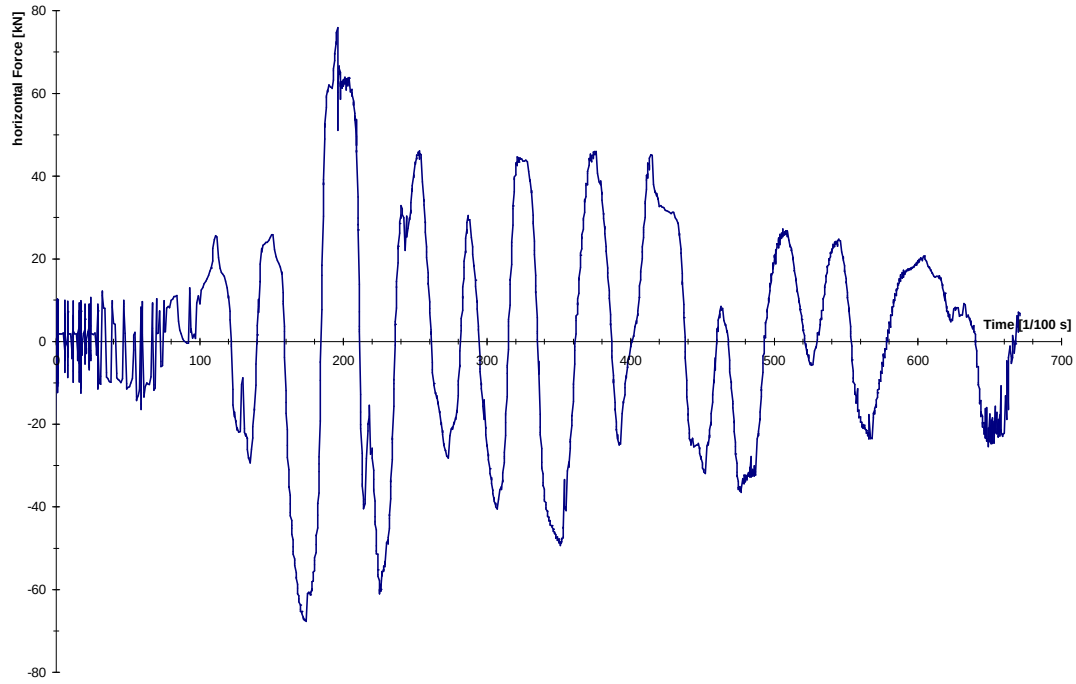

Figure 205: horizontal load history (earthquake time) Clay03

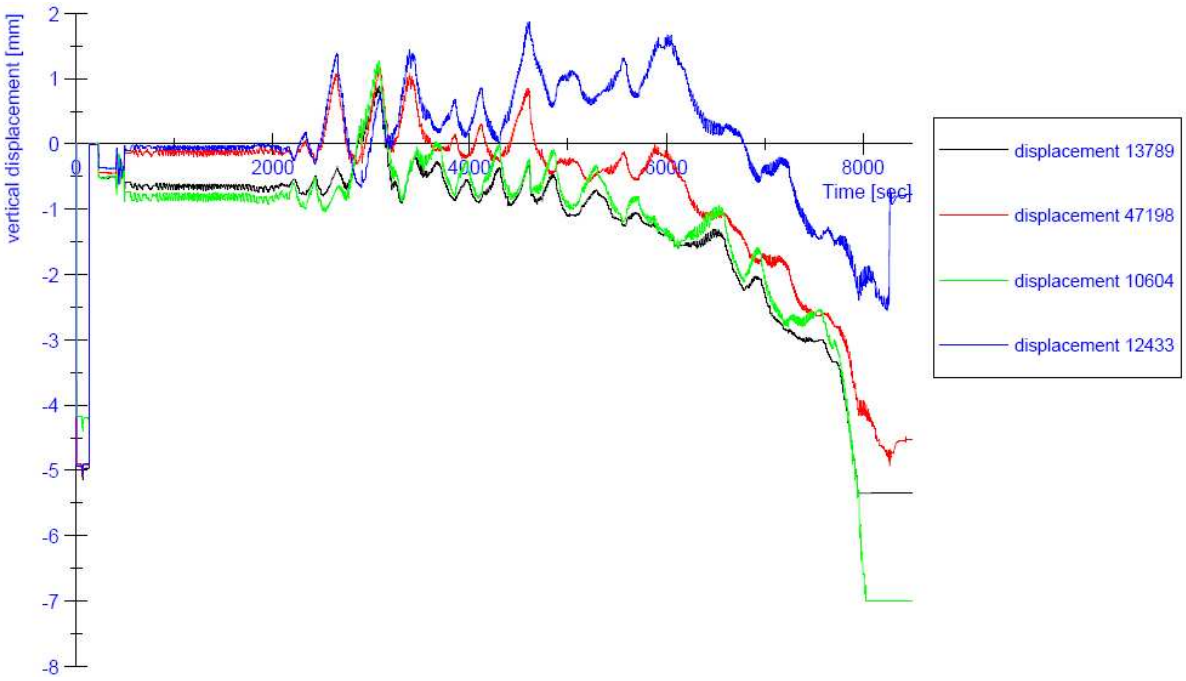

Figure 206: Progress of the vertical displacements (testing time) Clay03

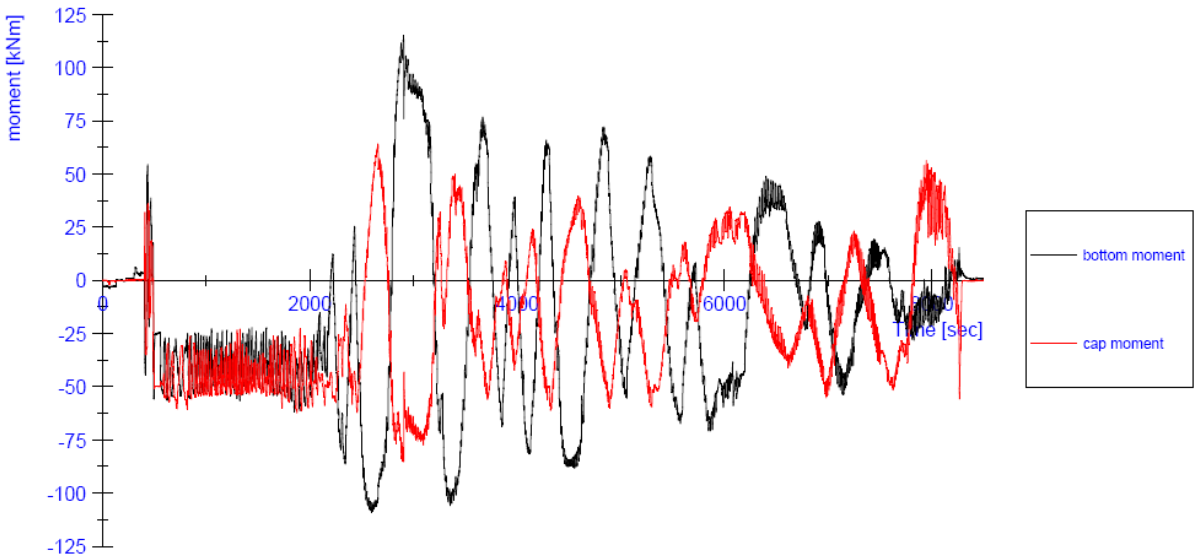

Figure 207: Progress of the in-plane bending moments at the top and at the bottom of the wall (testing time) Clay03

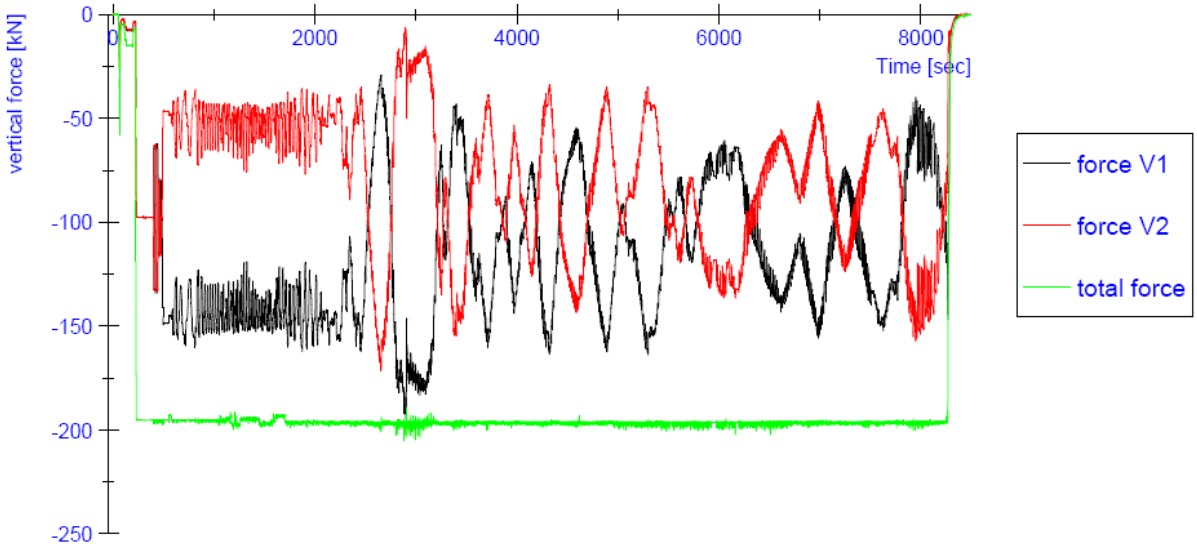

Figure 208: Progress of the vertical forces V1 and V2 (testing time) Clay03

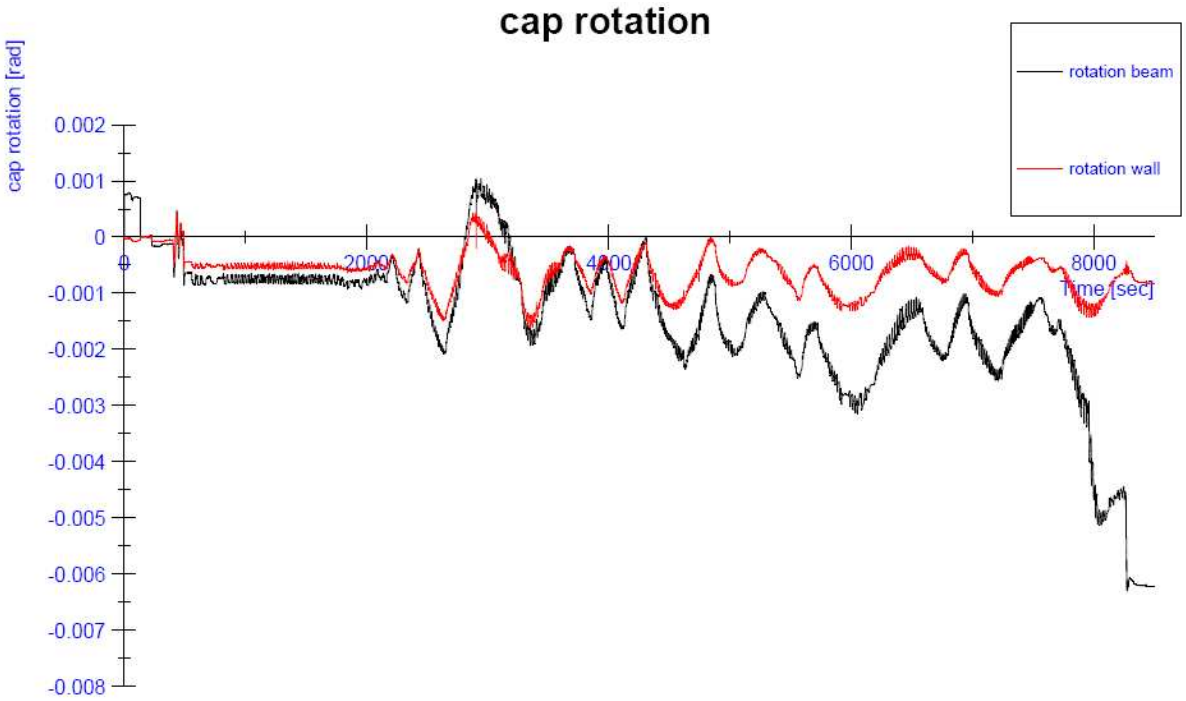

Figure 209: Progress of the in-plane rotation at the top of the wall (testing time) Clay03

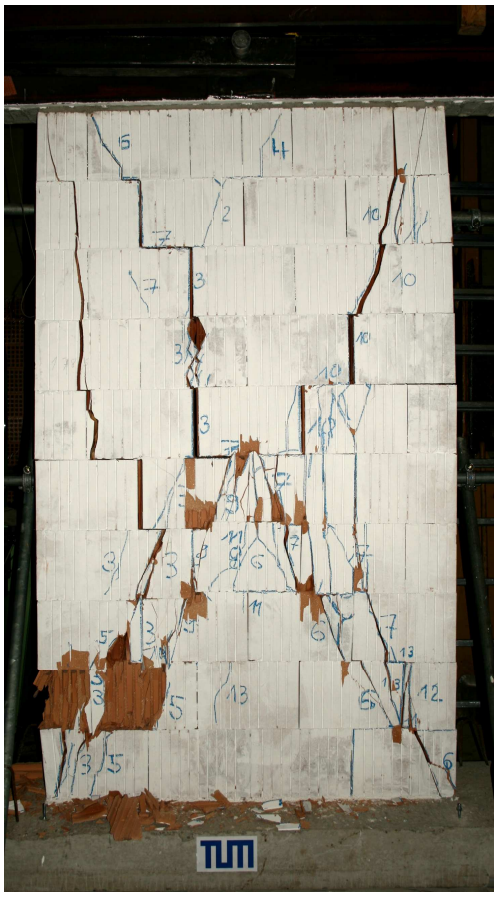

Figure 210: Crack pattern Clay03

7.12. Clay04

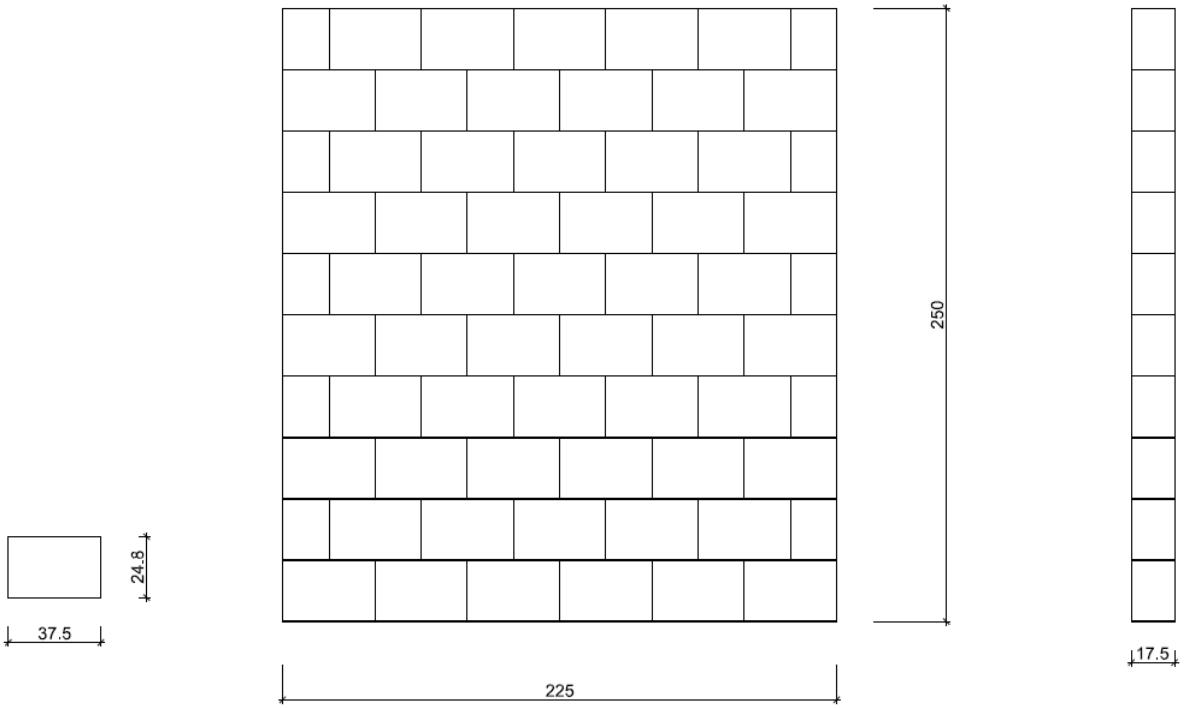

Figure 211: Dimension of the test specimen Clay04

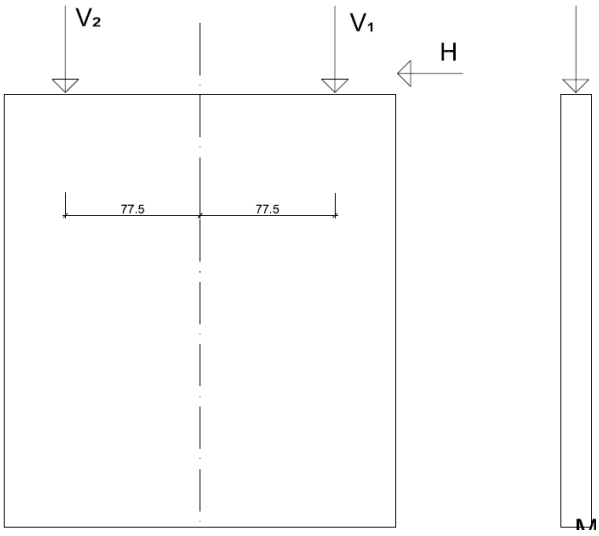

Figure 212: Position of the hydraulic actuators at test specimen Clay04

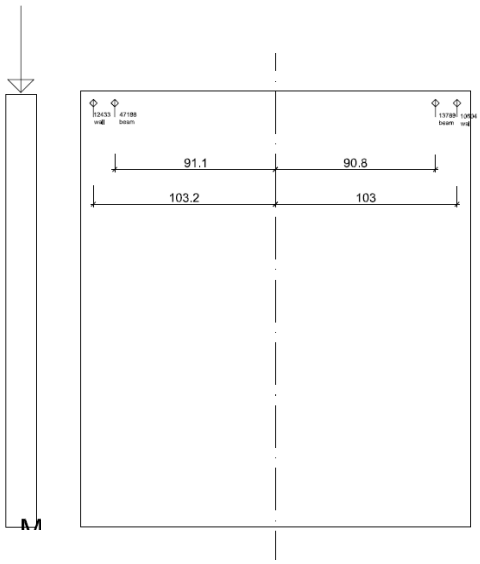

Figure 213: Position of the LVDTs at test specimen Clay04

7.12.1. Scale factor 2.5 (max 0.14 g)

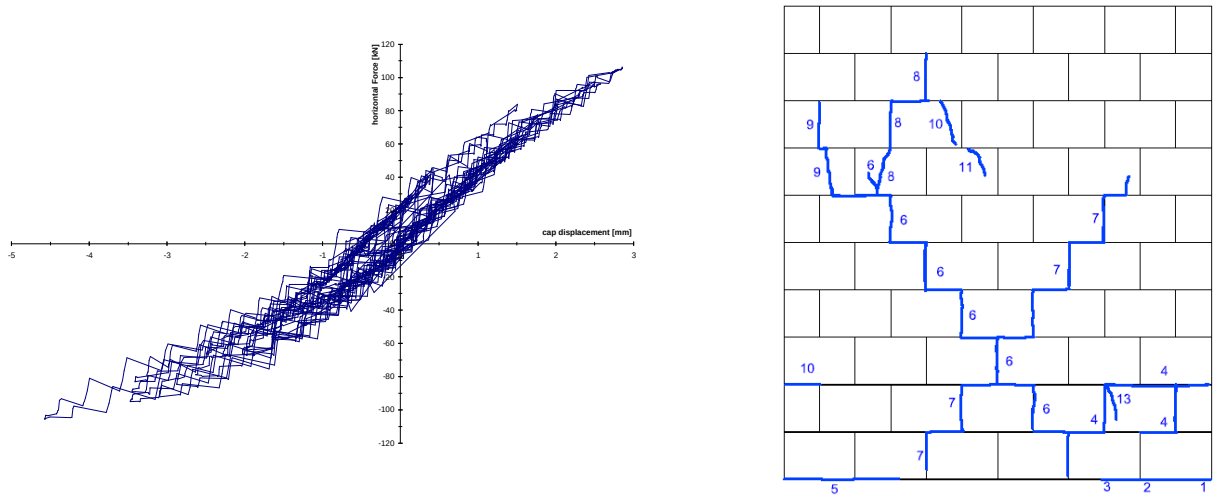

Figure 214: Load-displacement curve (hysteresis) and crack pattern of the test specimen Clay04

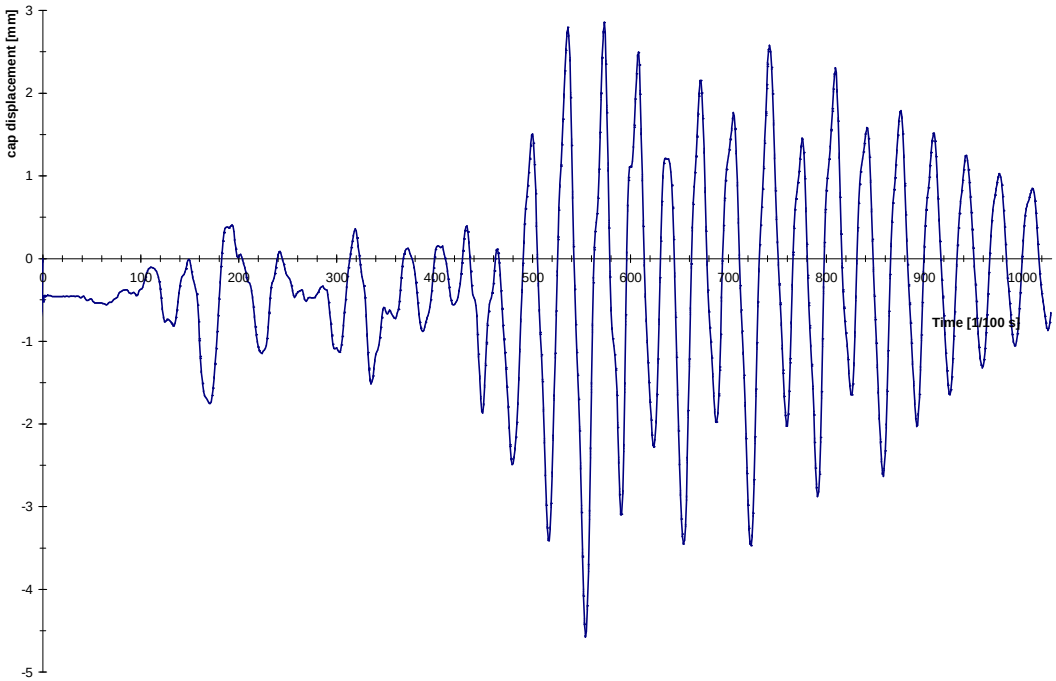

Figure 215: displacement history (earthquake time) Clay04

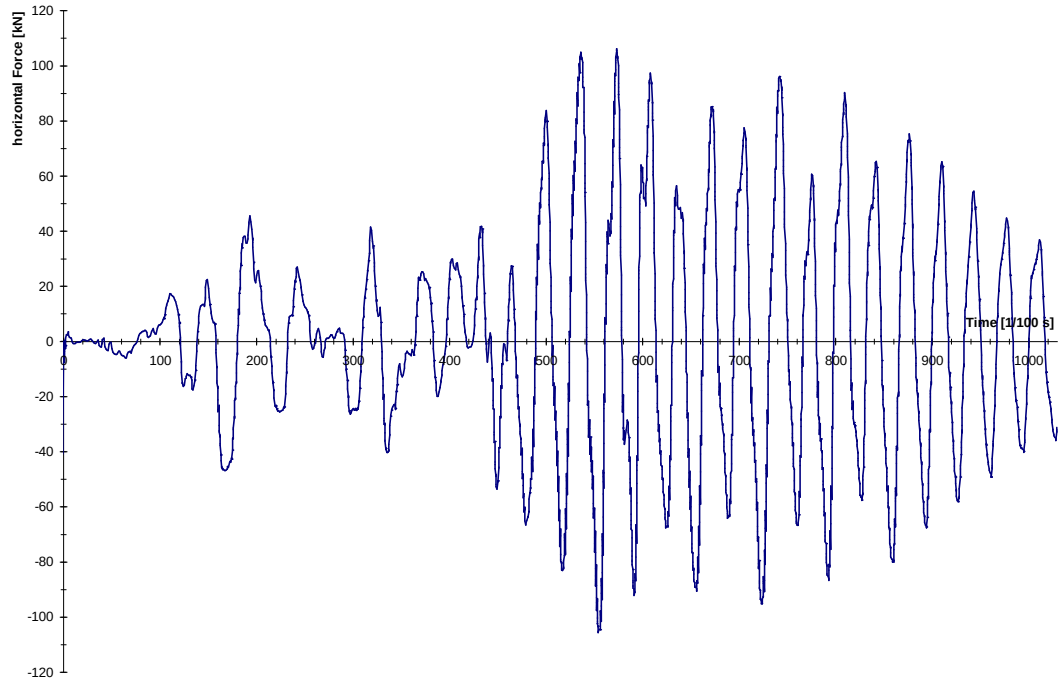

Figure 216: horizontal load history (earthquake time) Clay04

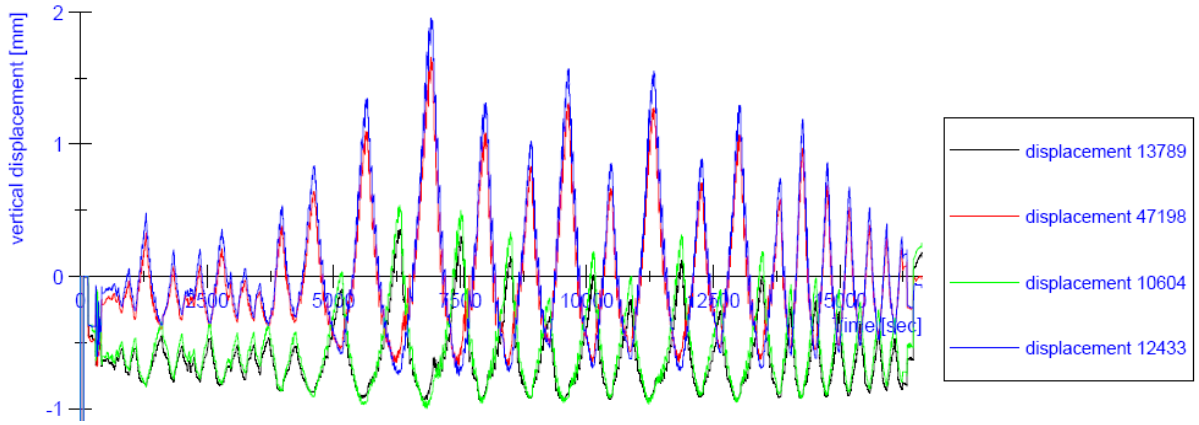

Figure 217: Progress of the vertical displacements (testing time) Clay04

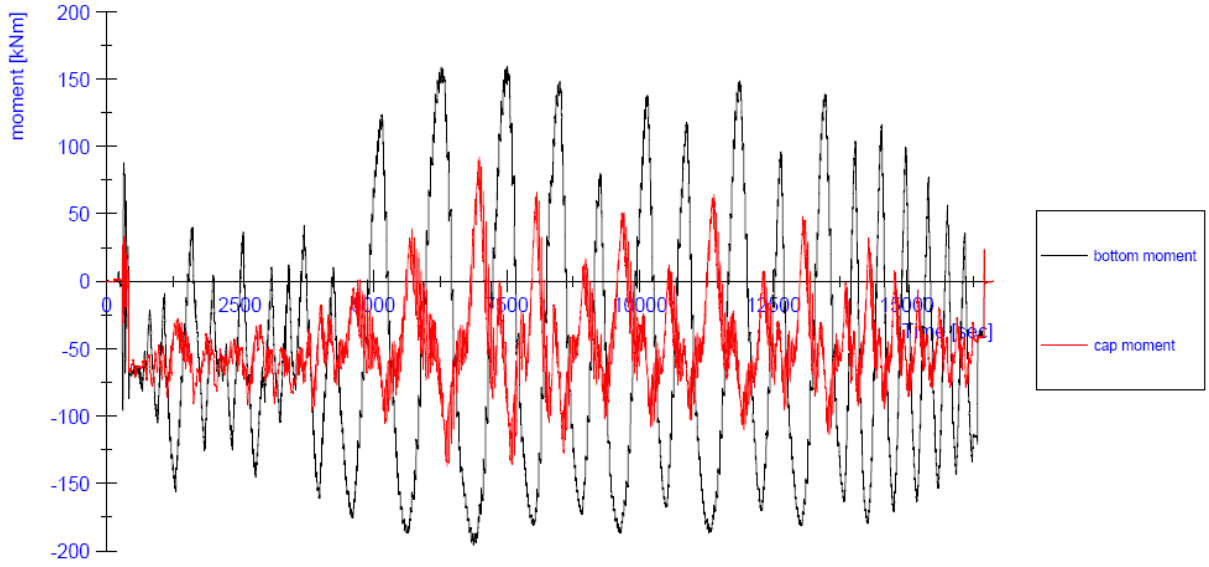

Figure 218: Progress of the in-plane bending moments at the top and at the bottom of the wall (testing time) Clay04

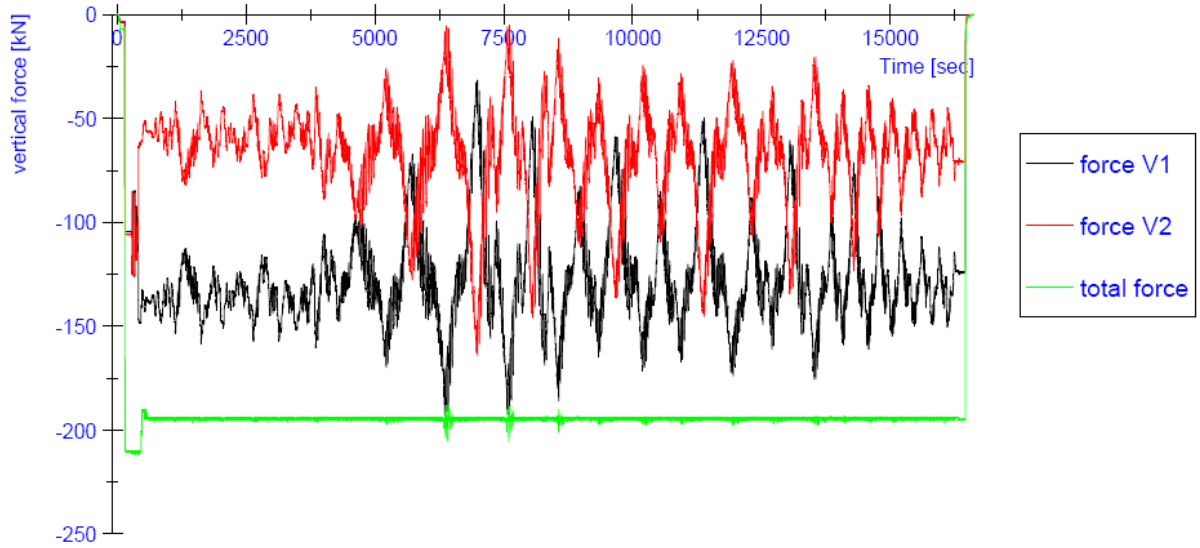

Figure 219: Progress of the vertical forces V1 and V2 (testing time) Clay04

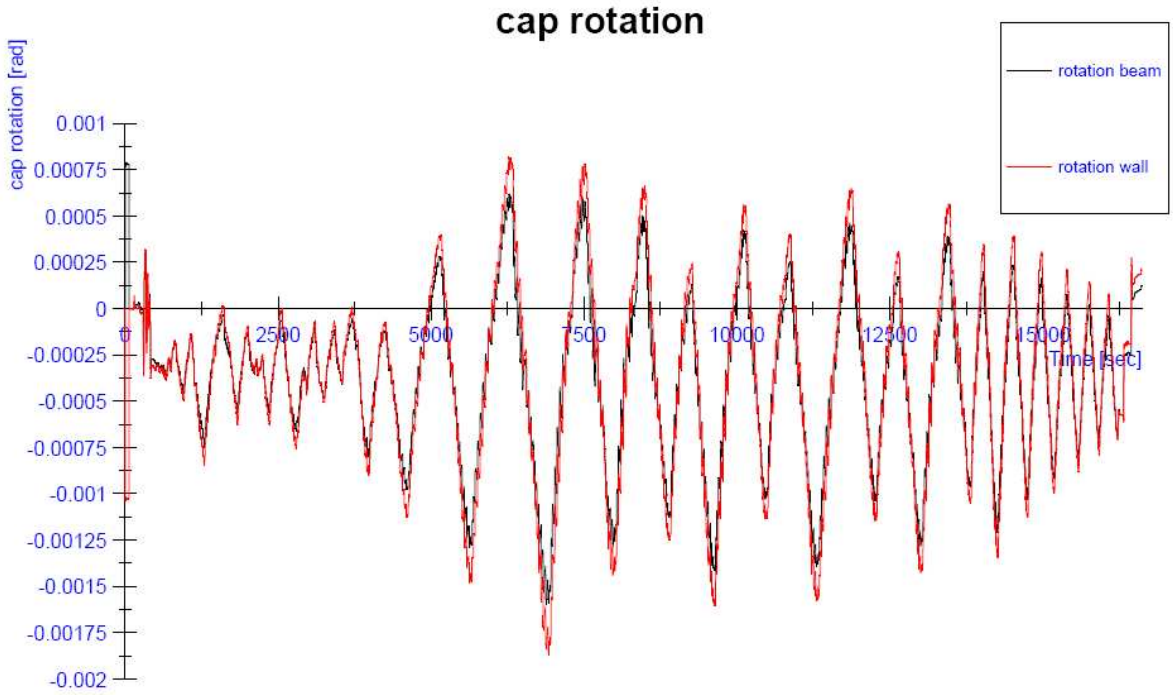

Figure 220: Progress of the in-plane rotation at the top of the wall (testing time) Clay04

7.12.2. Scale factor 4 (max 0.23 g)

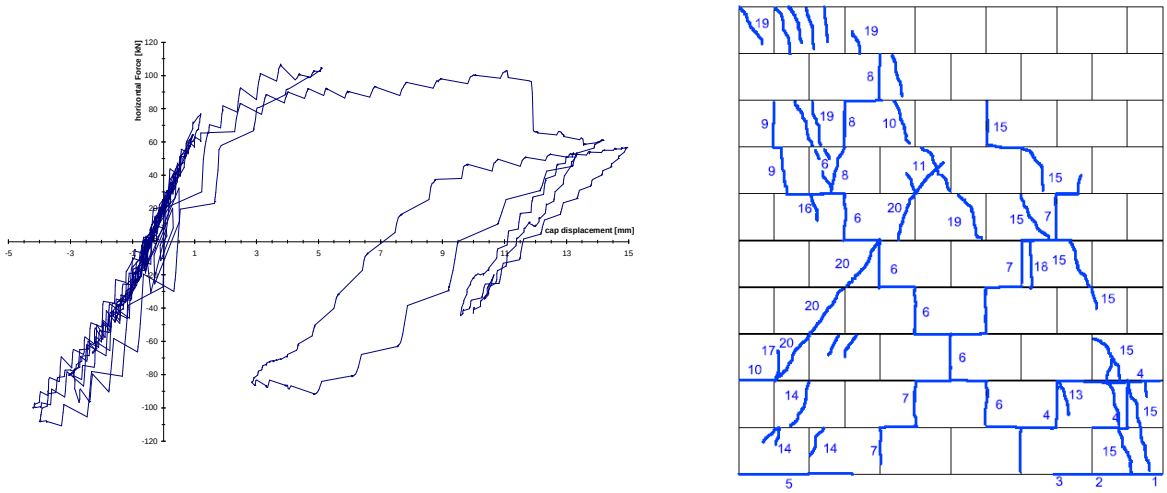

Figure 221: Load-displacement curve (hysteresis) and crack pattern of the test specimen Clay04

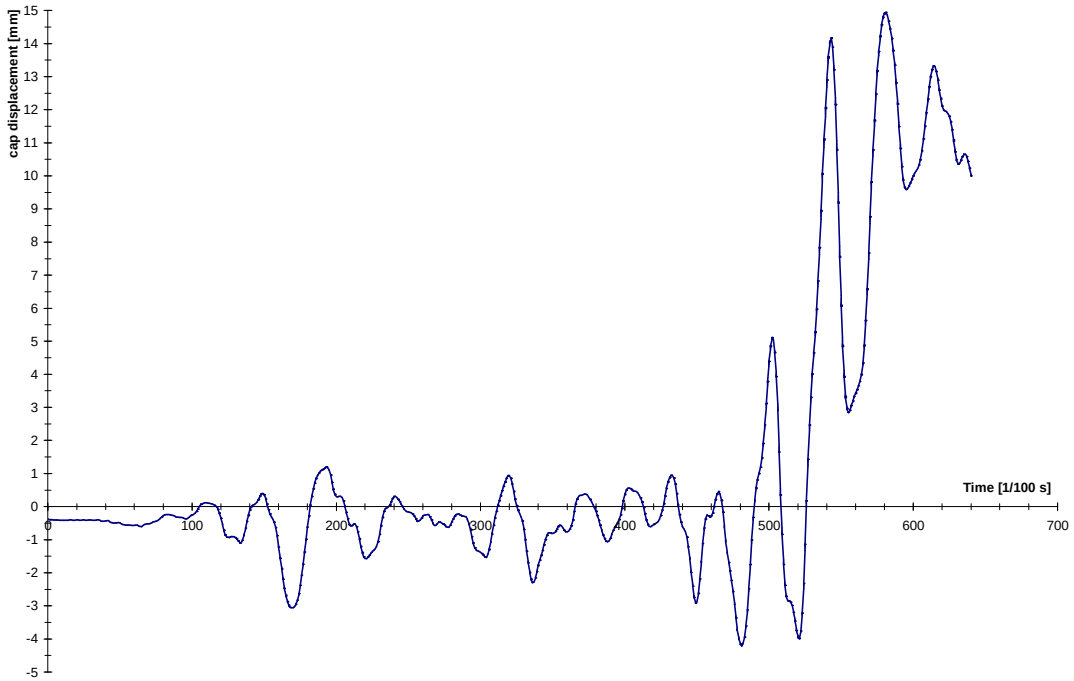

Figure 222: displacement history (earthquake time) Clay04

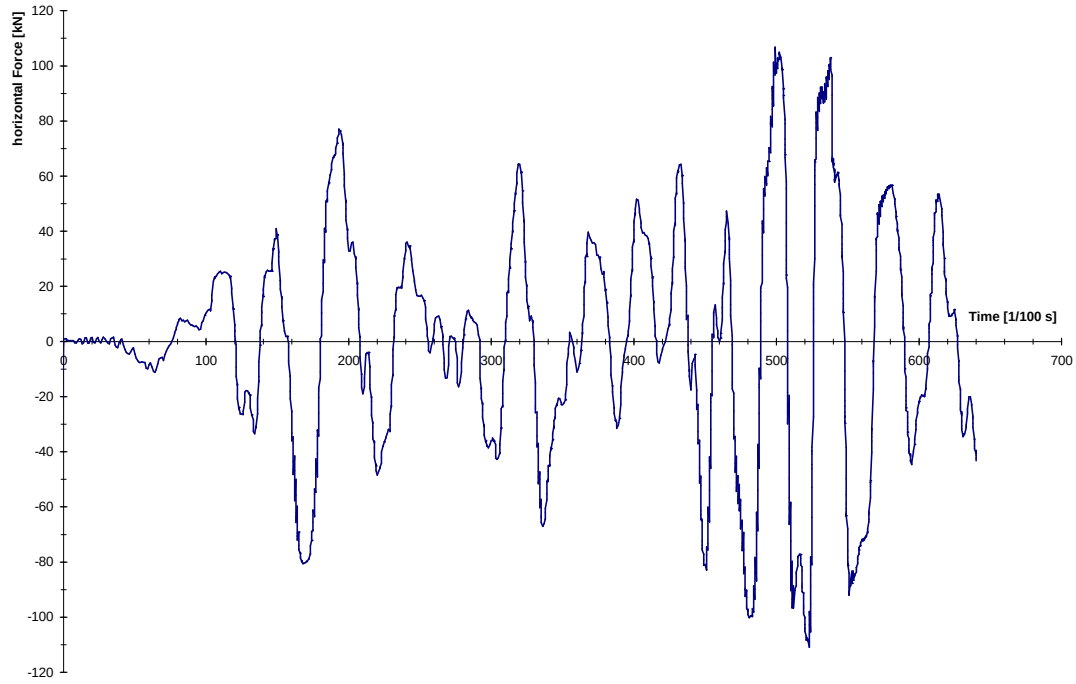

Figure 223: horizontal load history (earthquake time) Clay04

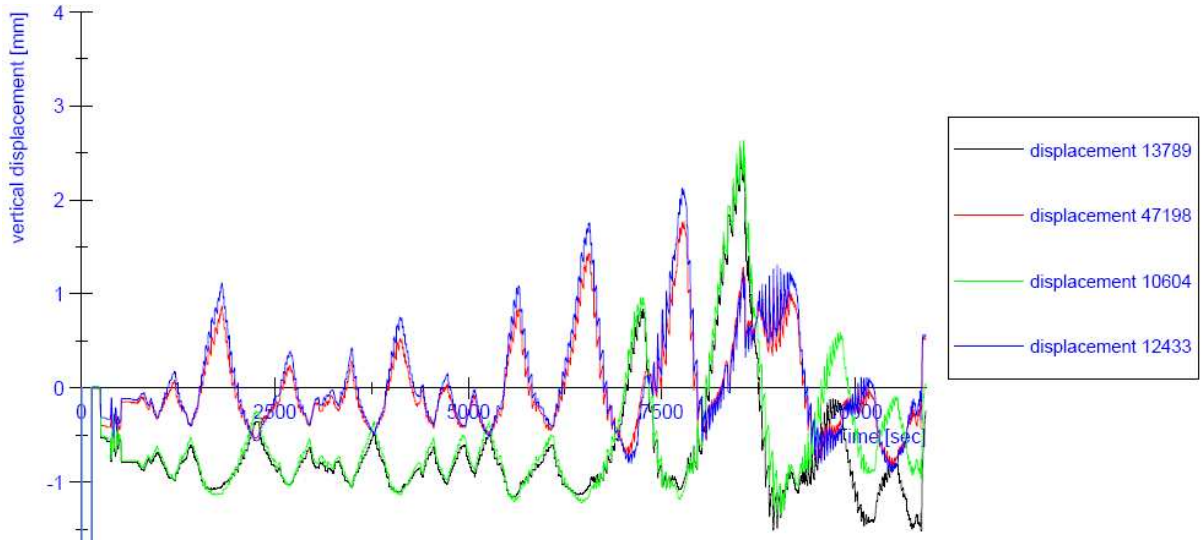

Figure 224: Progress of the vertical displacements (testing time) Clay04

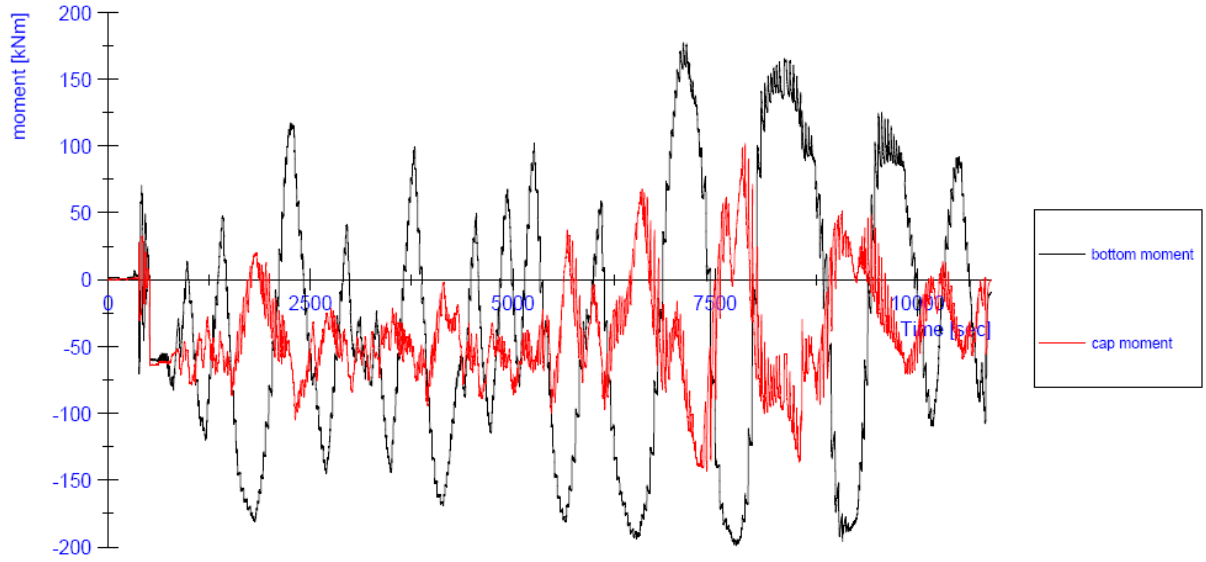

Figure 225: Progress of the in-plane bending moments at the top and at the bottom of the wall (testing time) Clay04

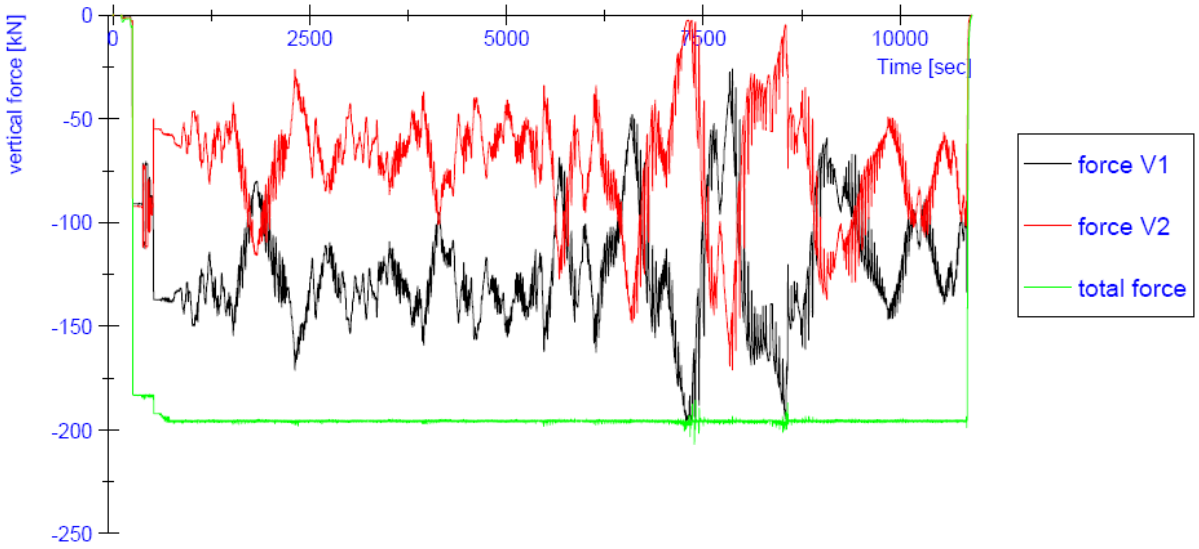

Figure 226: Progress of the vertical forces V1 and V2 (testing time) Clay04

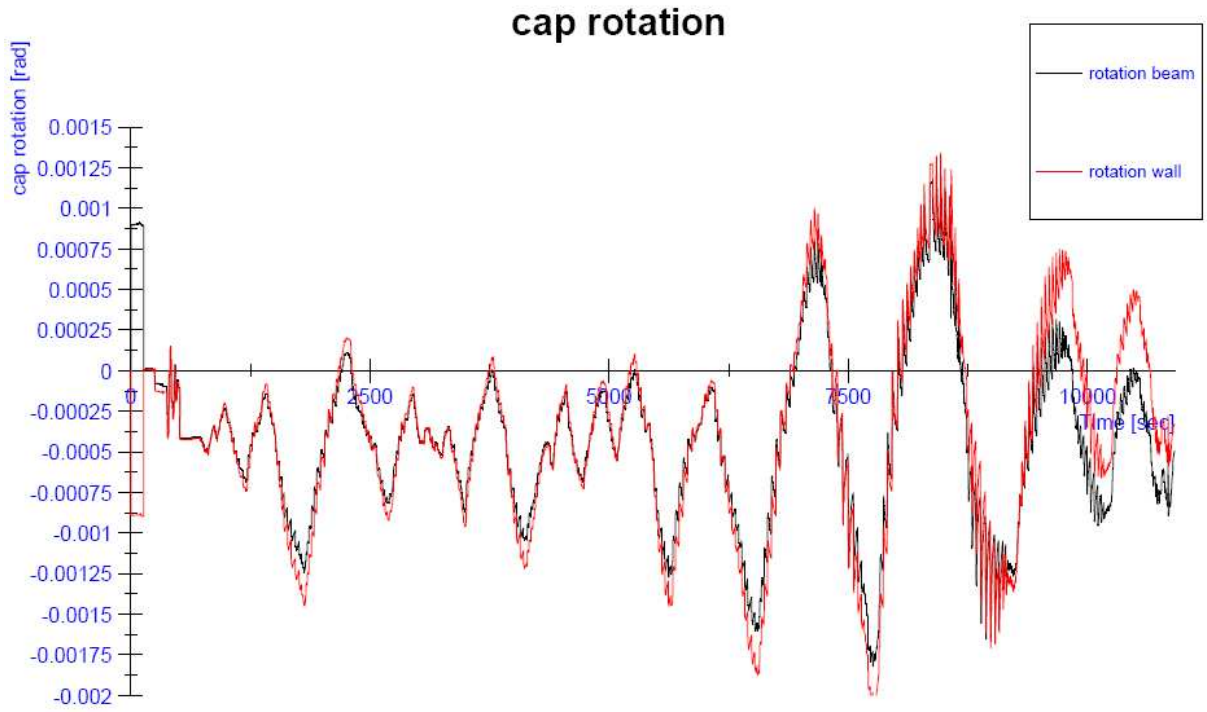

Figure 227: Progress of the in-plane rotation at the top of the wall (testing time) Clay04

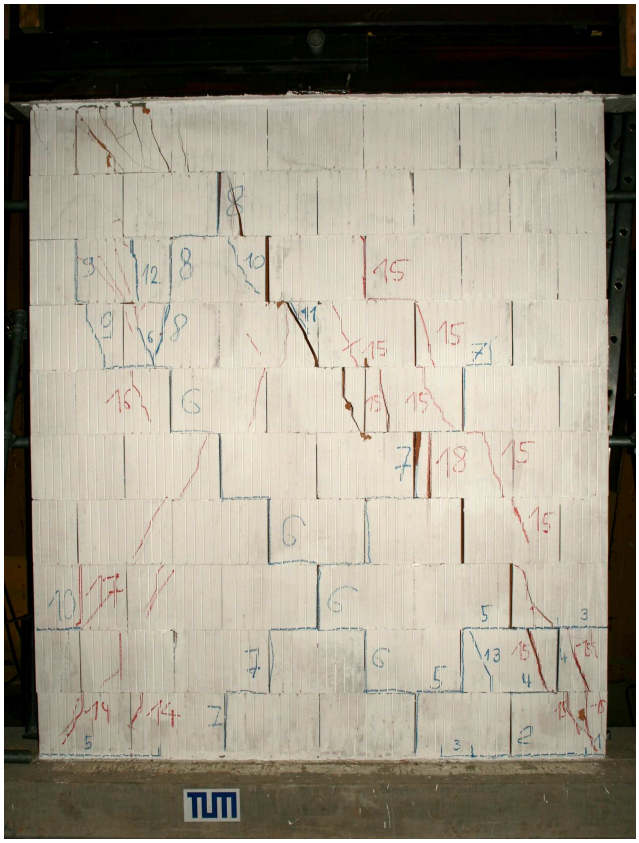

Figure 228: Crack pattern Clay04